

***Kalanchoe blossfeldiana*, a tool for comparatively studying
stomatal physiology, guard cell and mesophyll metabolism
in C₃ and crassulacean acid metabolism tissues**

Daniel Cowan-Turner

Doctor of Philosophy

School of Natural and Environmental Sciences

December 2022

Declaration

This thesis is submitted to Newcastle University for the degree of Doctor of Philosophy. The research detailed within was performed between the years 2018-2022 and it was supervised by Professor Anne Borland and Dr Maxim Kapralov. I certify that none of the material offered in this thesis has been previously submitted by me for a degree or any other qualification at this or any other university.

A handwritten signature in black ink, appearing to read 'Daniel Cowan-Turner', with a stylized, cursive script.

Daniel Cowan-Turner

Abstract

Engineering crassulacean acid metabolism (CAM) into C_3 crops has potential to significantly improve crop plant water usage efficiency (WUE) without significantly effecting yield. Despite the importance of stomata in efforts to engineer CAM into C_3 plants our understanding of CAM stomatal physiology and guard cell metabolism are still lacking. In C_3 plants, guard cell metabolism provides energy and osmolytes essential for proper stomatal regulation. Recent studies have suggested that CAM stomata differ in the timing of guard cell metabolism compared to C_3 . Guard cell metabolism may be of especial importance in CAM plants as it needs to provide energy to sustain nocturnal stomatal opening without photosynthesis. Furthermore, this thesis tackles a key question in CAM engineering, will stomata follow the pattern of mesophyll driven changes in C_i or will guard cells require separate changes to their regulation and metabolism to support nocturnal opening and diurnal closure? These questions will be tackled using C_3 and CAM tissues in *Kalanchoe blossfeldiana* and a CAM deficient *Kalanchoe fedtschenkoi pepc1* mutant. This thesis provides evidence of the retiming of guard cell starch metabolism in CAM tissues and suggests that nocturnal carboxylation driven reductions in C_i are not enough to drive nocturnal stomatal opening in C_3 tissues.

To date, most sequenced inducible CAM plants require inducement through an abiotic stress e.g. drought or salt stress, whereas CAM in *K. blossfeldiana* is also induced with ageing. This thesis develops the inducible CAM plant *K. blossfeldiana* as a system for investigating C_3 and CAM physiologies and mesophyll and guard cell metabolism by presenting a physiological and biochemical characterisation of *K. blossfeldiana* along with its genome and a comparative C_3 /CAM dusk transcriptome; identifying key components of the CAM cycle upregulated in response to age-induced CAM induction.

Acknowledgments

Firstly I would like to thank my great supervisors Prof. Anne Borland and Dr Maxim Kapralov for taking me on this great adventure into the world of CAM, for your countless hours of invaluable advice and support over many years; and for teaching me and countless others about CAM in the first place. Your wisdom and enthusiasm has kept me standing!

I would like to thank and acknowledge Bethan Morris, who agrees that *Kalanchoe blossfeldiana* is a great plant, for collaborating with me on the nucleic acid extractions, protein/western blot work and saturated water content experiments in chapters 2 and 4 and for many great conversations about CAM, plants and the wider world. I would also like to thank my collaborators at Kew Gardens (Dr Ilia Leitch and Dr Robyn Powel) who provided flowcytometry data to estimate the genome size of *Kalanchoe blossfeldiana*. And I would like to express my great thanks to the e-plants group at Linköping University (Dr Iwona Bernacka Wojcik, Dr Eleni Stavrinidou, Alexandra Sandéhn) and Lund University (Till Dreier), who again really like *Kalanchoe blossfeldiana*, for many great conversations and their tireless work on malate injections and *Kalanchoe blossfeldiana* cell size data. I would also like to thank Mercédesz Orosz for helping with collecting data on *Kalanchoe fedtschenkoi* epidermal peel soluble sugars and starch in Chapter 3. In addition I would like to express my great thanks to the plant and lab technicians (Helen Martin, Gillian Davidson, Tracey Stevenson, Mike Robinson, Seann Keith, Sammy Logan, Liam Thompson) for all of their help over the years, not least the time when we had to get a generator installed on the fifth floor for a night to cover an ongoing gas exchange experiment! I would also like to thank Dr Emma Foster and Dr George Merces at the Bioimaging unit for all their great help with imaging guard cell starch. And I would like to thank Dr Jon Marles-Wright for his assistance with getting started with nanopore sequencing and help over the years; and I would also like to thank Dr Vasilios Andriotis for his help, his great laugh and continual mischief!

I would especially like to thank the architects and designers of the Devonshire building for their thoughtful and well considered approach to heat management and almost all things; and for providing such fantastic cooling systems that really stand the test of time.

I would like to thank all of friends for all ways being great fun, especially when I've had to hide away in my 'plant' cave over recent years. For all the great people and friends I've met along the way and in the Devonshire building, especially the members of Max's RUBSICO group (Iain Hope, Wasim Iqbal, Bethan Morris and Rebecca Moore), Ashwinie Nagarajah, Alex Laverick, Ali Leverett, Hannah Gibson, Natalia Hurtado Castano, Tom Reed, Niall Convoy, Joshua Loh, Alex Finney, Osita Nwokeocha, Abdul Alhudhaibi, Feras Afifi, Ryan Thompson, Cassie Bakshani, and many others who have made doing this PhD great. I would also like to express my gratitude to the BBSRC for funding this work. I would also like to especially thank Alec Jones and Jules Falk for being wonderful people and for always being up for an adventure! And a big cheers to all the members of the pub club!

And finally I would like to express my heartfelt gratitude to my partner in life and crime, Laura Kennedy, for their unwavering support and encouragement throughout the writing of this thesis. I'd also like to thank my dog Woody for looking after my parents all of these years. And of course I would like to thank my parents, from whom I learnt my great curiosity and love for the living world. And a final thanks to all the shed loving tinkerers past and present.

Contents

Chapter 1. General Introduction	25
1.1 Climate and CAM	25
1.2 CAM Overview - Everything you need to know about CAM but were afraid to ask	28
1.2.1 PEP Regeneration Pathway / transitory carbon stores	30
1.2.2 ATP/energy supply for CAM	32
1.2.3 Carboxylation pathway of CAM	33
1.2.4 Malate Storage and pH regulation	34
1.2.5 Malate remobilisation and decarboxylation	35
1.2.6 Stomatal regulation and Guard Cell metabolism in CAM	36
1.2.7 The role of C_i in linking mesophyll CAM and stomatal conductance.	38
1.2.8 Guard Cell CO_2 sensing and regulation in CAM	40
1.2.9 Blue and red light mediated stomatal and guard cell starch regulation.	42
1.2.10 Guard Cell Metabolism	45
1.2.11 Guard Cells need energy – where do they get it?	46
1.2.12 Guard Cell Carbon	48
1.2.13 Rescheduling of guard cell starch metabolism in CAM	49
1.2.14 Key Areas for Investigation in CAM	51
1.3 Approaches to CAM engineering and progress so far	51
1.4 Tools to study CAM - CAM in the Omics Era	52
1.5 Approach of this thesis	54
1.6 Kalanchoe genus	54
1.6.1 <i>K. blossfeldiana</i> - Age Induced CAM	55
1.7 Core Questions to be addressed in this thesis - divided by chapter and approaches	57
Chapter 2. Comparative systems for studying crassulacean acid metabolism	59
2.1 Introduction	59
2.1.1 <i>K. blossfeldiana</i> - Age Induced CAM	59
2.1.2 Chapter Aims	61
2.2 Materials and Methods	62
2.2.1 Summary of Experiments	62

2.2.2 Plant Growth Conditions	62
2.2.3 Diel Gas Exchange	63
2.2.4 Long term Gas Exchange (Walz Binos-100)	63
2.2.5 Metabolite Sampling and Analysis	64
2.2.6 Protein Extraction and Western blots	65
2.2.7 Morphological analysis	66
2.3 Results	67
2.3.1 Young and mature <i>K. blossfeldiana</i> leaves have distinct photosynthetic physiotypes	67
2.3.2 Crassulacean acid metabolism is rapidly induced in young <i>K. blossfeldiana</i> leaves by drought	67
2.3.3 Young <i>K. blossfeldiana</i> leaves are more photosynthetically active than Mature <i>K. blossfeldiana</i> leaves	
2.3.4 Young <i>K. blossfeldiana</i> leaves did not accumulate titratable acids at night	72
2.3.5 Significant differences in whole leaf metabolism between young and mature leaves of <i>K. blossfeldiana</i>	
2.3.6 PEPC Protein	74
2.3.7 Morphology and the development of CAM traits	75
2.3.8 <i>K. fedtschenkoi pepc1.1</i> mutants are impaired in CAM	77
2.4 Discussion	79
2.4.1 <i>Kalanchoe blossfeldiana</i> – A tale of two physiotypes	79
2.4.2 Whole Leaf Metabolism in <i>Kalanchoe blossfeldiana</i>	80
2.4.3 The PEPC1 isoform is essential for CAM in <i>K. fedtschenkoi</i>	82
Chapter 3. Self-determined stomata - PEPC-mediated nocturnal carboxylation alone is not enough to drive nocturnal conductance in Kalanchoe	84
3.1 Introduction	84
3.1.1 The role of C_i in linking mesophyll PEPC-driven carboxylation and stomatal conductance.	85
3.1.2 Guard Cell Metabolism – Essential for powering nocturnal opening in CAM.	86
3.1.3 Whole Leaf Carbon Assimilation and its influence on stomatal behaviour in C_3 and CAM systems	87
3.1.4 Key questions and approach	89
3.2 Methods	90
3.2.1 Summary of Experiments and Conditions	90
3.2.2 Plant Materials and Growth Conditions	91
3.2.3 Gas Exchange and Low $[CO_2]$ Stomatal response assays	91
3.2.4 Stomatal Kinetic Responses	93
3.2.5 Metabolite Analysis	95
3.2.6 Epidermal Peel Soluble Sugar Analysis	95
3.2.7 Guard Cell Starch Analysis	96
3.3 Results	98
3.3.1 <i>K. blossfeldiana</i> age specific photosynthetic and stomatal responses.	98

3.3.2 <i>K. fedtschenkoi</i> genotype specific photosynthetic and stomatal responses.	101
3.3.3 Guard Cell Metabolism across different photosynthetic physiotypes	102
3.3.4 Comparing C ₃ and CAM stomatal responses to low [CO ₂]	105
3.3.5 Reduced CO ₂ is not enough to trigger CAM-like nocturnal opening in young C ₃ <i>K. blossfeldiana</i>	112
3.3.6 Reduced [CO ₂] can restore CAM-like nocturnal opening in CAM-deficient <i>K. fedtschenkoi pepc1.1</i> mutant	112
3.3.7 The role of whole leaf carbon assimilation on stomatal conductance, including both C ₃ RUBISCO and PEPC-mediated assimilation.	113
3.3.8 Reduced photo-assimilate reduced daytime stomatal response in C ₃ tissues but reduced malate accumulation had no effect on daytime stomatal responses in CAM tissues	113
3.3.9 Growth at reduced light intensity had differing effects on stomatal behaviour in C ₃ and CAM tissues in <i>K. blossfeldiana</i>	115
3.4 Discussion	117
3.4.1 C ₃ and CAM leaves have distinct patterns of diel stomatal conductance.	117
3.4.2 Guard Cell Starch Metabolism is rescheduled between C ₃ and CAM tissues	117
3.4.3 The role of C _i in linking mesophyll PEPC-driven carboxylation and stomatal conductance.	119
3.4.4 Diel sensitivity to reduced C _i varies between C ₃ and CAM tissues	120
3.4.5 Reduced [CO ₂] can restore CAM-like nocturnal opening in CAM-deficient <i>K. fedtschenkoi pepc1.1</i> mutant but not young C ₃ <i>K. blossfeldiana</i>	121
3.4.6 Increased stomatal conductance in C ₃ /CAM-deficient tissues is driven by increased photo-assimilate and stomatal density	122
3.4.7 What role does nocturnal malate accumulation play in daytime stomatal closure in CAM?	123
3.4.8 Conclusions	124
Chapter 4. The <i>Kalanchoe blossfeldiana</i> Genome	125
4.1 Introduction	125
4.2 Materials and Methods	127
4.2.1 Plant Materials	127
4.2.2 Estimating <i>K. blossfeldiana</i> genome size	127
4.2.3 <i>K. blossfeldiana</i> DNA Extraction	128
4.2.4 <i>K. blossfeldiana</i> RNA Extraction	129
4.2.5 <i>K. blossfeldiana</i> Genome Sequencing	130
4.2.6 <i>K. blossfeldiana</i> Genome Assembly	130
4.2.7 <i>K. blossfeldiana</i> Genome Annotation	131
4.2.8 <i>K. blossfeldiana</i> Chloroplast Genome and Phylogenetics	132
4.2.9 <i>K. blossfeldiana</i> Dusk RNA-seq	132
4.3 Results and Discussion	133

4.3.1 <i>K. blossfeldiana</i> genome size	133
4.3.2 <i>K. blossfeldiana</i> Genome Assembly	134
4.3.3 <i>K. blossfeldiana</i> Genome Annotation	136
4.3.4 Phylogenetics of <i>K. blossfeldiana</i>	138
4.3.5 Shift in transcript expression pattern in mature CAM <i>K. blossfeldiana</i> leaves	141
4.3.6 Core CAM genes upregulated in mature CAM <i>K. blossfeldiana</i> leaves	143
4.3.7 PEP Regeneration and Starch	144
4.3.8 Switch to phosphorolytic starch degradation in CAM <i>K. blossfeldiana</i> leaves	145
4.3.9 Down regulation of RUBISCO	147
4.3.10 Vacuolar Transporters	147
4.3.11 Overlap between ageing, drought and ABA CAM induction pathways.	148
4.3.12 Identifying Guard Cell genes upregulated in mature CAM <i>K. blossfeldiana</i> leaves	149
4.3.13 Guard cell regulatory genes upregulated in mature CAM <i>K. blossfeldiana</i> leaves	152
4.3.14 Guard cell metabolic genes upregulated in mature CAM <i>K. blossfeldiana</i> leaves	153
4.3.15 Endoreplication increases as <i>K. blossfeldiana</i> leaves age	154
4.3.16 Conclusions	155
Chapter 5. General Discussion	157
5.1 Key Findings	157
5.1.1 <i>Kalanchoe blossfeldiana</i> as a comparative system for studying C ₃ /CAM	157
5.1.2 Changes in guard cell metabolism and regulation in CAM are required for sustained nocturnal stomatal opening	159
5.1.3 ATP/Carbon supply for CAM	161
5.1.4 Core set of genes up-regulated in response to age, ABA, drought and NaCl-induced CAM	163
5.2 Future Directions – where next on the road to CAM?	165
5.2.1 Lots of omics data, but what to do with it?	165
5.2.2 New Approaches – The role of methylation in age-induced CAM	166
5.2.3 Temporal and Spatial Approaches to studying CAM	166
5.2.4 High Throughput Phenotyping	167
5.2.5 CAM modelling and Engineering	169
5.3 Overall Conclusions	170
Chapter 6. References	171
Chapter 7. Appendix	209
7.1 Appendix 1. Supplementary Data for Chapter 3.	209
7.2 Appendix 2. Supplementary Data for Chapter 4.	212

7.3 Appendix 3 Investigating differential methylation in age induced CAM in <i>K. blossfeldiana</i>	217
7.4 Appendix 4. Testing transformations of <i>K. blossfeldiana</i>	219
7.5 Appendix 5. Reduced Light Intensity Reduces CAM	220

List of figures

- FIGURE 1.1 AN OVERVIEW OF GLOBAL LAND USAGE, HIGHLIGHTING THE AREA OF DRYLANDS (ARID, SEMI-ARID AND DRY SUB-HUMID LANDS THAT MAKE UP 39.7% OF GLOBAL LAND MASS. ADAPTED FROM UNEP (2012). 25
- FIGURE 1.2 CAM PLANTS ARE MORE WATER USAGE EFFICIENT (WUE) THAN C_3 OR C_4 REQUIRING SIGNIFICANTLY LESS WATER WITHOUT A MAJOR IMPACT ON YIELD (LEFT, SHAMEER ET AL., 2018). C_3 PLANTS CAN LOSE UP TO 400 MOLES OF H_2O PER MOLE OF CO_2 FIXED (RIGHT). 26
- FIGURE 1.3 AN OVERVIEW OF DIEL MESOPHYLL CAM IN STARCH STORING CAM PLANTS ADAPTED FROM SCHILLER & BRÄUTIGAM (2021). TEXT IN BOLD REFERS TO ENZYMES. ABBREVIATIONS SHOWN INCLUDE: PHOSPHOGLYCEROMUTASE (PGLYM); TONOPLAST DICARBOXYLATE TRANSPORTER (TDT); ALUMINIUM ACTIVATED MALATE TRANSPORTER (ALMT);BILE ACID SODIUM SYMPORTER 2 (BASS2); DEBRANCHING ENZYME (DBE); GLUCOSE-1-PHOSPHATE (G1P);GLUCOSE-6-PHOSPHATE (G6P); MALATE DEHYDROGENASE (MDH); NAD(P)-DEPENDENT MALIC ENZYME (NAD(P)-ME); SODIUM HYDROGEN ANTIPOINTER 1 (NHD1); OXALOACETATE (OAA); PHOSPHOENOLPYRUVATE (PEP); PHOSPHOENOLPYRUVATE CARBOXYLASE (PEPC); PHOSPHOGLYCERATE (PGA); PYRUVATE PHOSPHATE DIKINASE (PPDK); PPK REGULATORY PROTEIN (PPDK-RP); PPT, PHOSPHOENOLPYRUVATE PHOSPHATE TRANSLOCATOR; TRIOSEPHOSPHATE/PHOSPHATE TRANSLOCATOR (TPT); AMY3 (A-AMYLASE 3); BAM1 (B-AMYLASE 1); BAM3 (B-AMYLASE 3); PHOSPHOGLUCOMUTASE (PGM);BCA5 (B-CARBONIC ANHYDRASE 1); PPCK (PHOSPHOENOLPYRUVATE CARBOXYLASE KINASE); DPE1 (CHLOROPLASTIC DISPROPORTIONATING ENZYME); PHS1 (CHLOROPLASTIC A-GLUCAN PHOSPHORYLASE); CYTOSOLIC DISPROPORTIONATING ENZYME (DPE2); MEX1 (MALTOSE TRANSPORTER); PGLCT (PLASTIDIC GLUCOSE TRANSPORTER), GPT1 (GLUCOSE PHOSPHATE TRANSLOCATOR 1); AND GPT2 (GLUCOSE PHOSPHATE TRANSLOCATOR 2). 29
- FIGURE 1.4 DIEL CO_2 ASSIMILATION IN C_3 AND CAM PLANTS, WITH DIEL PATTERN OF STOMATAL CONDUCTANCE INDICATED BELOW, ADAPTED FROM MALES & GRIFFITHS (2017). 36
- FIGURE 1.5 A SUMMARY OF KEY POTENTIAL LINKS BETWEEN MESOPHYLL METABOLISM AND GUARD CELL REGULATED STOMATAL CONDUCTANCE INCLUDING; PHOTOSYNTHETIC CONTROL MEDIATED VIA SUCROSE OR OTHER CARBOHYDRATES, MALATE PRODUCTION OR USAGE BY CAM, OR CHANGES IN CI DRIVEN BY CAM 38
- FIGURE 1.6 A SUMMARY OF THE CO_2 SIGNALLING PATHWAYS IN ARABIDOPSIS, ADAPTED FROM (ZHANG ET AL., 2018). 40
- FIGURE 1.7 A SUMMARY OF THE BLUE AND RED LIGHT SIGNALLING PATHWAYS IN ARABIDOPSIS GUARD CELLS, ADAPTED FROM (INOUE AND KINOSHITA, 2017) AND (ANDO AND KINOSHITA, 2018). 42
- FIGURE 1.8 KEY ELEMENTS OF GUARD CELL METABOLISM DURING LIGHT INDUCED OPENING IN C_3 PLANTS, WITH A FOCUS ON ATP DEMAND AND SUPPLY, ADAPTED FROM (FLÜTSCH & SANTELIA, 2021; LIM ET AL., 2022). 45
- FIGURE 1.9 COMPARISON OF DIEL CHANGES IN GUARD CELL STARCH GRANULE AREA IN ARABIDOPSIS (C_3) AND KALANCHOE FEDTSCHENKOI (CAM), SHOWING A RESCHEDULING OF STARCH METABOLISM IN K. FEDTSCHENKOI GUARD CELLS (ABRAHAM ET AL., 2020; HERRER ET AL. 2016). 49

FIGURE 2.1 *K. BLOSSFELDIANA* AGE SPECIFIC PHOTOSYNTHETIC TRAITS AND CAM INDUCTION. DIURNAL NET CO₂ UPTAKE (PANEL A, $\mu\text{MOL CO}_2 \text{ M}^{-1} \text{ S}^{-1}$) AND STOMATAL CONDUCTANCE (PANEL B, $\text{MOL H}_2\text{O M}^{-1} \text{ S}^{-1}$) OF *K. BLOSSFELDIANA* YOUNG LEAVES (RED POINTS, 10TH LEAF PAIR FROM THE BOTTOM) AND MATURE LEAVES (BLUE POINTS, 2ND LEAF PAIR FROM THE BOTTOM) BETWEEN 60-90 DAYS AFTER PROPAGATION. FOR PANEL A AND B POINTS REPRESENT THE MEAN OF THREE REPEATS AND THE SHADED INTERVAL \pm SEM. HORIZONTAL BLUE LINE EQUALS ZERO, PANEL A. CAM INDUCTION BY DROUGHT (PANEL C). NET CO₂ ASSIMILATION ($\mu\text{MOL CO}_2 \text{ M}^{-1} \text{ S}^{-1}$) OF A *K. BLOSSFELDIANA* YOUNG LEAF (10TH LEAF PAIR FROM THE BOTTOM) AT 90 DAYS AFTER PROPAGATION DROUGHTED FOR 10 DAYS AND RE-WATERED ON DAY 11. HORIZONTAL RED LINE INDICATES ZERO NET CO₂ ASSIMILATION. VERTICAL BLUE LINE INDICATES TIME OF RETURN TO NORMAL WATERING REGIME. 69

FIGURE 2.2 INTEGRATED WATER USE EFFICIENCY (WUE, LEFT TOP), OVERALL NET CO₂ ASSIMILATION ($\mu\text{MOL CO}_2 \text{ M}^{-1} \text{ S}^{-1}$), AND OVERALL TRANSPIRATION OVER A FULL 24HRS, THE DAY OR NIGHT PERIOD IN *K. BLOSSFELDIANA* YOUNG (LEFT SIDE, 10TH LEAF PAIR FROM THE BOTTOM) OR MATURE LEAVES (RIGHT SIDE, 2ND LEAF PAIR FROM THE BOTTOM) AT 60-90 DAYS AFTER PROPAGATION. VALUES ARE THE MEAN OF THREE REPLICATES \pm SEM. PLANTS WERE GROWN IN STANDARD CONDITIONS WITH 400 PPM CO₂ AND 190 $\mu\text{MOL M}^{-2} \text{ S}^{-1}$ LIGHT. STATISTICAL ANALYSIS WAS PERFORMED BY USING A TWO-WAY ANOVA, SIGNIFICANT DIFFERENCES ($P < 0.05$) ARE INDICATED BY DIFFERENT LOWERCASE LETTERS. 71

FIGURE 2.3 *K. BLOSSFELDIANA* AGE SPECIFIC WHOLE LEAF TITRATABLE ACIDITY AND METABOLITES. TITRATABLE ACIDITY ($\text{MMOL H}^+ \text{ G}^{-1} \text{ FWT}$) OVER 24HRS (PANEL A), DIFFERENCES IN DAWN/DUSK TITRATABLE ACIDITY ($\text{MMOL H}^+ \text{ G}^{-1} \text{ FWT}$) INCREASE WITH LEAF AGE (PANEL B), SOLUBLE SUGARS ($\text{MMOL GLC EQUIV G}^{-1} \text{ FWT}$) OVER 24 HRS (PANEL C), STARCH ($\text{MMOL GLC EQUIV G}^{-1} \text{ FWT}$) OVER 24HRS (PANEL D). LEAF PAIR TWO IS THE OLDEST (2ND LEAF PAIR FROM BOTTOM) AND TEN THE YOUNGEST (10TH LEAF PAIR FROM BOTTOM). LEAVES WERE SAMPLED EVERY FOUR HOURS, WITH THE FIRST SAMPLING 4 HRS BEFORE DUSK. ALL PLANTS SAMPLED 90 DAYS AFTER PROPAGATION. VALUES ARE MEANS OF FOUR REPLICATES \pm SEM. STATISTICAL ANALYSIS WAS PERFORMED BY USING A TWO-WAY ANOVA, SIGNIFICANT DIFFERENCES ($P < 0.05$) ARE INDICATED BY DIFFERENT LOWERCASE LETTERS FOR PANEL B. 73

FIGURE 2.4 *K. BLOSSFELDIANA* AGE SPECIFIC WESTERN BLOT ANALYSIS OF PEPC1 (UPPER BAND) AND RBCL (LOWER BAND) ABUNDANCE IN YOUNG LEAVES (10TH LEAF PAIR FROM THE BOTTOM, PANEL A), MATURE LEAVES (2ND AND 3RD LEAF PAIRS FROM THE BOTTOM, PANEL B AND C) OVER 24HRS; AND A COMPARISON ON EXPRESSION BETWEEN YOUNG LEAVES (10TH LEAF PAIR FROM THE BOTTOM) AND MATURE LEAVES (2ND LEAF PAIR FROM THE BOTTOM) AT DUSK (PANEL D). PROTEINS WERE SEPARATED BY SDS-PAGE, BLOTTED WITH PEPC1 AND RBCL ANTIBODIES. EQUAL LOADING WAS SHOWN BY PONCEAU STAINING THE BLOT (LOWER SECTION) PRIOR TO ANTIBODY INCUBATION; THE BLOT IS REPRESENTATIVE OF AT LEAST THREE REPLICATES. THE 20 PM TIMEPOINT WAS CARRIED OUT IN DARKNESS, WHILE THE 8 AM TIMEPOINT WAS IN THE LIGHT. THE TRIANGLE REPRESENTS THE POSITION OF PEPC1 (GREEN TRIANGLE) AND RBCL (ORANGE TRIANGLE). 74

FIGURE 2.5 CAM TRAITS ACROSS DIFFERENT LEAF PAIRS IN *K. BLOSSFELDIANA* PLANTS SAMPLED 90 DAYS AFTER PROPAGATION, GROWN IN NORMAL LIGHT (NORMAL BARS, 190 $\mu\text{MOL PHOTONS}$). DAWN/DUSK WHOLE LEAF TITRATABLE ACIDITY (PANEL A), LEAF SATURATED WATER CONTENT (SWC, PANEL B), LEAF

WATER MASS PER LEAF AREA (PANEL C, WMA), LEAF DRY MASS PER LEAF AREA (LMA, PANEL D). LEAF PAIRS ARE NUMBERED UP THE PLANT, WITH 12 BEING THE YOUNGEST SAMPLED. NUMBERS ABOVE BARS ON THE TOP LEFT PANEL INDICATE SAMPLE NUMBER, VALUES ARE MEANS OF THE NOTED NUMBER OF REPLICATES \pm SEM. STATISTICAL ANALYSIS WAS PERFORMED USING ONE-WAY ANOVA, SIGNIFICANT DIFFERENCES ($P < 0.05$) ARE INDICATED BY DIFFERENT LOWERCASE LETTERS. 76

FIGURE 2.6 *K. FEDTSCHENKOI* GENOTYPE SPECIFIC PHOTOSYNTHETIC TRAITS AND WHOLE LEAF TITRATABLE ACIDITY. DIURNAL NET CO₂ UPTAKE (PANEL A, $\mu\text{MOL CO}_2 \text{ M}^{-1} \text{ S}^{-1}$) AND STOMATAL CONDUCTANCE (PANEL B, $\text{MOL H}_2\text{O M}^{-1} \text{ S}^{-1}$) OF WILD TYPE *K. FEDTSCHENKOI* LEAVES (BLUE POINTS) AND *PEPC1.1* LEAVES (RED POINTS) BETWEEN 90-120 DAYS AFTER PROPAGATION. LEAF PAIR 6 WAS USED IN BOTH GENOTYPES. PLANTS GROWN IN 12HR/12HR DAY/NIGHT CYCLES. DARK SHADED AREA REPRESENTS NIGHT. FOR BOTH GRAPH, POINTS REPRESENT THE MEAN OF THREE REPEATS AND THE SHADED INTERVAL \pm SEM. DIFFERENCES IN DAWN/DUSK TITRATABLE ACIDITY ($\text{MMOL H}^+ \text{ G}^{-1} \text{ FWT}$) BETWEEN WILD TYPE *K. FEDTSCHENKOI*, *PEPC1.1* AND *PEPC1.2* LEAVES (PANEL C). POINTS REPRESENT THE MEAN OF AT LEAST FIVE SAMPLES AND \pm SEM. THE DARK BLUE LINE ON THE CO₂ UPTAKE GRAPH EQUALS ZERO. STATISTICAL ANALYSIS WAS PERFORMED USING ONE-WAY ANOVA, SIGNIFICANT DIFFERENCES ($P < 0.05$) ARE INDICATED BY DIFFERENT LOWERCASE LETTERS. 78

FIGURE 3.1 DIEL *K. BLOSSFELDIANA* AGE SPECIFIC PHOTOSYNTHETIC AND STOMATAL RESPONSES (PANELS A AND B) AND *K. FEDTSCHENKOI* GENOTYPE SPECIFIC PHOTOSYNTHETIC AND STOMATAL RESPONSES (PANEL C AND D). DIEL NET CO₂ UPTAKE (PANEL A AND C, $\mu\text{MOL CO}_2 \text{ M}^{-1} \text{ S}^{-1}$) AND STOMATAL CONDUCTANCE (PANEL B AND D, $\text{MOL H}_2\text{O M}^{-1} \text{ S}^{-1}$) OF *K. BLOSSFELDIANA* YOUNG LEAVES (RED POINTS, 10TH LEAF PAIR FROM BOTTOM) AND MATURE LEAVES (BLUE POINTS, 2ND LEAF FROM BOTTOM) BETWEEN 60-90 DAYS AFTER PROPAGATION OR WILD TYPE *K. FEDTSCHENKOI* LEAVES (BLUE POINTS) AND *PEPC1.1* LEAVES (RED POINTS) BETWEEN 100-120 DAYS AFTER PROPAGATION. LEAF PAIR 6 WAS USED IN BOTH GENOTYPES. PLANTS GROWN IN 12HR/12HR DAY/NIGHT CYCLES WITH 25°C DAYS/ 19°C NIGHTS. DARK SHADED AREA REPRESENTS NIGHT. FOR EACH GRAPH POINTS REPRESENT THE MEAN OF THREE REPEATS AND THE SHADED INTERVAL \pm SEM. THE DARK BLUE LINE ON THE CO₂ UPTAKE GRAPHS EQUALS ZERO. 99

FIGURE 3.2 CORELATIONS BETWEEN DIEL STOMATAL CONDUCTANCE AND NET CARBON UPTAKE IN *K. BLOSSFELDIANA* YOUNG AND MATURE LEAVES (PANEL A) AND *K. FEDTSCHENKOI* WILD TYPE AND *PEPC1.1* LEAVES (PANEL B). BLUE LINE REPRESENTS PLOTTED LINEAR REGRESSION. 100

FIGURE 3.3 GUARD CELL METABOLITES IN C₃/CAM TISSUES. DAWN/DUSK SOLUBLE SUGARS IN GUARD CELL ENRICHED EPIDERMAL PEEL TISSUE (PANEL A AND B). PANEL C, DIURNAL GUARD CELL STARCH GRANULE AREA OF *K. BLOSSFELDIANA* YOUNG LEAVES (RED POINTS, 10TH LEAF PAIR FROM BOTTOM), INTERMEDIATE LEAVES (GREEN POINTS, 4TH LEAF PAIR FROM BOTTOM), AND MATURE LEAVES (BLUE POINTS, 2ND LEAF FROM BOTTOM). DAWN/DUSK GUARD CELL STARCH GRANULE AREA OF *K. FEDTSCHENKOI* WILT TYPE AND *PEPC1.1* LEAVES. *K. BLOSSFELDIANA* PLANTS WERE SAMPLED AT 90 DAYS AFTER PROPAGATION, *K. FEDTSCHENKOI* PLANTS WERE SAMPLED AT 120 DAYS AFTER PROPAGATION. PLANTS GROWN IN 12HR/12HR DAY/NIGHT CYCLES. DARK SHADED AREA REPRESENTS NIGHT.

STATISTICAL ANALYSES WERE PERFORMED USING TWO-WAY ANOVA, SIGNIFICANT DIFFERENCES ($P < 0.05$) ARE INDICATED BY DIFFERENT LOWERCASE LETTERS. 104

FIGURE 3.4 DIEI STOMATAL CONDUCTANCE RESPONSES TO REDUCED $[CO_2]$ IN *K. BLOSSFELDIANA* YOUNG LEAVES (RED POINTS, 10TH LEAF PAIR FROM BOTTOM) AND MATURE LEAVES (BLUE POINTS, 2ND LEAF FROM BOTTOM) BETWEEN 60-90 DAYS AFTER PROPAGATION (PANELS A AND C) AND WILD TYPE *K. FEDTSCHENKOI* LEAVES (BLUE POINTS) AND *PEPC1.1* LEAVES (RED POINTS) BETWEEN 100-120 DAYS AFTER PROPAGATION (PANELS B AND D). LOW CO_2 STOMATAL RESPONSE ASSAY (PANELS A AND B, $MOL\ H_2O\ M^{-1}\ S^{-1}$). PLANTS WERE ASSAYED AT 6 TIMEPOINTS (2HRS, 6HRS, 10HRS FROM DAWN; AND 3 HRS, 6 HRS, 10 HRS FROM DUSK). FOR EACH TIMEPOINT CO_2 WAS HELD AT LOW CO_2 ($70\ \mu MOL\ MOL^{-1}$, OPEN POINTS) FOR 30 MINUTES FOLLOWED BY A RETURN TO AMBIENT ($400\ \mu MOL\ MOL^{-1}\ CO_2$, CLOSED POINTS) FOR 30 MINUTES, WITH MEASUREMENTS TAKEN EVERY MINUTE. DIEI STOMATAL CONDUCTANCE (PANELS C AND D) OF LEAVES HELD AT AMBIENT ($400\ \mu MOL\ MOL^{-1}\ CO_2$, CLOSED POINTS) FOR 24 HRS OR LOW CO_2 ($70\ \mu MOL\ MOL^{-1}$, OPEN POINTS), MEASUREMENTS TAKEN EVERY 15 MINUTES. FOR EACH GRAPH POINTS REPRESENT THE MEAN OF THREE REPEATS AND THE SHADED INTERVAL \pm SEM. 106

FIGURE 3.5 *K. BLOSSFELDIANA* AGE SPECIFIC LOW CO_2 RESPONSE STOMATAL KINETICS. *K. BLOSSFELDIANA* YOUNG LEAVES (RED BARS, 10TH LEAF PAIR FROM BOTTOM) AND MATURE LEAVES (BLUE BARS, 2ND LEAF FROM BOTTOM) ASSAYED AT 6 TIMEPOINTS (2 HRS, 6 HRS, 10 HRS FROM DAWN; AND 3 HRS, 6 HRS, 10 HRS FROM DUSK). FOR EACH TIMEPOINT CO_2 WAS HELD AT LOW CO_2 ($50\ \mu MOL$) FOR 30 MINUTES FOLLOWED BY A RETURN TO AMBIENT ($400\ \mu MOL\ CO_2$) FOR 30 MINUTES. A) MEAN INCREASE IN STOMATAL CONDUCTANCE OVER 30 MINUTES IN RESPONSE TO REDUCED CO_2 . B) TOTAL RESPONSE INTEGRATED OVER 60-MINUTE PERIOD. C) MAXIMUM OPENING RATE OF RESPONSE TO REDUCED CO_2 . D) MAXIMUM CLOSING RATE OF RESPONSE TO RETURN TO AMBIENT REDUCED CO_2 . ALL VALUES ARE MEANS OF THREE REPLICATES \pm SEM. DIFFERENT LETTERS REPRESENT A SIGNIFICANT DIFFERENCE (POST HOC TUKEY HSD TEST, $P < 0.05$). 109

FIGURE 3.6 *K. FEDTSCHENKOI* GENOTYPE SPECIFIC LOW CO_2 RESPONSE STOMATAL KINETICS OF WILD TYPE *K. FEDTSCHENKOI* LEAVES (BLUE POINTS) AND *PEPC1.1* LEAVES (RED POINTS) BETWEEN 90-120 DAYS AFTER PROPAGATION) ASSAYED AT 6 TIMEPOINTS (2 HRS, 6 HRS, 10 HRS FROM DAWN; AND 3 HRS, 6 HRS, 10 HRS FROM DUSK). FOR EACH TIMEPOINT CO_2 WAS HELD AT LOW CO_2 ($50\ \mu MOL$) FOR 30 MINUTES FOLLOWED BY A RETURN TO AMBIENT ($400\ \mu MOL\ CO_2$) FOR 30 MINUTES. A) MEAN INCREASE IN STOMATAL CONDUCTANCE OVER 30 MINUTES IN RESPONSE TO REDUCED CO_2 . B) TOTAL RESPONSE INTEGRATED OVER 60-MINUTE PERIOD. C) MAXIMUM OPENING RATE OF RESPONSE TO REDUCED CO_2 . D) MAXIMUM CLOSING RATE OF RESPONSE TO RETURN TO AMBIENT REDUCED CO_2 . ALL VALUES ARE MEANS OF THREE REPLICATES \pm SEM. DIFFERENT LETTERS REPRESENT A SIGNIFICANT DIFFERENCE (POST HOC TUKEY HSD TEST, $P < 0.05$). 110

FIGURE 3.7 *K. FEDTSCHENKOI* (PANELS A AND B) OR *K. BLOSSFELDIANA* (PANELS C AND D) STOMATAL RESPONSES TO REDUCED CO_2 AFTER 24 HRS OF AMBIENT ($400\ \mu MOL\ MOL^{-1}$ BLUE POINTS) OR REDUCED CO_2 ($70\ \mu MOL\ MOL^{-1}$ RED POINTS). SINGLE LEAVES WERE HELD AT $70\ \mu MOL\ MOL^{-1}\ CO_2$ IN A LICOR-6400XT CHAMBER OR KEPT AT AMBIENT $400\ \mu MOL\ MOL^{-1}\ CO_2$ AND ASSAYED. *K. FEDTSCHENKOI* WILD TYPE (PANEL A) AND *K. FEDTSCHENKOI PEPC1* MUTANT LEAVES (PANEL B) AND *K. BLOSSFELDIANA* YOUNG

LEAVES (LEFT, PANEL C) AND MATURE LEAVES (RIGHT, PANEL D) WERE ASSAYED AT 6 TIMEPOINTS (2HRS, 6HRS, 10 HRS FROM DAWN; AND 3 HRS, 6 HRS, 10 HRS FROM DUSK). THE CO₂ CONCENTRATION OF THE PREVIOUS 24 HRS WAS DENOTED BY BLUE POINTS (400 μMOL CO₂) OR RED POINTS (70 μMOL CO₂). FOR EACH TIMEPOINT CO₂ WAS HELD AT LOW CO₂ (70 μMOL CO₂, OPEN POINTS) FOR 30 MINUTES FOLLOWED BY A RETURN TO AMBIENT (400 μMOL CO₂, CLOSED POINTS) FOR 30 MINUTES, WITH MEASUREMENTS TAKEN EVERY MINUTE. FOR EACH GRAPH POINTS REPRESENT THE MEAN OF THREE REPEATS AND THE SHADED INTERVAL ± SEM. 114

FIGURE 3.8 IMPACT OF GROWING *K. BLOSSFELDIANA* AT REDUCED LIGHT INTENSITY ON AGE SPECIFIC PHOTOSYNTHETIC AND STOMATAL RESPONSES. PLANTS WERE GROWN AT REDUCED OR AMBIENT LIGHT (50 μMOL M⁻² S⁻¹, FILLED POINTS, OR 190 μMOL M⁻² S⁻¹, EMPTY POINTS). DIURNAL NET CO₂ ASSIMILATION (PANEL A, μMOL CO₂ M⁻¹ S⁻¹) AND STOMATAL CONDUCTANCE STOMATAL (PANEL B, MOL H₂O M⁻¹ S⁻¹) OF *K. BLOSSFELDIANA* YOUNG LEAVES (RED POINTS, 10TH LEAF PAIR FROM BOTTOM) AND MATURE LEAVES (BLUE POINTS, 2ND LEAF FROM BOTTOM) BETWEEN 60-90 DAYS AFTER PROPAGATION. PLANTS GROWN IN 12HR/12HR DAY/NIGHT CYCLES. DARK SHADED AREA REPRESENTS NIGHT. LOW CO₂ STOMATAL RESPONSE ASSAY (PANEL C AND D, MOL H₂O M⁻¹ S⁻¹). PLANTS FROM THE DIURNAL EXPERIMENT WERE ASSAYED AT 6 TIMEPOINTS (2HRS, 6HRS, 10HRS FROM DAWN; AND 3 HRS, 6 HRS, 10 HRS FROM DUSK). YOUNG LEAVES (LEFT, PANEL C) AND MATURE LEAVES (RIGHT, PANEL D) WERE COMPARED. LOW CO₂ ASSAYS WERE CARRIED OUT AT THE SAME RESPECTIVE LIGHT INTENSITIES 50 μMOL M⁻² S⁻¹ (RED POINTS) OR 190 μMOL M⁻² S⁻¹ (BLUE POINTS) AS THE DIURNAL EXPERIMENT. FOR DAY TIMEPOINTS A THIRD LIGHT CONDITION WAS USED WERE PLANTS GROWN AT 50 μMOL M⁻² S⁻¹ LIGHT AND THEN RECEIVED 190 μMOL M⁻² S⁻¹ LIGHT FOR THE DURATION OF EACH TIMEPOINT (YELLOW POINTS). FOR EACH TIMEPOINT CO₂ WAS HELD AT LOW CO₂ (50 μMOL, OPEN POINTS) FOR 30 MINUTES FOLLOWED BY A RETURN TO AMBIENT (400 μMOL CO₂, CLOSED POINTS) FOR 30 MINUTES, WITH MEASUREMENTS TAKEN EVERY MINUTE. FOR EACH GRAPH POINTS REPRESENT THE MEAN OF THREE REPEATS AND THE SHADED INTERVAL ± SEM. THE DARK BLUE LINE ON THE CO₂ UPTAKE GRAPHS EQUALS ZERO. 116

FIGURE 4.1 *K. BLOSSFELDIANA* COMPUTATIONAL GENOME SIZE AND PLOIDY ESTIMATES. LEFT PANEL, K-MER GRAPH AND FITTED MODELS GENERATED BY GENOMESCOPE 2 (VURTURE ET AL., 2017) USING K-MER FREQUENCIES COUNTED BY JELLYFISH 2.3.0 (MARÇAIS & KINGSFORD, 2011) USING ILLUMINA SHORT READS. RIGHT PANEL, SMUDGE PLOT 0.2.5 (RANALLO-BENAVIDEZ ET AL., 2020) GENERATED ESTIMATE OF GENOME PLOIDY. 133

FIGURE 4.2 THE GENOME OF *K. BLOSSFELDIANA*, SCAFFOLDED INTO 18 CHROMOSOME SCALE PSEUDOMOLECULES (377 MB) AND 155 SMALLER SCAFFOLDS (NOT SHOWN, 268 MB) USING THE *KALANCHOE LAXIFLORA* GENOME (PHYTOZOME). *K. BLOSSFELDIANA* IS THOUGHT TO HAVE 17 OR 18 CHROMOSOMES PER HAPLOTYPE. DENSITY OF GENES UP-REGULATED (RED, OUTWARD) OR DOWN-REGULATED (BLUE, INWARD) IN THE MATURE CAM *K. BLOSSFELDIANA* LEAVES (3RD LEAF PAIR FROM THE BOTTOM) COMPARED TO THE YOUNG C₃ *K. BLOSSFELDIANA* LEAVES (9TH LEAF PAIR FROM THE BOTTOM). INNER IMAGE IS OF *K. BLOSSFELDIANA*. 134

FIGURE 4.3 *K. BLOSSFELDIANA* GENOME CONTENT. GENOME COMPLETENESS WAS ASSESSED USING BUSCO WITH THE EMBRYOPHYTE ODB10 DATABASE OF SINGLE COPY GENES (A), SHOWING PERCENTAGE OF COMPLETE (C) PRESENT IN SINGLE COPIES (S) OR DUPLICATED (D), FRAGMENTED (F) OR MISSING (M) GENES DETECTED. PROPORTIONS OF REPETITIVE ELEMENTS DETECTED WITHIN THE *K. BLOSSFELDIANA* GENOME (B). 136

FIGURE 4.4 ANNOTATED FEATURES OF THE *KALANCHOE BLOSSFELDIANA* CHLOROPLAST GENOME. GENES TRANSCRIBED ARE DISPLAYED ON THE OUTERING, ON THE INSIDE IF TRANSCRIBED CLOCKWISE OR OUTSIDE IF COUNTER CLOCKWISE. THE CHLOROPLASTIC GENOME IS DIVIDED INTO A LARGE SINGLE COPY REGION, A SMALL SINGLE COPY REGION AND A PAIR OF INVERTED REPEAT REGIONS. THE INTERTRACK CONVEYS GC CONTENT. THE ANNOTATION AND DIAGRAM WAS PRODUCED USING GESEQ (TILLICH ET AL., 2017). 137

FIGURE 4.5 THE PHYLOGENETIC POSITION OF *KALANCHOE BLOSSFELDIANA*. WHOLE CHLOROPLAST GENOME SEQUENCES FROM 79 SPECIES ACROSS THE ORDER SAXIFRAGALES WERE ALIGNED AND RECONSTRUCTED INTO A PHYLOGENETIC TREE WITH A FOCUS ON THE CRASSULACEAE FAMILY, SPECIES FROM THE HALORAGACEAE FAMILY WERE USED AS OUTGROUPS. WHOLE CHLOROPLAST GENOME SEQUENCES WERE ALIGNED USING MAFFT 7.505 (KATO & STANDLEY, 2013). IQ-TREE 2.2.0.3 (MINH ET AL., 2020) WAS USED TO CONSTRUCT A PHYLOGENETIC TREE USING MAXIMUM LIKELIHOOD, WITH 1000 ULTRAFAST BOOTSTRAP REPLICATES (THI HOANG ET AL., 2017), WITH NODE LABELS REPRESENTING % BOOTSTRAP SUPPORT. 140

FIGURE 4.6 CHANGE IN TRANSCRIPT ABUNDANCES BETWEEN MATURE (3RD LEAF PAIR FROM THE BOTTOM) AND YOUNG *KALANCHOE BLOSSFELDIANA* LEAVES (9TH LEAF PAIR FROM THE BOTTOM) SAMPLED AT DUSK 90 DAYS AFTER PROPAGATION. ABBREVIATIONS: *PPDK* (PYRUVATE ORTHOPHOSPHATE DIKINASE), *RBCS* (RIBULOSE BISPHOSPHATE CARBOXYLASE SMALL CHAIN), *DI21* (DROUGHT INDUCED 21). 141

FIGURE 4.7 CHANGES IN TRANSCRIPT ABUNDANCE OF KEY GENES INVOLVED IN CAM IN THE MATURE CAM *KALANCHOE BLOSSFELDIANA* LEAVES COMPARED TO YOUNG C₃ LEAVES AT DUSK (PANEL A). UPREGULATED GENES (RED), DOWNREGULATED GENES (BLUE) AND GENES WITH NO CHANGE IN EXPRESSION (WHITE) ARE SHOWN IN ITALICS. BOLD LINES INDICATE THE UPREGULATION OF THE PHOSPHOROLYTIC STARCH DEGRADATION PATHWAY IN THE MATURE LEAVES. GO-TERM ENRICHMENT FOR TOP 100 GENES UPREGULATED (PANEL B) OR DOWNREGULATED (PANEL C) COMPARED BETWEEN MATURE (3RD LEAF PAIR FROM THE BOTTOM) AND YOUNG *KALANCHOE BLOSSFELDIANA* LEAVES (9TH LEAF PAIR FROM THE BOTTOM) SAMPLED AT DUSK. ABBREVIATIONS SHOWN INCLUDE: PHOSPHOGLYCEROMUTASE (PGLYM); TONOPLAST DICARBOXYLATE TRANSPORTER (TDT); ALUMINIUM ACTIVATED MALATE TRANSPORTER (ALMT);BILE ACID SODIUM SYMPORTER 2 (BASS2); DEBRANCHING ENZYME (DBE); GLUCOSE-1-PHOSPHATE (G1P);GLUCOSE-6-PHOSPHATE (G6P); MALATE DEHYDROGENASE (MDH); NAD(P)-DEPENDENT MALIC ENZYME (NAD(P)-ME); SODIUM HYDROGEN ANTIPOINTER 1 (NHD1); OXALOACETATE (OAA); PHOSPHOENOLPYRUVATE (PEP); PHOSPHOENOLPYRUVATE CARBOXYLASE (PEPC); PHOSPHOGLYCERATE (PGA); PYRUVATE PHOSPHATE DIKINASE (PPDK); PPK REGULATORY PROTEIN (PPDK-RP); PPT, PHOSPHOENOLPYRUVATE PHOSPHATE TRANSLOCATOR; TRIOSEPHOSPHATE/PHOSPHATE TRANSLOCATOR (TPT); AMY3 (A-AMYLASE 3); BAM1 (B-AMYLASE 1); BAM3 (B-AMYLASE 3);

PHOSPHOGLUCOMUTASE (PGM);BCA5 (B-CARBONIC ANHYDRASE 1); PPCK (PHOSPHOENOLPYRUVATE CARBOXYLASE KINASE); DPE1 (CHLOROPLASTIC DISPROPORTIONATING ENZYME); PHS1 (CHLOROPLASTIC A-GLUCAN PHOSPHORYLASE); CYTOSOLIC DISPROPORTIONATING ENZYME (DPE2); MEX1 (MALTOSE TRANSPORTER); PGLCT (PLASTIDIC GLUCOSE TRANSPORTER), GPT1 (GLUCOSE PHOSPHATE TRANSLOCATOR 1); AND GPT2 (GLUCOSE PHOSPHATE TRANSLOCATOR 2). 142

FIGURE 4.8 GO TERM ENRICHMENT OF GENES BOTH UPREGULATED IN MATURE CAM *K. BLOSSFELDIANA* LEAVES AT DUSK AND EPIDERMAL PEELS IN BOTH TRANSCRIPT (PANEL A, JAMES HARTWELL, UNPUBLISHED) AND PROTEIN (PANEL B, ABRAHAM ET AL., 2020) ABUNDANCE FROM CONSTITUTIVE CAM *K. FEDTSCHENKOI* LEAVES. UPREGULATION OF GENES IN THE EPIDERMAL PEELS WERE CALCULATED AS MEANS OF EXPRESSION OVER THE DIEL PERIODS. LOWER SECTION, DIEL TISSUE SPECIFIC TRANSCRIPT EXPRESSION OF KEY GENES IMPLICATED IN CAM STOMATAL REGULATION (LEFT) AND GUARD CELL METABOLISM (RIGHT) IN EPIDERMAL (RED CIRCLES) OR MESOPHYLL (BLUE CIRCLES) TISSUE IN THE CONSTITUTIVE CAM IN *K. FEDTSCHENKOI* (FROM JAMES HARTWELL, UNPUBLISHED). TISSUES SAMPLED EVERY 2HRS FROM RESPECTIVE LEAF PARTS OVER A 12HR NIGHT/12HR DAY DIEL CYCLE. 151

FIGURE 5.1 ROADMAP FOR THE FUTURE OF CAM RESEARCH AND ENGINEERING CAM INTO C₃ SPECIES 165

List of tables

TABLE 1. <i>K. BLOSSFELDIANA</i> GENOME STATISTICS	135
TABLE 2 CORE CAM GENES UP REGULATED IN MATURE <i>K. BLOSSFELDIANA</i> LEAVES AT DUSK.	143
TABLE 3 CHANGES IN TCA CYCLE GENES IN MATURE <i>K. BLOSSFELDIANA</i> LEAVES AT DUSK.	146
TABLE 4. STOMATAL GENES UPREGULATED IN MATURE <i>K. BLOSSFELDIANA</i> LEAVES AT DUSK AND HOMOLOGOUS TO GENES UPREGULATED IN BOTH TRANSCRIPT (JAMES HARTWELL, UNPUBLISHED) AND PROTEIN (ABRAHAM ET AL., 2020) ABUNDANCE IN <i>K. FEDTSCHENKOI</i> GUARD CELL ENRICHED EPIDERMAL PEELS, APART FROM <i>CIPK5</i> , <i>MPK19</i> , <i>SUS3</i> THAT WERE DETECTED ONLY IN THE TRANSCRIPTOME.	150

Abbreviations

ABCB	ATP-binding cassette transporter
ABI	ABA Insensitive
ADP	Adenosine diphosphate
AGPase	ADP Glucose pyrophosphorylase
AHA	Proton H ⁺ -ATPase
ALMT	Aluminium-activated malate transporter
AMY	α -amylase
ANOVA	Analysis of variance
APS	Ammonium persulfate
ATP	Adenosine triphosphate
BAM	β -amylase
BASS2	bile acid sodium symporter 2
BCA	β -carbonic anhydrase
Bicine	N, N-Bis (2-hydroxyethyl) glycine
BLUS1	Blue light signalling 1
C₃	C ₃ carbon fixation pathway with all CO ₂ fixed by Rubisco.
C₄	C ₄ carbon fixation pathway with primary CO ₂ fixation by PEPC to form a C ₄ acid.
CA	Carbonic anhydrase

CaCl₂	Calcium chloride
CAM	Crassulacean acid metabolism
CBC	Calvin–Benson cycle
C_i	Internal CO ₂ concentration
Cl⁻	Chloride
CO₂	Carbon dioxide
cTPs	Chloroplastic transit peptides
cwINV	cell wall invertase
DBE	Debranching enzyme
DHAP	Dihydroxyacetone phosphate
DNA	Deoxyribonucleic acid
DPE	Disproportionating enzyme
DPE1	chloroplastic disproportionating enzyme
DPE2	cytosolic disproportionating enzyme
DTT	Dithiothreitol
EDTA	Ethylenediaminetetraacetic acid
EGTA	Egtazic acid
FPKM	Fragments per kilobase of exon model per million reads mapped
Fru6P	Fructose 6-phosphate
FUM	fumarase

G1P	glucose-1-phosphate
G6P	glucose-6-phosphate
G6PDH	Glucose 6-phosphate dehydrogenase
GBSS	Granule-bound starch synthase
Glc	Glucose
Glc1P	Glucose 1-phosphate
Glc6P	Glucose 6-phosphate
GLCT	Glucose transporter
GPT	Glucose phosphate translocator
g_s	Stomatal conductance
GWD	Glucan water dikinase
HCl	Hydrochloric acid
HCO_3^-	Bicarbonate
HEPES	4-(2-hydroxyethyl)-1-piperazineethanesulfonic acid
HT1	High Leaf Temperature 1
HXK	Hexokinase
INV	Invertase
IPCC	Intergovernmental panel on climate change
ISA	Isoamylase
K^+	Potassium

KI	Potassium iodide
LSF	Like starch excess four
Mal	Malate
MDH	Malate dehydrogenase
MEX	Maltose exporter
MgCl₂	Magnesium chloride
MPK	Mitogen-Activated Protein Kinase
NAD	Nicotinamide adenine dinucleotide
NAD-MDH	Nicotinamide dinucleotide malate dehydrogenase
NAD-ME	NAD-malic enzyme
NADP	Nicotinamide adenine dinucleotide phosphate
NADP-ME	NADP-dependent malic enzyme
NaOH	Sodium hydroxide
NHD1	sodium hydrogen antiporter 1
NO₃	Nitrate
OAA	oxaloacetate
OST1	Open stomata 1
PEG	Polyethylene glycol
PEP	Phosphoenolpyruvate

PEPC	Phosphoenolpyruvate carboxylase
PEPCK	PEP carboxykinase
PFK	Phosphofructokinase
PGA	phosphoglycerate
PGI	Phosphoglucose isomerase
PGlyM	Phosphoglyceromutase
PGM	Phosphoglucomutase
PHOT	Phototropin
PHS	α -glucan phosphorylase
PHS1	chloroplastic α -glucan phosphorylase
Pi	Inorganic phosphate
PIP	Plasma Membrane Intrinsic Protein
PK	Pyruvate kinase
PPCK	Phosphoenolpyruvate carboxylase kinase
PPDK	Pyruvate phosphate dikinase
PPDK-RP	PPDK regulatory protein
PPFD	Photosynthetic photon flux density
PPi	Inorganic pyrophosphate
	Phosphoenolpyruvate phosphate
PPT	translocator
PWD	Phosphoglucan water dikinase

QUAC1	Quick-Activating Anion Channel 1
RNA	Ribonucleic acid
RNAi	RNA interference
RT-qPCR	Real time quantitative PCR
Rubisco	Ribulose-1,5-bisphosphate carboxylase/oxygenase
SDS- PAGE	Sodium dodecyl sulphate polyacrylamide gel electrophoresis
SEX4	Starch excess 4
SLAC1	Slow Anion Channel 1
SPP	Sucrose phosphatase
SS	Starch synthase
STP	Sugar Transport Protein
SUCs	Sucrose transporters
SUS	Sucrose synthase
SWEETs	Sugar Will Eventually be Exported Transporters
TCA	Tricarboxylic acid
TDT	tonoplast dicarboxylate transporter
TEMED	Tetramethyl ethylenediamine
TP	Triose phosphate
TPT	Triose phosphate translocator

Tris	Tris aminomethane
UDPG	Uridine diphosphate glucose
VPD	Vapour-pressure deficit
WT	Wild type
WUE	Water Use Efficiency

Chapter 1. General Introduction

1.1 Climate and CAM

The combined effects of a steadily rising population and climate change are major threats to global food security. Climate change will bring about a multitude of problems that will challenge modern agriculture by reducing yields and arable land including, and certainly not limited to, drought and desertification, flooding and sea level rise, disruption of plant-animal interactions and altered climate patterns (IPCC, 2013). This reduction of food production capacity coupled with a rising demand for food is likely to challenge the foundations of modern civilisation, with recent research suggesting that climate change-driven drought may have contributed to the early stages of the Syrian civil war (Kelley et al., 2015). An IPCC report stated vast changes in economic model, industry and society are needed to tackle greenhouse gas emissions (Shukla et al., 2022). The past few years have had many widespread and sustained climatic anomalies, where temperatures or precipitation were outside normal expected levels. These conditions have had severe and sustained negative effects on growth conditions. For instance in the first ten days of August 2022 47% of Europe was in soil moisture deficit, leading to a substantial reduction in crop yields, with grain maize, soybeans, and sunflowers most effected and satellite observed reductions in photosynthesis in key areas effected by drought (Toreti et al., 2022).

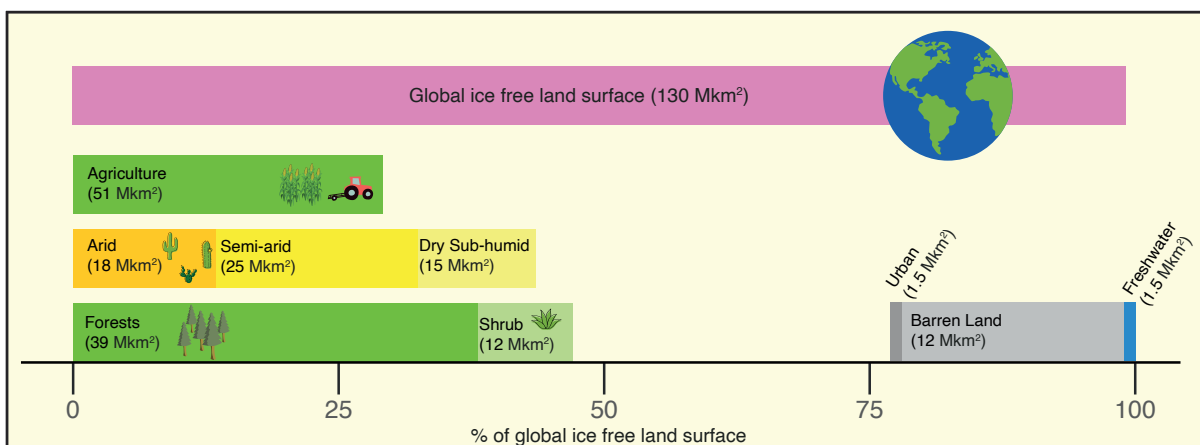


Figure 1.1 An overview of global land usage, highlighting the area of drylands (arid, semi-arid and dry sub-humid lands that make up 39.7% of global land mass. Adapted from UNEP (2012).

With this in mind there is a clear need for major sustained efforts to develop methods to improve food production capacity. This could be achieved by improving crop traits to improve yields and resilience to weather extremes on arable lands; or by engineering plants to grow in non-arable lands. Dry and arid lands that would not traditionally be considered arable make up ~40% of Earth's land area (Figure 1, UNEP, 2012), with 2.4 million ha of arable land lost in the EU 27 between 2010 and 2020 (Eurostat, 2020). These areas could be utilised by plants engineered to improve their water usage efficiency (WUE) and therefore their resilience to low water conditions.

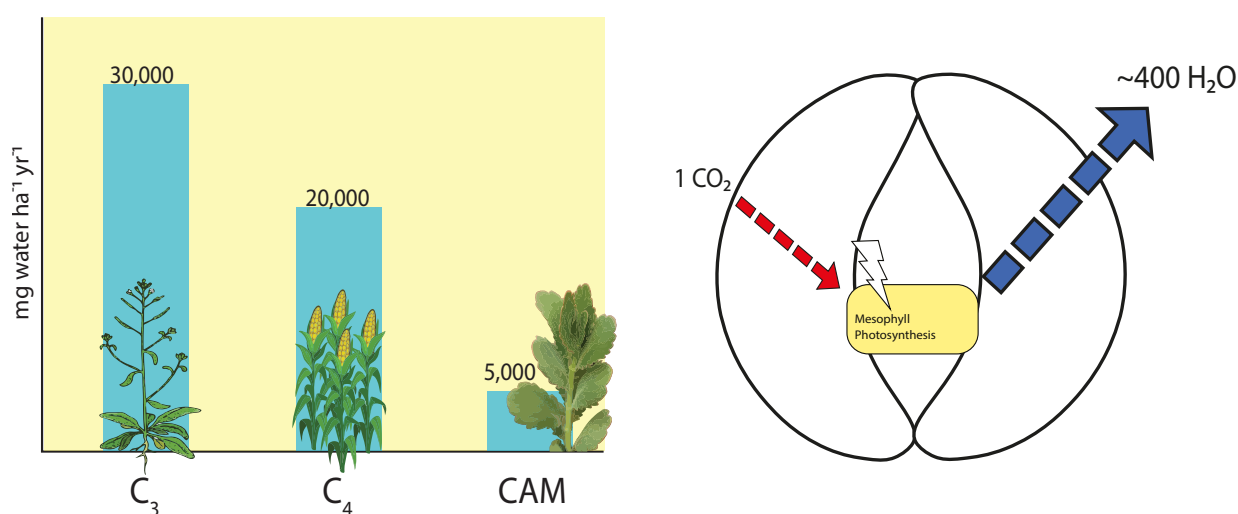


Figure 1.2 CAM plants are more water usage efficient (WUE) than C₃ or C₄ requiring significantly less water without a major impact on yield (left, Shameer et al., 2018). C₃ plants can lose up to 400 moles of H₂O per mole of CO₂ fixed (right).

Engineering crassulacean acid metabolism (CAM) into C₃ crops could be a potential method of significantly improving crop plant WUE (Borland et al., 2014), without substantially reducing productivity (Shameer et al., 2018). CAM is an alternate form of photosynthetic metabolism that confers a ~6-fold greater WUE compared to the C₃ and C₄ modes of photosynthesis (Borland et al., 2009) and makes up ~6% of land plants, see figure 2. CAM involves the nocturnal fixation of CO₂ (as HCO₃⁻) by phosphoenolpyruvate carboxylate (PEPC) into a C₄ acid, which is stored in the vacuole as malic acid until subsequent daytime decarboxylation and re-carboxylation into the Calvin cycle by Ribulose-1,5-bisphosphate carboxylase (RUBISCO). CAM plants are therefore able to shift atmospheric net CO₂ uptake to the night, allowing nocturnal stomatal opening, the inverse of C₃ and C₄ plants, to occur. By moving gas exchange and

stomatal opening to the night CAM plants reduce water losses by curtailing day-time evapotranspiration. The additional energetic demands of CAM are offset by the advantage of the carbon concentrating effect of malate decarboxylation during the day behind close stomata (Shameer et al., 2018). Thus, CAM provides an improved WUE over C_3 while not substantially affecting plant productivity.

CAM plants are highly resilient to long periods of drought and increased temperature; this makes them ideal candidates for growth on lands that are less suitable for drought sensitive plants (Borland et al., 2015). CAM plants have the potential to tackle both the causes and the symptoms of greenhouse gas emissions, as CAM plants could be used to remove atmospheric carbon by planting campaigns in drought prone areas. Efforts to remove atmospheric carbon by reforestation have gained significant traction in recent years, e.g. the One Trillion Trees project announced by World Economic Forum and the Bonn Challenge to restore 860 million acres of forestland. However, many such reforestation projects have failed, suggesting a need for the use of more resilient and effective plants, and the use of transgenic plants, that sequester greater amounts of carbon are currently under development (Eckhardt et al., 2022). Lessons from the CAM pathway also could provide a route to increasing the carbon efficiencies of plants, as CAM allows them to recycle CO_2 from nocturnal respiration. Globally, plants are estimated to lose ~50 billion tons of CO_2 annually (Five times that of total human outputs) to nocturnal respiration and take up ~130 billion tons of CO_2 via photosynthesis (Jung et al., 2011).

CAM plants could also provide feedstocks for agriculture and other biological processes. There has been much recent interest in genetically transforming plants to produce key biological compounds of value, such as protein-based vaccines or compounds that are often produced via petrochemical processes (Molina-Hidalgo et al., 2021; Warzecha & Mason, 2003). CAM plants could be of use here, due to their large vacuoles which could be used to sequester high-value compounds and through their ability to grow on drought prone uncultivated land, allowing these technologies to grow without displacing drought sensitive plants from cultivated land. The crisis in biodiversity, which is often overlooked, where anthropogenic activities have vastly reduced species number across the world, will also put pressure on land usage (Davison et al., 2021), with a need to shift land usage to allow native species to inhabit suitable land.

1.2 CAM Overview - Everything you need to know about CAM but were afraid to ask

For CAM to emerge from C_3 photosynthesis, it is believed that substantial rewiring and retiming of core metabolism is required (Borland & Dodd, 2002; Shameer et al., 2018). It is thought that CAM evolved from C_3 photosynthesis primarily by the recruitment of enzymes and pathways that are already present in C_3 plants (Borland et al., 2014; Lim et al., 2019). Thus, there is a core assumption to CAM engineering that most of the changes between C_3 and CAM are due to differences in the regulation of core metabolic enzyme expression and activity rather than an entirely novel system of enzymes and pathways. CAM can be split into a number of core 'modules' for the purpose of engineering CAM into non-CAM plants. This section explains the current knowledge on the workings of CAM by dividing CAM into its core modules, and is broadly split into two sections: firstly, CAM in the mesophyll, the site of photosynthesis and CAM; and secondly with greater focus, the changes that occur to guard cells and stomatal regulation in CAM. This section will also highlight some of the remaining questions that will need to be addressed before being able to successfully engineer CAM into C_3 plants.

1.2.1 PEP Regeneration Pathway / transitory carbon stores

CAM occurs in a cyclic manner, with carbon skeletons being cycled between nocturnal carboxylation, daytime decarboxylation, processing through the Calvin-Benson cycle and storage in transitory carbon stores which can be either starch or sugars, depending on species. These transitory carbon stores are essential in providing PEP for nocturnal carboxylation for CAM (Cushman et al., 2008). In C₃ species, mesophyll cells often accumulate starch during the day providing a sink for photoassimilates and a steady depletion overnight to supply carbon for nocturnal respiration, maintenance and growth; in a tightly controlled process that helps ensure a balance between early depletion and over investment in transitory starch (Flis et al., 2018; Santelia & Lunn, 2017).

To provide PEP for nocturnal carboxylation in CAM as much as 20% of leaf dry mass can be utilised as carbohydrates (Borland & Dodd, 2002). Starch storing CAM plants such as *Kalanchoe fedtschenkoi* (Abraham et al., 2020) and *Mesembryanthemum crystallinum* (Cushman et al., 2008) have similar patterns of mesophyll starch accumulation to that of C₃ species, with starch accumulated over the course of the day from carbon assimilated via RUBISCO. Overnight, starch is remobilised to support the regeneration of PEP for nocturnal carboxylation as well as nocturnal respiration, maintenance and growth. Other CAM species such as *Ananas comosus* supply carbon for PEP regeneration from transitory hexose sugar stores (Holtum et al., 2005). To date it is not clear why CAM species diverge in their transitory carbon stores, whether it be environmental or phylogenetic reasons. This might be important when deciding which method to use in CAM engineering.

Starch storing CAM plants have been shown to re-route starch degradation via the phosphorolytic pathway instead of the hydrolytic pathway which is used in C₃ *Arabidopsis* (Ceusters et al., 2021). In CAM, starch is broken down to form glucose-6-phosphate that is exported from the chloroplasts to ultimately regenerate PEP for the CAM cycle. CAM was impaired in *K. fedtschenkoi* α -glucan phosphorylase (*PHS1*) mutants which were unable to degrade starch via the phosphorolytic pathway (Ceusters et al., 2021). On CAM induction in the facultative species *M. crystallinum*, increased glucose-6-phosphate export from the chloroplasts was noted along with increased transcript abundance of *GLUCOSE PHOSPHATE TRANSLOCATOR* (*GPT*), thought to import/export G6P from chloroplasts (Hausler et al., 2000;

Kore-eda et al., 2013; Koreeda & Kanai, 1997; Neuhaus & Schulte, 1996). Increases in transcript abundances of genes involved in the phosphorolytic starch degradation pathway were also observed following ABA and drought-induced CAM induction in *T. triangulare* (Brilhaus et al., 2016; Maleckova et al., 2019). It has been suggested that this move to the phosphorolytic starch degradation pathway could be an effort to energetically balance the CAM cycle, as it provides cytosolic ATP during the conversion of G6P to PEP (Ceusters et al., 2021; Shameer et al., 2018). How this switch is regulated and how resultant carbon released is partitioned between nocturnal respiration, plant growth and PEP regeneration is not known. Upregulation of the enzymes in the phosphorolytic starch degradation pathway could be a key target for CAM engineering.

In both C_3 and starch storing CAM species the turnover of starch must be tightly regulated and responsive to time and the amount of carbon assimilated via photosynthesis to avoid carbon starvation by early depletion. Despite recent efforts in this area the mechanisms of starch turnover regulation are not fully understood. In C_3 *Arabidopsis* diel starch turnover is controlled in a complex process that is robust even in severely perturbed circadian clock mutants, with the suggestion that semi-autonomous oscillators along with circadian clock inputs may regulate starch turnover (Flis et al., 2018; Moraes et al., 2022). The careful and responsive regulation of starch turnover in starch storing CAM plants may help enable them to remain robust to carbon starvation in severe droughted conditions, with limited carbon assimilation. Thus, understanding the regulation of starch turnover in starch storing CAM plants is of great importance.

There are gaps in our knowledge of how photosynthetic metabolism is regulated and how the output carbon is partitioned in both C_3 and CAM plants. Carbon partitioning has been shown to change with development (Borland & Dodd, 2002), environmental conditions (Ceusters et al., 2010) and the induction of CAM, with up to 70% of leaf carbohydrate used in CAM (Haider et al., 2012). One suggested point of control in the PEP regeneration pathway in starch storing CAM species is the export of G6P from the chloroplasts via GPT 1 and 2 (Borland et al., 2016), which have been shown to have diel transcript expression patterns in *Ananas comosus* (Ming et al., 2015). In C_3 *Arabidopsis* there has been significant recent work in uncovering the role of carbohydrates in regulating both metabolism and development in C_3 plants, with various sugars and sugar sensing enzymes implicated (Fichtner & Lunn, 2021; Smith & Stitt, 2007; van

Dingenen et al., 2019), how these processes work in CAM species is yet unstudied, making it an area that will need further focus when considering targets for CAM engineering. Furthermore, CAM and especially inducible CAM could provide a good platform for studying carbohydrate partitioning with lessons applied to both photosynthetic modes.

1.2.2 ATP/energy supply for CAM

Flux balance analysis of CAM by Shameer et al. (2018) suggested CAM plants consume substantially higher amounts of ATP during both the day and the night. Most of the predicted increase in nocturnal ATP consumption was due to ATP- dependent proton pumps at both the tonoplast and plasma membrane, required to enable vacuolar malate accumulation; and the high flux through ATP consuming phosphofructokinase. This consumption was predicted to be balanced by increased ATP production over the diel period, with an increase in mitochondrial respiration across the diel period and a nocturnal increase in substrate level phosphorylation due to the high glycolytic flux required to regenerate PEP.

Recent experimental data have given support to these flux balance predictions; with transcript expression of mitochondrial genes upregulated in constitutive CAM *Agave americana* (Abraham et al., 2016) and on CAM induction in the facultative CAM *Talinum triangulare* (Brilhaus et al., 2016; Maleckova et al., 2019). Nocturnal respiratory rates were found to be higher on CAM induction by droughting in the facultative CAM species *Clusia pratensis* but reduced, as typical for a C₃ plant (Atkin & Macherel, 2009), in the obligate C₃ species *Clusia tocuchensis* (Leverett et al., unpublished). Increases in the size, number and presence of mitochondria and key mitochondrial enzymes have also been observed in some C₄ plants (Fan et al., 2022), which should also be investigated in CAM species. There is also evidence that CAM plants use pathways that are more energy efficient, for example the switch to the phosphorolytic starch degradation pathway in starch storing CAM species provides cytosolic ATP (Ceusters et al., 2021; Shameer et al., 2018). Together, there is growing evidence of the need to balance the energetic requirements of CAM with increased ATP production, and thus this will need to be a key area of future research to further the engineering of CAM into C₃ plants. Increased mitochondrial respiratory capacity is also a requirement in C₄ photosynthesis; and efforts to engineer the C₄ pathway into C₃ plants have shown that

constitutive expression of maize GOLDEN2-LIKE genes in rice could significantly increase the volume and metabolic capacity of mitochondria (Wang et al., 2017).

1.2.3 Carboxylation pathway of CAM

Central to the CAM cycle is the nocturnal carboxylation of phosphoenolpyruvate (PEP) by PEP carboxylase (PEPC) using HCO_3^- . PEPC is partially regulated by a diel pattern of transcript/protein abundance peaking in the night as shown in *A. americana* (Abraham et al., 2016) and *K. fedtschenkoi* (Abraham et al., 2020; Yang et al., 2017); and by PEPC kinase to be active primarily at night, avoiding futile cycling into malate and competition with RUBISCO during the day (Carter et al., 1991; Dodd et al., 2002).

PEPC kinase, which activates PEPC by the allosteric phosphorylation of the PEPC N-terminal, has been shown to be regulated by changes in transcript abundance (Hartwell et al., 1999), which is greater at night but can also be influenced by malate concentrations (Borland et al., 1999). PEPC activity can be influenced by malate and Glc 6-P concentration and cytosolic pH (Borland et al., 1999). Recent work in *C₃ Arabidopsis* has suggested regulation by post translational modification that links PEPC activity and sucrose concentration, via Tre6P, with increased [Tre6P] leading to increased PEPC activity and greater [malate] (Figueroa et al., 2016; O'Leary & Plaxton, 2020), however this has not been confirmed in CAM species and its exact mechanism is yet to be elucidated. The multilevel regulation of PEPC highlights the importance of understanding metabolic regulation in CAM plants, which will need to be understood to ensure proper flux through the CAM cycle.

In CAM species, the recruitment of a single PEPC isoform for CAM seems well conserved, with CAM species tending to have four to six PEPC isoforms, one of which is recruited for CAM (Cushman & Borland, 2002), though the functions of the other isoforms are not known. The *PEPC1* isoform has been shown to be essential for CAM in *K. laxiflora* (Boxall et al., 2020) and is the most abundantly expressed isoform in the mesophyll in *K. fedtschenkoi* (Abraham et al., 2020). Molecular evolution studies have identified convergent residue changes in PEPC *C₄* species (Aubry et al., 2014; Christin et al., 2007). Yang et al., (2017) identified a conserved residue change in *PEPC2* shared between CAM species *Phalaenopsis equestris* and *K. fedtschenkoi* and showed it increased PEPC activity; but this was ubiquitous across other CAM

species or present in *kfPEPC1* (Heyduk et al., 2022; Yang et al., 2017). It is unclear as to the role of *PEPC2* and if it is required for CAM, but a more efficient PEPC might be beneficial in CAM engineering efforts.

1.2.4 Malate Storage and pH regulation

The nocturnal accumulation of malate, recorded to average $\sim 10 \text{ mM h}^{-1}$ (Lüttge et al., 1981) in *Kalanchoe tubiflora* leaves, puts tremendous acidic strain on the cytosol, which is relieved by the activity of tonoplast H^+ pumps, V-ATPase and V-PPase, also energising the transport of malic acid into the vacuole (Hedrich et al., 1989; Martinoia et al., 2007). Both V-ATPase and V-PPase require energy in the form of ATP or Pi, respectively, to pump H^+ into the vacuole. V-ATPase, a multimeric protein, can be regulated transcriptionally and posttranscriptionally by phosphorylation and redox status (Hong-Hermesdorf et al., 2006; Tavakoli et al., 2001); with expression of V-ATPase seen to increase on CAM induction in *M. crystallinum* (Cushman et al., 2008). Malate can be transported into the vacuole by the *tonoplast dicarboxylate transporter (TDT)* and/or by members of the aluminium-activated malate transporter (ALMT) family (Emmerlich et al., 2003; Kovermann et al., 2007). ALMT6 was shown to be expressed at night in *K. fedtschenkoi* (Yang et al., 2017) and two ALMT isoforms were upregulated in CAM induction by drought in *Talinum triangulare* (Brilhaus et al., 2016).

Vacuolar malate storage also requires larger vacuoles with the vacuoles of CAM species using up to 95% of cell volume (Steudle et al., 1980) compared to 70-80% in C_3 species (H. Winter et al., 1993). It also appears that CAM vacuoles can withstand greater acidity than other species, with yeast vacuoles disintegrating at pH 4 (Shimada et al., 2006), whereas vacuoles in some CAM species have been reported to have a pH of 2.9 (Franco et al., 1990). It has also been suggested that some CAM plants accumulate citrate to buffer pH in the vacuole (Lüttge, 2010), and carbohydrates or even proteins could also provide extra buffering capacity. Efforts to engineer CAM will need to consider the vacuolar buffering and storage capacity of C_3 species to decide whether further capacity is needed and how to increase it.

1.2.5 Malate remobilisation and decarboxylation

During the day, malate is remobilised from the vacuole and decarboxylated by either malic enzyme (ME) or malate dehydrogenase (MDH) and PEP carboxykinase (PEPCK), depending on species (Borland et al., 2011). Members of the *Kalanchoe* genus tend to use malic enzyme (Dever et al., 2015), while Shammer et al. (2018) suggested via modelling that the PEPCK route may be more efficient.

A number of key questions remain about daytime malate remobilisation, that are well addressed by (Ceusters et al., 2021); namely which components pace the rate of vacuolar malate remobilisation to ensure a proper balance between CO₂ release and refixation and avoiding futile cycling, and how does malate remobilisation respond to changes in environmental conditions? Ceusters et al (2021) postulated that the vacuolar efflux of malate might be a key control point that triggers and regulates the rate of malate decarboxylation, highlighting this process as a key area of research for CAM engineering. The exact identity of vacuolar malate exporters are not known; *tDT* has been suggested to be involved in malate efflux out of the vacuole to drive malate decarboxylation, with greater diurnal transcript abundance in *K. fedtschenkoi* (Yang et al., 2017), it is also possible that members of the aluminium-activated malate transporter (ALMT) family could also be involved in malate efflux. Other critical questions remain as to how vacuolar malate exporters are regulated, how vacuolar H⁺ efflux occurs and how the cytosol manages pH during this period.

1.2.6 Stomatal regulation and Guard Cell metabolism in CAM

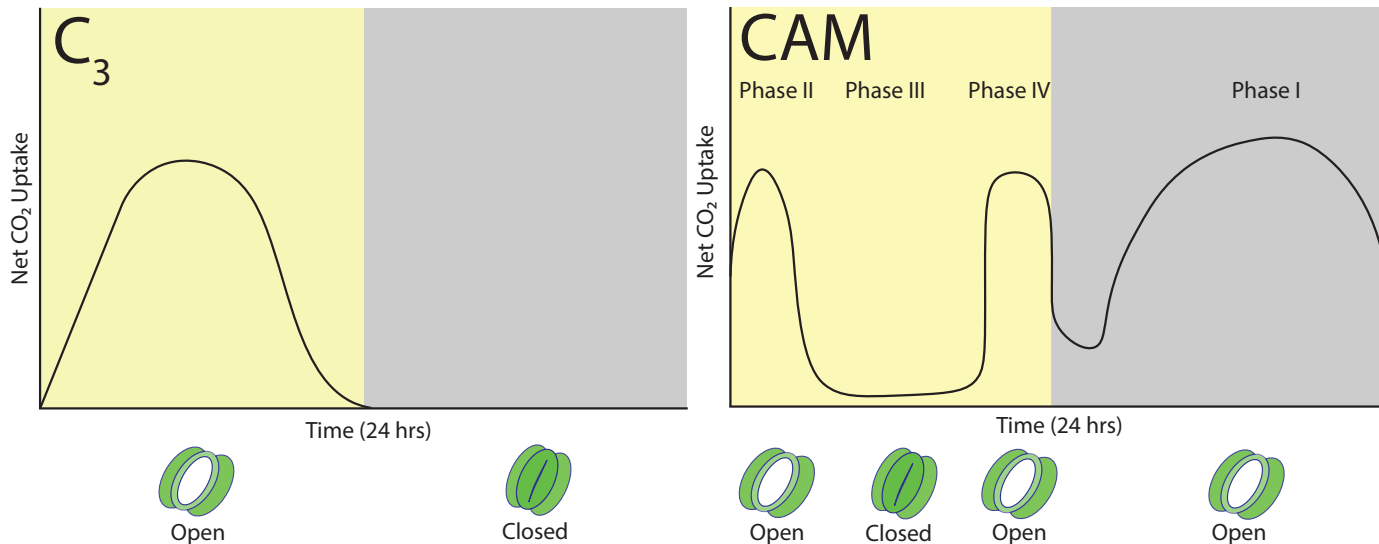


Figure 1.4 Diel CO_2 assimilation in C_3 and CAM plants, with diel pattern of stomatal conductance indicated below, adapted from Males & Griffiths (2017).

The inverted diel pattern of stomatal conductance in CAM species plays a central role in increased WUE, with CAM plants nocturnally opening their stomata and limiting diurnal opening to dusk and dawn, when conditions allow (Borland et al., 2014). Closed stomata during the day also allows CAM plants to concentrate CO_2 around RUBISCO reducing photorespiration. Despite the importance of engineering CAM stomatal behaviour in efforts to engineer this water conserving pathway into C_3 plants our understanding of how CAM stomatal physiology and guard cell metabolism differs compared to that in C_3 plants are still lacking. There are two schools of thought within CAM research – firstly that stomatal conductance will follow the changes in C_i (internal partial pressure of CO_2) due to nocturnal carboxylation and diurnal decarboxylation (Borland et al., 2014; Males & Griffiths, 2017), or secondly, that CAM guard cells fundamentally differ from C_3 guard cells in terms of their physiology, metabolism and regulation (Abraham et al. 2021; Hurtado-Castano et al. 2019). This has obvious implications for CAM engineering, and if the latter is true a sound understanding of these changes in stomatal regulation and guard cell metabolism will be needed.

The characteristic pattern of stomatal conductance in CAM species is separated into four phases: a nocturnal phase of *PEPC*-mediated carboxylation with open stomata (phase I); followed by an overlap of *PEPC* and *RUBISCO* carboxylation in the early day period with a peak in conductance (Phase II); then the main day period of malate decarboxylation and

recarboxylation by *RUBSICO* behind closed stomata (Phase III); and a final opening peak towards the end of the day alongside an overlap of *RUBSICO* and *PEPC* activity (Phase IV).

CAM is plastic and there is a diversity of strictness to the CAM pattern of stomatal conductance, with conductance in phases II and III absent in droughted or strict CAM plants. Some less strict C_3 /CAM phenotypes have also been observed with substantial day time *RUBSICO* carboxylation and nocturnal *PEPC* carboxylation.

Plant leaves are encapsulated by relatively impermeable epidermal layers punctuated by stomatal pores that account for up to 95% of leaf gas exchange in C_3 plants (Keenan et al., 2013; Lawson & Matthews, 2020). Stomatal aperture is regulated by two flanking guard cells through changes in their turgor, to control gas exchange that varies over the diel period and in response to both environmental (light, $[CO_2]$, water status and temperature) and endogenous signals (Aasamaa & Sober, 2011; Lawson & Blatt, 2014; Mott et al., 2008; K. Shimazaki et al., 2007). The development, density and size of stomata are also responsive to changes in their environment (Qu et al., 2017). Guard cells must balance the demands of reducing water loss and ensuring enough gas exchange for photosynthesis. Low stomatal conductance reduces CO_2 diffusion into the leaf and thus photosynthesis, while too much stomatal conductance will increase water loss and reduce WUE (Matthews et al., 2017). The importance of stomata is arguably even greater in CAM plants, as the CAM leaf epidermis has been shown to be less permeable to gas exchange allowing CO_2 to be concentrated around *RUBSICO* during daytime photosynthesis and preventing water loss (Leverett et al., 2022). Leaky stomata or a more gas permeable epidermis in CAM leaves would reduce the benefits of CAM as it would lead to water loss and CO_2 loss.

Changes in stomatal aperture are driven by the influx or efflux of water and osmolytes into guard cell vacuoles (Eisenach & de Angeli, 2017; Gao et al., 2005), which can increase the volume of guard cells by up to 50% (MacRobbie & Kurup, 2007). Stomatal opening is triggered by the hyperpolarisation of the guard cell plasma membrane (PM), by the action of PM H^+ ATPase driven H^+ efflux, which, in turn, activates voltage gated K^+ and other anion channels (Hedrich, 2012). The influx of potassium (K^+) and its counter ions chloride (Cl^-), nitrate (NO_3^-), and malate (Mal^{2-}) (Jezek & Blatt, 2017) into the guard cells and ultimately the vacuole drives water influx also into the guard cells and vacuole, increasing guard cell turgor and stomatal

aperture. The process occurs in reverse for stomatal closure, with K^+ and anion efflux driving water from the guard cells (Hedrich, 2012).

Our knowledge of stomatal regulation is mainly based on how these processes work in C_3 plants, with light induced diel stomatal opening. There will likely be fundamental differences in how stomatal regulation and guard cell metabolism functions in CAM plants that open stomata predominately nocturnally in the absence of light.

1.2.7 The role of C_i in linking mesophyll CAM and stomatal conductance.

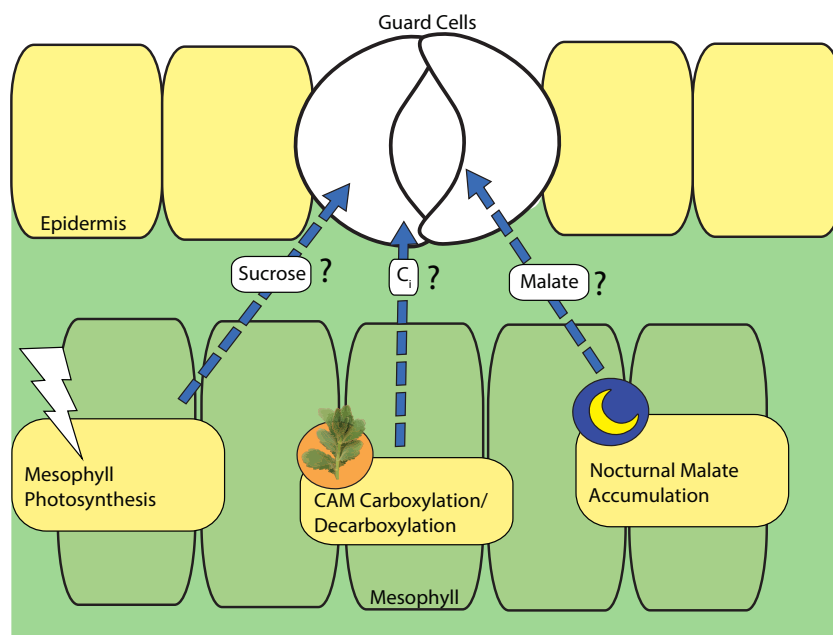


Figure 1.5 A summary of key potential links between mesophyll metabolism and guard cell regulated stomatal conductance including; photosynthetic control mediated via sucrose or other carbohydrates, malate production or usage by CAM, or changes in C_i driven by CAM

Photosynthesis and stomatal conductance are closely linked in both function and regulation, often positively correlating with each other (Buckley & Mott, 2013); and the same can be observed with net carbon assimilation in CAM plants, with high stomatal conductance occurring during nocturnal carboxylation and closure during decarboxylation. However, conductance and assimilation can be decoupled when environmental conditions vary quickly (Lawson et al., 2011; McAusland et al., 2016); and in instances of nocturnal conductance in C_3 leaves (de Dios et al., 2016; Zeppel et al., 2014). Despite ample evidence of a close link between conductance and assimilation it is still unclear what exactly links them (Buckley & Mott, 2013; Farquhar & Sharkey, 1982; Wong et al., 1979). In both C_3 and CAM plants carbon

assimilation decreases C_i which is a key signal for inducing stomatal opening. It has long been hypothesised that mesophyll cells could communicate assimilation status via changes in C_i .

There have been a number of other suggestions for links between guard cell conductance and mesophyll carbon assimilation such as red light (Gotoh et al., 2018) or a metabolic signal, such as ATP, NADPH, ribulose biphosphate (RuBP), malate or a sugar that could act upon the guard cells to respond to mesophyll photosynthesis (Fujita et al., 2013; Hedrich et al., 1994; Lee et al., 2008; Marigo et al., 1982; Tominaga et al., 2001; Zeiger & Zhu, 1998).

It has been thought that the key link between mesophyll CAM and stomatal conductance is C_i (Griffiths et al., 2007; von Caemmerer & Griffiths, 2009; Wyka et al., 2005); with nocturnal conductance driven by reduced C_i as a result of carbon assimilation at night and daytime closure driven by increased C_i due to the decarboxylation of accumulated malate, to levels reportedly as high as $10,000 \mu\text{mol mol}^{-1}$ (Cockburn et al., 1979). In the constitutive CAM species *Kalanchoe daigremontiana* and *Kalanchoe pinnata* Wyka 2005, Griffiths et al., 2007 and Von Caemmerer and Griffiths, 2009 showed strong responses to experimentally reduced atmospheric CO_2 at key points in the diel CAM cycle; and as expected no response during day time closure in phase III. Interestingly the same publications reported that this day-time closure remained and was largely unchanged even after they starved the plants of CO_2 overnight reducing acid accumulation. Transcript abundance of key elements of the CO_2 response pathway were shown to be rescheduled in a comparison between C_3 *Arabidopsis* and the constitutive CAM species *Agave americana* (Abraham et al., 2016). Together these studies suggest that there may be other, yet unexplained, mechanisms acting on CAM guard cells preventing daytime opening and maintaining a CAM-like pattern of diel conductance.

1.2.8 Guard Cell CO₂ sensing and regulation in CAM

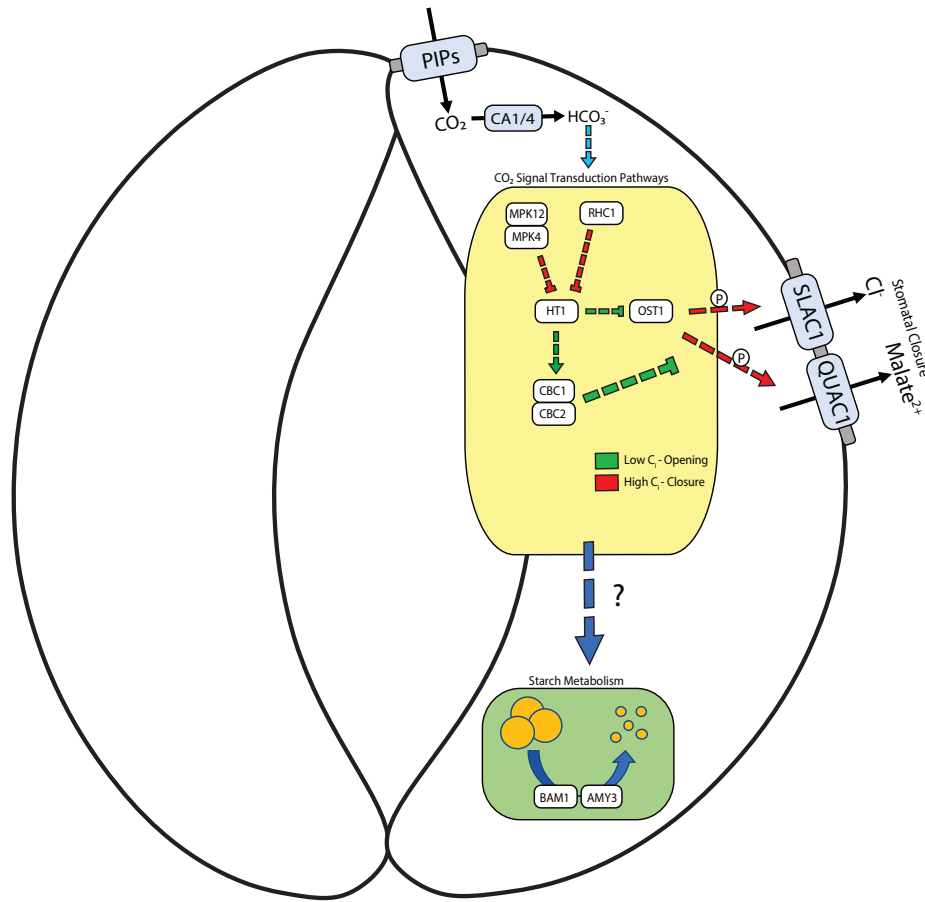


Figure 1.6 A summary of the CO₂ signalling pathways in *Arabidopsis*, adapted from (Zhang et al., 2018).

High internal CO₂ (C_i) concentration can trigger stomatal closure in both C₃ and CAM plants whilst stomatal opening is triggered by low C_i. CO₂ can be sensed in the mesophyll and guard cells, and while it is thought both contribute to stomatal regulation no CO₂ sensor has been discovered in the guard cells nor has any signal linking the guard cells and the mesophyll been identified in regard to CO₂ (Zhang et al., 2018). A guard cell CO₂ signal transduction pathway has been characterised in *Arabidopsis*, summarised in figure 1.6, with elements that are responsive to high and low C_i and shown to be important for proper stomatal CO₂ regulation. Despite having a CO₂ responsive pathway, no CO₂ sensor upstream of the pathway has been discovered (Zhang et al., 2018). *SLOW ANION CHANNEL-ASSOCIATED 1* (*SLAC1*) is a key element of guard cell closure, that upon activation exports Cl⁻ which depolarises the guard cell plasma membrane and ultimately leads to stomatal closure in response to many stomatal closure signals including increased CO₂, ABA and water stress. (Vahisalu et al., 2008; Zhang et al., 2018). The S-type ion channels appear to be towards the bottom of any CO₂ response in

the guard cells, and their activity is also regulated by the guard cell CO₂ signal transduction pathway. OPEN STOMATA 1, (*OST1*), a SnRK2 kinase, has been shown to function in high CO₂ induced closure in C₃ with mutants displaying greater stomatal conductance and impaired ability to close in response to increased CO₂ (Xue et al., 2011) by activating *SLAC1* driven Cl⁻ efflux from the guard cells resulting in plasma membrane depolarisation and ultimately stomatal closure (Geiger et al., 2009).

The photosynthetic mesophyll is likely to also affect stomatal regulation and guard cell metabolism. Photosynthesis and CO₂ assimilation will reduce C_i inducing stomatal opening, and when demand for CO₂ falls when photosynthesis and CO₂ assimilation is less active C_i can rise inducing closure (Lawson et al., 2014). Beyond this there is mounting evidence for a direct signal from the mesophyll to the guard cells conferring the status of photosynthesis or CO₂ assimilation. Much of this evidence is from experiments in which epidermal tissue containing guard cells are assayed for responsiveness to CO₂ or red/blue light with or without their corresponding mesophyll tissue. In these experiments it was observed that responses to CO₂ or red/blue light were impaired when the mesophyll was removed (Mott et al. 2008; Mcadam and Brodribb, 2012; Fujita et al., 2013)

If these signals were assimilates from photosynthesis it could also be possible that they would not only function as a signal for regulation but could also provide energy or osmolytes for stomatal opening. This idea might be supported by evidence that the mesophyll signal might be aqueous (Mott et al., 2008; Mcadam and Brodribb, 2012; Fujita et al., 2013). A candidate for such a signal could be malate, especially in CAM plants in which malate is accumulated over night by mesophyll CO₂ assimilation. Apoplastic malate has been shown to activate R-type and recently *SLAC1* (Hedrich et al., 1994; Wang et al., 2018). Questions remain as to how sensing CO₂ or mesophyll CO₂ assimilation might affect stomatal aperture, the identities of CO₂ sensors, or how this pathway might differ in CAM plants compared to C₃.

1.2.9 Blue and red light mediated stomatal and guard cell starch regulation.

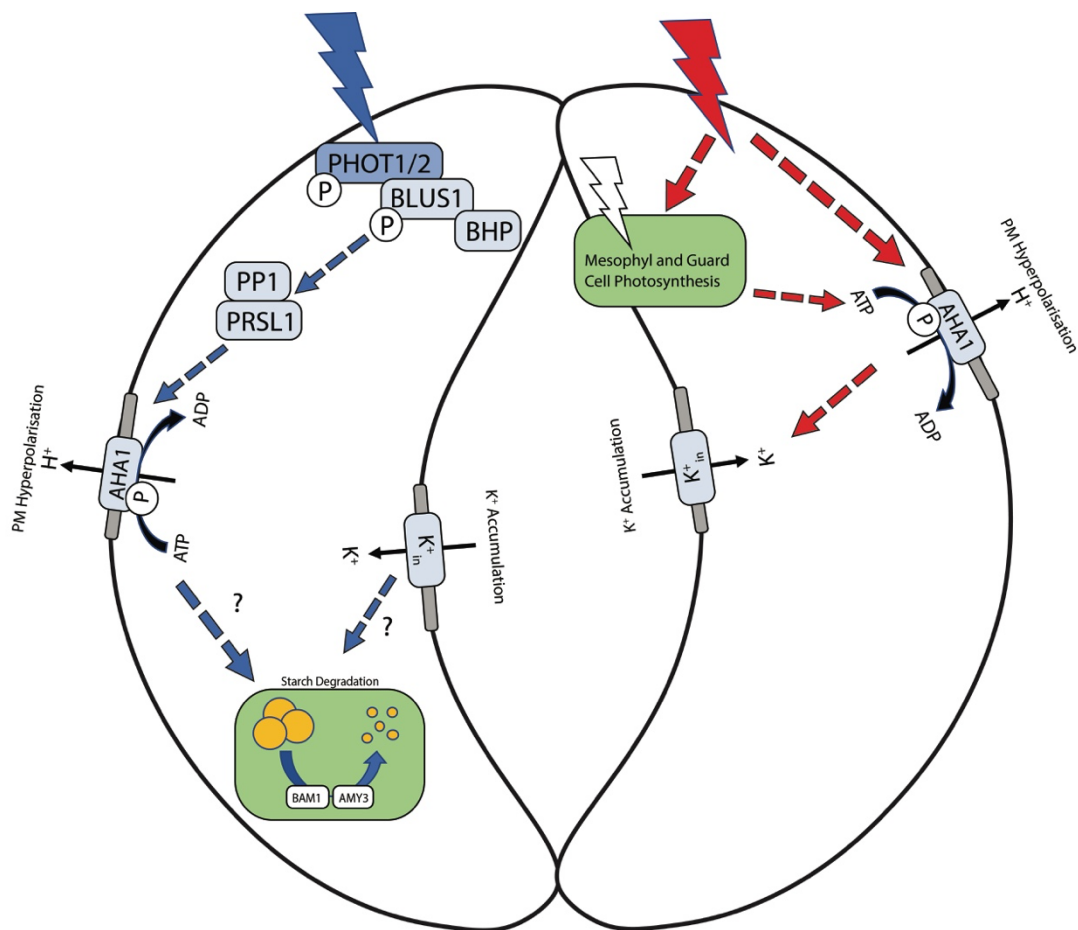


Figure 1.7 A summary of the blue and red light signalling pathways in Arabidopsis guard cells, adapted from (Inoue and Kinoshita, 2017) and (Ando and Kinoshita, 2018).

Light has long been known to induce stomatal opening in C₃ plants (Meinhard & Schnabl, 2001; Outlaw & Manchester, 1979), but its relevance to the opening of stomata in CAM plants is less clear. Red and blue light both induce stomatal opening via distinct mechanisms (summarised in figure 1.7), that both lead to the activation of plasma membrane H⁺ ATPases, the hyperpolarisation of the guard cell plasma membrane (PM), K⁺ influx and ultimately stomatal opening (Ando & Kinoshita, 2018; Inoue & Kinoshita, 2017). This process of light driven guard cell H⁺ efflux leading to stomatal opening was first described in the 1970's in *Vicia faba* (Assmann et al., 1985; Shimazaki, Iino and Zeiger, 1986) yet the pathway behind it has only been characterised over the last two decades.

Both red and blue light are required for proper day time opening of stomata, with significant reductions in stomatal conductance observed in the absence of either (Shimazaki et al., 2007). Despite distinct mechanisms, illumination by red or blue light leads to the phosphorylation of plasma membrane (PM) H⁺ ATPases (Ando & Kinoshita, 2018; Inoue & Kinoshita, 2017). The PM H⁺ ATPases are large PM spanning proteins with ten transmembrane and three cytosolic domains, that pump H⁺ across the PM using ATP. There are 11 PM H⁺ ATPase genes in *Arabidopsis* (*AHA1-AHA11*) (Haruta et al., 2010), with *AHA1* and *AHA2* shown to play a role in stomatal opening and are expressed in *Arabidopsis* guard cells (Merlot et al., 2007; Osakabe et al., 2016; Yamauchi et al., 2016). Mutants of *aha1*, *aha1-9* and *aha1-10* (Yamauchi et al., 2016; Ando and Kinoshita, 2018), show significantly impaired stomatal conductance in response to blue or red light. Conversely, *Arabidopsis AHA1* mutants that exhibit constitutive H⁺-ATPase activity show constitutively open stomata (Merlot et al., 2007). Over expression of *AHA2* specifically in *Arabidopsis* and other C₃ species guard cells has been shown to increase stomatal conductance (Wang et al., 2014; Yang et al., 2008).

The PM H⁺ ATPase is activated in response to blue and red light and phosphorylated on its penultimate C-terminal Thr, allowing the binding of a 14-3-3 protein to the C-terminal region (Inoue & Kinoshita, 2017; T. Kinoshita & Shimazaki, 1999, 2002). The PM H⁺ ATPase is also phosphorylated in residues other than the penultimate C-terminal Thr, but it is not understood what effect this has on its activity (Inoue & Kinoshita, 2017). The phosphorylation of the penultimate C-terminal Thr has also been shown to be modulated by a number of other environmental and physiological stimuli – salt, auxin, gibberellin and ABA. Of these stimuli ABA has been shown to suppress both blue and red light responsive stomatal opening and the phosphorylation of PM H⁺ ATPase (Ando & Kinoshita, 2018; Hayashi et al., 2011). Together this suggests the PM H⁺ ATPases may be a key regulatory hub in stomatal signalling, an argument that would be strengthened by examining its activation in response to other stimuli. Although, there are still unanswered questions about how the guard cell PM H⁺ ATPase becomes phosphorylated in response to blue or red light as no protein kinase has been identified (Inoue & Kinoshita, 2017); the roles of the other sites of phosphorylation; and the potential roles of the other PM H⁺ ATPase isoforms in stomatal opening.

It has been suggested that the ATP required for the PM H⁺ ATPase and the blue light signal transduction pathway is provided by photosynthesis (Suetsugu et al., 2014) and the light

induced breakdown of triacylglycerols (McLachlan et al., 2016). Mutants that lacked chloroplasts showed reduced guard cell ATP and impaired light induced stomatal opening (Wang et al., 2014). In contrast, the red light induction and phosphorylation of PM H⁺ ATPases does not appear to occur via guard cell phototropins or cryptochromes (Ando & Kinoshita, 2018). Until recently the involvement of red light in the induction of PM H⁺ ATPases was not clear, with earlier studies suggesting red light did (Serrano et al., 1988) and conversely did not induce them (Roelfsema et al., 2001; Taylor & Assmann, 2001). There is consistent evidence that red light induces stomatal opening and is required for proper blue light induced opening (Ando & Kinoshita, 2018; Inoue & Kinoshita, 2017).

It was long thought that red light induced mesophyll photosynthesis, which in turn reduced guard cell C_i inducing stomatal opening. In fact, mutants of two proteins involved in low C_i stomatal opening *HIGH LEAF TEMPERATURE1 (HT1)* (Hashimoto et al., 2006) and *CONVERGENCE OF BLUE LIGHT AND CO₂ 1 (CBC1 and 2)* (Hiyama et al., 2017), show no stomatal response to red light. Inversely, high CO₂ concentration can inhibit PM H⁺ ATPase activity (Edwards & Bowling, 1985). Despite this overlap in signalling, there is increasing evidence that a mechanism distinct of changes in C_i might be responsible for red light induction of PM H⁺ ATPases and stomatal opening. Studies have shown that red light can induce stomatal opening under constant C_i (Lawson et al., 2008; Messinger, 2006).

Until recently the role of these pathways had not been examined in CAM plants. A recent study has shown the stomata of two CAM species *Kalanchoe pinnata* and *Kalanchoe daigremontiana* are responsive to blue and red light (Gotoh et al., 2018). Furthermore, this work also showed that a similar mechanism of action to that of *Arabidopsis* was acting in this response. The response to blue light was suppressed by the application of inhibitors of PP1 and PM H⁺ ATPase, tautomycin and vanadate. The PM H⁺ ATPase activating compound fusicoccin strongly induced the phosphorylation of PM H⁺ ATPase and the opening of stomata.

Kalanchoe fedtschenkoi has also been shown to have stomatal responsiveness to blue and red light, with plants showing increased stomatal conductance in response to bursts of red/blue light during the night (Hurtado-Castano, 2019). Interestingly, this response was impaired in a starchless *K. fedtschenkoi phosphoglucomutase (pgm1)* mutant, suggesting that like *Arabidopsis* the starch metabolism plays a role in blue light responsive stomatal regulation.

1.2.10 Guard Cell Metabolism

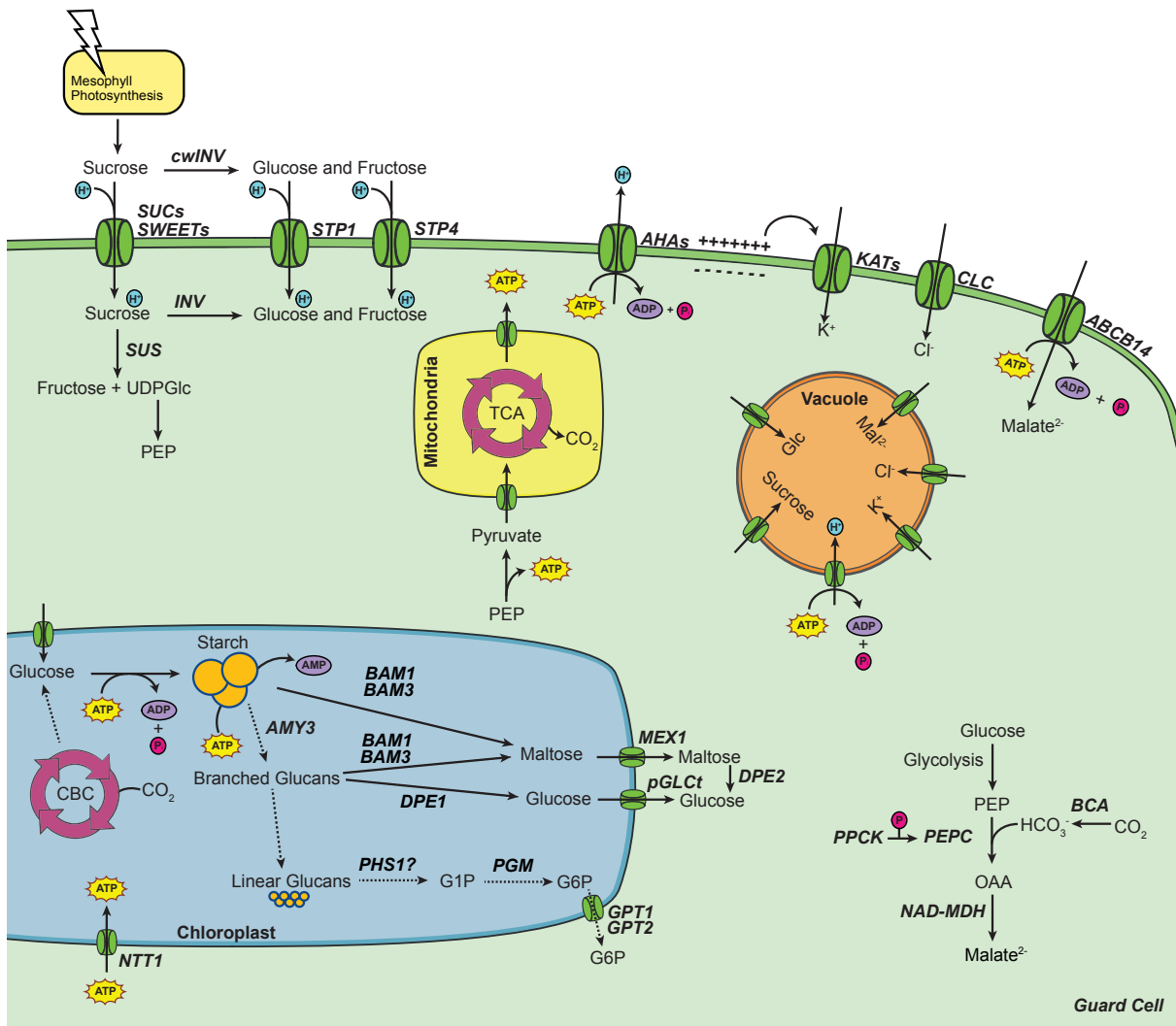


Figure 1.8 Key elements of guard cell metabolism during light induced opening in C3 plants, with a focus on ATP demand and supply, adapted from (Flütsch & Santelia, 2021; Lim et al., 2022).

Metabolism differs in the guard cells compared to that of the mesophyll in both C₃ and CAM plants (Abraham et al., 2020; Santelia & Lawson, 2016). This is exemplified by recent 'omics' studies that have shown considerable differences in the transcriptomes of guard cells compared to mesophyll (Bates et al., 2012; Bauer et al., 2013; Kong et al., 2020; Leonhardt et al., 2004; Yang et al., 2008); and in proteomes between mesophyll and guard cells in C₃ (Zhao et al., 2008; Zhu et al., 2009) and CAM (Abraham et al., 2020). These differences in transcripts and protein abundancies are also accompanied by changes in the enzyme activities of key metabolic enzymes, summarised by Daloso et al., (2017). Metabolomic studies have further supported key differences between guard cell and mesophyll metabolism (Daloso et al., 2015; Williams et al., 2016; Jin et al., 2013; McLachlan et al., 2016; Misra et al., 2015).

1.2.11 Guard Cells need energy – where do they get it?

In order to regulate stomatal aperture guard cells need energy. The hyperpolarisation of the guard cell plasma membrane by PM H⁺ ATPases consumes a large amount of cytosolic ATP (Tominaga et al., 2001; Wang et al., 2014) and is required to drive the influx of both ions and sugars into the guard cells (Flütsch & Santelia, 2021; Kinoshita et al., 2001). Organic compounds such as sugars and malate are also thought to act as osmolytes promoting guard cell opening, with their production or import also dependent on ATP consumption (Daloso et al., 2017). Guard cell starch metabolism, covered later, is thought to also play a key role in regulating metabolic osmoticum and thus stomatal opening, will also require ATP (Flütsch et al., 2020; Horrer et al., 2016).

The source of guard cell ATP is long debated, with glycolysis, mitochondrial respiration and photosynthesis all suggested as sources. Evidence that glycolysis provides at least a portion of this ATP is strong, with high glycolytic activity in guard cells (Daloso et al., 2015; Hedrich et al., 1985; Medeiros et al., 2018); and mutants impaired in glycolysis have impaired stomatal opening (Zhao & Assmann, 2011). There is also substantial support for ATP supply from mitochondrial respiration, with a tendency for significantly more mitochondria in guard cells compared to mesophyll cells (Allaway & Setterfield, 1972). Guard cell protoplasts have also been shown to have higher respiratory rates than mesophyll protoplasts (Mawson, 1993; Vani & Raghavendra, 1994) and reduced stomatal opening in epidermal strips in the presence of respiratory inhibitors (Raghavendra, 1981).

The role of photosynthesis in supplying ATP for guard cell function is less clear. There is agreement that guard cell photosynthesis occurs, but it is not clear how much of it contributes to guard cell sugar or ATP production (Daloso et al., 2017; Lawson & Matthews, 2020; Santelia & Lawson, 2016). Guard cell chloroplasts are lesser in number and smaller, with lower chlorophyll content compared to mesophyll cells (Wille & Lucas, 1984) and have low content and activity of RUBISCO (Madhavan & Smith, 1982; Outlaw et al., 1979; Reckmann et al., 1990; Shimazaki et al., 1989). However, some studies have detected Calvin-Benson-Bassham cycle activity, demonstrating CO₂ uptake into 3-PGA and ribulose-1,5-bisphosphate in guard cell chloroplasts (Goh et al., 1997; Gotow et al., 1988; Tallman & Zeiger, 1988). The guard cell chloroplast electron transport chain has been shown to be active and RUBISCO is a major sink for the end products for electron transport chain (Lawson et al., 2003). Notably, recent mass spec ¹³C isotope labelling in *Nicotiana tabacum* showed that guard cells are able to fix carbon by both RUBISCO and PEPC (Daloso et al., 2015).

In terms of ATP supply, studies have suggested that most ATP is supplied via photosynthesis and exported from the guard cells, with evidence that stomatal responses are impaired by photosynthesis inhibitor DCMU (Schwartz & Zeiger, 1984; Suetsugu et al., 2014; Tominaga et al., 2001). However, no route for ATP export from the guard cell chloroplasts has been identified, with suggestions that PGA/DHAP shuttle may carry out this function (Shimazaki et al., 1989). Recent work has cast doubt over this theory, Lim et al., (2022) showed that guard cells produce little ATP or NADPH via photosynthesis with that the majority of ATP being supplied via oxidative phosphorylation in the mitochondria. They also showed that guard cell chloroplasts possess the novel ability to import ATP, via an ADP/ATP translocator *NUCLEOTIDE TRANSPORTER 1 (NTT1)* that is not present in mesophyll chloroplasts and may allow ATP import to energise starch synthesis in the guard cell chloroplasts (Lim et al., 2022) and is consistent with other results that downregulation of *NTT1* reduced guard cell starch accumulation (Andersson et al., 2018). Notably, recent proteomics work in CAM *K. fedtschenkoi* also suggested an increase in mitochondrial respiration in guard cell enriched epidermal peels, with increased expression of mitochondrial respiration proteins, those involved in the TCA cycle and redox related genes (Abraham et al., 2020).

1.2.12 Guard Cell Carbon

Guard cell metabolism takes a position in between being heterotrophic and autotrophic (Flütsch et al., 2022; Lim et al., 2022), with modelling showing that C_3 guard cells are flexible in terms of their metabolism (Tan & Cheung, 2020). It is thought that a large portion of the carbon in the guard cells comes from the mesophyll in the form of sucrose (Lim et al., 2022) and/or malate (Lee et al., 2008). The majority of carbon is assimilated in the guard cells via PEPC to form malate (Daloso et al., 2015; Lima et al., 2021; Robaina-Estévez et al., 2017; Willmer & Ditttrich, 1974), with malate thought to contribute to stomatal opening as osmotically as a K^+ counter ion and also as a source of energy. Guard cell starch also contributes to the pool of available sugars but it is thought that the majority of carbon skeletons used in starch synthesis originate from imported sugars from the mesophyll, with some essential contribution from guard cell photosynthesis (Azoulay-Shemer et al., 2015; Lim et al., 2022). The pool of mesophyll imported and starch derived sugars are needed for glycolysis and mitochondrial metabolism during the day and for proper guard cell functioning (Flütsch et al., 2020; Flütsch et al., 2022; Horrer et al., 2016). Sucrose breakdown has also been shown to be important for stomatal opening. Sucrose has long been thought of as an osmolyte (Talbot & Zeiger, 1996), but recent evidence is lacking and points to an energetic role for sucrose in enabling stomatal opening (Antunes et al., 2012; Daloso et al., 2016; Daloso et al., 2015; Kelly et al., 2013).

The source of guard cell carbon and ATP is of especial importance to CAM plants as they must be able to maintain stomatal opening during the night in the absence of photosynthesis. CAM guard cells, like C_3 , accumulate starch during the day. This starch accumulation is likely also dependent on guard cell photosynthesis and mesophyll imported sugars, though this will need to be confirmed. The idea that the majority of guard cell ATP is sourced from the mitochondrial respiration and glycolysis, and the suggestion that guard cell chloroplasts can import ATP would provide a potential ATP supply for nocturnal guard cell opening in CAM plants when photosynthesis is not active.

1.2.13 Rescheduling of guard cell starch metabolism in CAM

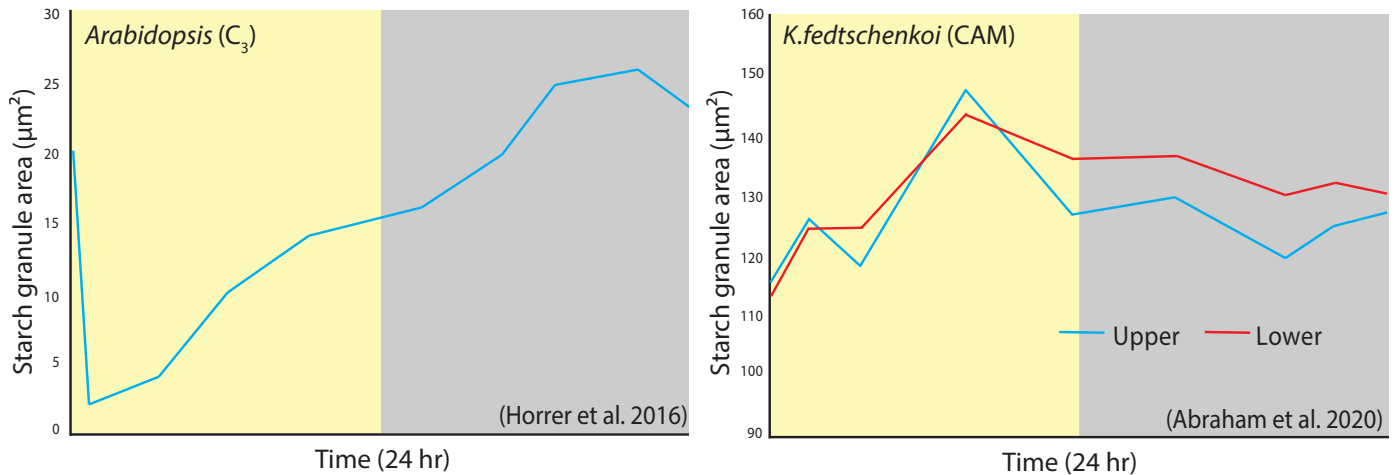


Figure 1.9 Comparison of diel changes in guard cell starch granule area in *Arabidopsis* (C₃) and *Kalanchoe fedtschenkoi* (CAM), showing a rescheduling of starch metabolism in *K. fedtschenkoi* guard cells (Abraham et al., 2020; Horrer et al. 2016).

It has been hypothesised that the pattern of guard cell metabolism may differ between C₃ and CAM plants, in order to provide energy and osmolytes over the night for nocturnal opening. In *Arabidopsis*, starch metabolism differs between the mesophyll and the guard cells. Both show a similar pattern of starch metabolism, with an accumulation of starch during the day providing a sink for photoassimilates and a steady depletion overnight to supply carbon for nocturnal metabolism, maintenance and growth (Flis et al., 2018; Santelia & Lunn, 2017). Yet In *Arabidopsis*, guard cell starch is also rapidly degraded towards the end of the night and in the early morning. It is thought that this rapid degrading of guard cell starch at the start of the day provides osmolytes that increase guard cell turgor and assist in stomatal opening (Santelia & Lunn, 2017). Recent data has shown that starch metabolism in CAM *K. fedtschenkoi* guard cells has been rescheduled compared to C₃ plants, with starch broken down overnight in CAM as opposed to breakdown in the early day in *Arabidopsis* (Abraham et al., 2020). Guard cell starch metabolism is thought to play a key role in guard cell function (Lloyd, 1908), with a distinct pattern of starch metabolism compared to that of the mesophyll. Guard cell starch could provide a carbon sink that can be hydrolysed to provide sugars and malate to be used as osmolytes and energy for stomatal opening (Tallbott & Zeiger, 1993). This carbon sink may be of especial importance in CAM plants to sustain nocturnal opening without any direct energy input from photosynthesis.

In *Arabidopsis* guard cell starch is important both for the provision of osmolytes and carbohydrates for stomatal opening when degraded, but also to act as a sink for osmolytes and carbohydrates in stomatal closure (Horrer, Flütsch, et al., 2016; Santelia & Lunn, 2017). This degradation of starch in C₃ plants is thought to be induced by light, with epidermal accumulation of sucrose and products of the starch hydrolytic pathway like maltose observed during stomatal opening in *Vicia faba* (Talbot & Zeiger, 1993) and a similar sudden degradation of starch at the start of the day in *Arabidopsis* (Horrer et al., 2016). Over the course of the day guard cell starch accumulates, and likely acts as a sink for osmolytes during stomatal closure (Horrer et al., 2016; Santelia & Lunn, 2017). It should, however, be noted that starch may not play this role in all C₃ plants; for example it has been recently suggested that changes in guard cell sugars and not starch are responsible for light induced opening in the C₃ plant tobacco (Daloso et al., 2015).

An *Arabidopsis* double mutant deficient in two key enzymes implicated in the guard cell hydrolytic starch degradation pathway, *amy3bam1*, that could not properly degrade starch, showed impaired stomatal opening and starch (Horrer et al., 2016). Importantly a similar impairment of guard cell starch degradation was observed in *phot1phot2* and *blus1* mutants. Furthermore, activation of the PM H⁺ ATPase by fusicoccin treatment in epidermal peels lead to both stomatal opening and almost total degradation of starch (Horrer et al., 2016). Treatment of *phot1phot2* mutants with fusicoccin rescued their phenotype and induced proper guard cell starch degradation. Interestingly illumination of *Arabidopsis* with red light induced starch degradation independently of blue light (Horrer et al., 2016), as both pathways induce the phosphorylation of PM H⁺ ATPase this could suggest that these proton pumps are a key hub in regulating light induced starch degradation in guard cells.

Together these results suggest that both blue and red light can trigger starch degradation in *Arabidopsis* guard cells via the PM H⁺ ATPases. Yet there are many questions remaining as to how the activation of these proton pumps induce starch degradation and how this pathway might be modulated in CAM plants to ignore red/blue light during daytime stomatal closure? The activation of PM H⁺ ATPases result in the efflux of H⁺ from the cytosol, this could mean that enzymes sensitive to such a change might activate. One such interesting example is PEPC, an isoform of which was shown to activate in response to a reduction in cytosolic [H⁺] in *Arabidopsis* guard cell protoplasts (Meinhard & Schnabl, 2001). Activation of such an enzyme

and the resultant flux of carbon into malate might provide a potential route for activating starch degradation.

1.2.14 Key Areas for Investigation in CAM

This section has highlighted a number of key questions for investigation. A major outstanding question in CAM that has implications for CAM engineering is how the regulation of stomatal conductance and the mesophyll CAM cycle are linked and if there are regulatory and metabolic changes that are required to enable the inverted diel pattern of stomatal opening in CAM plants. How do CAM plants meet the high demand for ATP at night in the absence of photosynthesis to carry out mesophyll CAM and support nocturnal stomatal opening, both of which require substantial amounts of ATP? And how well conserved are processes already shown to be used to tackle ATP demand, like the switch to phosphorolytic starch degradation in starch using CAM species?

1.3 Approaches to CAM engineering and progress so far

Over the past decade there have been a few first steps into engineering components of the CAM pathway into C_3 plants. An early effort expressed PEPC from *Solanum tuberosum* in both a constitutive and dark induced manner in *A. thaliana*, which resulted in increased stomatal conductance, likely due to increased CO_2 consumption (Kebeish et al., 2012), adding to previous works constitutively overexpressing PEPC in various plants (Hudspeth et al., 1992; Kogami et al., 1994; Ku et al., 1999). Recently, a more comprehensive study demonstrated the separate constitutive overexpression of many key metabolic components of both the carboxylation and decarboxylation pathways of CAM from *M. crystallinum* into *A. thaliana* (Lim et al., 2019). Transgenic plants with carboxylation and decarboxylation components showed increases or decreases in titratable acidity, respectively, however the study did not attempt to express any of the genes in a CAM-like pattern. They have also not attempted to express the genes in a mesophyll specific manner or make any transgenic changes to the guard cells. Interestingly, overexpression of *PEPC-kinase* also led to increased PEPC activity and accumulation of titratable acidity (Lim et al., 2019). This gives support to an alternative approach to CAM engineering. Rather than overexpress all the genes implicated in CAM, a

more elegant approach may be to identify the key control points of metabolic flux and upregulate them instead. For example instead of overexpressing all the elements of the carboxylation pathway at night, it might be possible to achieve CAM-like carboxylation by increasing expression or activity of the key controlling points. These top down metabolic approaches are likely to be less complex in terms of implementation, with less transgenes needed, but may require a greater understanding on how these pathways are regulated. Reducing the complexity will be especially important if other elements of CAM will also need to be engineered in, for example if CAM stomatal regulation and guard cell metabolism also need substantial alteration. Identifying bottlenecks or key control points in CAM may also raise the possibility of improving the efficiencies of CAM.

1.4 Tools to study CAM - CAM in the Omics Era

As previously described, CAM is a complex trait that recruits many metabolic enzymes and pathways present in C_3 species, with genes upregulated or their expression patterns re-timed to fit the CAM diel cycle (Abraham et al., 2016; Wai et al., 2019; Yang et al., 2017). Efforts to understand CAM, its induction and regulation will need to consider genome scale changes in gene expression. Consequently, over recent years there has been a flurry of 'CAM-omics' studies, with the genomes of constitutive and facultative CAM species from across plant life sequenced, including: *Ananas comosus* (Ming et al., 2015), *Agave* (Abraham et al., 2016; Gross et al., 2013), *Kalanchoe fedtschenkoi* (Yang et al., 2017a), *Kalanchoe laxiflora* (unpublished, Phytozome), *Sedum Album* (Wai et al., 2019), *Talinum triangulare* (Brilhaus et al., 2016; Maleckova et al., 2019, 2020), *Isoetes taiwanensis* (Wickell et al., 2021) and most recently *Cistanthe longiscapa* (Ossa et al., 2022)

Many of these CAM genomics studies also compared diel transcript expression between the CAM species and C_3 species to identify genes that were either upregulated in the CAM species or showed a significant diel shift in expression pattern compared to that in the C_3 species (e.g. Moseley et al., 2019). This approach has identified and corroborated the importance of many key CAM genes. These works may, however, be complicated by intraspecific differences in gene expression, especially as many of these comparisons are made between the CAM species and *Arabidopsis* which differ significantly in their morphology, geography and phylogenetic placing. More recently, efforts have been made to compare the gene expressions of more

closely related species, such as comparisons between C₃, CAM and C₃/CAM hybrids in *Yucca* (Heyduk et al., 2019).

Another approach, highlighted by Winter et al. (2008), is to study changes in gene expression that occur when CAM is induced in facultative CAM plants, usually by an abiotic stress. Such as drought in *Sedum album* (Wai et al., 2019), *Cistanthe longiscapa* (Ossa et al., 2022) and *Portulaca amilis* (Gilman et al., 2022); NaCl in *Mesembryanthemum crystallinum* (Cushman et al., 2008); and ABA (Maleckova et al., 2019) or drought (Brilhaus et al., 2016) in *Talinum triangulare*. This approach compares abiotically induced CAM and C₃ transcription, physiologies and sometimes metabolites (Maleckova et al., 2019) within the same respective species, reducing potential conflation from intraspecific differences. Yet, such studies, while useful in identifying many key elements of CAM that are upregulated upon CAM induction, also suffer from potential overlap with between CAM induction and abiotic stress response. A method of CAM induction that may be less 'stressful' and provide insights from a different angle is CAM induction by ageing and is thus the main focus of this thesis. Undoubtedly, experiments that explore all of the different modes of induction within one species will give the strongest contrast between the key components of CAM induction compared to abiotic stress response. Also, there will be overlap between CAM induction and the abiotic stress response pathways, for instance there was substantial overlap between the response to ABA and drought in *Talinum triangulare* (Brilhaus et al., 2016; Maleckova et al., 2019).

A final approach to establishing the key elements required for CAM is to genetically manipulate constitutive CAM plants to impair their ability to do CAM. Knocking down the PEPC isoform recruited for nocturnal carboxylation is arguably the most direct way to impair nocturnal carboxylation and CAM (Boxall et al., 2020). An issue with this approach is that this will only partially turn off CAM and there will be many elements of CAM that would be still active. However this approach may be useful in differentiating between the role of nocturnal carboxylation and other CAM components.

Functional genetics studies will, however, be key for understanding the core components of CAM and have already advanced the field considerably (Boxall et al., 2017; Boxall et al., 2020; Ceusters et al., 2021; Dever et al., 2015). A recent study created a library of CRISPR guide DNA sequences for targeting genes in *K. fedtschenkoi* (Liu et al., 2019), which may help open the door for high throughput phenotypic analysis of key CAM mutants. Combining the previously

mentioned 'omics' methods to identify key CAM components and transgenic manipulations will help provide answers to key remaining CAM questions.

1.5 Approach of this thesis

This thesis aims to develop the inducible CAM plant *K. blossfeldiana* as a system for comparatively studying C₃ and CAM whole leaf and stomatal physiology and metabolism across the mesophyll and guard cells. Ultimately, the aim is to address some of the questions raised above, a key one being, how the regulation of stomatal conductance and the mesophyll CAM cycle are linked and if there are regulatory and metabolic changes that are required to enable the inverted diel pattern of stomatal opening in CAM plants? The thesis will also make use a recently characterised CAM-deficient *K. fedtschenkoi pepc1* mutant to cross compare with C₃/CAM tissues from *K. blossfeldiana* and to explore the role of nocturnal carboxylation on stomatal regulation in CAM.

1.6 Kalanchoe genus

A substantial portion of studies over the last near century of CAM research have been carried out using plants from the genus *Kalanchoe* (Abraham et al., 2020; Gregory et al., 1954; Moseley et al., 2019; Rustin & Queiroz-Claret, 1985; Taybi et al., 1995; von Caemmerer & Griffiths, 2009; Winter et al., 2008; Yang et al., 2017). The *Kalanchoe* genus is estimated to have diverged from the *Sempervivoideae* between 22.78–44.29 million years ago (Messerschmid et al., 2020). The current *Kalanchoe* genus is made of up species from three previous genera, *Kalanchoe* (of which *K. blossfeldiana* was a member), *Kitchingia* and *Bryophyllum* (of which *K. fedtschenkoi* and *K. laxiflora* were members and carry out leaf margin embryogenesis (Mort et al., 2010). *K. blossfeldiana* shows some morphological and physiological differences from *K. fedtschenkoi* and *K. laxiflora* - it is predominantly green leafed, lacks the ability to reproduce from leaf tip pups, and performs inducible CAM vs constitutive CAM as found in *K. fedtschenkoi* and *K. laxiflora*.

1.6.1 *K. blossfeldiana* - Age Induced CAM

The potential for using inducible CAM plants for studying CAM has long been recognised (Osmond, 1978), as they provide a system that is less prone to being affected by potential intraspecific differences between C₃ and CAM species; and they allow for a system that can be monitored as it transitions into CAM. Inducible CAM plants are often induced by the application of abiotic stress, such as drought or salt. With plants quickly transitioning, usually into a strong form of CAM where there is limited, if any, daytime conductance, or CO₂ assimilation. This provides an issue for studying CAM, the pathways associated with the response to abiotic stresses are complex and it may be difficult to separate the actions of these abiotic stress pathways from CAM induction pathways. Here *K. blossfeldiana* is of potential utility as CAM is induced by ageing, with CAM activity increasing down the plant as leaves age. This therefore provides a system for comparing C₃ and CAM within the same plant at the same time, without the activation of any abiotic stress pathways., thus saving both time, space and reducing the risk of conflation with abiotic stress.

K. blossfeldiana naturally occurs in the high-altitude (~1500-2000+M) humid forests of the Tsaratanana mountain range, Madagascar, alongside its close relative *K. globulifera* (Klein et al., 2021). The *Kalanchoe* genus consists of over 150 currently known species that all perform CAM to varying amounts and is found in Madagascar (Kluge et al., 1991), Southern Africa (Gehrig et al., 2001), Arabia and tropical Asia (Klein et al., 2021). *K. blossfeldiana* is within *Kalanchoe* subg. *Kalanchoe* and was discovered by the botanist Perrier de la Bathie in 1924 on the slopes of the aforementioned mountains (van Voorst & Arends, 1982). *K. blossfeldiana* is morphologically similar to *K. globulifera* and the recently described *K. darainensis* (Klein et al., 2021). It has had a confused naming history, which is well described by (Klein et al., 2021). It rose to horticultural significance when it was introduced to Potsdam by Robert Blossfeld in 1932 and has ever since been a popular and significant house plant (Pertuit, 1992).

K. blossfeldiana was first shown to assimilate CO₂ nocturnally in 1942 (Bode, 1942). Its importance in the comparative study of CAM was realised in the late 20th century with the observations that CAM in *K. blossfeldiana* can be induced by short days (Lerman & Queiroz, 1974), nitrogen deficiency (Ota, 1988), ABA and drought (Taybi et al., 1995) and leaf aging (Brulfert et al., 1982). *K. blossfeldiana* is awkward to categorise; it has previously been

described as a facultative CAM plant (Gehrig et al., 1995) and may have been the first plant described as such (Gregory et al., 1954). There have been recent efforts to more clearly define the various different forms of CAM (Winter, 2019), under which a facultative CAM plant would be defined as a plant in which CAM could be induced and un-induced depending on environmental conditions. As CAM in *K. blossfeldiana* is induced by ageing it would appear inevitable that it would become CAM and from previous studies there is no evidence of CAM being reversible in this species (Gehrig et al., 1995; Lerman & Queiroz, 1974; Taybi et al., 1995). It is also unclear what contribution each form of photosynthesis would make to carbon gain over the entire lifespan of *K. blossfeldiana*. For the interests of simplicity in this thesis *K. blossfeldiana* is referred to as an inducible CAM species.

1.7 Core Questions to be addressed in this thesis - divided by chapter and approaches

This thesis sets out to develop *Kalanchoe blossfeldiana* as a system for comparatively studying C₃ and CAM, and to use this system to identify key differences in metabolism and physiology between these photosynthetic types with a focus on stomatal physiology and guard cell metabolism.

Chapter 2 – Comparative systems for studying crassulacean acid metabolism.

The first experimental chapter characterises the induction of CAM by ageing in young and mature *Kalanchoe blossfeldiana* leaves. A key aim is to characterise photosynthetic metabolism and CAM traits and thereby determine if *Kalanchoe blossfeldiana* would be useful as a comparative system to study C₃/CAM. This chapter also explores the morphology and the development of CAM traits in *K. blossfeldiana*. Additionally, the chapter uses a CAM deficient *Kalanchoe fedtschenkoi pepc1* mutant to investigate and characterise the effects of impairing nocturnal carboxylation on CAM and photosynthetic metabolism.

Chapter 3- Self determined stomata - PEPC-mediated nocturnal carboxylation alone is not enough to drive nocturnal conductance in *Kalanchoe*.

This chapter explores differences between C₃ and CAM stomatal physiology and guard cell metabolism making use of the two C₃/CAM comparative systems described in chapter 2, i.e. young C₃ and mature CAM *Kalanchoe blossfeldiana* leaves and *Kalanchoe fedtschenkoi* WT and a *pepc1* mutant. The chapter compares C₃ and CAM stomatal diel conductance and guard cell metabolism and investigates the role of C_i in linking mesophyll PEPC-driven carboxylation and stomatal conductance, with the hope of addressing whether there are regulatory and metabolic changes that are required to enable the inverted diel pattern of stomatal opening in CAM plants? The chapter also examines the role of whole leaf carbon assimilation on stomatal conductance including both C₃ RUBISCO and PEPC-mediated assimilation.

Chapter 4 – The *Kalanchoe blossfeldiana* Genome

This chapter presents the genome of *Kalanchoe blossfeldiana* and a comparative C₃/CAM dusk transcriptome; and explores the key differences in gene expression between C₃ and CAM tissues with a focus on genes involved in mesophyll CAM, guard cell metabolism and stomatal regulation. By investigating the changes in transcript abundance in age induced CAM it is hoped that this chapter can be used to identify the core elements of CAM that are conserved across different CAM species and different induction modes.

Chapter 2. Comparative systems for studying crassulacean acid metabolism

2.1 Introduction

2.1.1 *K. blossfeldiana* - Age Induced CAM

The potential for using inducible CAM plants for studying CAM has long been recognised (Osmond, 1978), as they provide a system for investigating the physiological and metabolic changes that occur within a plant between from C₃ to CAM that is less prone to being affected by potential intraspecific differences between C₃ and CAM species; and allow for a system that can be monitored as it transitions into CAM. CAM is often induced by the application of abiotic stress, such as drought or salt with plants quickly transitioning, usually into a strong form of CAM where there is limited, if any, daytime conductance, or CO₂ assimilation. This stress-induced CAM provides an issue for studying the mechanisms of CAM since the pathways associated with the response to abiotic stresses are complex and it may be difficult to separate the actions of these abiotic stress pathways from CAM induction pathways. Here, *Kalanchoe blossfeldiana* is of potential utility for studying the genes/proteins required for CAM since the pathway is induced by ageing, with CAM activity increasing down the plant from youngest leaves at the top. This could provide a system for comparing C₃ and CAM within the same plant at the same time, without the activation of any abiotic stress pathways, thus saving both time, space and reducing the risk of conflation with abiotic stress.

K. blossfeldiana was first shown to assimilate CO₂ nocturnally in 1942 (Bode, 1942). Its importance in the comparative study of CAM was realised in the late 20th century with the observations that CAM in *K. blossfeldiana* can be induced by short days (Lerman & Queiroz, 1974), nitrogen deficiency (Ota, 1988), ABA and drought (Taybi et al., 1995) and leaf aging (Brulfert et al., 1982). *K. blossfeldiana* is awkward to categorise, it has previously been described as a facultative CAM plant (Gehrig et al., 1995) and may have been the first plant described as such (Gregory et al., 1954). There have been recent efforts to more clearly define the various different forms of CAM (Winter, 2019), under which a facultative CAM plant would be defined as a plant in which CAM could be induced and un-induced depending on environmental conditions. As CAM in *K. blossfeldiana* is induced by ageing it would appear

inevitable that it would become CAM and from previous studies there is no evidence of it being reversible (Gehrig et al., 1995; Lerman & Queiroz, 1974; Taybi et al., 1995a). It is also unclear what contribution each form of photosynthesis would make to carbon gain over its entire lifespan. This chapter builds on these works, with the use of newer techniques, to focus on metabolic and physiological comparisons between young C₃ leaves and mature CAM leaves in *K. blossfeldiana*.

A second *Kalanchoe* species, *Kalanchoe fedtschenkoi*, along with a CAM deficient *phosphoenolpyruvate carboxylase isoform 1 (pepc1)* mutant were used to complement comparisons made between C₃ and CAM tissues in *K. blossfeldiana*. *K. fedtschenkoi* is a well-established obligate CAM plant, that has been extensively studied, with a recent plethora of omics datasets, including its genome, diel mesophyll vs guard cell enriched epidermal peel proteome, and a number of transcriptomes under different conditions (Abraham et al., 2020; Hu et al., 2022; Yang et al., 2017; Zhang et al., 2020). Its small genome size (diploid ~256 Mb) and the relative ease to which it is genetically transformed has highlighted *K. fedtschenkoi* as a potential target for further genetic manipulation and study in order to further our knowledge of CAM (Hartwell et al., 2016).

PEPC is central to CAM, responsible for the nocturnal fixing of CO₂ as HCO₃⁻ into OAA which is rapidly stored overnight in the vacuole as malic acid. PEPC1 (Kaladp0095s0055) has been hypothesised to be the main “CAM” PEPC isoform in *K. fedtschenkoi*, with greater transcript expression than the other five isoforms in *K. fedtschenkoi* (Yang et al., 2017). This has been supported by recent work in close relative *K. laxiflora* that showed RNAi silencing of PEPC1 resulted in an CAM-deficient phenotype with an inability to accumulate malate overnight and a shift to a ‘C₃’ pattern of daytime carbon assimilation (Boxall et al., 2020). In this chapter I exploit a recently created CRISPR driven knock down of *phosphoenolpyruvate carboxylase isoform 1 (PEPC1)* to examine the impact on nocturnal CO₂ uptake, nocturnal stomatal conductance, and nocturnal accumulation of titratable acidity.

This chapter makes use of two systems for comparing C₃ and CAM tissues, age induced CAM between young and mature *K. blossfeldiana* leaves and comparisons between wild type and a CAM deficient *pepc1 K. fedtschenkoi* mutant. Across the two systems both CAM tissues, the mature *K. blossfeldiana* and wild type *K. fedtschenkoi* are likely to have a similar phenotype with both performing CAM. Whereas comparisons of the two C₃ tissues, young *K. blossfeldiana*

and *K. fedtschenkoi pepc1* mutants, might provide a way of studying the role of CAM-related pathways independent of PEPC1.

2.1.2 Chapter Aims

The aims of this chapter are to characterise the primary metabolism and physiology of the inducible CAM plant *K. blossfeldiana* and to establish it as a comparative system for studying C₃ and CAM tissues within the same plant. It also explores a second comparative system, comparing the constitutive CAM plant *Kalanchoe fedtschenkoi* and CAM deficient CRISPR generated *K. fedtschenkoi pepc1* mutants. Across the two systems, it is hypothesised that both CAM tissues, the mature *K. blossfeldiana* and wild type *K. fedtschenkoi* will have a similar phenotype in terms of gas exchange profiles and metabolite turnover. It is further hypothesized that comparisons of the two C₃ tissues, young *K. blossfeldiana* and *K. fedtschenkoi pepc1* mutants, might provide a way of studying the role of CAM-related pathways independent of PEPC1. The overall aim of this chapter is to provide evidence to decide whether these systems will be useful in comparatively studying C₃ and CAM with regard to stomatal behaviour, and if so to optimise these comparisons. This will then be used to optimise sampling in the comparative study of C₃ and CAM guard cell physiology and metabolism in subsequent chapters.

This chapter is divided into three parts:

- The characterisation of C₃/CAM photosynthetic traits in *K. blossfeldiana*
- Morphology and the development of CAM traits in *K. blossfeldiana*
- The effect of PEPC1 knockout in *Kalanchoe fedtschenkoi* on diel gas exchange and nocturnal malate accumulation.

2.2 Materials and Methods

2.2.1 Summary of Experiments

Throughout this chapter comparisons were made between C₃ and CAM physiotypes using two comparative systems; 1) between *K. blossfeldiana* young (10th leaf pair from bottom) and mature leaves (2nd leaf from bottom), and 2) between wild type *K. fedtschenkoi* and CAM-deficient *pepc1.1* mutants. The *K. fedtschenkoi pepc1* mutants were produced by CRISPR targeted gene silencing of the *K. fedtschenkoi* PEPC1 gene by Xiaohan Yang with a method described in Zhang et al. (2020). The overall aim of this chapter is to characterise the basic CAM metabolic and gas exchange traits within the comparative systems.

2.2.2 Plant Growth Conditions

All plants were grown under 190 μ mol light, unless otherwise noted, with 12/12hrs day/night cycles and with 25°C days and 19°C nights. Plants were watered twice weekly. *K. blossfeldiana* plants were propagated by cutting. Briefly, side shoots were cut from the main stem with all but a small emerging leaf bud at the apex of the shoot and the top two leaf pairs. Care was taken to ensure all cuttings were the made to the same length and were uniform in leaf sizes. Individual cuttings were placed in 5 cm pots with John Innes No.2 compost and grown under cover for 2 weeks. After 6 weeks cuttings were re-potted into 12 cm pots with a 3:1 mix of John Ins No.2: Perculite. *K. fedtschenkoi* plants were propagated by leaf edge pupping. Removed leaves were placed on trays with a 3:1 mix of John Innes No.2: Perculite. Plantlets were grown for 8 weeks before being re-potted three per 12 cm pot. *K. fedtschenkoi* plants were sampled 120 days after propagation.

2.2.3 Diel Gas Exchange

Short term (up to 48 hrs) diurnal stomatal conductance ($\text{mol H}_2\text{O m}^{-1} \text{s}^{-1}$) and net CO_2 assimilation ($\mu\text{mol CO}_2 \text{m}^{-1} \text{s}^{-1}$) were measured using a Li-Cor Portable Photosynthesis System Li-6400XT (Li-Cor, USA) over full 24 hr periods. All such measurements were run successively in triplicate. For all measurements, zero CO_2 and H_2O readings were taken before a run of experiments and CO_2 was zeroed before every run; with desiccant and CO_2 scrub replaced for every run. Chamber conditions were set to track the conditions of the growth cabinet, with $190 \mu\text{mol m}^{-2} \text{s}^{-1}$ light, unless otherwise noted, with 12/12hrs day/night cycles and with 25°C days and 19°C nights, relative humidity was held between ~ 25 and 35% . Importantly, the chamber fan was set to 4 (Slow), which was found to substantially improve fan longevity. For a standard 24 hr diurnal run measurements were taken every 15 minutes with automatic matching every 30 minutes and ambient CO_2 set to $400 \mu\text{mol mol}^{-1} \text{CO}_2$. For experiments with *K. blossfeldiana* leaves at leaf pairs two and ten (counted from the bottom up) were used with plants 60-90 days after propagation, for those involving *K. fedtschenkoi* leaves at leaf pair 6 were used with plants 100-120 days after propagation

In order to monitor the Li-6400XT remotely throughout these experiments, the Li-6400XT was attached to a Raspberry Pi 3B (Raspberry Pi, UK) which ran a python script that queried the Li-6400XT at two-minute intervals. A second, internet connected, computer would then query the Raspberry Pi at two-minute intervals and display an automatically updating web app. This web app was written in R (version 4.0.2) and Shiny (version 1.6.0) and ran inside a docker container.

2.2.4 Long term Gas Exchange (Walz Binos-100)

Longer term net CO_2 assimilation ($\mu\text{mol CO}_2 \text{m}^{-1} \text{s}^{-1}$) was measured *K. blossfeldiana* young leaves (10th leaf pair from bottom) over multiple diurnal cycles using a Walz CMS-400 compact mini-cuvette system equipped with a BINOS-100 infra-red gas analyser (Walz, Germany). Leaves were placed in a cuvette that tracked ambient temperature in the growth cabinet. Net CO_2 assimilation was calculated every 15 minutes over the course of each run, resulting data was transferred off and analysed in Diagas (Walz, Germany).

2.2.5 Metabolite Sampling and Analysis

Whole leaves were sampled from *K. blossfeldiana* and *K. fedtschenkoi* to determine levels of titratable acidity, soluble sugars, and starch. For the 24 hr sampling (Figure 2.3) *K. blossfeldiana* young leaves (leaf pairs 9 and 10 from the bottom) and mature leaves (leaf pairs 2 and 3 from the bottom) were sampled every four hours from four hours before dusk onwards. For the dawn/dusk samplings *K. blossfeldiana* 1 cm leaf punches were sampled up the plant from the 2nd leaf pair at the bottom until the 10th leaf pair at the top and *K. fedtschenkoi* were sampled at the 6th leaf pair from the top. All samples were immediately frozen in liquid nitrogen and subsequently stored at -80 °C before analysis.

A methanol extraction method was used for all metabolite analyses. Whole leaves or five epidermal peels were used, both were collected by flash freezing in liquid nitrogen. Whole leaves were ground by mortar and pestle with liquid nitrogen, with of 250 mg of tissue collected for analysis. Epidermal peels were smashed with a prechilled TissueLyser II (Qiagen, USA) for 2 minutes at 30 Hz with a single 2 mm metal beads. Then 80% methanol was added, 1 ml for whole leaves and 500 µl for epidermal peels. Samples were then incubated at 60°C for 40 minutes and then spun down at 13,000 rpm for 10 mins and stored at 4°C until further analysis. Titratable acidity of 200 µl methanol extracted tissue was calculated by titrating against 5 mM NaOH until neutrality, using phenolphthalein as indicator, determining titratable acidity per fresh weight. Whole leaf total soluble sugars were determined by measuring glucose equivalents using a phenol–sulfuric acid colorimetric method (Dubois et al., 1956), with 50 µl methanol extract diluted with 450 µl ddH₂O and 0.5 ml 5% phenol then 2.5 ml concentrated sulphuric acid added. After incubation for 15 minutes absorbance was read at 482 nm. A glucose standard curve with concentrations between zero and 150 µg glucose was used to calculate total glucose equivalents per fresh weight. Whole leaf starch content was determined from the insoluble fraction of the methanol extraction. The supernatant was removed and the insoluble pelleted washed twice in ddH₂O, followed by the addition of 1.5 ml acetate buffer (0.1 M sodium acetate, pH 4.5, adjusted with acetic acid) and incubation at 90°C for one hour. Starch extracts were digested over night at 40°C with 300 units of amyloglucosidase (Sigma-Aldrich). Starch content was determined as glucose equivalents per fresh weight as described above (Dubois et al., 1956).

2.2.6 Protein Extraction and Western blots

Protein was extracted from *K. blossfeldiana* whole leaf tissue for western blots. Leaf tissue was flash frozen in liquid nitrogen and stored at -80°C until mortar and pestle grinding with liquid nitrogen, with 200 mg ground tissue used for protein extraction. Then 500 μl protein extraction buffer (0.5 M Tris-HCl (pH8), 10 mM EDTA, 1% (v/v) Triton-X, 5 mM Urea, 2% (w/v) PEG 20,000, 10 mM DTT) was added followed by immediate re-freezing in liquid nitrogen, samples were then thawed on ice and spun at 13,000 rpm for 10.5 minutes at 4°C . 300 μl supernatant was recovered and added to 700 μl acetone on ice, samples were again re-frozen in liquid nitrogen, and left to thaw on ice. After thawing, samples were spun at 13,000 rpm for 7.5 minutes at 4°C , acetone supernatant was discarded, and samples resuspended in 100 μl 4x SDS Lamelli buffer (20% glycerol, 240 mM Tris/HCl pH 6.8, 8% (w/v) SDS, 0.4% (w/v) bromophenol blue, 100 mM DTT). Samples were incubated while shaking at 65°C for 20 minutes and spun down at full speed for five minutes. Extracted proteins were separated using SDS-page and transferred to nitrocellulose using a Trans-Blot Turbo Transfer System (Bio-Rad, USA). Ponceau stain was washed off and the blot was incubated overnight with 1:3000 anti-PEPC (Agrisera, AS09458) and 1:3000 anti-Rubisco large subunit (Agrisera, AS03037, RbcL) polyclonal antibodies to identify PEPC and RbcL bands. Goat anti-Rabbit IgG secondary antibody (Agrisera,AS09602) was used at 1:50000 dilution and detection was performed using chemiluminescence with SuperSignal West Pico PLUS Chemiluminescent substrate (Thermo Scientific, USA).

2.2.7 Morphological analysis

Single leaves of *K. blossfeldiana* plants were removed at every two leaf pair intervals down the plant, with the opposite leaf in the pair used for dawn/dusk methanol extractions to calculate corresponding changes in titratable acidity. Leaves were removed underwater, with great care taken to ensure their petiole remained submerged, and hydrated to full turgor for 24 hrs in the same growth conditions as they were grown in. After 24 hrs leaves were dabbed dry, weighed to determine fresh mass at full turgor and imaged in a scanner, leaf area was calculated using ImageJ (Schneider et al., 2012). Leaves were then dried at 75°C for 48 hrs and re-weighed to determine dry mass. Leaf dry mass per area was calculated as dry mass divided by leaf area (Equation 2.1). Water mass per area was calculated as fresh mass at full turgor subtracted by dry mass and then divided by leaf area (Equation 2.1). Saturated water content was calculated by dividing water mass area by leaf mass area.

Equation 2.1 - Leaf dry mass per area, dry mass (DM) divided by leaf area (LA)

$$LMA = \frac{DM}{LA}$$

Equation 2.2 – Water mass per area (WMA), with fresh mass at full turgor (FM_{FT})

$$WMA = \frac{FM_{FT} - DM}{LAK}$$

Equation 2.3 – Saturated Water Content (SWC)

$$SWC = \frac{WMA}{LMA}$$

2.3 Results

2.3.1 Young and mature *K. blossfeldiana* leaves have distinct photosynthetic phenotypes

The young and mature *K. blossfeldiana* leaves had distinct patterns of gas exchange. The young leaves (10th leaf pair from the bottom) assimilated all of their CO₂ during the day with no nocturnal net CO₂ assimilation; and the mature leaves (2nd leaf pair from the bottom) assimilated most of their CO₂ during the night with some assimilation during the day (Figure 2.1.A). The young leaves assimilated a substantially higher amount of CO₂ over the entire diurnal period than the mature leaves. Accordingly, stomatal conductance in the young leaves was much greater during the day period (Figure 2.1.A). Conductance in the mature leaves peaked at the start of the day and overnight. Interestingly, nocturnal stomatal conductance was positive in the young leaves despite no nocturnal net CO₂ assimilation. Differences in stomatal conductance between these C₃ and CAM performing tissues are explored in more detail in chapter 3.

2.3.2 Crassulacean acid metabolism is rapidly induced in young *K. blossfeldiana* leaves by drought

CAM can also be rapidly induced in the young *K. blossfeldiana* leaves by drought (Figure 2.1.C, 10th leaf pair from the bottom). Some 90 days after propagation, plants were droughted for ten days with water withheld from the end of day one until plants were re-watered after eleven days. Two days after the withholding of watering, these young leaves showed some net nocturnal CO₂ assimilation, increasing in magnitude until day ten. Daytime net CO₂ assimilation reduced over the same period (Figure 2.1.C). A CAM-like pattern of daytime gas exchange developed after two days, with a noticeable reduction of CO₂ assimilation during the middle of the day and phase two and four peaks appearing at the early day and late night (Figure 2.1.C). This continued until a marked reduction in daytime assimilation five days after droughting to an apparent zero. Total assimilation stayed relatively flat after this transition to nocturnal only net CO₂ assimilation until the recommencing of watering after eleven days of drought (Figure 2.1.C). Upon rewatering there was a fast increase in nocturnal assimilation,

within less than 24hrs. This was followed by a return to daytime CO₂ assimilation one day after re-watering (Figure 2.1.C). Notably, even after re-watering there was no return to the original C₃ physiotype in the young droughted *K. blossfeldiana* leaves but a continuation of nocturnal CO₂ assimilation along with daytime CO₂ assimilation. This daytime CO₂ assimilation and total CO₂ assimilation over each diurnal period was substantially reduced in the young droughted *K. blossfeldiana* leaves, even after re-watering, compared to the pre-drought levels.

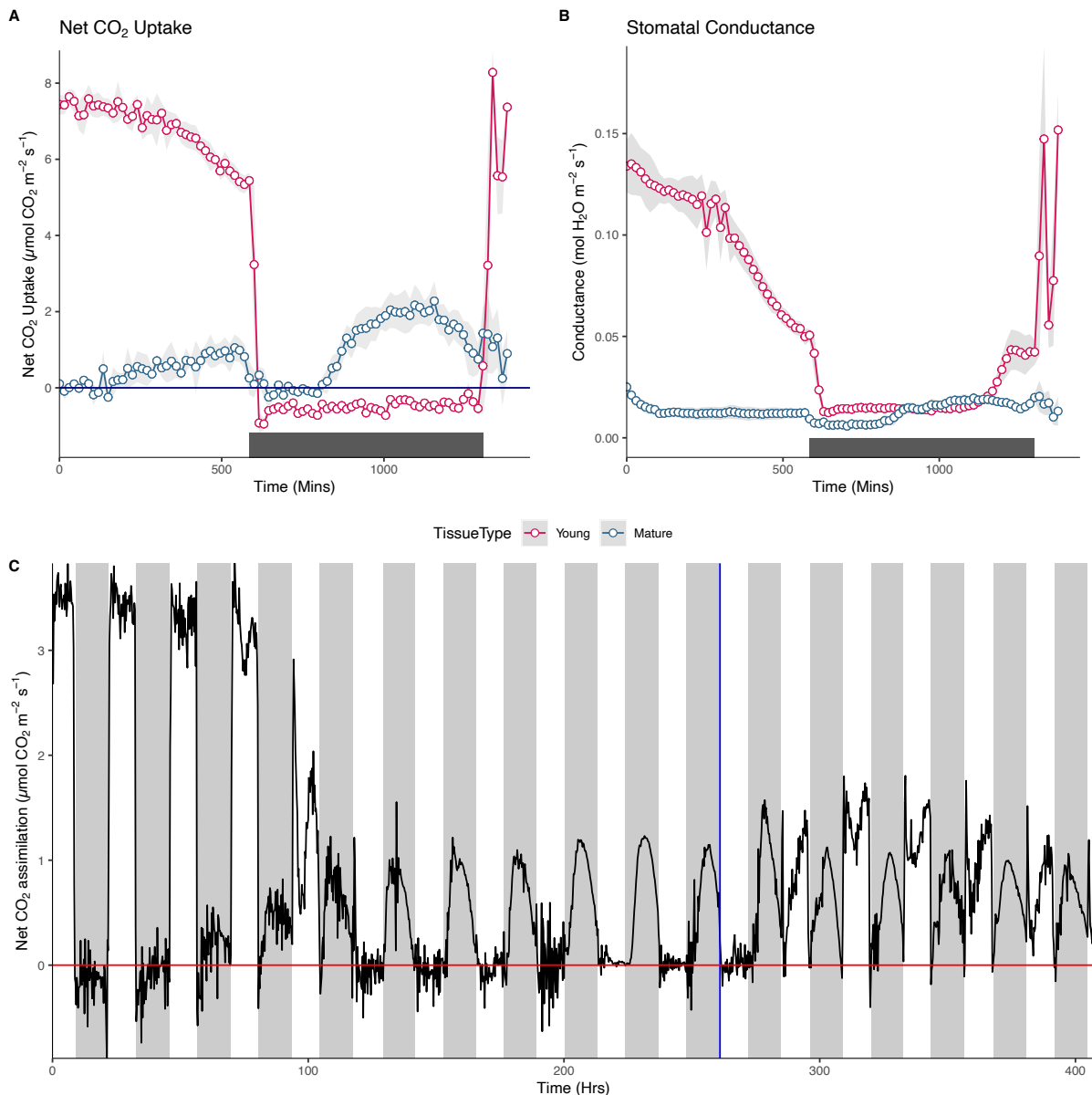


Figure 2.1 *K. blossfeldiana* age specific photosynthetic traits and CAM induction. Diurnal net CO₂ uptake (panel A, µmol CO₂ m⁻¹ s⁻¹) and stomatal conductance (panel B, mol H₂O m⁻¹ s⁻¹) of *K. blossfeldiana* young leaves (red points, 10th leaf pair from the bottom) and mature leaves (blue points, 2nd leaf pair from the bottom) between 60-90 days after propagation. For panel A and B points represent the mean of three repeats and the shaded interval ± SEM. Horizontal blue line equals zero, panel A. CAM induction by drought (Panel C). Net CO₂ assimilation (µmol CO₂ m⁻¹ s⁻¹) of a *K. blossfeldiana* young leaf (10th leaf pair from the bottom) at 90 days after propagation droughted for 10 days and re-watered on day 11. Horizontal red line indicates zero net CO₂ assimilation. Vertical blue line indicates time of return to normal watering regime.

2.3.3 Young *K. blossfeldiana* leaves are more photosynthetically active than Mature *K. blossfeldiana* leaves

Over 24 h, young *K. blossfeldiana* leaves assimilated substantially more CO₂ than the mature leaves, with all net gains made during the day and a net loss at night (Figure 2.2). Notably, the young C₃ leaves had a greater daytime water usage efficiency (WUE, μmol CO₂ mol H₂O⁻¹), compared to mature CAM *K. blossfeldiana* leaves which was driven by their greater level of daytime CO₂ assimilation. Overall WUE was slightly but not significantly (Wilcox test, P>0.05) higher in the mature CAM leaves, which was driven by greater nocturnal net CO₂ assimilation when total transpiration is lower, with ~3/4 of net CO₂ assimilation occurring at night in the mature leaves (Figure 2.2). While assimilating a much greater amount of CO₂ the young leaves were also losing significantly more water via overall transpiration than the mature CAM performing leaves, especially during the day. The WUE of the young leaves was also negatively impacted by substantial nocturnal conductance and thus water loss but without net carbon assimilation at night (Figure 2.2).

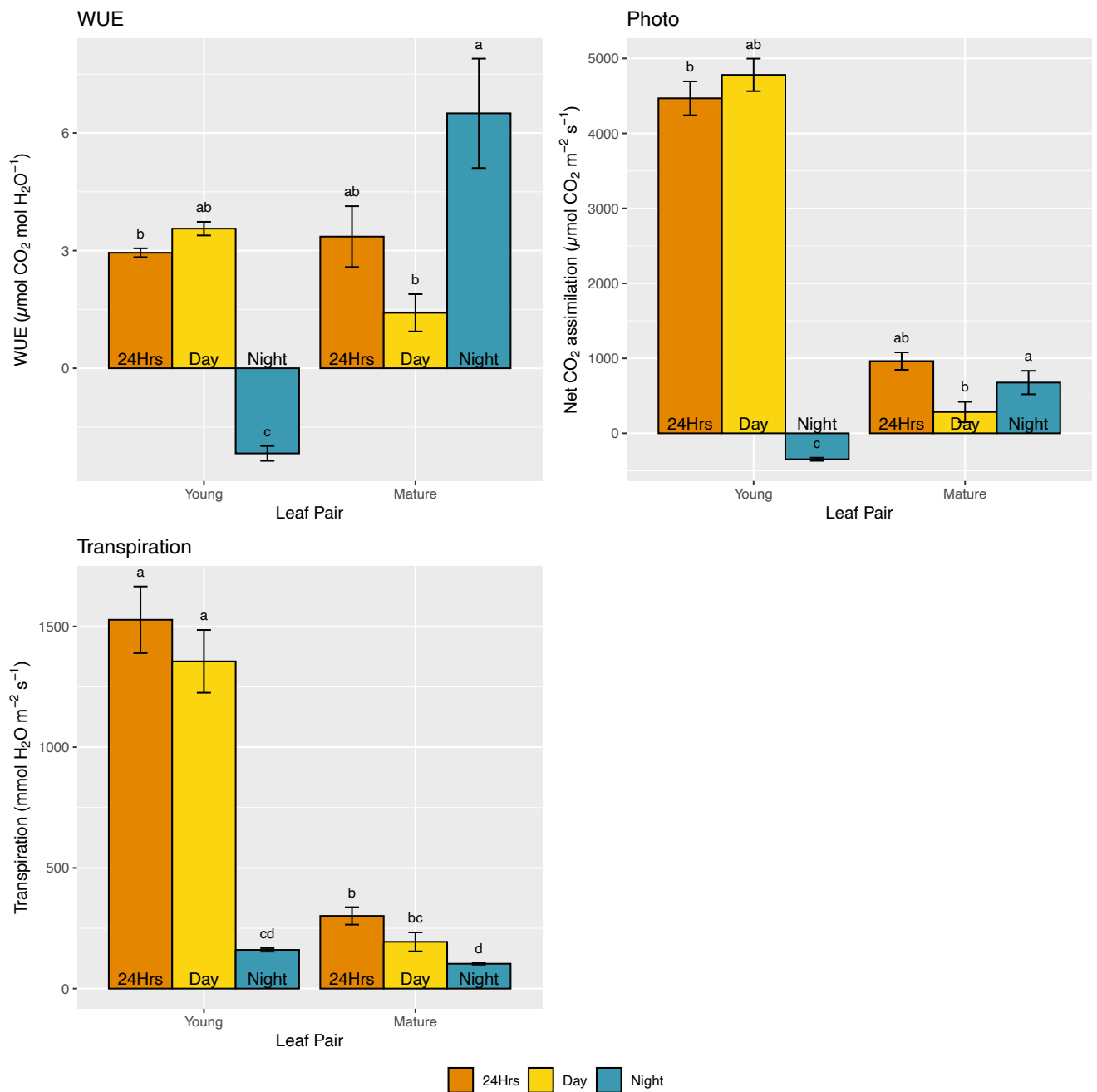


Figure 2.2 Integrated water use efficiency (WUE, left top), overall net CO₂ assimilation ($\mu\text{mol CO}_2 \text{ m}^{-1} \text{ s}^{-1}$), and overall transpiration over a full 24hrs, the day or night period in *K. blossfeldiana* young (left side, 10th leaf pair from the bottom) or mature leaves (right side, 2nd leaf pair from the bottom) at 60-90 days after propagation. Values are the mean of three replicates \pm SEM. Plants were grown in standard conditions with 400 ppm CO₂ and 190 $\mu\text{mol m}^{-2} \text{ s}^{-1}$ light. Statistical analysis was performed by using a two-way ANOVA, significant differences ($P < 0.05$) are indicated by different lowercase letters.

2.3.4 Young *K. blossfeldiana* leaves did not accumulate titratable acids at night

In keeping with the above gas exchange data, the young *K. blossfeldiana* leaves (10th leaf pair from the bottom) did not accumulate titratable acidity overnight, with no accumulation observed overnight in the tenth leaf pair from bottom ($P > 0.05$, Figure 2.3 A and B). In contrast, the mature leaves (2nd leaf pair from the bottom) did accumulate substantial amounts of titratable acidity overnight. There was also a slight but not significant ($P > 0.05$) accumulation of titratable acidity in the ninth leaf pair from the bottom, suggesting the presence of some CAM activity. In figure 3, nocturnal accumulation of titratable acidity appeared to increase progressively down the plant. The 24 hr graph of titratable acidity also shows a strong and steady accumulation of titratable acidity overnight in the mature leaves, with little change in the young leaves (Figure 2.3 A).

2.3.5 Significant differences in whole leaf metabolism between young and mature leaves of *K. blossfeldiana*

Soluble sugar contents were substantially, ~2-3x higher (Figure 2.3.B), in the young *K. blossfeldiana* leaves compared to the mature leaves, which was consistent with the ~4x difference in total net CO₂ uptake over 24 hrs (figures 2.1 and 2.2). There was also a difference in the diurnal content of whole leaf starch, with the younger leaves showing greater peaks in starch contents at dusk compared to that in mature leaves (Figure 2.3.D). However, overall this difference in starch content between young and mature leaves was not as large as that seen with soluble sugars (Figure 2.3). There was a much more defined pattern of diel starch metabolism than that of soluble sugars across all leaf ages, with whole leaf starch accumulating to peak at the end of the day and then steadily decline overnight (Figure 2.3.D). The nocturnal degradation of starch was also greatest in the younger leaves. Over the diel period, soluble sugar contents remained fairly stable in the mature leaves, while there was a slight degree of soluble sugar accumulation in the young leaves during the day (Figure 2.3.C).

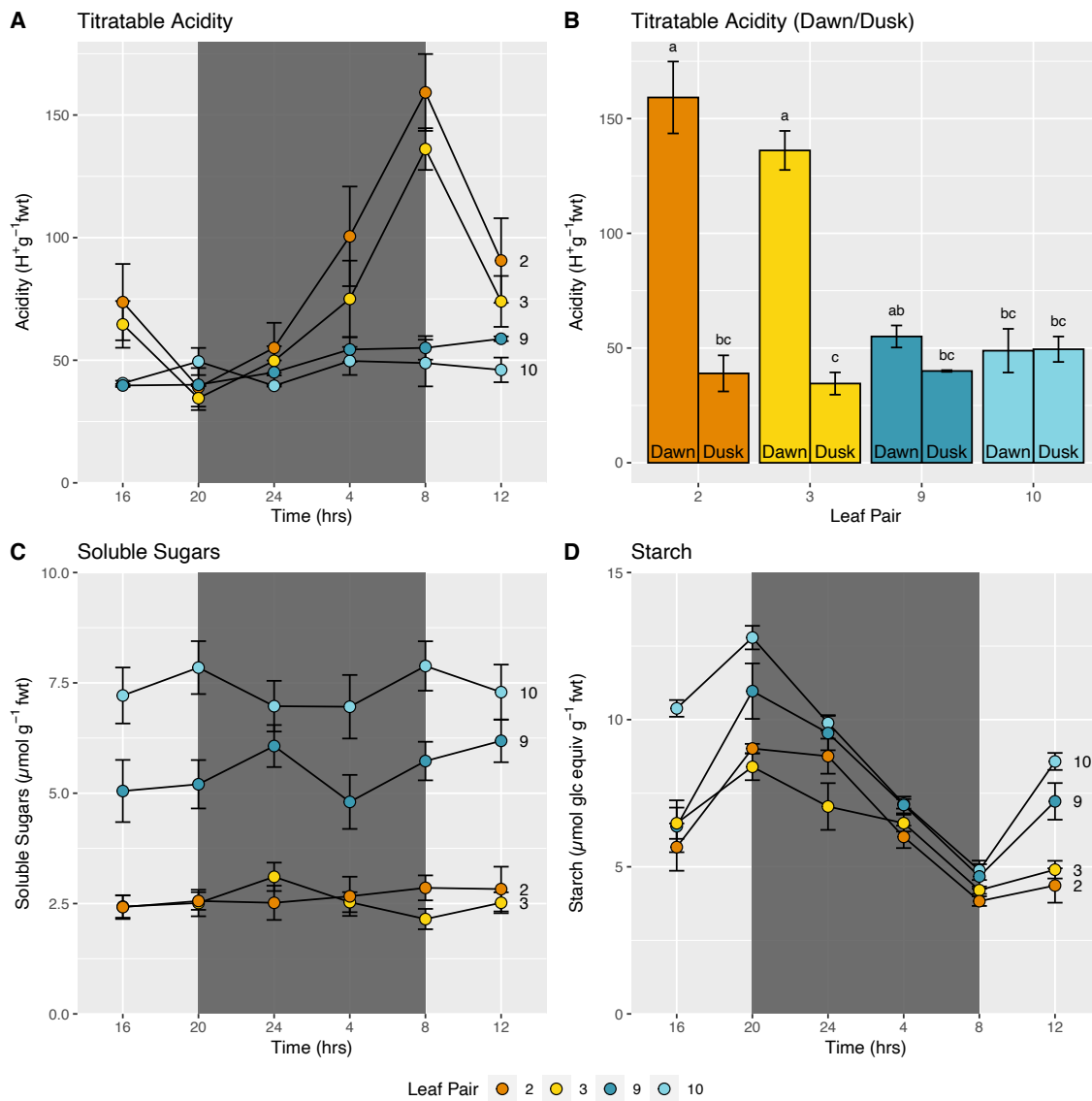


Figure 2.3 *K. blossfeldiana* age specific whole leaf titratable acidity and metabolites. Titratable acidity ($\mu\text{mol H}^+ \text{g}^{-1} \text{fwt}$) over 24hrs (Panel A), differences in dawn/dusk titratable acidity ($\mu\text{mol H}^+ \text{g}^{-1} \text{fwt}$) increase with leaf age (Panel B), soluble sugars ($\mu\text{mol Glc equiv g}^{-1} \text{fwt}$) over 24 hrs (Panel C), starch ($\mu\text{mol Glc equiv g}^{-1} \text{fwt}$) over 24hrs (Panel D). Leaf pair two is the oldest (2nd leaf pair from bottom) and ten the youngest (10th leaf pair from bottom). Leaves were sampled every four hours, with the first sampling 4 hrs before dusk. All plants sampled 90 days after propagation. Values are means of four replicates \pm SEM. Statistical analysis was performed by using a two-way ANOVA, significant differences ($P < 0.05$) are indicated by different lowercase letters for Panel B.

2.3.6 PEPC Protein

The abundance *PEPC1* protein over the diel period in both young and mature were relatively stable (Figure 2.4 A,B,C). The mature *K. blossfeldiana* leaves expressed substantially higher detectable levels of *PEPC1* protein than the young leaves, as shown in the western blot in figure 2.4.D, which in line with the previous results on their differences in CAM activity.

This difference was also apparent between the young and mature leaves in the 24hr *PEPC1* and *RBCL* blots, however, comparisons between blots are less robust. Between the young and mature leaves there appeared to be some differences in the abundance of *RBCL*, with slightly higher levels in the young leaves (Figure 2.4.D).

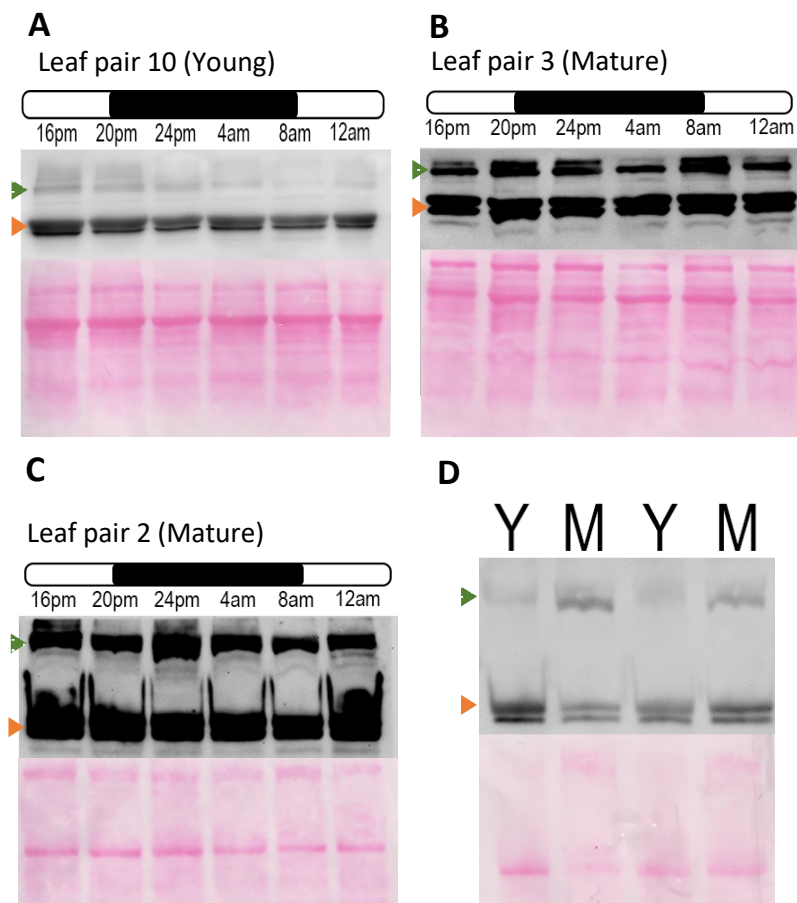


Figure 2.4 *K. blossfeldiana* age specific western blot analysis of *PEPC1* (upper band) and *Rbcl* (lower band) abundance in young leaves (10th leaf pair from the bottom, Panel A), mature leaves (2nd and 3rd leaf pairs from the bottom, Panel B and C) over 24hrs; and a comparison on expression between young leaves (10th leaf pair from the bottom) and mature leaves (2nd leaf pair from the bottom) at dusk (Panel D). Proteins were separated by SDS-Page, blotted with *PEPC1* and *Rbcl* antibodies. Equal loading was shown by ponceau staining the blot (lower section) prior to antibody incubation; the blot is representative of at least three replicates. The 20 pm timepoint was carried out in darkness, while the 8 am timepoint was in the light. The triangle represents the position of *PEPC1* (green triangle) and *RBCL* (orange triangle).

2.3.7 Morphology and the development of CAM traits

Whilst figure 2.3 shows a progressive increase in nocturnal titratable acidity accumulation down the plant (i.e. as leaves age), the true peak of nocturnal titratable acidity accumulation was found in the middle of the plant. This is shown in figure 2.5 with a peak in the accumulation of nocturnal acidity found in leaf pair six (six leaves from bottom), in plants grown in normal lighting conditions ($\sim 190 \mu\text{mol m}^{-2} \text{s}^{-1}$). Changes in light intensity, had a substantial effect on the nocturnal accumulation of titratable acidity, with *K. blossfeldiana* plants grown in normal lighting conditions ($\sim 190 \mu\text{mol m}^{-2} \text{s}^{-1}$) for 90 days after propagation showing much higher changes in dawn/dusk titratable acidity than those grown in low light ($\sim 90 \mu\text{mol m}^{-2} \text{s}^{-1}$, Appendix Figure A5.1). While nocturnal accumulation of dawn/dusk titratable acidity peaked in leaf pair six, interestingly, saturated water content increased progressively with leaf age in *K. blossfeldiana* (Figure 2.5).

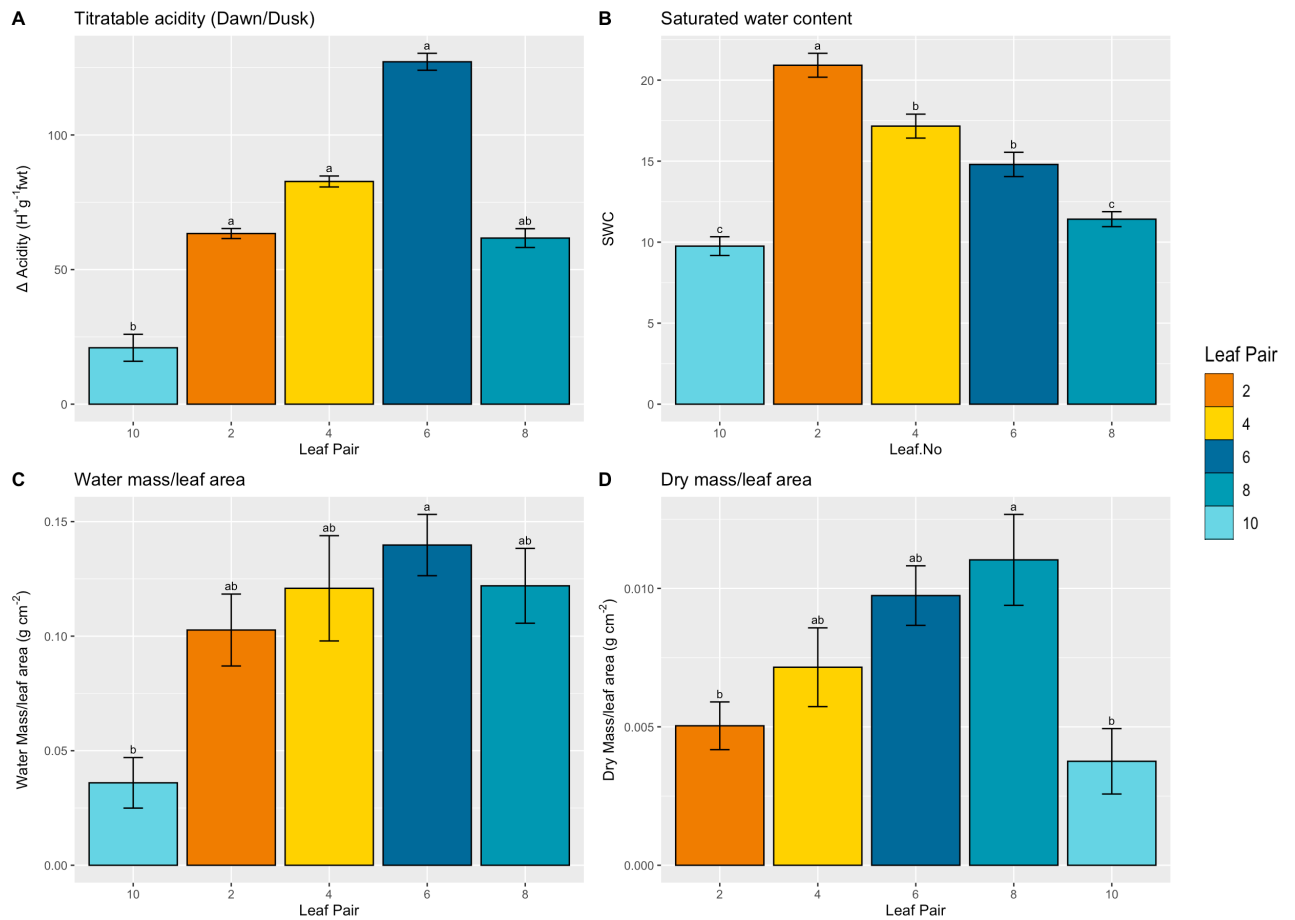


Figure 2.5 CAM traits across different leaf pairs in *K. blossfeldiana* plants sampled 90 days after propagation, grown in normal light (normal bars, 190 $\mu\text{mol Photons}$). Dawn/Dusk whole leaf titratable acidity (Panel A), leaf saturated water content (SWC, Panel B), leaf water mass per leaf area (Panel C, WMA), leaf dry mass per leaf area (LMA, Panel D). Leaf pairs are numbered up the plant, with 12 being the youngest sampled. Numbers above bars on the top left panel indicate sample number, values are means of the noted number of replicates \pm SEM. Statistical analysis was performed using one-way ANOVA, significant differences ($P < 0.05$) are indicated by different lowercase letters.

2.3.8 *K. fedtschenkoi pepc1.1* mutants are impaired in CAM

CRISPR driven knock down of *phosphoenolpyruvate carboxylase isoform 1 (PEPC1)* led to an almost complete reversal of photosynthetic phenotype in *K. fedtschenkoi pepc1.1* mutant compared to wild type (Figure 2.6). Wild type leaves assimilated most of their carbon during the night with a limited amount of net CO₂ assimilation towards the end of the day (Figure 6.A). The wild type *K. fedtschenkoi* also showed a reduced period of assimilation during the early part of the night, like that observed in the mature CAM performing *K. blossfeldiana* leaves (Figure 2.1). Alongside this reversal of photosynthetic phenotype between mutant and wild type *K. fedtschenkoi*, there was a similar reversal of stomatal conductance, with the *pepc1.1* mutants showing highest values of stomatal conductance during the day and this was significantly reduced at night. Interestingly, the *pepc1.1* mutant did show some net nocturnal stomatal conductance during the night (Figure 2.6.B), which may have been driven by some residual nocturnal carbon assimilation. The *pepc1.1* mutants also showed a significant, almost 10 fold, reduction in nocturnal titratable acidity accumulation compared to the wild type (Figure 2.6.C). A second independent mutant *pepc1.2* showed a less significant and more variable reduction in nocturnal titratable acidity (Figure 2.6.C) and showed a more CAM like phenotype compared to *pepc1.1* in gas exchange experiments (Nwokeocha, 2022).

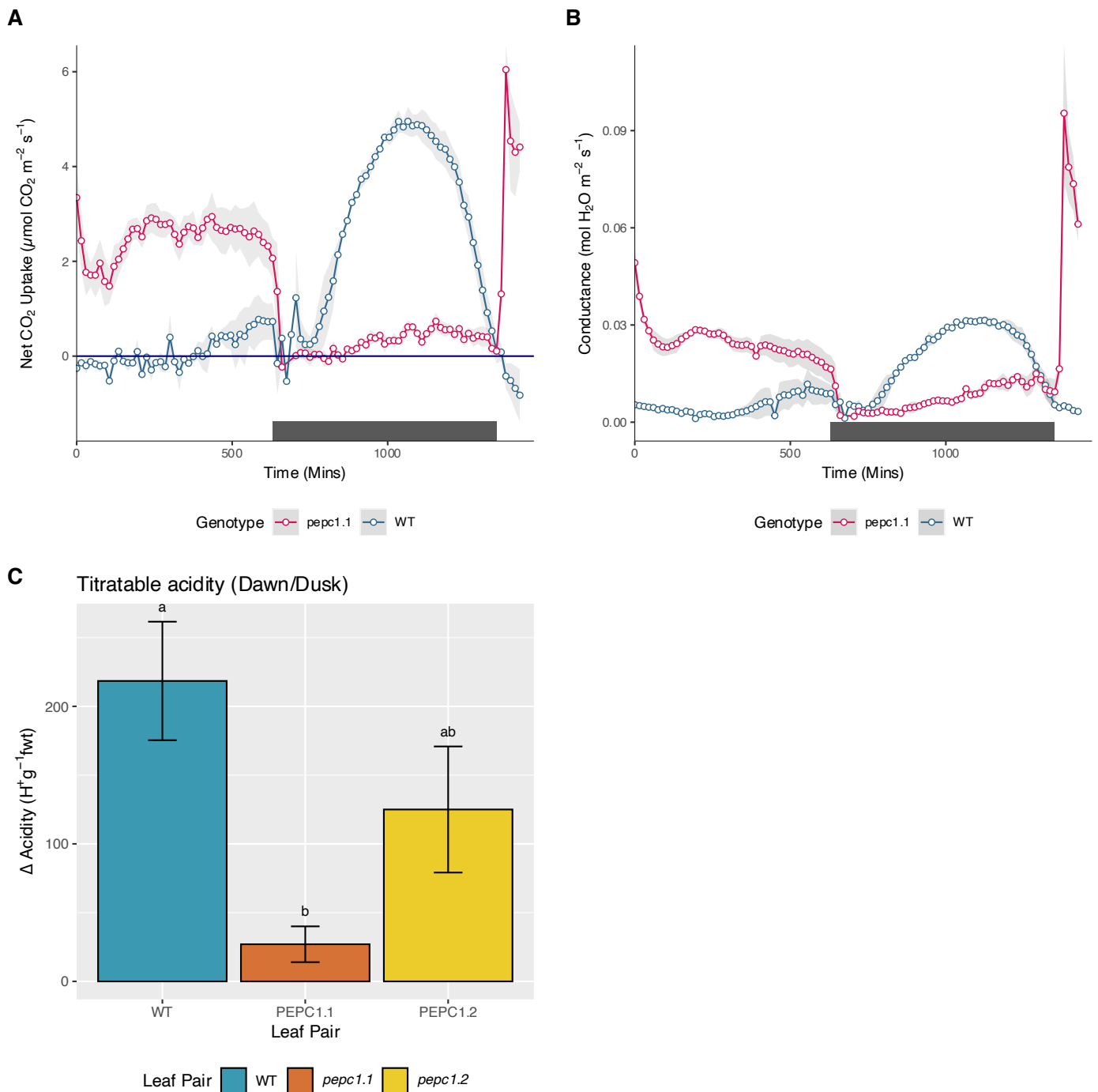


Figure 2.6 *K. fedtschenkoi* genotype specific photosynthetic traits and whole leaf titratable acidity. Diurnal net CO₂ uptake (panel A, $\mu\text{mol CO}_2 \text{ m}^{-2} \text{ s}^{-1}$) and stomatal conductance (panel B, $\text{mol H}_2\text{O m}^{-2} \text{ s}^{-1}$) of wild type *K. fedtschenkoi* leaves (blue points) and *pepc1.1* leaves (red points) between 90-120 days after propagation. Leaf pair 6 was used in both genotypes. Plants grown in 12hr/12hr day/night cycles. Dark shaded area represents night. For both graph, points represent the mean of three repeats and the shaded interval \pm SEM. Differences in dawn/dusk titratable acidity ($\mu\text{mol H}^+ \text{ g}^{-1} \text{ fwt}$) between wild type *K. fedtschenkoi*, *pepc1.1* and *pepc1.2* leaves (Panel C). Points represent the mean of at least five samples and \pm SEM. The dark blue line on the CO₂ uptake graph equals zero. Statistical analysis was performed using one-way ANOVA, significant differences ($P < 0.05$) are indicated by different lowercase letters.

2.4 Discussion

2.4.1 *Kalanchoe blossfeldiana* – A tale of two phenotypes

Young and mature *K. blossfeldiana* leaves, grown to 90 days after propagation from cutting, showed distinct phenotypes. The young leaves (10th leaf pair from bottom) displayed C₃ metabolism with no net nocturnal accumulation of CO₂ (Figure 2.2) and no overnight accumulation of titratable acidity (Figure 2.3). Whereas the mature leaves (2nd leaf pair from bottom) performed CAM, assimilating ~2/3 of their CO₂ overnight, nocturnally accumulating substantial amounts of titratable acidity, and expressing greater levels of PEPC protein than the young leaves (Figure 2.4). The accumulation of titratable acidity in the mature leaves was comparable to that seen in *K. fedtschenkoi* and *K. pinnata* but lower than that of *K. daigremontiana* (Ceusters et al., 2021; Griffiths et al., 2008).

CAM was rapidly induced in *K. blossfeldiana* young leaves by drought, with nocturnal net CO₂ assimilation observed two days after droughting and no net daytime assimilation after six days of drought (Figure 2.1). This rapid induction of strong CAM has also been observed in other members of the *Kalanchoe* genus – *K. porphyrocalyx* and *K. miniate* (Brulfert et al., 1996); and is in line with previous reports that PEPC activity is rapidly increased in response to drought in *K. blossfeldiana* (Taybi et al., 1995). However, unlike facultative CAM plants, it appears that once CAM is induced in the young *K. blossfeldiana* leaves it remains active even after the return to watering; in keeping with previous reports (Queiroz and Brulfert, 1982) and the suggestion that CAM is not optional in *K. blossfeldiana* (Winter and Holtum, 2014). Once watering recommenced the young leaves rapidly restarted daytime net CO₂ assimilation while continuing to assimilate CO₂ at night, which is similar to observations made of *K. porphyrocalyx* and *K. miniate* (Brulfert et al., 1996). It is also unlikely that the leaf ever returns to C₃ after this point as this period will coincide with age induced CAM induction. The effects of drought on CAM induction in *K. blossfeldiana* on the whole plant level need further study as questions remain, for instance, would CAM be immediately induced in the new emerging leaves or are they constrained by the metabolic costs of CAM.

Levels of CAM in *K. blossfeldiana* leaves can be modulated by changing light intensity, with much greater amounts of titratable acidity accumulated overnight in plants grown with

normal light intensity (~190 μmol Photons) compared to those grown in low light (~90 μmol Photons, figure 9.1). This has also been observed in *K. fedtschenkoi* (Zhang et al., 2020) and is likely driven by a reduction in available carbon due to decreased photosynthesis, which in turn would reduce the amount of available carbon skeletons for CAM. A view that is supported by a reduction in soluble sugar contents and leaf starch and dawn/dusk net turnover of both, as also observed in *K. fedtschenkoi* plants grown in reduced light intensity by (Zhang et al., 2020).

2.4.2 Whole Leaf Metabolism in *Kalanchoe blossfeldiana*

Leaf soluble sugar contents were significantly, ~2-3x higher, in the young *K. blossfeldiana* leaves compared to the mature leaves, which is consistent with the ~4x difference in total net CO_2 assimilated over 24 hrs (Figures 2.2 and 2.3). There were also greater levels of whole leaf starch in the young leaves compared to mature, however, this difference was not as large as that in soluble sugar contents. The nocturnal depletion of starch was also greatest in the younger leaves. Both of these observations are in keeping with previous work with the facultative/inducible CAM plant *Mesembryanthemum crystallinum*, which showed similarly higher levels of soluble sugars and starch prior to the induction of CAM (Taybi et al., 2017). However, it is not clear whether this is due to CAM or is a by-product of ageing.

It is likely that the transition from C_3 to CAM requires a build-up of carbon, and that the substantially greater levels of carbohydrates observed, mainly in the form of soluble sugars in the young leaves, are preparation for this transition. CAM requires a supply of carbon skeletons to build up PEP for nocturnal carboxylation. Recent flux balance analysis and experimental data have also suggested that CAM requires higher nocturnal respiration rates (Shameer et al., 2018; Töpfer et al., 2020; Tay et al., 2021; Leverett et al., unpublished). Shameer et al. (2018) modelled that CAM required more ATP than C_3 overnight to drive the ATP-tonoplast proton pump to ensure malate can be stored in the vacuole; and to also ensure the high flux through phosphofructokinase to produce PEP for nocturnal carboxylation. CAM plants can store carbon as starch for regenerating PEP, which has been predicted to be more efficient than sugar storing CAM plants (Shameer et al., 2018). Due to the observed diel cycling of starch it appears likely that *K. blossfeldiana* mature leaves use starch as their carbon store for PEP regeneration, with soluble sugar contents appearing fairly flat over the 24 hr period

(Figure 2.3), which is in keeping with other members of the *Kalanchoe* genus (Borland et al., 2016). However, it is possible that the leaves transitioning into CAM may use soluble sugars or a mix, which may be advantageous in a fast transition. Further work is needed to explore the fluxes of carbon over the diel period between the C₃ and CAM tissues; and how these fluxes change during the transition to CAM. Figure five shows that that CAM activity, as shown by nocturnal acid accumulation, peaks midway down the plant at leaf pair six. This would suggest that the reduction of soluble sugar contents down the plant may be due to ageing and fulfilling carbon demand for leaf growth rather than being a result of the transition to CAM, however this could be investigated by further study of soluble sugar contents of leaves as they transition to CAM.

It is both likely that the young *K. blossfeldiana* leaves build up carbon, that could allow for a rapid transition to CAM, as seen in figure 2.1.C in response to drought; and that the mature leaves have reached a point in which they have a reduced demand for carbon and reduced access to light due to overlapping leaf growth above. Interestingly, after droughting, the young leaves do not return to a C₃ state when re-watered unlike most other facultative CAM plants which can reversibly switch and return from CAM (Winter & Holtum, 2014). It is not clear why this is the case; further investigations will be needed to explore why some inducible CAM species and revert to C₃ and others like *K. blossfeldiana* cannot. It would also be informative to study drought induction on the whole plant level.

The drought-induced CAM leaves also do not return to the same levels of carbon assimilation after water was returned. It is possible that this might be in anticipation of further droughts or that there is a post-drought metabolic constraint preventing either the return to C₃ only or previous levels of carbon assimilation. At the whole plant level, it may be more efficient and effective to invest in a new C₃ performing leaf than revert from CAM to C₃. Further work is needed to unpick these processes and establish the interplay between C₃ and CAM performing leaves on a whole plant level.

The strongest difference in photosynthesis phenotype was observed between the young leaf pair ten and the mature leaf pair two. This clear distinction between C₃ photosynthesis in the young leaves and CAM in the mature leaves make it a good system for comparing C₃ and CAM physiology; and will be the basis for further study in this thesis. The middle leaf pair six, that showed a substantial amount of both daytime and nocturnal carbon assimilation may also

make for an interesting phenotype for future works and CAM bioengineering, as it shows an example of how productive the C₃/CAM phenotype can be in terms of 24 h net CO₂ assimilation. The striking difference in carbon uptake and soluble sugars between the young and mature *K. blossfeldiana* leaves raises some interesting questions as to how carbon is assimilated and utilised on the whole plant level, with young C₃ leaves appearing to act like source tissue and the mature CAM performing leaves like sink tissues. Such questions may be answered by carbon isotope and whole plant gas exchange experiments. Answering these questions may help to unravel the carbon mechanics behind CAM plants ability to avoid carbon starvation during long periods of drought.

2.4.3 The PEPC1 isoform is essential for CAM in *K. fedtschenkoi*

Nocturnal carboxylation of PEP is a key step in the CAM cycle. In the *K. fedtschenkoi* genome there are reportedly five PEPC isoforms, compared to four in C₃ Arabidopsis, each of which could catalyse the formation of oxaloacetate from HCO₃ and phosphoenolpyruvate. In C₃ plants PEPC has been shown to play a key role in guard cell opening (Daloso et al., 2015) and carbon and nitrogen metabolism (Shi et al., 2015). *PEP* isoforms one (Kaladp0095s0055.1) and two (Kaladp0048s0578.1) have been shown to have CAM-like patterns of transcript expression in *K. fedtschenkoi*, suggesting that they may be the isoforms involved in the nocturnal carboxylation of PEP. The transcript abundance of *PEPC1* is, however, much greater (~30 times) than that of *PEPC2* and peaks towards the end of the day rather than the middle of the night (Yang et al., 2017). In recent *K. fedtschenkoi* proteomic data (Abraham et al., 2020) the *PEPC1* isoform also shows the greatest abundance and is phosphorylated only at night, which is essential for restricting PEPC activity to the night (Boxall et al., 2017). Data here showed that the *PEPC1* isoform is crucial for nocturnal carbon assimilation in *K. fedtschenkoi*, and that without it there is a reversion to a 'C₃-like' phenotype with much greater daytime carbon assimilation and only low levels of nocturnal carbon assimilation (Figure 2.6). Previous work has confirmed that the *pepc1* mutant shows substantial knockdown in the protein abundance of *PEPC1* and PEPC enzymatic activity (Nwokeocha, 2020). The remaining nocturnal assimilation and accumulation of acidity may be due to residual expression of *PEPC1* or the activity of the other PEPC isoforms. It is unclear what drives variation in reduction in nocturnal acidity accumulation between *pepc1.1* and *pepc1.2* mutants, but it may be down to a

homozygous vs heterozygous insertion of the CRISPR mutation (Figure 2.6.C). Further work will be needed to investigate the roles that the different PEPC isoforms play in CAM, guard cell opening, and mesophyll metabolism.

Previous genetic perturbations of different components of the CAM cycle have shown similar phenotypes with regard to reduced CAM expression. With impairments in starch synthesis via the knockdown or mutation of *PGM* in *K. fedtschenkoi* (Hurtado-Castano, 2019) or *M. crystallinum* (Cushman et al., 2008); impairments in phosphorolytic starch degradation by knockdown of *PHS1* in *K. fedtschenkoi* (Ceusters et al., 2021); and direct knockdown of *PEPC1* in *Kalanchoë laxiflora* (Boxall et al., 2020) all resulting in reduced nocturnal malate accumulation and impaired CAM activity.

2.4.4 Conclusions

This chapter has explored the physiological and metabolic differences between C₃ and CAM tissues in two comparative systems, young (10th leaf pair from bottom) vs mature (2nd leaf pair from bottom) *K. blossfeldiana* leaves and wild type vs CAM deficient *K. fedtschenkoi pepc1* mutants. The two systems provide clear distinctions between the two photosynthetic phenotypes. Both comparative systems provide a platform for investigating key questions on CAM physiology and for this thesis in the comparison of guard cell physiology and metabolism between C₃ and CAM within and between the two systems.

There is, however, an important difference between the two systems that may be useful in differentiating between different elements of CAM. CAM is a complex process that requires the coordinated rescheduling of multiple components. While of these components need to be present to transition to CAM, the components that underpin the progression to CAM are still unclear. It is possible that some of these components are activated or can function independently of *PEPC1* and nocturnal carbon assimilation. The comparison of these two different systems for studying C₃ and CAM, i.e. the young and mature *K. blossfeldiana* leaves and wild type vs CAM deficient *K. fedtschenkoi pepc1* mutants provides a potential way of studying which elements of CAM remain intact without a functioning a *pepc1* and/or net nocturnal carbon assimilation. This may be of especial importance in the study of how stomatal conductance changes between C₃ and CAM, where the level of guard cell autonomy from mesophyll metabolism is currently unclear.

Chapter 3. Self-determined stomata - PEPC-mediated nocturnal carboxylation alone is not enough to drive nocturnal conductance in *Kalanchoe*

3.1 Introduction

In CAM plants it is not known how nocturnal mesophyll PEPC-driven carboxylation and guard cell conductance are coordinated nor is it currently understood how reliant nocturnal opening is on PEPC activity. Understanding the mechanistic basis of nocturnal stomatal opening is key for efforts to engineer CAM into C_3 species (Borland et al., 2014), as it is not clear whether adding the capacity for nocturnal carboxylation into a C_3 plant would lead to nocturnal stomatal opening or daytime closure or both. This chapter investigates links between mesophyll carbon assimilation and guard cell behaviour by comparing the stomatal physiology and metabolism of guard cells in two comparative systems, described in chapter one: C_3 young and CAM mature *K. blossfeldiana* leaves, and wild type constitutive CAM *K. fedtschenkoi* and the CAM deficient *pepc1.1* mutant. These two comparative systems are used in a series of experiments to explore the role of C_i and whole leaf carbon status in determining stomatal conductance. Ultimately, this chapter aims to answer the question: to what extent is stomatal conductance in CAM plants determined by PEPC-mediated carboxylation?

To answer this question it is important to note a key difference between the two C_3 tissues. The previous chapter has shown that *K. blossfeldiana* young leaves could be considered fully C_3 as they lack any CAM features – no titratable acidity, no nocturnal net carbon assimilation, and no CAM-like pattern of stomatal conductance. Whereas the *K. fedtschenkoi pepc1.1* mutants are deficient in PEPC-driven carboxylation but likely retain many other components related to CAM. This chapter hypothesises that if there is a regulatory or metabolic element of the guard cells that needs to change to enable nocturnal stomatal conductance there may be a difference in guard cell response to key stomatal conductance inducing stimuli between the fully C_3 young *K. blossfeldiana* leaves and the PEPC1-impaired *K. fedtschenkoi pepc1.1* mutant leaves.

The way in which mesophyll carbon assimilation influences guard cell behaviour can be considered in two parts: the role of C_i in linking mesophyll PEPC-driven carboxylation and stomatal opening and the role of carbon assimilation in the build-up of sugars and malate and how this influences stomatal behaviour.

3.1.1 The role of C_i in linking mesophyll PEPC-driven carboxylation and stomatal conductance.

Photosynthesis and stomatal conductance are closely linked in both function and regulation, often positively correlating with each other (Buckley & Mott, 2013); and the same can be observed with net carbon assimilation in CAM plants. However, conductance and assimilation can be decoupled when environmental conditions vary quickly (Lawson et al., 2011; McAusland et al., 2016); and in instances of nocturnal conductance in C_3 leaves (de Dios et al., 2016; Zeppel et al., 2014). Despite ample evidence of a close link between conductance and assimilation it is still unclear what exactly links them (Buckley & Mott, 2013; Farquhar & Sharkey, 1982; Wong et al., 1979). In both C_3 and CAM plants carbon assimilation decreases C_i which is a key signal for inducing stomatal opening. It has long been hypothesised that mesophyll cells could communicate assimilation status via changes in C_i .

There have been a number of other suggestions for links between guard cell conductance and mesophyll carbon assimilation such as red light (Gotoh et al., 2018) or a metabolic signal, such as ATP, NADPH, ribulose biphosphate (RuBP), malate or a sugar that could act upon the guard cells to respond to mesophyll photosynthesis (Fujita et al., 2013; Hedrich et al., 1994; Lee et al., 2008; Marigo et al., 1982; Tominaga et al., 2001; Zeiger & Zhu, 1998). However, this chapter focuses on the roles of C_i and leaf carbon status.

It has long been thought that the key link between mesophyll CAM and stomatal conductance is C_i (Griffiths et al., 2007; von Caemmerer & Griffiths, 2009; Wyka et al., 2005); with nocturnal conductance driven by reduced C_i as a result of carbon assimilation at night and daytime closure driven by increased C_i due to the decarboxylation of accumulated malate, to levels reportedly as high as $10,000 \mu\text{mol mol}^{-1}$ (Cockburn et al., 1979). In the constitutive CAM species *Kalanchoe daigremontiana* and *Kalanchoe pinnata* (Wyka et al., 2005; Griffiths et al., 2007; Von Caemmerer and Griffiths, 2009) showed strong responses to experimentally

reduced atmospheric CO₂ at key points in the diel CAM cycle; and as expected no response during day time closure in phase III. Interestingly they found this closure remained and was largely unchanged even after they starved the plants of CO₂ overnight reducing acid accumulation. Transcript abundance of key elements of the CO₂ response pathway were shown to be rescheduled in a comparison between C₃ Arabidopsis and the constitutive CAM species *Agave americana* (Abraham et al., 2016). Together these studies suggest that there may be other, yet unexplained, mechanisms acting on CAM guard cells preventing daytime opening and maintaining a CAM-like pattern of diel conductance.

This chapter investigates the role of C_i in linking mesophyll carbon assimilation and stomatal conductances and compares the responsiveness to reduced C_i between the C₃ and CAM tissues. This is explored in two ways: a low [CO₂] response assay that measures the change in stomatal conductance at different points of the diel cycle in response to a lowering of external [CO₂] from 400 μmol mol⁻¹ CO₂ to 70 μmol mol⁻¹ CO₂ for 30 minutes; and a separate experiment where external [CO₂] is held at 70 μmol mol⁻¹ CO₂ for 24 hrs while stomatal conductance is measured. It is hoped that these two methods will provide a measure of responsiveness to reduced C_i over 24 hrs and will assess if and how the responses differ between the C₃ and CAM tissues. The reason for both approaches is to compare instantaneous and sustained responses of stomata to a change in C_i. This may provide extra information about how long a response may be sustained, which may be of importance if guard cell metabolism has to change to sustain long periods of stomatal conductance at night in CAM leaves. This section hypothesises that guard cell sensitivity to C_i will vary over the diel period and between C₃ and CAM tissues.

3.1.2 Guard Cell Metabolism – Essential for powering nocturnal opening in CAM.

Stomatal opening requires energy and carbon skeletons for osmolytes such as malate and soluble sugars. It is likely that most of guard cell carbon, in the form of sugars or starch, is provided by mesophyll photosynthesis via the apoplast (Talbot & Zeiger, 1998). The impairment of mesophyll photosynthesis, the impaired import of sugars into the guard cells, and the inhibition of guard cell photosynthesis all lead to reduced stomatal conductance. Raising a key question – how and where do CAM guard cells obtain carbon and energy to enable nocturnal opening?

It has been hypothesised that the pattern of guard cell metabolism may differ between C₃ and CAM plants, in order to provide energy and osmolytes over the night for nocturnal opening. Recent data has shown that starch metabolism in *K. fedtschenkoi* guard cells has been rescheduled compared to C₃ plants, with starch broken down overnight in CAM as opposed to breakdown in the early day in *Arabidopsis* (Abraham et al., 2020). Guard cell starch metabolism is thought to play a key role in C₃ guard cell function (Lloyd, 1908), with a distinct pattern of starch metabolism compared to that of the mesophyll. Guard cell starch could provide a carbon sink that can be hydrolysed to provide sugars and malate to be used as osmolytes and energy for stomatal opening (Tallbott & Zeiger, 1993). This carbon sink may be of especial importance in CAM plants to sustain nocturnal opening without any direct energy input from photosynthesis. This chapter aims to explore this further by investigating whether the pattern of guard cell starch metabolism changes on the transition from C₃ to CAM as leaves age in *K. blossfeldiana* or between wild type obligate-CAM *K. fedtschenkoi* and CAM deficient *pepc1.1* mutant.

Overall this series of experiments compares C₃ and CAM guard cell metabolism in order to identify any fundamental differences in guard cell metabolism that may suggest a degree of independence between guard cells and the mesophyll, though it is not clear whether guard cell metabolism is regulated by the guard cells themselves, the mesophyll or a via combination of both.

3.1.3 Whole Leaf Carbon Assimilation and its influence on stomatal behaviour in C₃ and CAM systems

C₃ plants accumulate carbon from RUBSICO driven carboxylation which is partitioned into sugars for respiration, growth, or storage in starch. CAM plants do the same, while also allocating a portion of net carbon assimilate for the cyclic regeneration of PEP and accumulating malate overnight.

A key observation in chapter one was that whole leaf soluble sugars and starch contents were substantially greater in the *K. blossfeldiana* young C₃ leaves than the mature CAM leaves. Stomatal opening is an energy requiring process, with previous works showing that reduced soluble sugar import into the guard cells reduced conductance (Flütsch et al., 2020). This has

led to the question: what effect does this increased photo-assimilate in the C₃ tissues have on stomatal conductance, and to what extent does that explain differences between C₃ and CAM stomatal responses? This chapter aims to explore the influence of whole leaf carbon status on stomatal conductance by comparing the stomatal responses of *K. blossfeldiana* grown under two contrasting light environments (90 vs 190 $\mu\text{mol m}^{-2} \text{s}^{-1}$) or by reducing leaf [CO₂] to 70 $\mu\text{mol mol}^{-1}$ for 24 hrs in the C₃ and CAM leaves from both *K. blossfeldiana* and *K. fedtschenkoi* wild type and *pepc1.1* mutants.

These experiments were also used to explore the role of malate accumulation in CAM plants. CAM is also an energy hungry process and reduction in carbon assimilation by growth in reduced light has been shown, in chapter one and previously, to delay CAM and reduce nocturnal carbon assimilation. CAM can also be inhibited by holding nocturnal [CO₂] low over the night. So, an experiment where carbon assimilation is limited by reduced light or low [CO₂] will reduce photo-assimilate in plants with C₃ photosynthesis; or reduce the amount of malate accumulated in CAM plants overnight. Thus, experiments which reduced leaf carbon assimilation were also used to explore the role of nocturnal malate accumulation and its subsequent decarboxylation on the daytime stomatal closure. Malate decarboxylation increases C_i which is thought to trigger day-time closure.

3.1.4 Key questions and approach

The previous chapter showed a clear distinction in photosynthetic physiotypes between *K. blossfeldiana* young and mature leaves and between wild type *K. fedtschenkoi* and the *pepc1.1* mutant. This chapter aims to further probe these systems and establish if there are fundamental differences in stomatal behaviour and responses to [CO₂] between these plant tissues that differ primarily in their photosynthetic physiotype.

These following key questions will be addressed:

1. How does stomatal conductance and guard cell metabolism vary between C₃ and CAM tissues over the day/night (diel) cycle?
2. Does guard cell sensitivity to C_i vary over the diel period and between C₃ and CAM tissues, and to what extent does C_i determine the differences in diel patterns of stomatal conductance between C₃ and CAM tissues?
3. Does the observation of increased soluble sugars in C₃ *K. blossfeldiana* young leaves explain differences in daytime stomatal conductance?
4. To what extent does the decarboxylation of nocturnally accumulated malate determine the daytime stomatal closure in CAM tissues?

3.2 Methods

3.2.1 Summary of Experiments and Conditions

Throughout this chapter comparisons were made between C₃ and CAM physiotypes using two comparative systems as described in the previous chapter; with comparisons made between in *K. blossfeldiana* young (10th leaf pair from bottom) and mature leaves (2nd leaf from bottom), and between wild type *K. fedtschenkoi* and CAM-deficient *pepc1.1* mutants.

This chapter is divided into three parts:

- A comparison of C₃ and CAM stomatal diel conductance and guard cell metabolism.
- The role of C_i in linking mesophyll PEPC-driven carboxylation and stomatal conductance.
- The role of whole leaf carbon status on stomatal conductance, including both C₃ RUBSICO and PEPC-mediated assimilation.

3.2.2 Plant Materials and Growth Conditions

Throughout this chapter comparisons were made between C₃ and CAM physiotypes using two comparative systems; 1) between *K. blossfeldiana* young (10th leaf pair from bottom) and mature leaves (2nd leaf from bottom), and 2) between wild type *K. fedtschenkoi* and CAM-deficient *pepc1.1* mutants. The *K. fedtschenkoi pepc1* mutants were produced by CRISPR targeted gene silencing of the *K. fedtschenkoi* PEPC1 gene by Xiaohan Yang with a method described in Zhang et al. (2020). All plants were grown under 190 $\mu\text{mol m}^{-2} \text{s}^{-1}$ light, unless otherwise noted, with 12/12hrs day/night cycles and with 25°C days and 19°C nights. Plants were watered twice weekly. *K. blossfeldiana* plants were propagated by cutting. Briefly, side shoots were cut from the main stem with all but a small emerging leaf bud at the apex of the shoot and the top two leaf pairs. Care was taken to ensure all cuttings were the same length and were uniform in leaf sizes. Individual cuttings were placed in 5 cm pots with John Ins No.2 compost and grown under cover for 2 weeks. After 6 weeks cuttings were repotted into 12 cm pots with a 3:1 mix of John Innes No.2: Perculite. *K. fedtschenkoi* plants were propagated by leaf edge pupping. Removed leaves were placed on trays of with a 3:1 mix of John Innes No.2:Perculite. Plantlets were grown for 8 weeks before being reported three per 12 cm pot. *K. fedtschenkoi* plants were sampled 120 days after propagation.

3.2.3 Gas Exchange and Low [CO₂] Stomatal response assays

All gas exchange measurements were carried out using the Li-6400XT (Li-Cor, USA) over 48 hr periods. In each experiment the rate of net CO₂ uptake and stomatal conductance were measured every 15 minutes over the first 24 hr period under conditions that tracked those in the growth cabinet and with [CO₂] held at 400 $\mu\text{mol mol}^{-1}$; followed by a second 24 hr period in which the response to reduced [CO₂] was assayed at six different time points in the 24hr period (Dawn +2,6,10 hrs; Dusk + 3,6,10 hrs). Each assay involved reducing CO₂ concentration to 70 $\mu\text{mol mol}^{-1}$ for 30 minutes to induce opening and then back to ambient (400 $\mu\text{mol CO}_2$) for 30 minutes while stomatal conductance was measured every minute. All gas exchange experiments in this chapter were carried out between 60-90 days or 100-120 days after propagation for *K. blossfeldiana* or *K. fedtschenkoi* respectively.

The following three gas exchange experiments were carried out:

1. A comparison of photosynthetic and stomatal responses between C₃ and CAM physiotypes of plants grown in standard growth conditions (190 μmol m⁻² s⁻¹ light, 12/12 hr day/night cycles, 25°C days and 19°C nights). Gas exchange measurements were made under normal conditions for 24 hrs followed by a second 24 hr period in which the response to reduced [CO₂] was assayed at six different time points in the 24 hr period (Dawn +2,6,10 hrs; Dusk + 3,6,10 hrs).
2. A comparison of C₃ and CAM physiotypes with leaves kept at reduced CO₂ (70 μmol mol⁻¹) for the first 24 hr period of experiment in order to reduce carbon assimilation and to simulate a longer period of reduced C_i. This was followed by a second 24 hr period in which the response to reduced [CO₂] was assayed at six different time points in the 24 hr period (Dawn +2,6,10 hrs; Dusk + 3,6,10 hrs), with [CO₂] was kept at ambient until each assay timepoint.
3. The impact of growing *K. blossfeldiana* at reduced light intensity (90 vs 190 μmol m⁻² s⁻¹) on age specific photosynthetic and stomatal responses between C₃ and CAM physiotypes. The aim of this experiment was to reduce carbon assimilation over a longer period, to study the effect of reduced photo-assimilate on both C₃ and CAM physiotypes and its effect on stomatal conductance and response to reduced [CO₂]. Gas exchange measurements were made under reduced light (90 μmol m⁻² s⁻¹) with *K. blossfeldiana* young and mature leaves 60-90 days after propagation and growth under reduced light (90 μmol m⁻² s⁻¹) for 24 hrs followed by a second 24 hr period in which the response to reduced [CO₂] was assayed at six different time points in the 24 hr period (Dawn +2,6,10 hrs; Dusk + 3,6,10 hrs). An extra experiment was performed in which the low [CO₂] response assays were performed under normal lighting (190 μmol m⁻² s⁻¹) for the assays to control for any light induced conductance effects.

3.2.4 Stomatal Kinetic Responses

The kinetics of stomatal response to reduced CO₂ (70 μmol mol⁻¹) and the subsequent return to ambient CO₂ (400 μmol) was further explored by separately fitting functions to each response individually.

Two approaches were explored. Firstly fitting responses to a simpler exponential function as described Vialet-Chabrand et al. (2017) which is as follows:

Equation 1.1 Stomatal increase exponential function:

$$g_s = G_{max} + (G_{min} - G_{max})e^{-\frac{t}{\tau_i}}$$

Equation 1.2 Stomatal decrease exponential function:

$$g_s = G_{min} + (G_{max} - G_{min})e^{-\frac{t}{\tau_d}}$$

Where g_{min} and g_{max} are the minimum and maximum g_s observed. τ_d and τ_i are time constants for the increase and decrease in g_s .

A second approach using a sigmoidal function that accounts for any delay that may be observed in the response (Violet-Chabrand et al., 2017) was also fitted to each response. In which k_d and k_i time constants for the increase and decrease in g_s and λ represents the initial lag time.

Equation 2.1 Stomatal increase sigmoidal function:

$$g_s = (G_{max} - G_{min})e^{-e^{\left(\frac{\lambda-t}{k_i}+1\right)}} + G_{min}$$

Equation 2.2 Stomatal decrease sigmoidal function:

$$g_s = (G_{min} - G_{max})e^{-e^{\left(\frac{\lambda-t}{k_d}+1\right)}} + G_{max}$$

A third and final set of equations were used to describe the maximum slope of the sigmoidal function (Ozeki et al., 2022).

Equation 3.1 Maximum slope of the increase in g_s :

$$Sl_{max} = \frac{(G_{min} - G_{max})}{k \cdot e}$$

Equation 3.2 Maximum slope of the decrease in g_s :

$$Sl_{max} = \frac{(G_{max} - G_{min})}{k \cdot e}$$

All data and statistical analysis were carried out using R version 4.0.2 (R Core Team, 2020). In both exponential and sigmoidal approaches the increase response was any change in g_s between t_0 and t_{30} ; and any decrease response was any change between t_{30} and t_{60} . Before attempting to fit any functions onto the data responses where there was no clear change in conductance (change less 0.5%) were removed. R core functions `lm` or `nls` were used to fit response data to exponential or sigmoidal functions respectively. Each response was graphed and fitted individually and the mean of three replicates of each parameter presented. Two parameters were used to characterise the amplitude of response the change in conductance observed within the first 30 minutes, and the area under the entire response integrated. For the integrated response the base R Spline function used to extrapolate between points and `pracma` version 2.3.8 was used for intergradation.

3.2.5 Metabolite Analysis

3.2.6 Epidermal Peel Soluble Sugar Analysis

Epidermal peels were collected from the abaxial side of *K. blossfeldiana* young (10th leaf pair from bottom) and mature leaves (2nd leaf from bottom), and wild type *K. fedtschenkoi* and CAM-deficient *pepc1.1* mutants (both 6th leaf pair from bottom). Peels were collected by snapping the leaves and pulling off the epidermal peel. For these analyses samples were collected at dusk and the subsequent dawn. A methanol extraction method was used for all metabolite analyses. Five epidermal peels were used, and these were collected by flash freezing in liquid nitrogen. Whole leaves were ground by mortar and pestle with liquid nitrogen, with of 250 mg of tissue collected for analysis. Epidermal peels were smashed with a prechilled TissueLyser II (Qiagen, USA) for 2 minutes at 30 Hz with 2 mm metal beads. 80% methanol was added, 1 ml for whole leaves and 500 μ l for epidermal peels. Samples were incubated at 60°C for 40 minutes and spun down at 13,000 rpm for 10 mins and stored at 4°C until further analysis. Whole leaf total soluble sugars were determined by measuring glucose equivalents using a phenol–sulfuric acid colorimetric method (Dubois et al., 1956), with 50 μ l methanol extract diluted with 450 μ l ddH₂O and 0.5 ml 5% phenol then 2.5 ml concentrated sulphuric acid added. After incubation for 15 minutes absorbance was read at 482 nm. A

glucose standard curve with concentrations between zero and 150 μg glucose was used to calculate total glucose equivalents per fresh weight.

3.2.7 Guard Cell Starch Analysis

Epidermal peels were collected from the abaxial side of *K. blossfeldiana* young (10th leaf pair from bottom) and mature leaves (2nd leaf from bottom), and wild type *K. fedtschenkoi* and CAM-deficient *pepc1.1* mutants (both 6th leaf pair from bottom). For the 24 hr *K. blossfeldiana* sampling tissues were sampled at eight time points over the diel period, commencing 4 hrs before dusk. For *K. fedtschenkoi* samples were collected at dusk and the subsequent dawn. Peels were collected by snapping the leaves and pulling off the epidermal peel and immediately fixing the peel in a fixative solution (50% v/v Methanol, 10% v/v Acetic acid) for 24 hrs. Before staining, tissues were rinsed with 1 ml of dH₂O to remove traces of fixative solution. Peels were stained for starch with Lugol's iodine solution (6 mM iodine, 43 mM KI) for five minutes, then rinsed with 3 ml of dH₂O. Stained peels were imaged at x 20 magnification on a Zeiss Axiomager2 (Zeiss, Germany). Once imaged a new method was used to rapidly analyse the stained starch granule areas, as described in diagram 1. Images were batch converted from .czi to .jpg using a custom ImageJ macro. A subset of 20 images were taken for model training. Image annotation and model training was carried out on roboflow. The subsequent model was tested on a second subset of images and used to identify guard cell granules. The model was used to sort and separate guard cells from images. Results were manually sorted to remove false positives or poorly focused guard cells. Adaptive thresholding was used to highlight stained starch granules and pixels were counted, both using OpenCV.

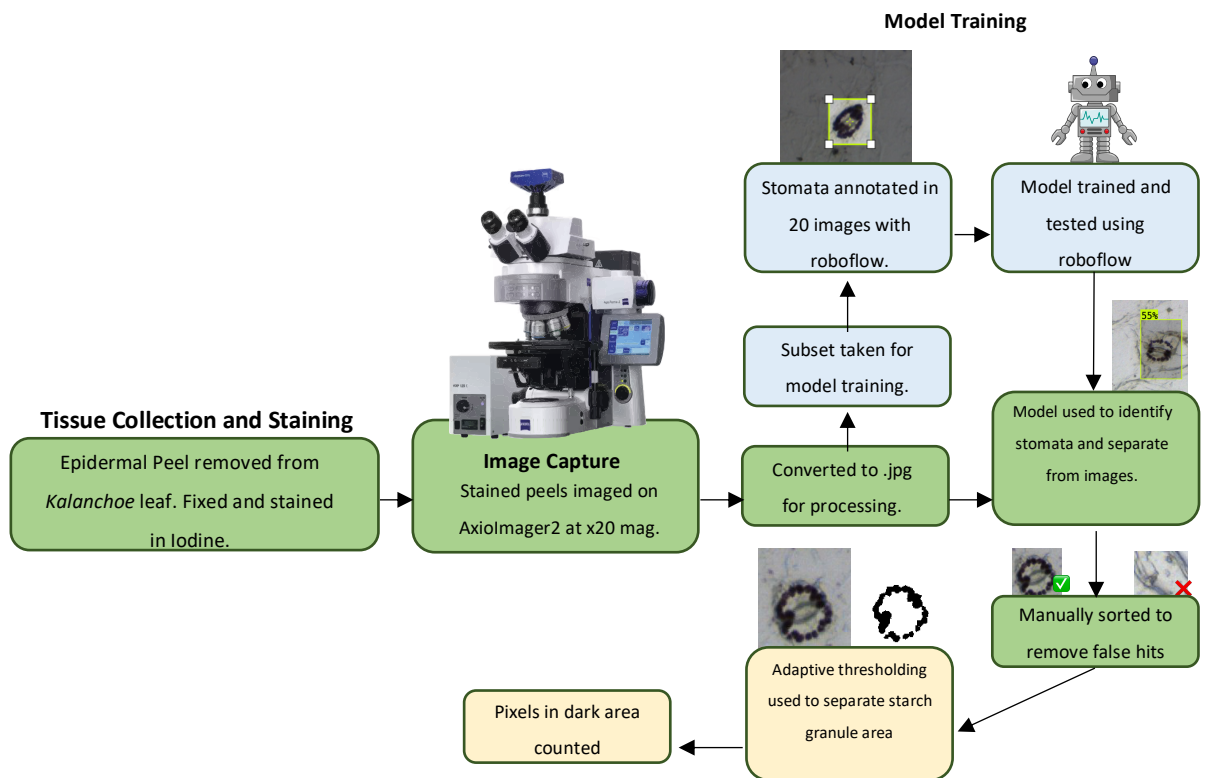


Diagram 1. Rapid automated guard cell granule area counter.

3.3 Results

3.3.1 *K. blossfeldiana* age specific photosynthetic and stomatal responses.

Diel Photosynthesis and Conductance

Net CO₂ assimilation was substantially higher in young leaves (2nd leaf pair from top) over the entire Diel period, with all net assimilation occurring during day and no net assimilation observed at night in young leaves (Figure 3.1.A). The lack of nocturnal CO₂ assimilation is supported by no corresponding increase in titratable acidity measured overnight (Chapter 2). In mature leaves (2nd leaf from bottom) there was comparatively lower overall net CO₂ assimilation over the diel period (~4.5x lower) with the majority of net CO₂ assimilation occurring at night and a steadily increasing amount occurring towards the end of the day period (Figure 3.1.A).

Stomatal conductance was similarly higher in young leaves compared to mature leaves over the diel period (Figure 3.1.B), with a peak towards the start of the day followed by a gradual decline and a large drop during the night. Interestingly, stomatal conductance started to increase over the latter part of the night in the young leaves despite no nocturnal net CO₂ assimilation. Mature leaves showed generally lower diel conductance with a peak towards the middle of the latter half of the night, corresponding with a peak in net CO₂ assimilation.

Diel Conductance vs Diel Photosynthesis

Notably there was poor correlation between net CO₂ assimilation and stomatal conductance in young leaves during the night ($R^2 = 0.07$ Figure 3.2A); this was driven by the observation of nocturnal conductance in the young leaves towards the end of the night but with no net CO₂ uptake at this time (Figure 3.1B). In both young and mature leaves there was a strong correlation between CO₂ assimilation and stomatal conductance during their respective periods of most assimilation, which was the day in young leaves ($R^2 = 0.96$ Figure 3.2A) and the night in mature leaves ($R^2 = 0.90$ Figure 3.2A).

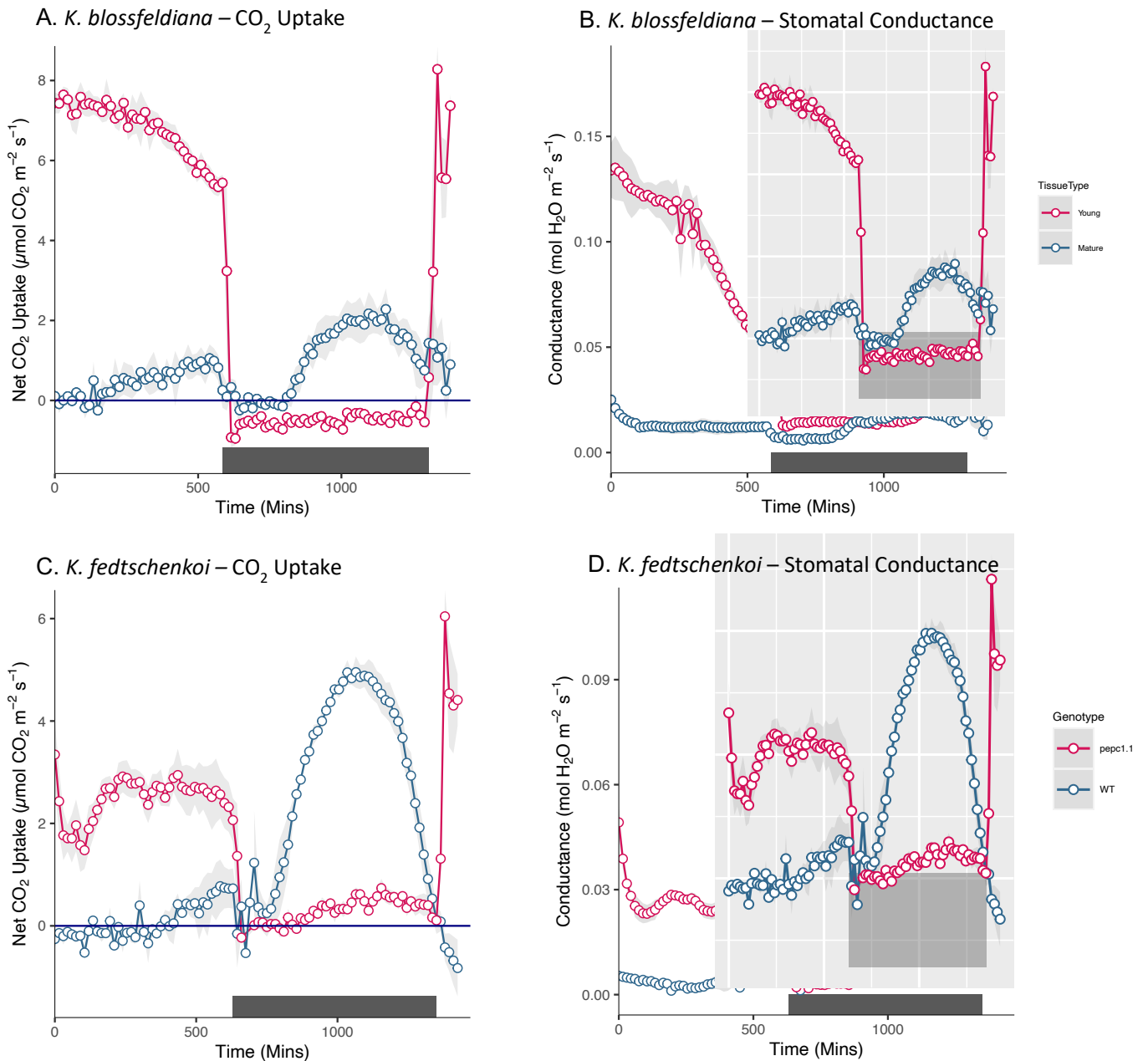


Figure 3.1 Diel *K. blossfeldiana* age specific photosynthetic and stomatal responses (Panels A and B) and *K. fedtschenkoi* genotype specific photosynthetic and stomatal responses (Panel C and D). Diel net CO₂ uptake (panel A and C, µmol CO₂ m⁻¹ s⁻¹) and stomatal conductance (panel B and D, mol H₂O m⁻¹ s⁻¹) of *K. blossfeldiana* young leaves (red points, 10th leaf pair from bottom) and mature leaves (blue points, 2nd leaf from bottom) between 60-90 days after propagation or wild type *K. fedtschenkoi* leaves (blue points) and *pepc1.1* leaves (red points) between 100-120 days after propagation. Leaf pair 6 was used in both genotypes. Plants grown in 12hr/12hr day/night cycles with 25°C days/ 19°C nights. Dark shaded area represents night. For each graph points represent the mean of three repeats and the shaded interval ± SEM. The dark blue line on the CO₂ uptake graphs equals zero.

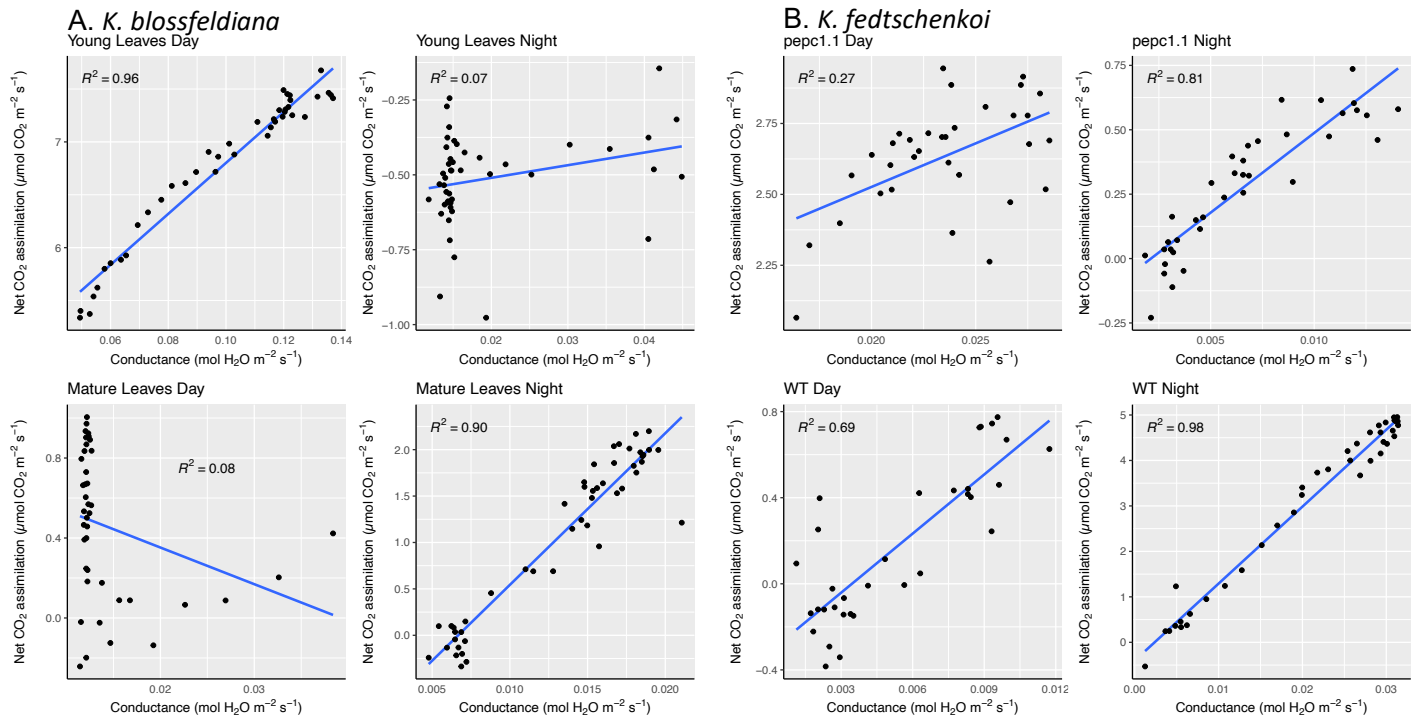


Figure 3.2 Correlations between diel stomatal conductance and net carbon uptake in *K. blossfeldiana* young and mature leaves (Panel A) and *K. fedtschenkoi* wild type and pepc1.1 leaves (Panel B). Blue line represents plotted linear regression.

3.3.2 *K. fedtschenkoi* genotype specific photosynthetic and stomatal responses.

Diel Photosynthesis and Conductance

The overall range of stomatal conductance and net CO₂ assimilation between *K. fedtschenkoi* and *pepc1.1* mutants over the diel period was smaller than that observed between *K. blossfeldiana* young and mature leaves. However, WT and *pepc1.1* mutants showed contrasting patterns of stomatal conductance and net CO₂ uptake that were consistent with their CAM and CAM deficient (C₃-like) phenotypes respectively.

Wild type *K. fedtschenkoi* leaves carried out most of their net CO₂ uptake at night with a limited amount towards the end of the day (Figure 3.1.C) and a period of reduced uptake in the early night. There was also a correlation between net CO₂ uptake and stomatal conductance over the day ($R^2 = 0.69$ Figure 3.2B) and night ($R^2 = 0.98$ Figure 3.2B). In comparison, the *pepc1.1* mutants took up most CO₂ during the day period with very limited net CO₂ uptake towards the end of the night. Stomatal conductance largely followed patterns of net CO₂ uptake in these mutants, and, unlike the young *K. blossfeldiana* leaves, there was little evidence of a decoupling between these processes at night ($R^2 = 0.81$ Figure 3.2B).

3.3.3 Guard Cell Metabolism across different photosynthetic physiotypes

Greater Epidermal Peel Soluble Sugar contents in C₃ tissues

In both C₃ tissues (i.e. young *K. blossfeldiana* leaves and leaves of the *K. fedtschenkoi pepc1.1* mutant), there was significantly greater amounts of soluble sugars in the guard cell enriched epidermal peels compared to peels from CAM tissues (mature *K. blossfeldiana* and wild type *K. fedtschenkoi* leaves, Figure 3.3.A, and B). The greatest difference in soluble sugar content was observed between physiotypes at dusk, with soluble sugar content nine and two times greater in young *K. blossfeldiana* and *K. fedtschenkoi pepc1.1* mutants compared to mature *K. blossfeldiana* and/or wild type *K. fedtschenkoi* respectively.

Differences between the contrasting photosynthetic physiotypes were less pronounced at dawn with 25% and 40% greater soluble sugar contents in young *K. blossfeldiana* and *K. fedtschenkoi pepc1.1* mutant compared to CAM tissues (Figure 3.3.A and B). The timing of peaks in epidermal soluble sugar contents also differed between the physiotypes, with peaks observed at dusk in both C₃ tissues and at dawn for the CAM tissues. The dawn-dusk change in epidermal soluble sugar contents was most pronounced in the C₃ tissues compared to the CAM tissues and was negligible in the wild type *K. fedtschenkoi*.

Guard cell starch metabolism is retimed between C₃ and CAM tissues

The diel pattern of guard cell starch content was progressively rescheduled as the leaves transitioned from C₃ to CAM in *K. blossfeldiana*. A two-way anova (Leaf Pair X Time) showed statistically significant effects of both leaf pair ($F(1)= 45.291$, $p < 0.001$) time ($F(2)= 41.514$, $p < 0.001$) and a significant interaction between both ($F(3)= 16.661$, $p < 0.001$). The youngest leaf (10th from the bottom) with a C₃ physiotype, increased starch granule area during the start of the night period, followed by a relatively stable period until a decline in the last four hours of the night and into the day. Starch granule area then increased as the day processed to peak four hrs before the night. The C₃-CAM intermediate (4th leaf pair from the bottom) showed an increase in starch granule area in the first two hours of the night followed by sharp decline in the middle of the night. Followed by an increase then decrease in the late night and two hours into the day, and then followed an increase into the late afternoon.

The CAM leaf (2nd from the bottom) showed a decline in starch granule area in the last four hours of the day. Followed by a stable period in the first two hours of the night, then a decline until the middle of the night. Starch then increased in area over the remainder of the night, then a sudden decline in starch was observed at the start of the day, followed by an increase until the late afternoon. Interestingly, in all tissues there was a sudden decrease in starch granule area before the start of the night, with the sharpest decrease observed in the C₃ leaf pair eight. Guard cell starch granule area also differed between wild type CAM *K. fedtschenkoi* and the CAM deficient *pepc1.1* mutant, with a significantly greater amount of starch observed at both time points in the *pepc1.1* mutant ($p < 0.05$, Figure 3.3.C). Guard cell starch significantly declined overnight in the wild type ($p = 0.02$), whereas in the *pepc1.1* mutant, guard cell starch showed a negligible difference between dawn and dusk overnight ($p > 0.1$).

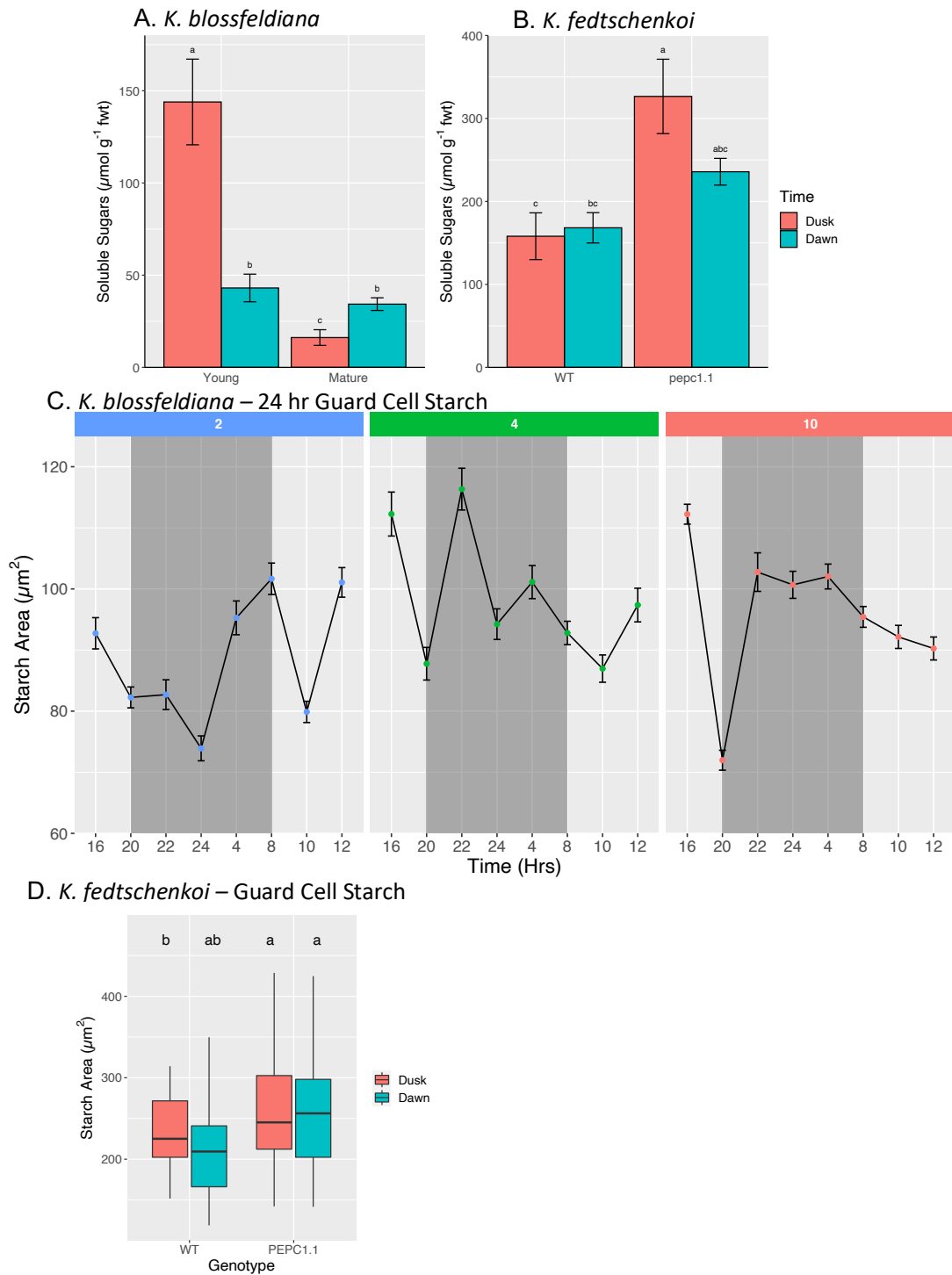


Figure 3.3 Guard Cell metabolites in C_3 /CAM tissues. Dawn/dusk soluble sugars in guard cell enriched epidermal peel tissue (Panel A and B). Panel C, Diurnal guard cell starch granule area of *K. blossfeldiana* young leaves (red points, 10th leaf pair from bottom), intermediate leaves (green points, 4th leaf pair from bottom), and mature leaves (blue points, 2nd leaf from bottom). Dawn/dusk guard cell starch granule area of *K. fedtschenkoi* wilt type and *pepc1.1* leaves. *K. blossfeldiana* plants were sampled at 90 days after propagation, *K. fedtschenkoi* plants were sampled at 120 days after propagation. Plants grown in 12hr/12hr day/night cycles. Dark shaded area represents night. Statistical analyses were performed using two-way ANOVA, significant differences ($P < 0.05$) are indicated by different lowercase letters.

3.3.4 Comparing C₃ and CAM stomatal responses to low [CO₂]

The responses of the contrasting photosynthetic physiotypes of young and mature leaves to altered [CO₂] was examined over the diel period. External CO₂ concentrations were reduced from 400 μmol mol⁻¹ to 70 μmol mol⁻¹ and stomatal conductance was monitored at 1 min intervals for 30 minutes followed by a return to ambient (400 μmol mol⁻¹ CO₂). The plants were subjected to these shifts in [CO₂] at 6 time points (2 hrs, 6 hrs and 10 hrs from dawn; and 3 hrs, 6 hrs and 10 hrs from dusk). The magnitude of the stomatal responses were compared using two metrics: the difference between G_{max} and G_{min} within the first 30 minutes (G_{diff}); and the integrated area under the curve over the entire 60 minutes (G_{int}). The rapidity of stomatal responses were primarily compared using the modelled maximum rate of opening/closure (S_{Iopen}/S_{Iclosed}).

Stomatal responses to low [CO₂] in *K. blossfeldiana*

In *K. blossfeldiana* the reduction of atmospheric CO₂ from 400 μmol to 70 μmol for 30 minutes elicited an increase in stomatal conductance at all time points examined for mature leaves and all at all time points apart from the early night for young leaves (Figure 2.1.C). Both the magnitude (G_{diff} and G_{int}) and rapidity (Max S_{Iopen}/S_{Iclose}) of the stomatal response varied significantly by tissue age and time point (Figure 2.2. G_{diff}, G_{int}, S_{Iopen}, S_{Iclosed} all P < 0.001). Young leaves showed significantly greater responses, in both magnitude and rapidity of opening and closure during the day and at the late night time point; the greatest response in the young leaves was 12 times that of the greatest response in the mature leaves. The [CO₂] responsiveness of stomata in young leaves peaked towards the start of the day and declined steadily but significantly as the day progressed which is seen most clearly by G_{int}. The difference (G_{int}) between early and mid-day stomatal responses in young leaves was due to a slowdown in the rate of the early day closing response after a rapid initial response. Responsiveness to [CO₂] in young leaves was absent in the early-night and was very slight (G_{diff} 0.02 ± 0.002 mol H₂O m⁻² s⁻¹) in the middle of the night.

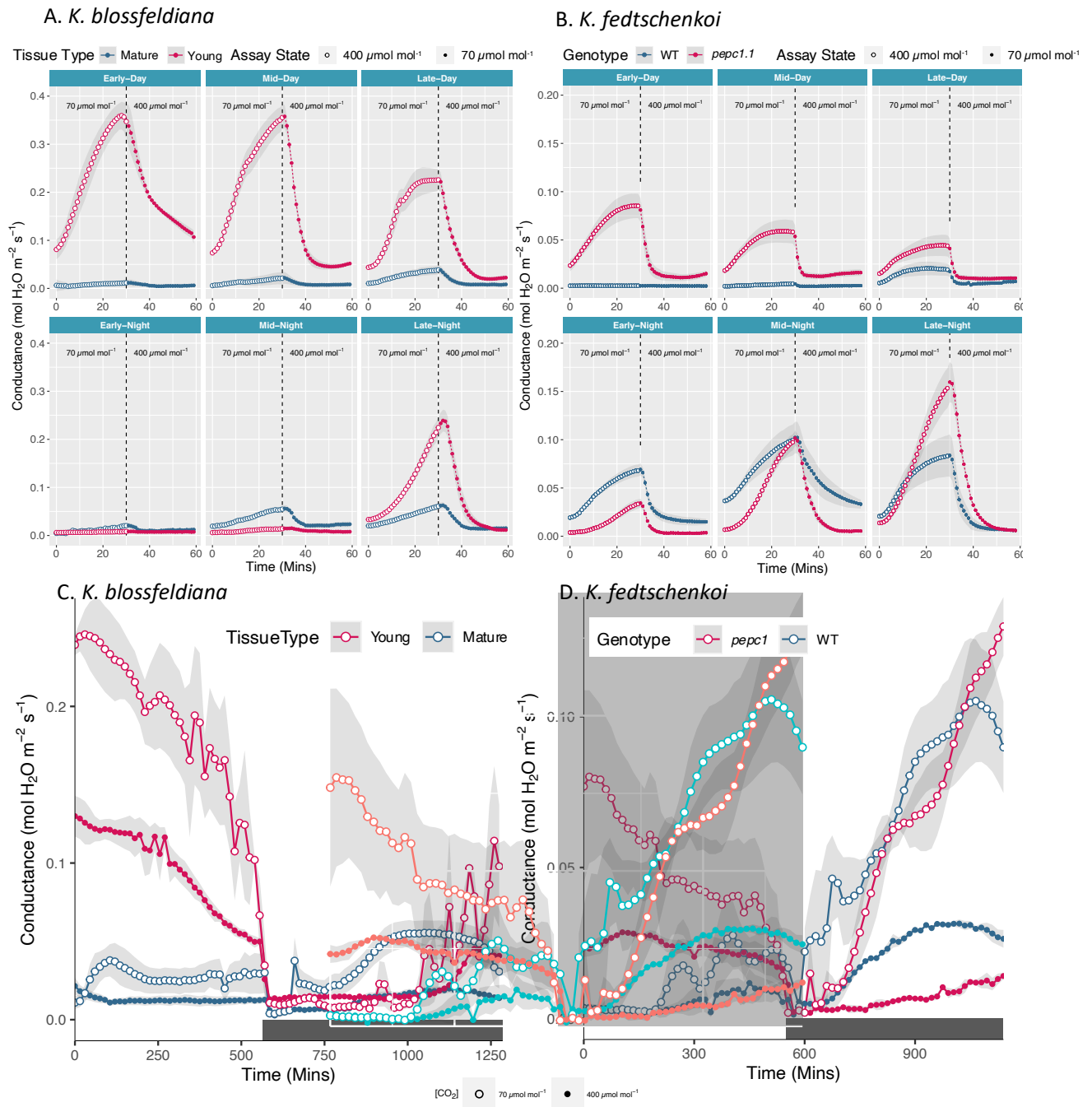


Figure 3.4 Diel stomatal conductance responses to reduced [CO₂] in *K. blossfeldiana* young leaves (red points, 10th leaf pair from bottom) and mature leaves (blue points, 2nd leaf from bottom) between 60-90 days after propagation (Panels A and C) and wild type *K. fedtschenkoi* leaves (blue points) and *pepc1.1* leaves (red points) between 100-120 days after propagation (Panels B and D). Low CO₂ stomatal response assay (panels A and B, mol H₂O m⁻² s⁻¹). Plants were assayed at 6 timepoints (2hrs, 6hrs, 10hrs from dawn; and 3 hrs, 6 hrs, 10 hrs from dusk). For each timepoint CO₂ was held at low CO₂ (70 μmol mol⁻¹, open points) for 30 minutes followed by a return to ambient (400 μmol mol⁻¹ CO₂, closed points) for 30 minutes, with measurements taken every minute. Diel stomatal conductance (Panels C and D) of leaves held at ambient (400 μmol mol⁻¹ CO₂, closed points) for 24 hrs or low CO₂ (70 μmol mol⁻¹, open points), measurements taken every 15 minutes. For each graph points represent the mean of three repeats and the shaded interval ± SEM.

Kinetics of stomatal responses to low [CO₂] in *K. blossfeldiana*

The maximum rate of opening and closing (S_{open} and S_{close}) was consistently higher in the younger leaves at times where there was a substantial response. Despite the gradual decrease in response amplitude observed in the young leaves over the day period such a pattern was not observed in the maximum rate of opening or closure (Figure 3.5.C and D). Over the diel period the lag time, the time taken for the response to become exponential, was greater in the late day and night time points where there was a response, with the least lag observed at mid-day. There is an opposite pattern of closure lag in the young leaf responses during the day, with a mid-day peak followed by a decline and an overall peak at late-night.

The stomata in the CAM-performing mature leaves showed significantly weaker responses to [CO₂] throughout the diel period, but also an opposite pattern of responsiveness. The CAM stomata had the weakest response at the start of the day, followed by a gradual increase through the day, then a reduction at the early night timepoint and an increase to peaks in stomatal conductance at middle- and late-night (Figure 3.5). Notably there was limited response in either tissue type in the early night timepoint, corresponding with a period of reduced conductance at the start of the night in the diel conductance graph. The rapidity of stomatal opening peaked at the end of the day in mature leaves with slightly slower stomatal responses in the mid to late night. The speed of stomatal closure increased as the day progressed and peaked at late day and mid to late night. There was no clear pattern in the lag period in opening, but lag closure peaked in the mid to late night in the mature leaves.

Stomatal responses to low [CO₂] in *K. fedtschenkoi*

Stomatal responses to low CO₂ were greater in the *pepc1.1* mutants compared to that of wild type *K. fedtschenkoi* at all time points examined apart from early/mid night (Figure 3.4.B).

However, the differences in stomatal responses to altered [CO₂] between C3 and CAM tissues in *K. fedtschenkoi* were smaller than those observed between *K. blossfeldiana* young and mature leaves. Like the stomata in young *K. blossfeldiana* leaves the stomatal responses of *pepc1.1* mutants to altered [CO₂] peaked at the start of day and declined as the day progressed (Fig. 3.4). Unlike the young *K. blossfeldiana* leaves the stomata in the *pepc1.1* mutants showed a response at all timepoints and responses at early/mid night were comparable to those of the wild type.

The strongest response was observed in *pepc1.1* mutants at late night. *K. fedtschenkoi* wild type plants showed a similar pattern of stomatal response to altered [CO₂] to those seen in mature *K. blossfeldiana* leaves, but with generally greater amplitude. Notably, in *K. fedtschenkoi* wild type leaves, at their lowest response (Early-Day) there was no response at all detected, unlike the slight 'leaky' responses seen at the lowest points of responsiveness in mature *K. blossfeldiana*. The responsiveness of stomatal conductance in wild type *K. fedtschenkoi* leaves to reduced [CO₂] peaked in the middle of the night, with a slight response at mid-day building up into the night, followed by a slight reduction in stomatal response to [CO₂] at the end of night time point.

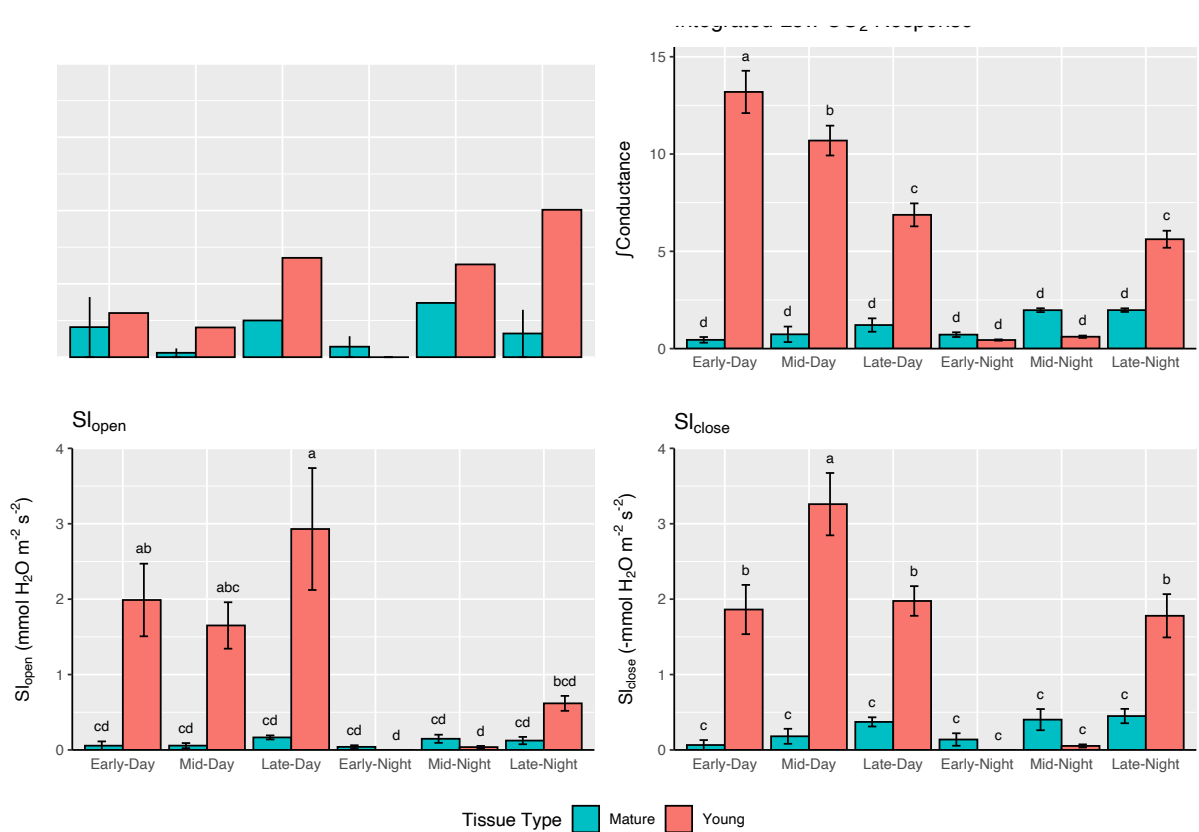


Figure 3.5 *K. blossfeldiana* age specific low CO₂ response stomatal kinetics. *K. blossfeldiana* young leaves (red bars, 10th leaf pair from bottom) and mature leaves (blue bars, 2nd leaf from bottom) assayed at 6 timepoints (2 hrs, 6 hrs, 10 hrs from dawn; and 3 hrs, 6 hrs, 10 hrs from dusk). For each timepoint CO₂ was held at low CO₂ (50 μmol) for 30 minutes followed by a return to ambient (400 μmol CO₂) for 30 minutes. a) Mean increase in stomatal conductance over 30 minutes in response to reduced CO₂. b) Total response integrated over 60-minute period. c) Maximum opening rate of response to reduced CO₂. d) Maximum closing rate of response to return to ambient reduced CO₂. All values are means of three replicates ± SEM. Different letters represent a significant difference (post hoc Tukey HSD test, p<0.05).

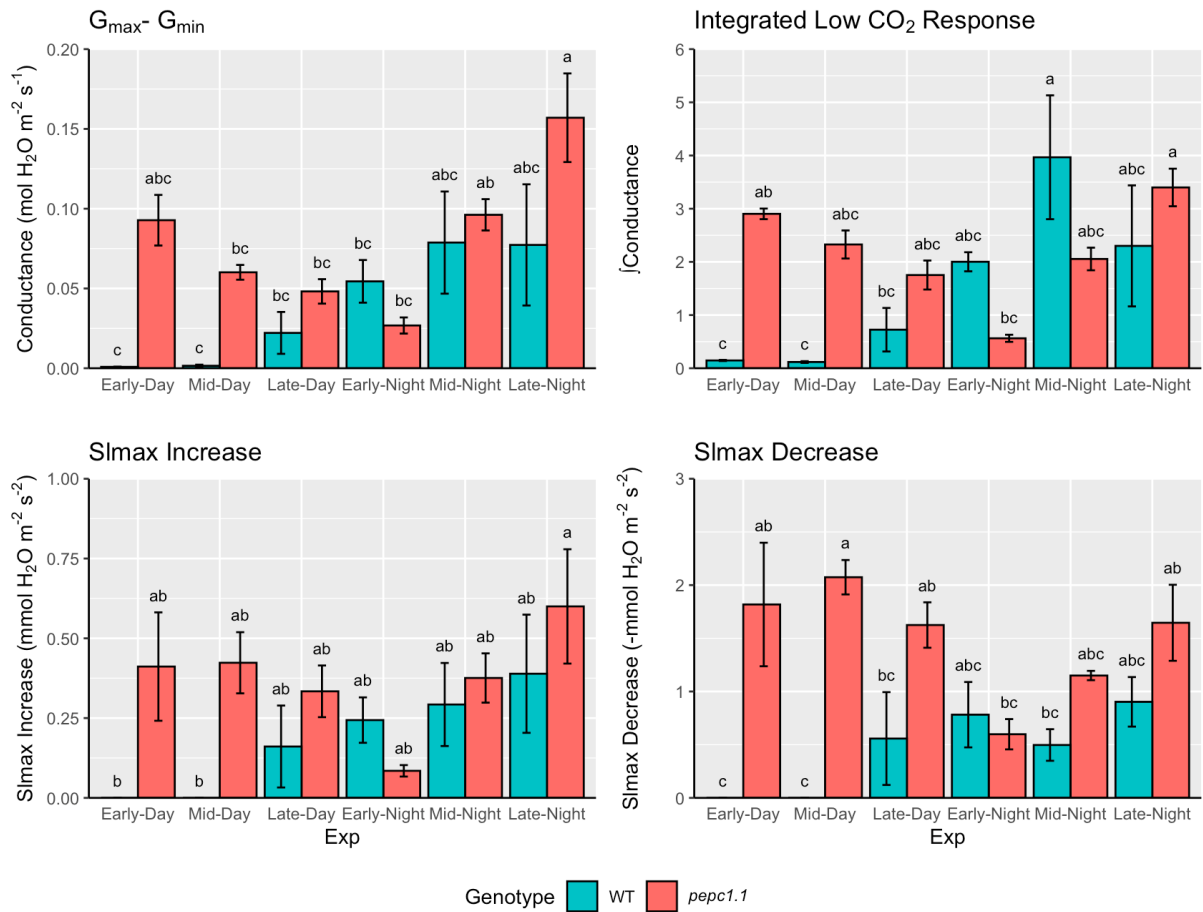


Figure 3.6 *K. fedtschenkoi* genotype specific low CO₂ response stomatal kinetics of wild type *K. fedtschenkoi* leaves (blue points) and *pepc1.1* leaves (red points) between 90-120 days after propagation) assayed at 6 timepoints (2 hrs, 6 hrs, 10 hrs from dawn; and 3 hrs, 6 hrs, 10 hrs from dusk). For each timepoint CO₂ was held at low CO₂ (50 μmol) for 30 minutes followed by a return to ambient (400 μmol CO₂) for 30 minutes. a) Mean increase in stomatal conductance over 30 minutes in response to reduced CO₂. b) Total response integrated over 60-minute period. c) Maximum opening rate of response to reduced CO₂. d) Maximum closing rate of response to return to ambient reduced CO₂. All values are means of three replicates ± SEM. Different letters represent a significant difference (post hoc Tukey HSD test, p<0.05).

Kinetics of stomatal responses to reduced [CO₂] in *K. fedtschenkoi*

The pattern of maximum rates of stomatal opening and closing in response to reduced [CO₂] (Figure 3.6.C/D) largely followed the pattern of response amplitude over the diel period in both *K. fedtschenkoi* wild type and *pepc1.1* mutants. In both wild type and *pepc1.1* mutants, when a stomatal response to reduced [CO₂] was observed the maximum rates of closure were substantially greater than the maximum rates of opening. In the wild type *K. fedtschenkoi* the maximum rate of stomatal opening (S_{open}) and closure (S_{close}) increased from the late day until its peak at the end of night, following the same pattern observed in its stomatal response amplitudes. The maximum rates of stomatal opening and closure also largely followed the pattern of amplitude in the *pepc1.1* mutants apart from during the day when the rate of stomatal closure peaked, which also occurred in the young *K. blossfeldiana* leaves.

Diel Stomatal responses to low [CO₂] over 24hrs in *K. blossfeldiana* and *K. fedtschenkoi*

This series of experiments aimed to investigate whether stomatal responses to reduced [CO₂] could be sustained for longer periods of time, and to simulate the drawdown of [CO₂] by carbon uptake by either rubisco during the day in the C₃ plants or PEPC nocturnally in the CAM plants. These experiments aimed to explore the responsiveness to reduced CO₂ (70 μmol CO₂) over the entire diel period. A key objective was to establish if a CAM-like pattern of nocturnal stomatal conductance could be observed in the young C₃ *K. blossfeldiana* leaves or in the CAM-deficient *K. fedtschenkoi pepc1.1* leaves, by simulating a nocturnal reduction in C_i that would be expected to occur in CAM leaves due to the draw-down in internal [CO₂] from carbonic anhydrase and PEPC activity.

3.3.5 Reduced CO₂ is not enough to trigger CAM-like nocturnal opening in young C3 *K. blossfeldiana*

Both young and mature *K. blossfeldiana* leaves generally showed increased stomatal conductance over the whole diel period under low [CO₂] (70 μmol mol⁻¹ CO₂, Figure 3.4.C). The increase in mature leaf stomatal conductance in response to low [CO₂] was greater during the night, with a gentle peak towards middle of the night. Young leaves also showed increased stomatal conductance in response to reduced CO₂ (70 vs at 400 μmol mol⁻¹) but with the greatest increases in stomatal conductance observed during the day.

Reduced [CO₂] (70 vs at 400 μmol mol⁻¹) did not trigger a CAM like pattern of nocturnal stomatal conductance in the young *K. blossfeldiana* leaves that was comparable to the mature leaves at reduced CO₂. Instead the young leaves showed a pattern of nocturnal stomatal opening in both [CO₂] that tends to occur closer to the end of the night and in reduced [CO₂] appears to zig-zag up/down suggesting they are unable to maintain high conductances.

3.3.6 Reduced [CO₂] can restore CAM-like nocturnal opening in CAM-deficient *K. fedtschenkoi pepc1.1* mutant

In *K. fedtschenkoi* stomatal conductance in both wild type and *pepc1.1* leaves increased in response to reduced 70 μmol mol⁻¹ CO₂ compared to that measured under 400 μmol mol⁻¹ over most of the diel period; with the exception of early mornings in the wild type where stomatal conductance remained negligible (Figure 3.4.D). Stomatal conductance under reduced CO₂ (70 μmol mol⁻¹) in the wild type was low during the start of the day increased throughout the day, whereas stomatal conductance in the *pepc1.1* peaked at the start of the day and then declined. Increases in stomatal conductance under reduced (70 vs at 400 μmol mol⁻¹) were greatest in both genotypes during the night, far surpassing that of leaves in ambient CO₂. This would suggest that in the CAM-deficient *pepc1.1* line it is possible to restore nocturnal stomatal conductance by simulating the drawdown of internal [CO₂] that occurs during CAM (Figure 3.4.D).

3.3.7 The role of whole leaf carbon assimilation on stomatal conductance, including both C₃ RUBISCO and PEPC-mediated assimilation.

This series of experiments aimed to explore the influence of whole leaf carbon status on stomatal conductance by modulating carbon status either by growth of *K. blossfeldiana* in reduced light (90 vs 190 $\mu\text{mol m}^{-2} \text{s}^{-1}$ light) or by holding the leaf $[\text{CO}_2]$ at 70 $\mu\text{mol mol}^{-1}$, within the Licor-6400 chamber, for 24 hrs in the different tissues from both *K. blossfeldiana* and *K. fedtschenkoi* wild type and *pepc1.1* mutants. Both of these conditions should reduce net CO_2 uptake and reduce the amount of photo assimilate available for stomatal opening. In the case of the CAM tissues reduced $[\text{CO}_2]$ overnight will also reduce the amount of nocturnal carboxylation and subsequent accumulation of malate. These experiments are therefore a way of exploring the importance of photo assimilate and the effect of malate accumulation on stomatal conductance across these C₃ and CAM tissues.

3.3.8 Reduced photo-assimilate reduced daytime stomatal response in C₃ tissues but reduced malate accumulation had no effect on daytime stomatal responses in CAM tissues

Stomatal response to reduced $[\text{CO}_2]$ after 24 hrs of low $[\text{CO}_2]$ was measured to explore the effect of reduced photo-assimilate on stomatal conductance response to reduced $[\text{CO}_2]$ in the subsequent day. Daytime stomatal response to reduced $[\text{CO}_2]$ decreased in both the C₃ young *K. blossfeldiana* and CAM-deficient *K. fedtschenkoi pepc1.1* leaves (Figure 3.7). In the CAM tissues 24 hrs of low CO_2 (70 $\mu\text{mol mol}^{-1}$) should reduce the amount of CO_2 assimilated into malate and reduce the amount of malate available for decarboxylation. Figure 3.7 showed that there was no significant change in the daytime responses to reduced CO_2 (70 $\mu\text{mol mol}^{-1}$) in any of the CAM tissues after being subjected to 24 hr of low CO_2 (70 $\mu\text{mol mol}^{-1}$).

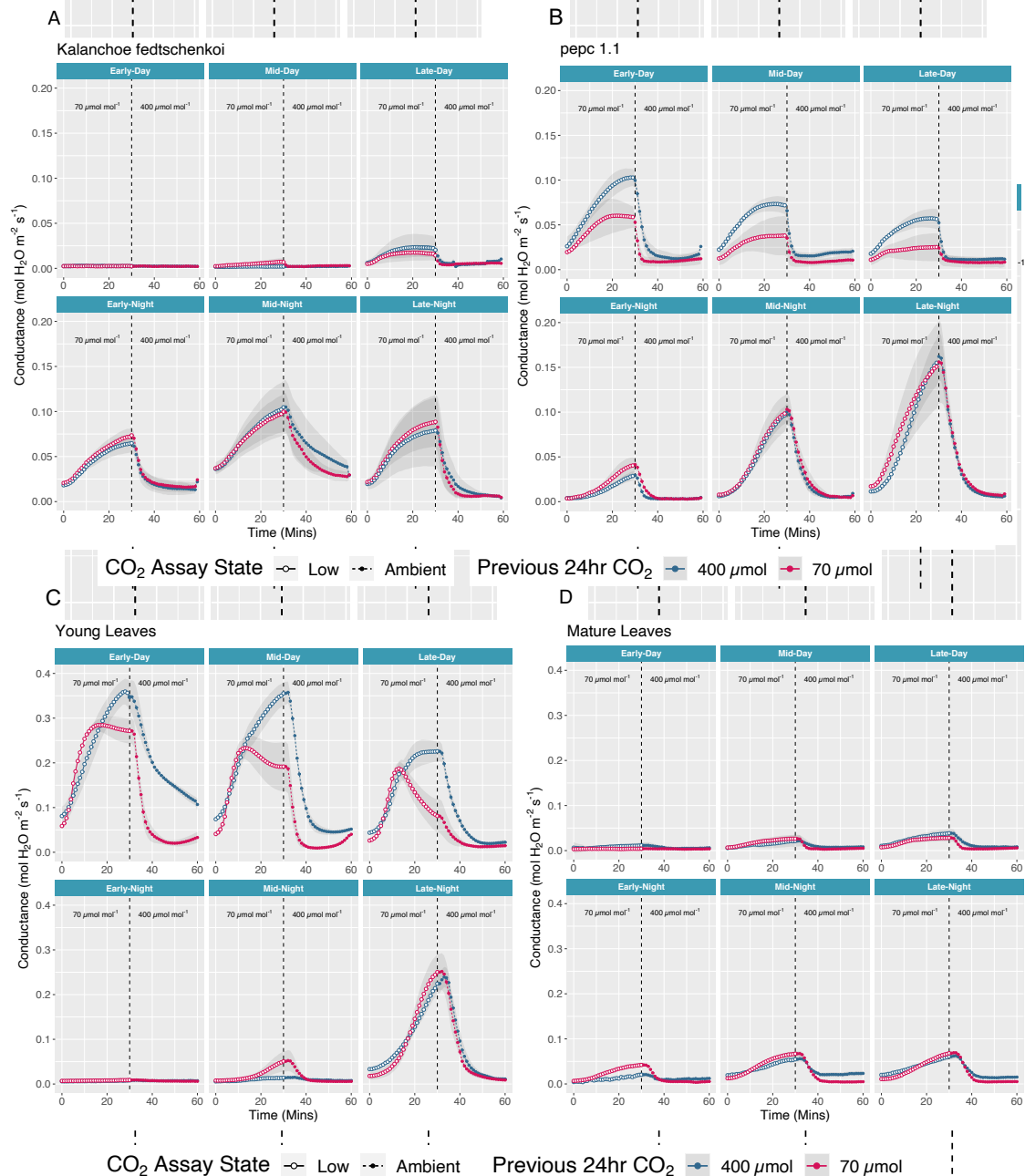


Figure 3.7 *K. fedtschenkoi* (Panels A and B) or *K. blossfeldiana* (Panels C and D) stomatal responses to reduced CO₂ after 24 hrs of ambient (400 μmol mol⁻¹ blue points) or reduced CO₂ (70 μmol mol⁻¹ red points). Single leaves were held at 70 μmol mol⁻¹ CO₂ in a Licor-6400xt chamber or kept at ambient 400 μmol mol⁻¹ CO₂ and assayed. *K. fedtschenkoi* wild type (panel A) and *K. fedtschenkoi pepc1* mutant leaves (panel B) and *K. blossfeldiana* young leaves (left, panel C) and mature leaves (right, panel D) were assayed at 6 timepoints (2hrs, 6hrs, 10 hrs from dawn; and 3 hrs, 6 hrs, 10 hrs from dusk). The CO₂ concentration of the previous 24 hrs was denoted by blue points (400 μmol CO₂) or red points (70 μmol CO₂). For each timepoint CO₂ was held at low CO₂ (70 μmol CO₂, open points) for 30 minutes followed by a return to ambient (400 μmol CO₂, closed points) for 30 minutes, with measurements taken every minute. For each graph points represent the mean of three repeats and the shaded interval ± SEM.

3.3.9 Growth at reduced light intensity had differing effects on stomatal behaviour in C₃ and CAM tissues in *K. blossfeldiana*

K. blossfeldiana plants were grown in reduced light (90 vs 190 $\mu\text{mol m}^{-2} \text{s}^{-1}$) from propagation onwards as an alternative means of reducing leaf carbon status (Figure 3.7). This had different effects on the diel patterns of net CO₂ uptake and stomatal conductance between the young (C₃) and mature (CAM) leaves. The young C₃ leaves grown at 90 $\mu\text{mol m}^{-2} \text{s}^{-1}$ showed a marked reduction in both diel CO₂ uptake and stomatal conductance. The mature CAM leaves showed an increase in daytime CO₂ uptake and a reduction in nocturnal PEPC-mediated CO₂ uptake. This was accompanied by an increase in daytime conductance in the mature CAM leaves and a reduction in nocturnal conductance. Thus, growth under low light resulted in reduced CAM in the mature leaves of *K. blossfeldiana*.

A CO₂ stomatal response assay was carried out on both tissue types under reduced light (90 vs 190 $\mu\text{mol m}^{-2} \text{s}^{-1}$), similar to those carried out in figure 3.4A/B. External CO₂ concentrations were reduced from 400 $\mu\text{mol mol}^{-1}$ to 70 $\mu\text{mol mol}^{-1}$ and stomatal conductance was monitored at 1 min intervals for 30 minutes followed by a return to ambient (400 $\mu\text{mol mol}^{-1}$ CO₂). The plants were subjected to these shifts in [CO₂] at 6 time points (2 hrs, 6 hrs and 10 hrs from dawn; and 3 hrs, 6 hrs and 10 hrs from dusk). An extra condition was added to this response assay, in which *K. blossfeldiana* plants grown at 90 $\mu\text{mol m}^{-2} \text{s}^{-1}$ since propagation were assayed at 190 $\mu\text{mol m}^{-2} \text{s}^{-1}$ at daytime timepoints. This was to control for the effect of reduced stomatal opening due to the reduced light.

Again, growth at reduced light intensity (90 $\mu\text{mol m}^{-2} \text{s}^{-1}$) had different effects on the low CO₂ stomatal response in the young and mature *K. blossfeldiana* leaves. Stomatal responses to reduced CO₂ in young C₃ leaves were significantly weakened by growth in low light, even when normal light was restored for the assay. The opposite occurred in the mature leaves, with stomatal responses, including amplitude and opening/closing rates, to reduced CO₂ increased during the day timepoints, slight but insignificant reductions were observed during the night.

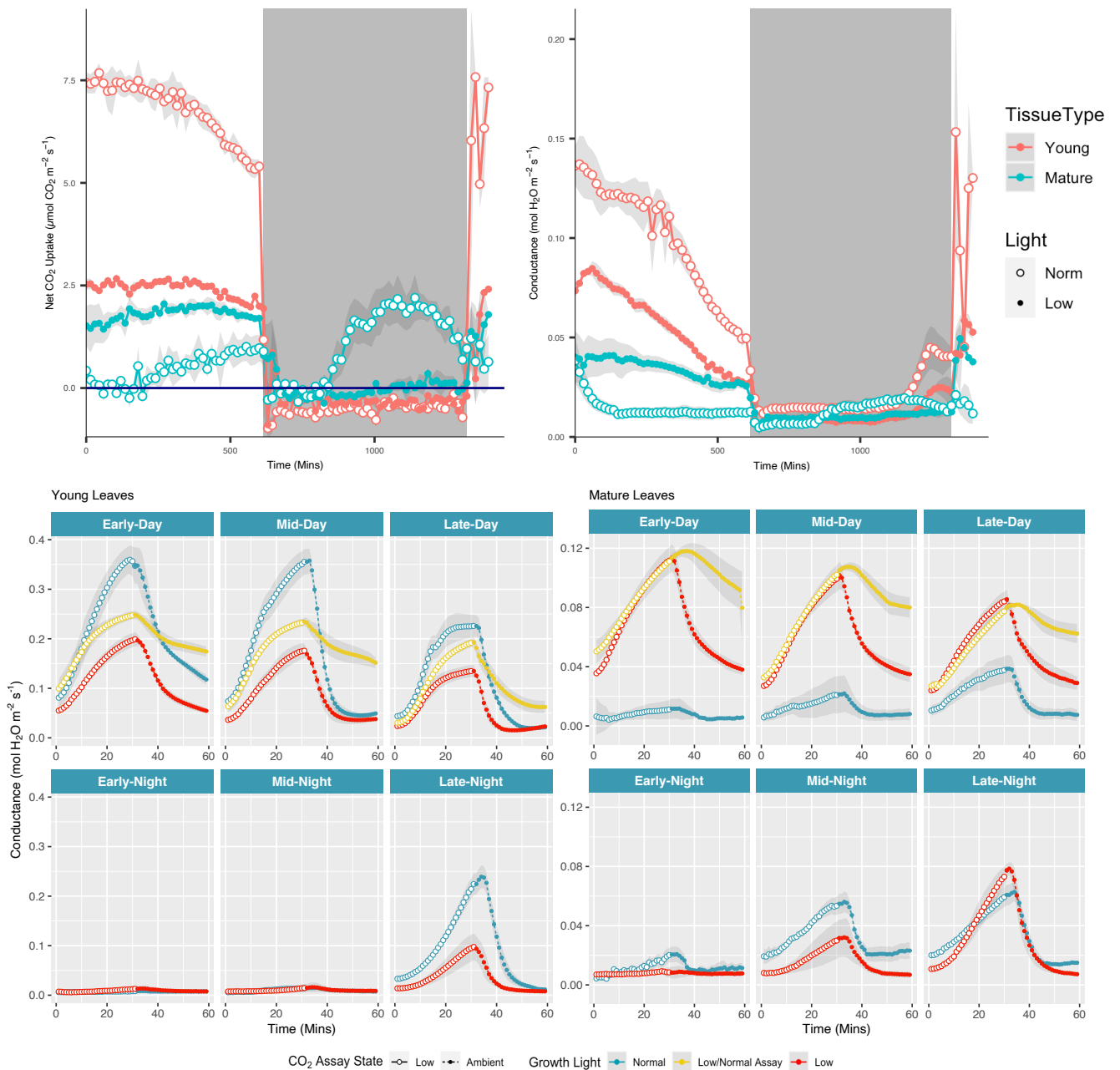


Figure 3.8 Impact of growing *K. blossfeldiana* at reduced light intensity on age specific photosynthetic and stomatal responses. Plants were grown at reduced or ambient light ($50 \mu\text{mol m}^{-2} \text{s}^{-1}$, filled points, or $190 \mu\text{mol m}^{-2} \text{s}^{-1}$, empty points). Diurnal net CO_2 assimilation (panel A, $\mu\text{mol CO}_2 \text{m}^{-1} \text{s}^{-1}$) and stomatal conductance stomatal (panel B, $\text{mol H}_2\text{O m}^{-1} \text{s}^{-1}$) of *K. blossfeldiana* young leaves (red points, 10th leaf pair from bottom) and mature leaves (blue points, 2nd leaf from bottom) between 60-90 days after propagation. Plants grown in 12hr/12hr day/night cycles. Dark shaded area represents night. Low CO_2 stomatal response assay (panel C and D, $\text{mol H}_2\text{O m}^{-1} \text{s}^{-1}$). Plants from the diurnal experiment were assayed at 6 timepoints (2hrs, 6hrs, 10hrs from dawn; and 3 hrs, 6 hrs, 10 hrs from dusk). Young leaves (left, panel C) and mature leaves (right, panel D) were compared. Low CO_2 assays were carried out at the same respective light intensities $50 \mu\text{mol m}^{-2} \text{s}^{-1}$ (red points) or $190 \mu\text{mol m}^{-2} \text{s}^{-1}$ (blue points) as the diurnal experiment. For day timepoints a third light condition was used were plants grown at $50 \mu\text{mol m}^{-2} \text{s}^{-1}$ light and then received $190 \mu\text{mol m}^{-2} \text{s}^{-1}$ light for the duration of each timepoint (yellow points). For each timepoint CO_2 was held at low CO_2 ($50 \mu\text{mol}$, open points) for 30 minutes followed by a return to ambient ($400 \mu\text{mol CO}_2$, closed points) for 30 minutes, with measurements taken every minute. For each graph points represent the mean of three repeats and the shaded interval \pm SEM. The dark blue line on the CO_2 uptake graphs equals zero.

3.4 Discussion

3.4.1 C₃ and CAM leaves have distinct patterns of diel stomatal conductance.

As predicted, both of the systems for comparing C₃ and CAM, the young C₃ and mature CAM *K. blossfeldiana* leaves and the CAM *K. fedtschenkoi* and CAM-deficient *pepc1.1* mutants, showed marked differences in patterns of stomatal conductance over the diel cycle. Wild type *K. fedtschenkoi* and mature *K. blossfeldiana* leaves, performing CAM, showed characteristic 'CAM-like' patterns of stomatal conductance (Males & Griffiths, 2017), with the highest values of conductance measured at night. Stomatal conductance in both young *K. blossfeldiana* and *pepc1.1 K. fedtschenkoi* leaves followed 'C₃-like' patterns. While both tissue types showed higher stomatal conductance during the day than the CAM tissues, this difference was more pronounced in the *K. blossfeldiana* young leaf versus mature leaf comparison; which is likely due to higher net daytime carbon assimilation in the young *K. blossfeldiana* leaves compared to the *pepc1.1* mutant line of *K. fedtschenkoi*. A similar reversion to 'C₃-like' stomatal conductance when expression of PEPC1 was perturbed was also observed in the constitutive CAM *Kalanchoë laxiflora* (Boxall et al., 2020).

3.4.2 Guard Cell Starch Metabolism is rescheduled between C₃ and CAM tissues

Guard cell starch metabolism plays a key role in guard cell function (Lloyd, 1908), with a distinct pattern of starch turnover compared to that of the mesophyll. It is thought that guard cell starch acts as a carbon sink that can be hydrolysed to provide sugars and malate to be used as osmolytes and/or energy for stomatal opening (Tallbott & Zeiger, 1993). Studies have shown the importance of guard cell starch synthesis in C₃ species in closure in response to increased CO₂ closure (Azoulay-Shemer et al., 2016) and starch degradation in blue light induced opening in the morning (Horrer et al., 2016; Lasceve et al., 1997; Tallbott & Zeiger, 1993). It has been hypothesised that the pattern of guard cell carbohydrate metabolism may differ between C₃ and CAM plants, with recent data showing that starch turnover in *K. fedtschenkoi* guard cells has been rescheduled compared to C₃ plants, with starch broken down in the night in CAM as opposed to breakdown in the early day in *Arabidopsis* (Abraham

et al., 2020). Figure 3.3. shows a similar rescheduling of guard cell starch turnover between C₃ and CAM tissues in both *K. blossfeldiana* and *K. fedtschenkoi* systems. In *K. blossfeldiana* as leaves age and increase CAM, guard cell starch metabolism shifts from a general pattern of nocturnal synthesis at night and breakdown towards the day to a pattern of breakdown towards and into the night and synthesis during the late night and day (Figure 3.3.C).

The pattern of dawn/dusk guard cell starch metabolism also differs between the wild type and *K. fedtschenkoi pepc1.1* mutant, with greatest starch granule area observed at dusk in the wild type but at dawn in *pepc1.1*. Together these results suggest that the retiming of guard cell starch metabolism may be key to enabling nocturnal conductance in CAM leaves. The role of guard cell starch as a possible energy store within the guard cells may be even more important in CAM leaves, as guard cells must be able to maintain nocturnal opening without any direct input from photosynthesis. Future work to perturb guard cells starch metabolism is needed to investigate the importance of this change - e.g. guard cell specific knockdown of key starch synthesis or degradation genes. And to explore whether this is also the case in other CAM genera.

Dawn/dusk soluble sugar contents in guard cell enriched epidermal peels changed between the C₃ and the CAM tissues (Figure 3.3). C₃ peels from young *K. blossfeldiana* and *K. fedtschenkoi pepc1.1* mutants showed greatest sugar content at dusk and a substantially reduced amount at dawn. Whereas CAM tissues in mature *K. blossfeldiana* leaves and *K. fedtschenkoi* wild type showed significantly greater and slightly greater levels at dawn, respectively. It is possible that this overnight reduction in sugar content in the C₃ tissues were driven by conversion of C-skeletons into guard cell starch, which occurred overnight in both C₃ tissues (Figure 3.3) but to a lesser extent in *pepc1.1*. Recent studies have highlighted the importance of guard cell sugars in maintaining proper stomatal opening (Daloso et al., 2016; Daloso et al., 2016; Flütsch, 2020), thus opposite patterns of epidermal sugar contents between the C₃ and CAM tissues may underpin differences in C₃ and CAM diel patterns of stomatal conductance.

3.4.3 The role of C_i in linking mesophyll PEPC-driven carboxylation and stomatal conductance.

CO_2 drawn down due to assimilation has long been thought to be a key link between mesophyll RUBISCO- or PEPC-mediated carbon assimilation and guard cell opening with C_i thought to be a key signal that links the diel shift in photosynthetic and stomatal behaviours (Griffiths et al., 2007; von Caemmerer & Griffiths, 2009; Wyka et al., 2005). In CAM nocturnal conductance is believed to be driven by reduced C_i as a result of carbon assimilation at night and daytime closure driven by increased C_i due to the decarboxylation of accumulated malate, to levels reportedly as high as $10,000 \mu\text{mol mol}^{-1}$ (Cockburn et al., 1979).

A key finding from the data presented in this chapter was that positive nocturnal stomatal conductance was observed towards the end of the night in the C_3 young *K. blossfeldiana* leaves without any net CO_2 uptake at this time or change in titratable acidity (Chapter 2, Figure 2.3). The values obtained for this nocturnal conductance was comparable and at times greater than nocturnal conductance in the mature leaves). This nocturnal opening observed the C_3 young *K. blossfeldiana* leaves towards the end of the night took a different pattern to that of the mature CAM leaves and may be a C_3 trait with stomata opening in advance of the morning. Instances of nocturnal stomatal opening in C_3 plants are common and show similar patterns to that of the C_3 young *K. blossfeldiana* with peaks towards the end of the night period (Zeppel et al., 2012, 2014; Cirelli et al., 2016; de Dios et al., 2016, 2019). It has been suggested that nocturnal stomatal opening prepare stomata for photosynthesis in the early day (de Dios et al., 2016). A reanalysis of many C_3 and C_4 species found that nocturnal conductance correlated with faster growth but also noted variation in magnitude between species (Resco de Dios et al., 2019).

It was unclear whether there was any CO_2 assimilation independent stomatal opening in *K. fedtschenkoi pepc1.1* mutant, as there was some residual nocturnal CO_2 assimilation observed along with stomatal conductance. However, some nocturnal conductance was observed in CAM deficient *Kalanchoe laxiflora pepc1* mutant (Boxall et al., 2020) that did not show any overnight net CO_2 assimilation. There was a reduced correlation between assimilation and conductance overnight in the *K. fedtschenkoi pepc1.1* mutant compared to the wild type overnight, which might suggest some element of decoupling between assimilation and conductance in the PEPC impaired mutant. In both the *K. fedtschenkoi* and *K. laxiflora* (Boxall

et al., 2020) *pepc1* mutants the amount of nocturnal opening was reduced versus the CAM performing wild types and tended to increase over the course of the night; conductance also peaked towards the end of the night in the young *K. blossfeldiana* leaves.

Overall it appears that nocturnal stomatal opening can occur without PEPC activity in the C₃ young *K. blossfeldiana* leaves towards the end of the night and to a lesser extent in the CAM deficient *K. fedtschenkoi pepc1.1* mutant. However, the majority of nocturnal stomatal opening in the CAM tissues is driven by PEPC-mediated carboxylation.

3.4.4 Diel sensitivity to reduced C_i varies between C₃ and CAM tissues

This uncoupling of nocturnal stomatal conductance from net CO₂ uptake in C₃ and/or CAM deficient *Kalanchoe* led to the two following questions: How does responsiveness to reduced CO₂ vary over the diel period and between C₃ and CAM tissues? Could an extended period of reduced external [CO₂] restore or induce a CAM-like pattern of opening in the C₃ systems?

Stomatal responsiveness to reduced [CO₂] changed over the 24 hr period and varied between C₃ and CAM photosynthetic physiotypes in both *K. blossfeldiana* and *K. fedtschenkoi*. Stomata in young *K. blossfeldiana* leaves were most responsive to altered [CO₂] in magnitude (G_{diff} and G_{int}) and rapidity ($Max SI_{open}/SI_{close}$) during the day; whereas stomata in the mature CAM leaves showed their greatest responses during the night period. Similar differences in stomatal responses to reduced [CO₂] between CAM wild type *K. fedtschenkoi* and CAM-deficient *pepc1.1* mutant leaves were observed. The CAM-deficient *pepc1.1* mutant stomata were responsive to reduced [CO₂] at all timepoints; and were significantly more responsive than wild type stomata during the day and at the late night timepoint (Figure 3.4.B). Stomatal responses to reduced C_i in wild type *K. fedtschenkoi* showed a CAM like pattern, with no or limited response throughout the day and responses present and building through the night. In general, stomatal responsiveness to reduced CO₂ occurred at times when CO₂ assimilation and stomatal conductance were well correlated which is consistent with the concept of C_i draw down linking mesophyll carbon assimilation and stomatal conductance in both C₃ and CAM tissues.

3.4.5 Reduced [CO₂] can restore CAM-like nocturnal opening in CAM-deficient *K. fedtschenkoi pepc1.1* mutant but not young C₃ *K. blossfeldiana*

In a further effort to explore the role of [CO₂] on stomatal conductance, an experiment was carried out in which external [CO₂] was held at 70 μmol mol⁻¹ for an entire 24 h diel cycle. The aim was to simulate the drawdown of internal [CO₂] or C_i during CO₂ assimilation during the day and the night.

There was a key distinction between the two different C₃/CAM-deficient model tissues in how reduced [CO₂] impacted stomatal conductance. In the *K. fedtschenkoi pepc1.1* mutant, reduced C_i over the night induced an increase in nocturnal stomatal conductance greater than that observed in the wild type performing CAM at normal CO₂ concentrations. This result indicates that it is possible to restore nocturnal stomatal opening in the CAM-deficient *pepc1.1* line by simulating the drawdown of CO₂ that occurs during CAM. Thus, despite being impaired in the ability to produce malate the *pepc1.1* mutant was still able to respond to reduced [CO₂] by opening stomata overnight. However, such an effect was not observed in the young C₃ leaves of *K. blossfeldiana* which showed increased (compared to mature leaves) but variable stomatal conductance towards the end of the night when CO₂ concentration was held at 70 μmol overnight and displaying a pattern of stomatal conductance that was not comparable to the mature leaves at ambient or low CO₂.

The distinction, that it is possible to induce a CAM-like pattern of nocturnal conductance in the CAM-deficient *K. fedtschenkoi pepc1.1* line but not in the young *K. blossfeldiana* leaves along with evidence of varying diel sensitivity to CO₂ concentration suggests the presence of a mechanism that alters guard cells sensing of or ability to respond to reduced CO₂ concentration that changes with transition from C₃ to CAM. This occurs despite the *K. fedtschenkoi pepc1.1* line being impaired in the ability to produce malate; that the *pepc1.1* mutant is still able to respond to reduced CO₂ overnight suggests that any change that occurs to allow nocturnal stomatal opening in transition from C₃ to CAM is independent of PEPC activity and is active in the *pepc1.1* mutant.

Together the results described above suggest that guard cell responsiveness to low [CO₂] varies over 24hrs and differs between C₃ and CAM physiotypes; that this responsiveness is well correlated with key periods of CO₂ assimilation (apart from C₃ and CAM-deficient tissues at night); and the drawdown of CO₂ due to mesophyll carbon assimilation alone is not enough to induce a CAM-like pattern of stomatal opening in young C₃ *K. blossfeldiana* and likely C₃ plants in general. However, from these experiments it is not clear by what mechanism the CAM-guard cells use to enable nocturnal opening. It is likely that there is a difference in guard cell regulation pathways that could act via starch metabolism to enable nocturnal opening, which could be detected by exploring changes in the expression of key guard cell regulatory genes. It is not entirely clear how the CAM guard cells sustain nocturnal opening, yet the nocturnal break down of starch observed in this chapter could provide osmolytes and carbohydrates to sustain nocturnal opening. It is also possible that a signal originating in the mesophyll may influence nocturnal stomatal opening in the CAM leaves, Santos et al. (2021) provided evidence for some level of autonomous guard cell behaviour in *K. fedtschenkoi* that was possibly influenced by a mesophyll signal. In C₃ guard cells there is substantial evidence that the mesophyll supports guard cell opening, summarised well by Lawson et al. (2014). From the data here, it is clear that nocturnal guard cell opening in CAM is independent of PEPC mediated malate accumulation yet further work is needed to unravel the PEPC- independent pathways that drive nocturnal low-C_i opening in CAM guard cells.

3.4.6 Increased stomatal conductance in C₃/CAM-deficient tissues is driven by increased photo-assimilate and stomatal density

Both C₃ tissues, the young *K. blossfeldiana* and CAM-deficient *K. fedtschenkoi pepc1.1* mutants had significantly greater diurnal net CO₂ uptake and diurnal stomatal conductance than the CAM tissues (Figure 3.1). Stomatal conductance responses to C_i were significantly reduced in both attempts to explore a link between the greater diurnal net CO₂ uptake and greater diurnal stomatal conductance in the C₃ tissues, either by growth under reduced light intensity (*K. blossfeldiana* only, 90 μmol m⁻² s⁻¹) or by 24 hrs of 70 μmol mol⁻¹ CO₂ (*K. blossfeldiana* and *K. fedtschenkoi*). Importantly, growth at reduced light intensity did not significantly affect stomatal density in the young or mature leaves (Appendix Figure A1.3, p<0.1), but some

contribution to the changes should not be ruled out. There was, however, a significant difference between the stomatal density of the young and mature *K. blossfeldiana* leaves.

Overall, the presence of increased photo-assimilate in the C₃ leaves in the form of soluble sugars likely explains, at least in part, their increased responsiveness and conductance during the day.

3.4.7 What role does nocturnal malate accumulation play in daytime stomatal closure in CAM?

In CAM tissues the release of CO₂ behind closed stomata from the decarboxylation of malate during the day will increase C_i, to levels reportedly as high as 10,000 μmol mol⁻¹ (Cockburn et al., 1979); which has long been thought to provide a simple mechanism to drive stomatal closure during the day period. A previous study showed exposing CAM-performing leaves of *Kalanchoe daigremontiana* *Kalanchoe pinnata* to reduced [CO₂] at night had little effect on stomatal conductance early to mid-day (Von Caemmerer & Griffiths, 2009). However, despite holding [CO₂] low over night and significantly reducing titratable acidity, the recorded remaining acidity was similar to levels observed in CAM-performing mature *K. blossfeldiana* and wild type *K. fedtschenkoi* leaves and may be enough to trigger closure via decarboxylation. In a similar experiment carried out here, where stomatal responses to low CO₂ were recorded after CO₂ was held low (70 μmol mol⁻¹) for 24 hrs, there was a limited effect on both CAM tissues (mature *K. blossfeldiana* and wild type *K. fedtschenkoi*, Figure 3.7). However, it is unclear if this reduced residual malate from previous night was enough to have a significant effect on daytime closure.

In all experiments in this chapter where nocturnal malate accumulation has been notably reduced, for example in the *K. fedtschenkoi pepc1* mutant or in the mature *K. blossfeldiana* grown at reduced (90 μmol m⁻² s⁻¹) light, daytime stomatal conductance, and daytime response to reduced [CO₂] increased. This chapter has also, suggested that an element of increased daytime stomatal opening and response to reduced [CO₂] in the C₃/CAM deficient tissues is due to increased photo-assimilate. Taken together, data from this chapter would suggest that daytime stomatal closure in the CAM tissues is being driven by increased C_i due to the decarboxylation of malate. It is also possible that other mechanisms may play a role in ensuring daytime stomatal conductance in CAM leaves, which may be of especial importance in periods of carbon starvation during prolonged drought with low carbon uptake.

3.4.8 Conclusions

Overall this chapter highlighted key differences in stomatal behaviour and carbohydrate metabolism of guard cells between C_3 and CAM photosynthetic tissues, with differences observed in stomatal conductance; stomatal responsiveness to C_i and a retiming of guard cell starch and soluble sugar metabolism between C_3 and CAM tissues across the two comparative systems (*K. blossfeldiana* young C_3 and mature CAM leaves, and wild type and CAM deficient *pepc1 K. fedtschenkoi* mutants).

Notably, *K. blossfeldiana* young C_3 guard cells were unable to sustain nocturnal stomatal opening in response to reduced C_i overnight, while CAM deficient *pepc1 K. fedtschenkoi* guard cells showed wild type levels of nocturnal opening in response to reduced C_i overnight. Together this suggested a change occurs in the *K. blossfeldiana* guard cells on the transition from C_3 to CAM to enable nocturnal opening that is distinct from mesophyll PEPC-driven carboxylation and demonstrating that C_i alone is likely not enough to induce a CAM nocturnal pattern of stomatal opening in C_3 plants.

The data collected in this chapter showed that the pattern of starch metabolism progressively changed as the leaves aged and CAM activity increased in *K. blossfeldiana*; it is therefore possible that the retiming of starch metabolism in CAM guard cells is to support nocturnal opening both energetically and by supplying osmoticum. The chapter also suggested that diurnal stomatal closure was largely driven by increases in C_i from the diurnal decarboxylation of malate, with CAM-deficient *pepc1 K. fedtschenkoi* mutants displaying C_3 levels of diurnal stomatal conductance. However, it is not clear if there are other, possibly regulatory elements, that assist in or enable daytime closure.

Chapter 4. The *Kalanchoe blossfeldiana* Genome

4.1 Introduction

Crassulacean acid metabolism (CAM) is a complex trait that recruits many of metabolic enzymes and pathways present in C₃ species, with genes upregulated or their expression patterns re-timed to fit the CAM diel cycle (Abraham et al., 2016; Wai et al., 2019; Yang et al., 2017). Efforts to understand CAM, its induction and regulation will need to consider genome scale changes in gene expression. Consequently, recent years have seen a flurry of ‘CAM-omics’ studies, with the genomes of constitutive and facultative CAM species from across plant life sequenced, including: *Ananas comosus* (Ming et al., 2015), *Kalanchoe fedtschenkoi* (Yang et al., 2017), *Kalanchoe laxiflora* (unpublished, Phytozome), *Sedum album* (Wai et al., 2019), *Talinum triangulare* (Brilhaus, Bräutigam, et al., 2016; Maleckova, 2020; Maleckova et al., 2019), *Isoetes taiwanensis* (Wickell et al., 2021) and most recently *Cistanthe longiscapa* (Ossa et al., 2022).

However, only a handful of omics studies have looked at the induction of CAM and there has yet to be a genome scale study focused on changes in gene expression in CAM induction by ageing. The ability of *K. blossfeldiana* to transition from C₃ to CAM as it ages could provide an important platform for the comparative study of C₃ and CAM. This is the first reported work exploring transcriptional changes after CAM induction by ageing, with previous focusing on CAM induction by ABA (Maleckova et al., 2019), drought (Wai et al., 2019) or salt stress (Cushman et al., 2008). This thesis hypothesises that identifying CAM-specific changes in the transcriptome in inducible CAM plants maybe be clearer in age-induced CAM compared to that of stress-induced CAM. This chapter presents the genome of the inducible CAM plant *K. blossfeldiana* along with a comparison of the transcriptome between the young C₃ and mature CAM *K. blossfeldiana* leaves at dusk. The aim of this work is to lay the foundations for future molecular genetic studies utilising *K. blossfeldiana* to compare C₃ and CAM physiologies within the same plant.

This chapter will address five hypotheses:

1. There may be a high level of conservation between key CAM genes in *K. blossfeldiana* and close relative *K. fedtschenkoi* in terms of both sequence identity and orthologs recruited for CAM.
2. Key elements of age-induced CAM in *K. blossfeldiana* may be identified by investigating the changes in transcript abundance in age induced CAM and cross comparing with genes upregulated in studies across different CAM species and different induction modes.
3. The induction of CAM by ageing may be less stressful and involve fewer elements than those in response to an abiotic stress such as drought, which could make it easier to dissect changes to the transcriptome that are specific to CAM.
4. Key elements of guard cell metabolism and stomatal regulation may show retimed patterns of gene expression between the young C₃ and CAM tissues in *K. blossfeldiana*.
5. Endoreplication may occur as the leaves become more succulent and transition to CAM as they age in *K. blossfeldiana*.

4.2 Materials and Methods

4.2.1 Plant Materials

The inducible CAM plant *Kalanchoe blossfeldiana* was sampled at 90 days after propagation for this chapter. For genome assembly all short read illumina sequencing was carried out on DNA extracted from young leaves (10th leaf pair from the bottom). Nanopore long read sequencing occurred on DNA extracted from both 10th leaf pair from the bottom) and mature (2nd leaf pair from the bottom) to allow for the analysis of differential methylation between these leaves. For RNA sequencing RNA was extracted from young (10th leaf pair from the bottom) and mature (2nd leaf pair from the bottom) leaves.

4.2.2 Estimating *K. blossfeldiana* genome size

Flow cytometry was carried out by Robyn Powel at Kew Gardens on both young (10th leaf pair from the bottom) and mature (2nd leaf pair from the bottom) leaves. The genome size of *Kalanchoe blossfeldiana* was estimated by flow cytometry using the fluorochrome propidium iodide and following the method described in (Pellicer et al., 2021). Briefly, a fresh razor blade was used to chop c. 1cm² of young leaf tissue of *K. blossfeldiana* with the internal standard (*Petroselinum crispum* (Mill) Nyman ex A.E. Hill 'Champion Moss Curled', 1C=2,171.16 Mbp; (Obermayer et al., 2002) in a petri dish containing 1 ml of General Purpose Buffer supplemented with 3% PVP (GPB) (Loureiro et al., 2007). A further 1 ml of GPB was added and the sample was gently mixed. The sample was passed through a 30 µm nylon filter and the resulting homogenate was stained with 100 µl propidium iodide (1 mg/ml) and incubated on ice for 10 minutes. The sample was run three times on a Sysmex CyFlow Space (Sysmex Europe GmbH, Norderstedt, Germany) flow cytometer fitted with a 100 mW green solid state laser and recording up to 1,000 nuclei per fluorescence peak each time. In total, four separate samples prepared from different leaves of two individual plants were analysed. The resulting histograms were analysed using the WindowsTM-based FlowMax software (v. 2.9 2014, Sysmex GmbH) and the average of each sample was used to estimate genome size. Genome size in base pairs was calculated as described by Doležel et al. (2003)

Genome size was also estimated computationally from genomic illumina short reads. A histogram of Kmer distribution was created from illumina short reads using Jellyfish 2.3.0 (Marçais & Kingsford, 2011) and passed to GenomeScope 2 (Vurture et al., 2017). Many varieties of *K. blossfeldiana* vary in their ploidy. Genome ploidy was estimated by first calculating kmer frequencies and a histogram of kmers using Jellyfish 2.3.0 (Marçais & Kingsford, 2011) followed by analysis with GenomeScope 2 and Smudgeplot 0.2.5 (Ranallo-Benavidez et al., 2020).

4.2.3 *K. blossfeldiana* DNA Extraction

Both RNA and DNA extractions were carried out in collaboration with another research student (Bethan Morris). For Illumina short reads genomic DNA was extracted using an adapted version of (Keb-Llanes et al., 2002) followed by a further clean up using the ChargeSwitch gDNA Mini Bacteria Kit (Invitrogen, USA). Samples were flash frozen in liquid nitrogen, then 300 mg of leaf tissue was ground in liquid nitrogen, then lysed and homogenised in a mix of two extraction buffers mixed just prior to extraction. 300 µl buffer A (2% Hexadecyltrimethylammonium bromide (CTAB) (w/v), 100 mM Tris-HCl (pH 8), 20 mM EDTA, 1.4 M NaCl, 4% polyvinylpyrrolidone (PVP-40) (w/v), 0.1% ascorbic acid (w/v), and 10 mM β-mercaptoethanol); and 900 µl buffer B (100 mM Tris-HCl (pH 8), 50 mM EDTA, 100 mM NaCl) were mixed along with 100 µl 20% SDS and 10 mM β-mercaptoethanol. Extracts were vortexed then incubated at for ten minutes at 65°C while shaking at 1500 rpm. Exactly 410 µl potassium acetate was added, samples were then spun down at 15,300 g for 15 minutes at 4°C. Supernatant (1 ml) was transferred to a fresh microcentrifuge tube and added to 540 µl ice cold isopropanol and incubated for 20 minutes. Samples were then washed three times as follows: samples centrifuged at 9600 g for ten minutes at 4°C; supernatant discarded, and pellet washed with 540 µl 70% ethanol and immediately air dried; pellet was then resuspended in 600 µl TE buffer (10 mM Tris, 1 mM EDTA (pH 8)), 60 µl 3M sodium acetate (pH 5.2) and 360 µl ice cold isopropanol; sample was then incubated for 20 minutes, and the process repeated. After three washes the sample was spun down at 9600 g for ten minutes at 4°C then resuspended in 50 µl resuspension buffer (R4, from the ChargeSwitch kit) containing RNase A. The ChargeSwitch protocol followed from this point on, as described in its manual. For long read nanopore sequencing the extraction was as above for with gDNA extracted from

both young (9th leaf pair from the bottom) and mature (3rd leaf pair from the bottom) leaves. All samples were accessed for quality by nanodrop 2000 (Thermo Fisher, Massachusetts) and agarose gel with a high molecular weight ladder (N3239S, NEB, Massachusetts).

4.2.4 *K. blossfeldiana* RNA Extraction

RNA was extracted from young (9th leaf pair from the bottom) and mature (3rd leaf pair from the bottom) leaves, at dusk. Samples were flash frozen in liquid nitrogen, then 100 mg of leaf tissue was ground in liquid nitrogen. The samples were the same as those used in chapter one for metabolite analysis. Ground tissue was combined with 900 μ l of pre-heated (65°C) extraction buffer: 3% Hexadecyltrimethylammonium bromide (CTAB) (w/v), 100 mM Tris-HCl (pH 8), 25 mM EDTA (pH 8), 2 M NaCl, 3% polyvinylpyrrolidone (PVP-40) (w/v), 0.5g/L spermidine and 4% β -mercaptoethanol added just prior to extraction and incubated at 65°C for ten minutes while shaking. Exactly 900 μ l of chloroform: isoamyl alcohol (24:1) was added and mixed by inversion for ten minutes. Samples were centrifuged at max speed for ten minutes at 4°C, with supernatants transferred to fresh tubes with an equal volume of chloroform: isoamyl alcohol (24:1), then incubated at 4°C for ten minutes while inverting. The upper phase was discarded and two times volume of ethanol added, followed by freezing at -20°C for two hours and centrifuged at 15,000 g for 30 minutes. The supernatant was discarded and 1 ml lithium chloride added, followed by two hours at -20°C and centrifuged at 15,000 g for 30 minutes. The supernatant was discarded and the RNA pellet was resuspended in 100 μ l of DEPC water, with gentle shaking at 65°C for ten minutes. Care was taken throughout to avoid RNase contamination. Samples were then DNase treated with an Invitrogen DNase kit, as described by its manual.

4.2.5 *K. blossfeldiana* Genome Sequencing

Short read whole genome library preparation and sequencing of *K. blossfeldiana* was carried out by Novogene (Beijing, China). Sample and library integrity was tested with an Agilent 2100 Bioanalyzer (Agilent Technologies, USA). Pair end 150 bp libraries were produced using the NEB Next Ultra DNA Library Prep Kit and sequencing was performed in three runs on the same library on an Illumina NovaSeq 6000. The three runs produced a total of 91.6 Gb, 305 million PE reads, and an estimated sequencing coverage of ~200x for a predicted haploid genome size of 450 Mb. Initial sequence QC and adaptor trimming was carried out by Novogene and then assessed in FastQC 0.11.9 (Andrews, 2010). Long read sequencing was carried out over three r9.4.1 minion flow cell using either the RAD004 or RBK004 kits, with libraries prepared as per their protocols. For one run the RBK004 was used to differentially barcode DNA from the young and mature leaves to allow for the analysis of differential methylation between these leaves. Basecalled and quality filtered by Guppy and read quality was assessed in LongQC

4.2.6 *K. blossfeldiana* Genome Assembly

Genome assembly was performed with a hybrid assembly approach using MaSuRCA 4.0.9 (Zimin et al., 2017), which combines accurate short and error prone long reads into super reads and is often used in the assembly of large plant genomes (Scott et al., 2020; Wang et al., 2020). Assemblies were also performed using only short reads with abyss 2.3.5 (Jackman et al., 2017) and only long reads with Flye 2.9.1 (Kolmogorov et al., 2019) for comparison. Assembly quality and size statistics were calculated at each step of assembly processing by BUSCO 5.4.3 (Manni et al., 2021) and the abyss-fac script from the abyss assembler.

The MaSuRCA assembly was scaffolded using Ragtag 2.1.0 (Alonge et al., 2019, 2021) with the *Kalanchoe laxiflora* genome (FTBG2000359A v3.1, unpublished, Phytozome) accessible on Phytozome (Goodstein et al., 2012). Scaffolds shorter than 100 kbp were removed. Multiple methods were used to reduce assembly ploidy to one haplotypic representation of the tetraploid genome. Purge Haplotigs 1.1.2 (Roach et al., 2018) and Purge Dups were run sequentially to reduced assembly ploidy. Scaffolds not contained within chromosome scale pseudomolecules were filtered using a BUSCO optimisation approach where a combination of scaffolds were retained to give the highest BUSCO score while reducing ploidy. After reducing ploidy the assembly was polished with the short reads using Pilon 1.24 (Walker et al., 2014).

BUSCO was used to assesses genome completeness by detecting the presence of key single copy genes from the embryophyta_odb10 database. The genome assembly was assessed using the long-terminal repeat (LTR) assembly index, which is the proportion of intact long terminal repeats (LAI) within the assembly, from the LTR retriever pipeline 2.9.0 (Ou et al., 2018). A higher score tends to suggest a more contiguous and complete assembly; and is improved by both short reads increasing accuracy per base and long reads providing resolution over long repetitive regions.

4.2.7 *K. blossfeldiana* Genome Annotation

RepeatModeler 2.02 (Flynn et al., 2020) and RepeatMasker 4.1.3 (Tarailo-Graovac & Chen, 2009) were used to annotate repetitive regions of the genome assembly. The assembly was soft masked using Bedtools 2.30 (Quinlan & Hall, 2010). BRAKER2 2.1.6 (Brůna et al., 2021) was used for gene annotation. Two methods were used, as recommended, firstly mRNA based gene predictions were made using BRAKER pipeline with the illumina RNA reads as described above. Simultaneously, in a separate BRAKER2 run, gene predictions were made using a set of training proteins from the OrthoDB plant database (Kriventseva et al., 2019) and *K. fedtschenkoi* (Yang et al., 2017). Annotations from both BRAKER runs were combined using the transcript selector TSEBRA (Gabriel et al., 2021). Protein sequences from gene models predicted by the BRAKER pipeline above were functionally characterised. This was primarily performed using OrthoFinder 2.5.4 (Emms & Kelly, 2019) to sort proteins into orthologous groups from *K. fedtschenkoi* (*Kalanchoe fedtschenkoi* v1.1), *K. laxiflora* (FTBG2000359A v3.1), *Vitis vinifera* (*Vvinifera_457_v2.1*), and *Arabidopsis thaliana* (TAIR10) from Phytozome

(Goodstein et al., 2012). Annotations present from these genomes in each orthogroup were used to fill in *K. blossfeldiana* annotation in the above order.

4.2.8 *K. blossfeldiana* Chloroplast Genome and Phylogenetics

The *K. blossfeldiana* chloroplast genome was assembled with GetOrganelle 1.7.5 (Jin et al., 2020) using the same Illumina PE reads as were used for nuclear genome. Functional and structural annotation of the chloroplast genome was performed using GeSeq (Tillich et al., 2017) with the *Arabidopsis thaliana* chloroplast genome used as a reference. For this chapter the *K. blossfeldiana* chloroplast genome was primarily used to explore the phylogenetic relationship between this variety of *K. blossfeldiana* and other members of the genus *Kalanchoe*, and the wider *Crassulaceae* family. Whole chloroplast genome sequences from 79 species across the order *Saxifragales* were used with a focus on the *Crassulaceae* family and species from the *Haloragaceae* family were used as outgroups. Whole chloroplast genome sequences were obtained from NCBI and aligned using MAFFT 7.505 (Kato & Standley, 2013). ModelFinder (Kalyaanamoorthy et al., 2017) determined used the Bayesian Information Criterion (BIC) to select a nucleotide substitution model. IQ-TREE 2.2.0.3 (Minh et al., 2020) was used to construct a phylogenetic tree using maximum likelihood, with 1000 ultrafast bootstrap replicates (Thi Hoang et al., 2017).

4.2.9 *K. blossfeldiana* Dusk RNA-seq

Short read RNA library preparation and sequencing of *K. blossfeldiana* was carried out by Novogene (Beijing, China), with RNA extracted from young (9th leaf pair from the bottom) and mature (3rd leaf pair from the bottom) leaves. Three biological replicates were collected and sequenced from each leaf age group, with samples taken at dusk. A total of 119 million PE reads, and 35.8 Gb were sequenced on an Illumina NovaSeq 6000, with a range of 15-22 million reads per sample. RNA sequencing QC, alignment and quantification were performed using the nf-core/rnaseq 3.8.1 pipeline (Ewels et al., 2020) with default settings. Briefly, read QC was performed using FastQC, adapters and quality trimming by Trim Galore. STAR was used to align reads to gene models predicted in the *K. blossfeldiana* genome, and Salmon was used to quantify transcript abundance (Patro et al., 2017). DESeq2 (Love et al., 2014) was used to analyse differential expression between samples.

4.3 Results and Discussion

4.3.1 *K. blossfeldiana* genome size

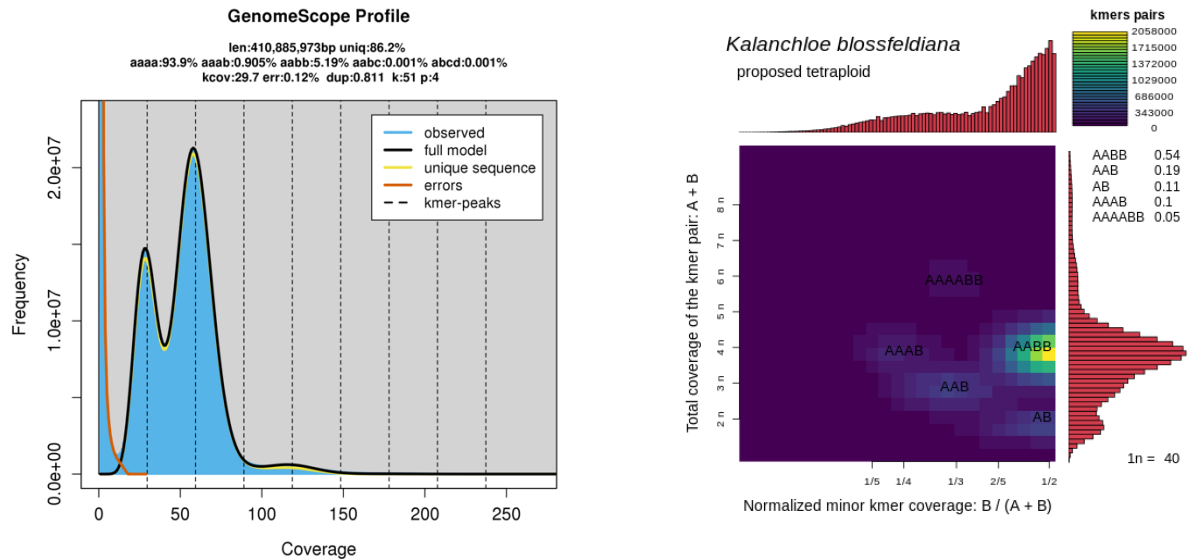


Figure 4.1 *K. blossfeldiana* computational genome size and ploidy estimates. Left panel, K-mer graph and fitted models generated by GenomeScope 2 (Vurture et al., 2017) using K-mer frequencies counted by Jellyfish 2.3.0 (Marçais & Kingsford, 2011) using illumina short reads. Right panel, Smudgeplot 0.2.5 (Ranallo-Benavidez et al., 2020) generated estimate of genome ploidy.

The variety of *Kalanchoe blossfeldiana* used in this thesis was estimated to be tetraploid with a genome size of ~1.94 Gb and with each haplotype 450-490 Mb (Figure 4.1). This was estimated by both by flow cytometry ($2C=1.98625 \pm 0.05$ pg, Appendix Table A2.5) and computationally from genomic Illumina short reads using Jellyfish 2.3.0 (Marçais & Kingsford, 2011), GenomeScope 2 (Vurture et al., 2017) and Smudgeplot 0.2.5 (Ranallo-Benavidez et al., 2020). Many varieties of *K. blossfeldiana* vary in their ploidy with diploid varieties reported with ($2n=34$) and tetraploid ($2n=68-72$) (van Voorst & Arends, 1982), with 17 or 18 chromosomes expected per haplotype.

4.3.2 *K. blossfeldiana* Genome Assembly

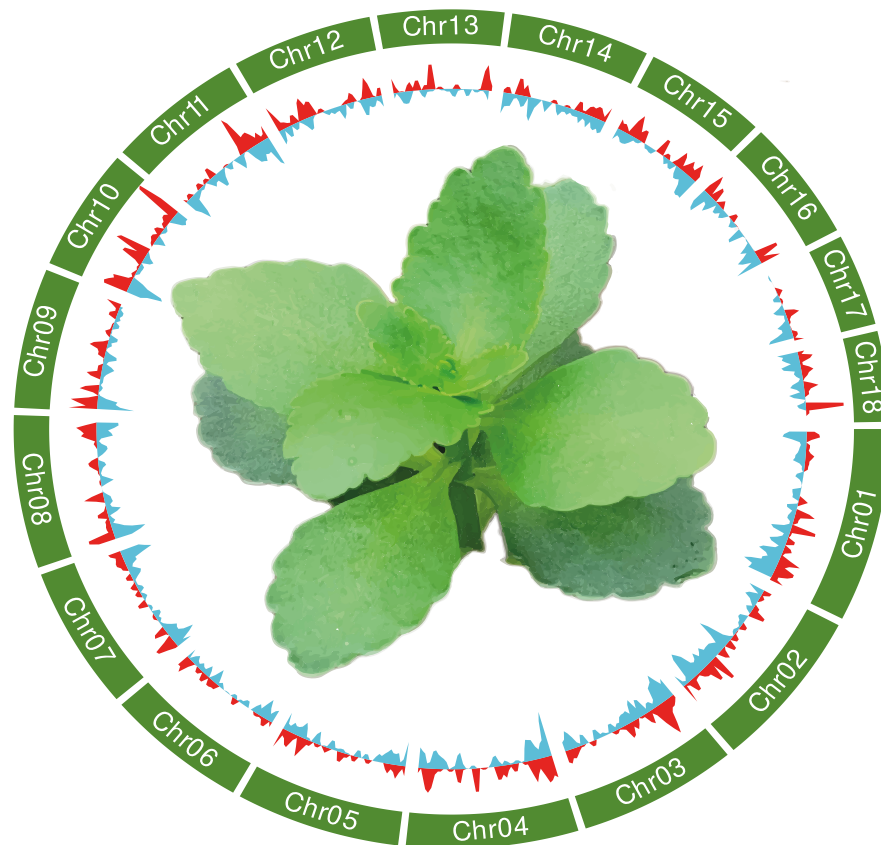


Figure 4.2 The genome of *K. blossfeldiana*, scaffolded into 18 chromosome scale pseudomolecules (377 Mb) and 155 smaller scaffolds (not shown, 268 Mb) using the *Kalanchoe laxiflora* genome (Phytozome). *K. blossfeldiana* is thought to have 17 or 18 chromosomes per haplotype. Density of genes up-regulated (red, outward) or down-regulated (blue, inward) in the mature CAM *K. blossfeldiana* leaves (3rd leaf pair from the bottom) compared to the young C₃ *K. blossfeldiana* leaves (9th leaf pair from the bottom). Inner image is of *K. blossfeldiana*.

An initial *K. blossfeldiana* genome assembly of 772 Mb and an N50 of 1 Mb was made using the hybrid MaSuRCA 4.0.9 (Zimin et al., 2017), with 91.6 Gb, 305 million PE illumina short reads and 10 Gb 3.49 million nanopore long reads (N50 ~10 Kb). Abyss-Fac (Jackman et al., 2017), Spades (Antipov et al., 2016) and Flye (Kolmogorov et al., 2019b) assemblers were also tested but produced assemblies with less contiguity. The MaSuRCA assembly was scaffolded with the *Kalanchoe laxiflora* genome (FTBG2000359A v3.1, unpublished, Yang et al. 2022) using Ragtag 2.1.0 (Alonge et al., 2019, 2021) into 18 chromosome scale pseudomolecules (377 Mb) and 155 smaller scaffolds (268 Mb), with fragments less than 100 Kb removed. To reduce assembly ploidy Purge Haplotigs 1.1.2 (Roach et al., 2018) and Purge Dups (Guan et al., 2020) were run sequentially, reducing assembly size to 556 Mb. Scaffolds not contained within chromosome scale pseudomolecules were filtered using a BUSCO optimisation approach where a combination of scaffolds were retained to give the highest BUSCO score while reducing ploidy, giving a final assembly size of 461 Mb, consisting of 18 chromosome scale pseudomolecules and 125 scaffolds with an N50 of 20.6 Mb. A number of methods were used to assess assembly quality and completeness. The final assembly had a genomic BUSCO score of 95.6% complete copies, with 70% present in single copies and 25.6% present in duplicated copies using the Embryophyte odb10 database of single copy genes. Efforts to reduce ploidy reduced the number of duplicated single copy genes present from 67% to 25.6%, however this also reduced the number of BUSCO genes found from 97.2% to 95.6%. The proportion of intact long terminal repeats (LAI) within the assembly was 11.12, from the LTR retriever pipeline 2.9.0 (Ou et al., 2018) and the assembly is made up of 0.138% gaps. The genome was also assessed by the aligning reads back to the genome, with 94.21% of long reads mapping and 80% of short reads mapping back to the genome (Table 1).

Table 1. *K. blossfeldiana* Genome Statistics

Scaffolds:	N50 (Mb)	Largest Scaffold (Mb)	Assembly Size (Mb)	Gaps (%)	Read Mapping Rate (%)	
					Short Reads	Long Reads
143	20.06	29.6	461	0.138	89.03	94.38

4.3.3 *K. blossfeldiana* Genome Annotation

Over half of the genome assembly was identified as repetitive elements (57.3%), the majority marked as LTRs (24.7%), DNA transposons (18.7%) and LINES (7.71%, Figure 4.3). The BRAKER2 and TSEBRA functional annotation pipeline (Gabriel et al., 2021) identified 38117 protein coding genes, with 95.3% of the BUSCO Embryophyte odb10 genes present. The majority (32096, 84%) of these proteins were functionally annotated by sorting into orthologous groups from *K. fedtschenkoi* (*Kalanchoe fedtschenkoi* v1.1), *K. laxiflora* (FTBG2000359A v3.1), *Vitis vinifera* (Vvinifera_457_v2.1), and *Arabidopsis thaliana* (TAIR10) from Phytozome (Goodstein et al., 2012). Annotations present from these genomes in each orthogroup were used to fill in *K. blossfeldiana* annotation in the above order. The remaining genes not sorted into orthogroup or present in orthogroup with no annotation were annotated by blasting protein sequences to *A. thaliana* (TAIR10).

A- Genome BUSCO



B- Repetitive Elements in the *Kalanchoe blossfeldiana* genome

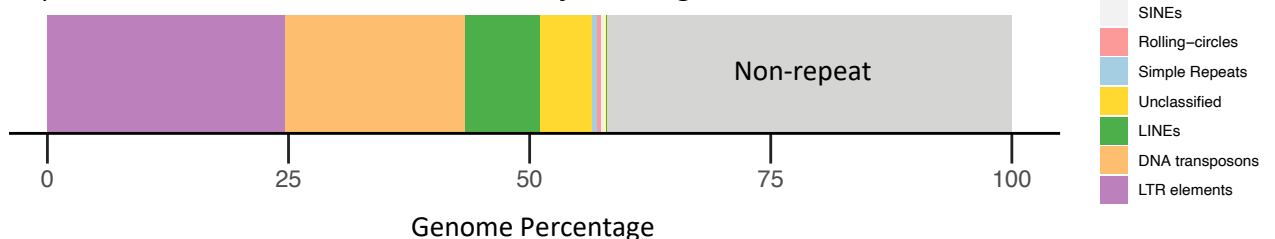


Figure 4.3 *K. blossfeldiana* genome content. Genome completeness was assessed using BUSCO with the Embryophyte odb10 database of single copy genes (A), showing percentage of complete (C) present in single copies (S) or duplicated (D), fragmented (F) or missing (M) genes detected. Proportions of repetitive elements detected within the *K. blossfeldiana* genome (B).

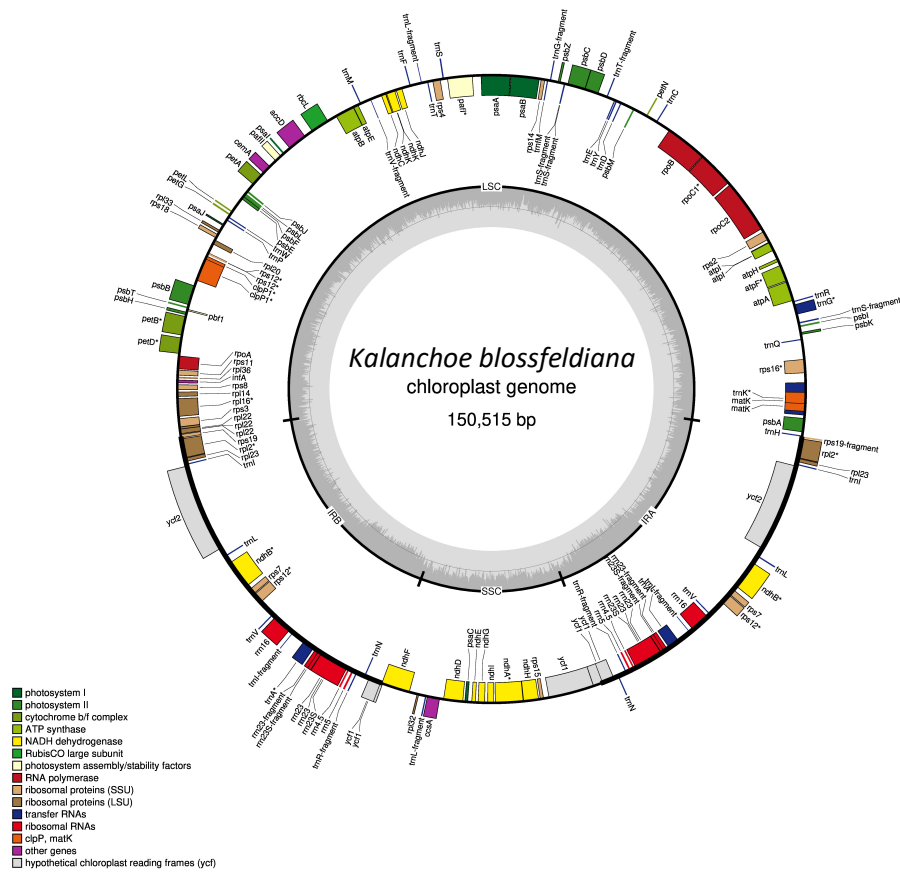


Figure 4.4 Annotated features of the *Kalanchoe blossfeldiana* chloroplast genome. Genes transcribed are displayed on the outer ring, on the inside if transcribed clockwise or outside if counter clockwise. The chloroplast genome is divided into a large single copy region, a small single copy region and a pair of inverted repeat regions. The intertrack conveys GC content. The annotation and diagram was produced using GeSeq (Tillich et al., 2017).

4.3.4 Phylogenetics of *K. blossfeldiana*

The *Kalanchoe* genus is estimated to have diverged from the *Sempervivoideae* between 22.78–44.29 million years ago (Messerschmid et al., 2020). The current *Kalanchoe* genus is made of up species from three previous genera, *Kalanchoe* (of which *K. blossfeldiana* was a member), *Kitchingia* and *Bryophyllum* (of which *K. fedtschenkoi* and *K. laxiflora* were members and carry out leaf margin embryogenesis (Mort et al., 2010). *K. blossfeldiana* shows some morphological and physiological differences from *K. fedtschenkoi* and *K. laxiflora* - it is predominantly green leafed, lacks the ability to reproduce from leaf tip pups, and performs inducible CAM vs constitutive CAM in the latter. Therefore, it was expected that *K. blossfeldiana* would phylogenetically be within the *Kalanchoe* genus but distinct from *K. fedtschenkoi* and *K. laxiflora*.

The chloroplast sequence is a useful tool for determining the phylogenetic relationship between *K. blossfeldiana* and other relative species, and recently chloroplasts of a large number of species within the Crassulaceae have been sequenced (Han et al., 2022; Tian et al., 2021). As expected, the *K. blossfeldiana* chloroplast genome was highly conserved between it and other members of the *Kalanchoe* genus with 99.01% sequence similarity to *K. fedtschenkoi* chloroplast genome. A *K. blossfeldiana* chloroplast genome sequence recently deposited on NCBI (OM320795, Liang et al. 2022, unpublished) was identical to the *K. blossfeldiana* chloroplast sequence presented here. Such findings suggest that the chloroplastic genome is highly conserved between *K. blossfeldiana* varieties as would be expected as the varieties are likely to have formed by horticultural breeding programs over the last century.

Whole chloroplast genome sequences from 79 species across the order Saxifragales were aligned and reconstructed into a phylogenetic tree with a focus on the Crassulaceae family and species from the Haloragaceae family were used as outgroups (Figure 4.5). In this phylogenetic reconstruction *K. blossfeldiana* chloroplast sequence sits within the *Kalanchoe* genus between *Kalanchoe longiflora* and *Kalanchoe tomentosa*, the latter like *K. blossfeldiana* does not perform leaf margin embryogenesis (Garcês et al., 2007).

A phylogeny was also made from single copy genes, from the genomic assemblies of related plant species with a focus on dicots, which positioned *K. blossfeldiana* within the *Kalanchoe* genus but slightly away from *K. fedtschenkoi* and *K. laxiflora* (Appendix Figure A2.1). Together as expected *K. blossfeldiana* phylogenetically lies within *Kalanchoe* but is distinct from *K. fedtschenkoi* and *K. laxiflora*. Its placement and the differences between the three historic genera would be further helped with the future genomic sequencing of close relatives of *K. blossfeldiana* such as *Kalanchoe globulifera* and *Kalanchoe darainensis* (Klein et al., 2021). Further work is also needed to determine the genetic makeup of the various *K. blossfeldiana* varieties that have been bred in the past century, as it is likely that many of these are hybrids of *K. blossfeldiana* and close relatives.

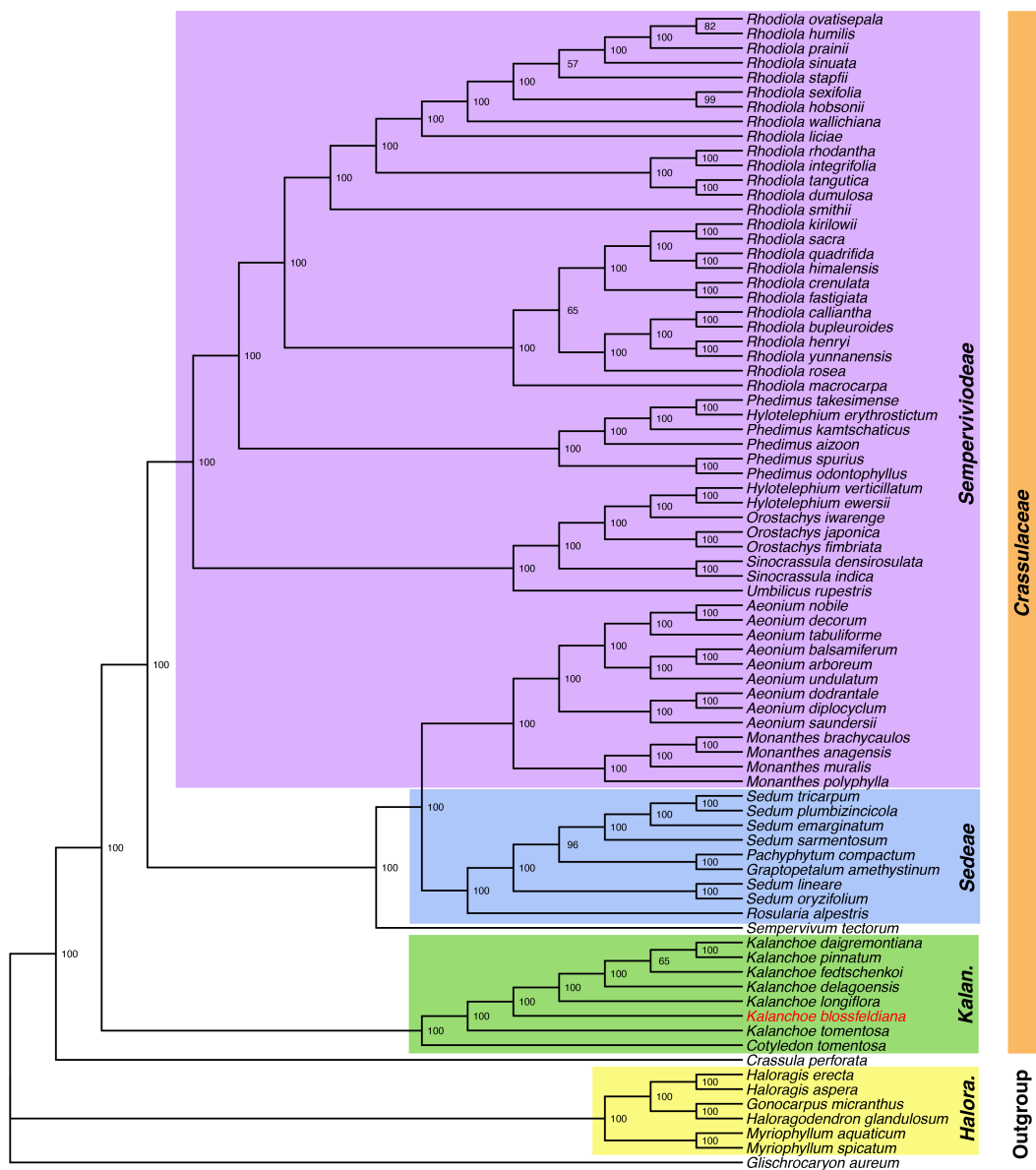


Figure 4.5 The phylogenetic position of *Kalanchoe blossfeldiana*. Whole chloroplast genome sequences from 79 species across the order *Saxifragales* were aligned and reconstructed into a phylogenetic tree with a focus on the *Crassulaceae* family, species from the *Haloragaceae* family were used as outgroups. Whole chloroplast genome sequences were aligned using MAFFT 7.505 (Kato & Standley, 2013). IQ-TREE 2.2.0.3 (Minh et al., 2020) was used to construct a phylogenetic tree using maximum likelihood, with 1000 ultrafast bootstrap replicates (Thi Hoang et al., 2017), with node labels representing % bootstrap support.

4.3.5 Shift in transcript expression pattern in mature CAM *K. blossfeldiana* leaves

Mature CAM vs Young C₃ leaves

○ NS △ Log₂ FC ● p-value and log₂ FC

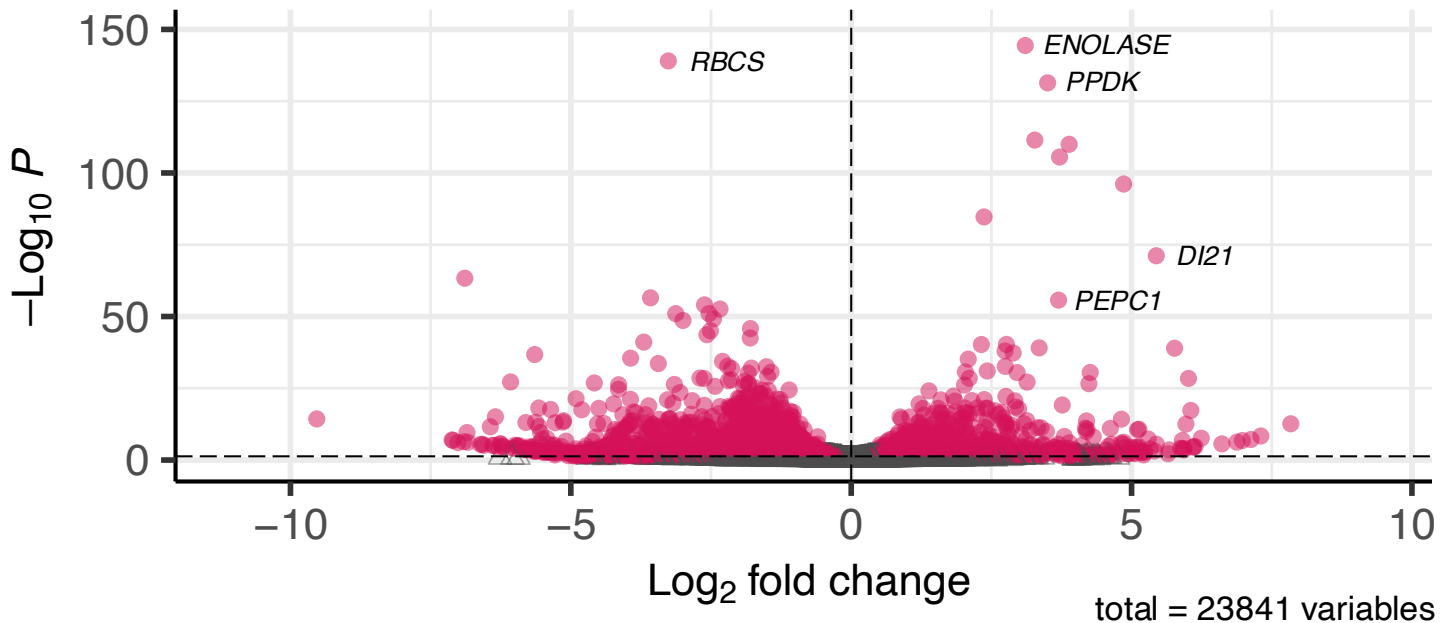
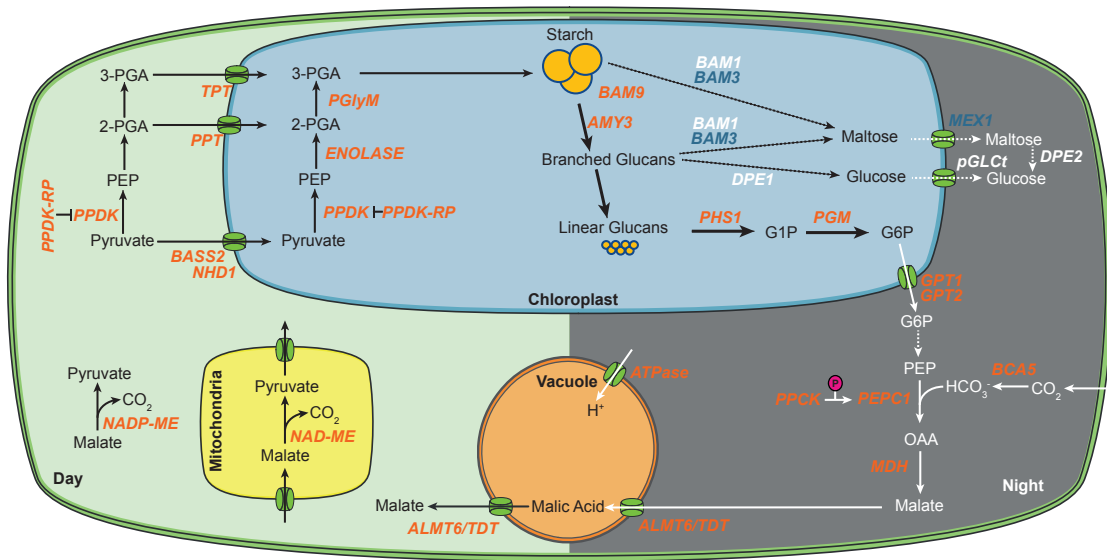


Figure 4.6 Change in transcript abundances between mature (3rd leaf pair from the bottom) and young *Kalanchoe blossfeldiana* leaves (9th leaf pair from the bottom) sampled at dusk 90 days after propagation. Abbreviations: PPDK (pyruvate orthophosphate dikinase), RBCS (Ribulose biphosphate carboxylase small chain), DI21 (Drought Induced 21).

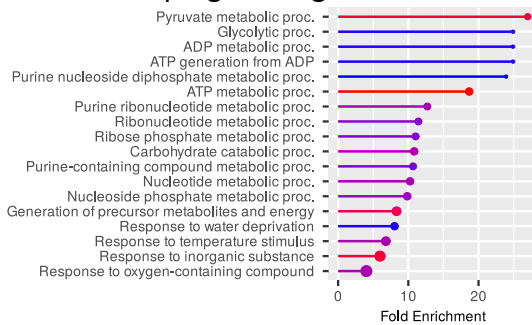
Data in the previous chapters have shown a clear distinction between the photosynthetic phenotypes of different aged *K. blossfeldiana* leaves, with the young leaves (9th and 10th leaf pair from the bottom) performing C₃ and the mature (2nd and 3rd leaf pair from the bottom) leaves performing CAM. The present chapter shows a substantial change in transcript abundances between the young C₃ (9th leaf pair from the bottom) and mature CAM leaves (3rd leaf pair from the bottom), with 685 genes significantly upregulated and 1491 downregulated in the mature leaves compared to young leaves at dusk (figure 4.6). Orthologs of many of these upregulated genes in the mature CAM *K. blossfeldiana* leaves have also been shown to be upregulated in the induction of CAM in inducible CAM species (Maleckova et al., 2019) and/or shown to have CAM-like patterns of expression in constitutive CAM species (Yang et al., 2017). This supports the suggestion made by Yang et al. (2017) and others that that genes recruited for CAM undergo a convergent shift in expression profile that is conserved in CAM species across many genera.

A. Core metabolism in mature *Kalanchoe blossfeldiana* leaves.



Enriched GO terms in mature *Kalanchoe blossfeldiana* leaves.

B. Upregulated genes



C. Downregulated genes

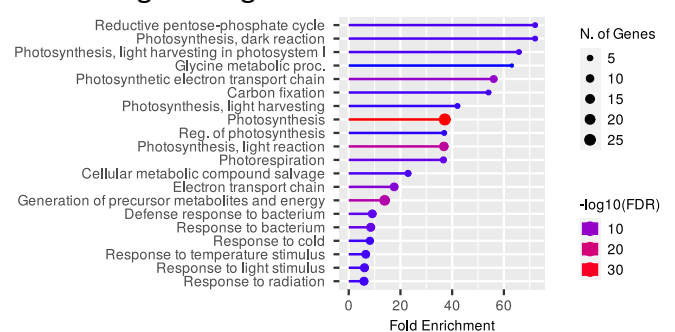


Figure 4.7 Changes in transcript abundance of key genes involved in CAM in the mature CAM *Kalanchoe blossfeldiana* leaves compared to young C_3 leaves at dusk (Panel A). Upregulated genes (orange), downregulated genes (blue) and genes with no change in expression (white) are shown in italics. Bold lines indicate the upregulation of the phosphorolytic starch degradation pathway in the mature leaves. GO-term enrichment for top 100 genes upregulated (Panel B) or downregulated (Panel C) compared between mature (3rd leaf pair from the bottom) and young *Kalanchoe blossfeldiana* leaves (9th leaf pair from the bottom) sampled at dusk. Abbreviations shown include: Phosphoglyceromutase (PGLyM); tonoplast dicarboxylate transporter (TDT); aluminium activated malate transporter (ALMT);bile acid sodium symporter 2 (BASS2); debranching enzyme (DBE); glucose-1-phosphate (G1P);glucose-6-phosphate (G6P); malate dehydrogenase (MDH); NAD(P)-dependent malic enzyme (NAD(P)-ME); sodium hydrogen antiporter 1 (NHD1); oxaloacetate (OAA); phosphoenolpyruvate (PEP); phosphoenolpyruvate carboxylase (PEPC); phosphoglycerate (PGA); pyruvate phosphate dikinase (PPDK); PPK regulatory protein (PPDK-RP); PPT, phosphoenolpyruvate phosphate translocator; triosephosphate/phosphate translocator (TPT); AMY3 (α -amylase 3); BAM1 (β -amylase 1); BAM3 (β -amylase 3); Phosphoglucomutase (PGM);BCA5 (β -carbonic anhydrase 1); PPKC (phosphoenolpyruvate carboxylase kinase); DPE1 (chloroplatic disproportionating enzyme); PHS1 (chloroplatic α -glucan phosphorylase); cytosolic disproportionating enzyme (DPE2); MEX1 (maltose transporter); pGLCT (plastidic glucose transporter), GPT1 (glucose phosphate translocator 1); and GPT2 (glucose phosphate translocator 2).

4.3.6 Core CAM genes upregulated in mature CAM *K. blossfeldiana* leaves

As expected, key genes involved in the CAM cycle were upregulated on the transition from C₃ to CAM between the young and mature *K. blossfeldiana* leaves (Table 2). Of the three carbonic anhydrase families beta appears to play a role in CAM (Ming et al., 2015). The transcript abundance of *BETA CARBONIC ANHYDRASE 5* (*BCA5*, kblos_g10271), responsible for converting CO₂ to HCO₃⁻, increased in mature CAM *K. blossfeldiana* leaves compared to the young C₃ leaves. An increase in *BCA5* transcript abundance also occurred on CAM induction in *Talinum triangulare* (Maleckova et al., 2019) and *BCA5* showed nocturnal pattern of expression in *K. fedtschenkoi* (Kaladp0095s0400, Yang et al., 2017). ALPHA CARBONIC ANHYDRASE was downregulated in the mature CAM *K. blossfeldiana* leaves, which also occurred on CAM induction in *T. triangulare* (Maleckova et al., 2019).

Table 2 Core CAM genes up regulated in mature *K. blossfeldiana* leaves at dusk.

Protein	Gene ID	EC no.	log2FoldChange	<i>A. thaliana</i> ID
<i>NADP-malic enzyme</i>	Kblos_g3772	1.1.1.40	3.17	AT5G25880.1, AT1G79750.1
<i>phosphoenolpyruvate carboxylase kinase</i>	Kblos_g22444	2.7.11.1	4.25	AT3G04530.1, AT1G08650.1
<i>phosphoenolpyruvate carboxylase 1</i>	Kblos_g8592	4.1.1.31	3.70	AT1G53310.1, AT3G14940.1
<i>malate dehydrogenase</i>	Kblos_g28939	1.1.1.37	3.20	AT3G47520.1
<i>NAD-dependent malic enzyme 1</i>	kblos_g1381	1.1.1.39	1.04	AT2G13560.1
<i>NAD-dependent malic enzyme 2</i>	kblos_g19016	1.1.1.39	0.57	AT4G00570.1
<i>beta carbonic anhydrase 5</i>	Kblos_g10289	4.2.1.1	1.19	AT4G33580.1
<i>plasma membrane intrinsic protein</i>	kblos_g12096		0.60	AT4G00430.1, AT4G23400.1

PEPC1 appears to be the key PEPC isoform involved in nocturnal malate accumulation in both *K. blossfeldiana* (kblos_g8596) and *K. fedtschenkoi* (Kaladp0095s0055, Yang et al., 2017), with a 3.7-fold increase in expression in the CAM mature *K. blossfeldiana* leaves. Previous works have suggested that CAM plants, including *K. blossfeldiana*, tend to have four to six PEPC isoforms, one of which is recruited for CAM (Cushman & Borland, 2002), though the functions of the other isoforms are not known. *K. blossfeldiana*, like *K. fedtschenkoi*, has five PEPC isoforms (Yang et al., 2017). Alongside this transcript abundance of the PEPC-activating PHOSPHOENOLPYRUVATE CARBOXYLASE KINASE 1/2 (PPCK, kblos_g22485) increased in the mature CAM *K. blossfeldiana* leaves.

An area where CAM performing plants have not converged, is the use of either NAD-/NADPH-malic enzymes (ME) or phosphoenolpyruvate carboxykinase (PEPCK) for daytime decarboxylation (Dittrich et al., 1973; Ming et al., 2015). Like other members of the *Crassulaceae* mature CAM *K. blossfeldiana* leaves appear to use malic enzyme as their main decarboxylating enzyme, with orthologs of both NAD- and NADP-MALIC ENZYME, upregulated in the CAM mature *K. blossfeldiana* leaves (Table 2). Whereas other CAM plants such as members of the *bromeliaceae* tend to use PEPCK instead of ME. Although, recent work has shown both to be important for CAM, with separate transgenic knockdown of NAD-ME or PPK significantly reducing CAM activity in *K. fedtschenkoi* (Dever et al., 2015).

4.3.7 PEP Regeneration and Starch

The regeneration of PEP in the CAM cycle is a key rate limiting step for nocturnal carboxylation and the overall CAM cycle (Ceusters et al., 2010; Dever et al., 2015; Dodd et al., 2003), and is driven by the allocation of a large proportion of fixed C into transitional carbohydrate stores during the day (Cushman et al., 2008; Haider et al., 2012). CAM performing plants diverge in their use of different transitional carbohydrate stores that support the regeneration of PEP, with CAM species like *K. fedtschenkoi* and *M. crystallinum* storing carbohydrate as starch or *Ananas comosus* storing as hexose sugars (Cushman et al., 2008; Haider et al., 2012; Holtum et al., 2005). The mature CAM *K. blossfeldiana* leaves appear to use starch as their transitional carbohydrate to drive PEP regeneration, with transcript abundance of key starch degradation genes (*AMY3*, *BAM9*, *PHS1*) all upregulated in the CAM mature *K. blossfeldiana* leaves (Table 3). *BAM9* was recently shown to positively regulate transitory starch degradation

in *Arabidopsis*, but like *BAM4* lacks a catalytic domain and appears to have no direct catalytic role in starch turnover (David et al., 2022).

4.3.8 Switch to phosphorolytic starch degradation in CAM *K. blossfeldiana* leaves

Starch storing CAM plants have been shown to re-route starch degradation via the phosphorolytic pathway instead of the hydrolytic pathway used in C_3 *Arabidopsis*, with starch broken down to form glucose-6-phosphate that is exported from the chloroplasts to ultimately regenerate PEP for the CAM cycle (Borland & Dodd, 2002; Neuhaus & Schulte, 1996). CAM was impaired in *K. fedtschenkoi* *PHS1* mutants unable to degrade starch with the phosphorolytic pathway (Ceusters et al., 2021). Following CAM induction in the facultative species *M. crystallinum* increased glucose-6-phosphate export from the chloroplasts has been reported along with increased transcript abundance of *GLUCOSE PHOSPHATE TRANSLOCATOR* (*GPT*), thought to export G6P from chloroplasts (Hausler et al., 2000; Koreeda et al., 2013; Koreeda & Kanai, 1997; Neuhaus & Schulte, 1996). During CAM induction, *K. blossfeldiana* also appears to upregulate the phosphorolytic starch degradation pathway with upregulation of *PHS1* and two *GPT* isoforms along with the down-regulation of the chloroplastic maltose exporter *MEX1* involved in the hydrolytic starch degradation pathway (Table 3). Increases in transcript abundances of genes involved in the phosphorolytic starch degradation pathway were also observed on ABA induced CAM induction in *T. triangulare* (Maleckova et al., 2019). It has been suggested that this move to the phosphorolytic starch degradation pathway could be an effort to energetically balance the CAM cycle, as it allows for the provision of cytosolic ATP during the conversion of G6P to PEP (Ceusters et al., 2021; Shameer et al., 2018). The switch to the phosphorolytic starch degradation pathway across *M. crystallinum*, *K. blossfeldiana* and *K. fedtschenkoi* implies its importance to CAM.

Table 3 Changes in TCA cycle genes in mature *K. blossfeldiana* leaves at dusk.

Protein	Gene ID	EC no.	log2FoldChange	<i>A. thaliana</i> ID
<i>succinate dehydrogenase 1-1</i>	kblos_g24913	1.3.5.1	1.13	AT5G66760.1
<i>aconitase 1/3</i>	kblos_g11093	4.2.1.3	0.88	AT2G05710.1, AT4G35830.1
<i>Isocitrate dehydrogenase</i>	kblos_g20786	1.1.1.42	1.59	AT1G65930.1, AT5G14590.1
<i>ATP-citrate lyase A-3</i>	kblos_g23278	2.3.3.8	-3.02	AT1G09430.1
<i>ATP-citrate lyase B-1</i>	kblos_g25707	2.3.3.8	-1.24	AT3G06650.1
<i>ATP-citrate lyase A-3</i>	kblos_g30737	2.3.3.8	-0.84	AT1G09430.1
<i>ATP-citrate lyase A-3</i>	kblos_g29429	2.3.3.8	-1.48	AT1G09430.1

4.3.8 Upregulation of TCA cycle

Recent flux balance analysis and experimental data have suggested that CAM requires greater levels of nocturnal respiration rates (Shameer et al., 2018; Töpfer et al., 2020; Tay et al., 2021; Leverett et al., unpublished). Shameer et al. (2018) modelled that CAM required more ATP than C₃ overnight to drive the ATP-tonoplast proton pumps to ensure malate can be stored in the vacuole; and the high flux through phosphofructokinase to produce PEP for carboxylation. They also suggested that these ATP costs will be reduced by the switch to the phosphorolytic starch degradation pathway, which has been observed in the mature CAM *K. blossfeldiana* leaves. To further provide increased ATP it appears the mature CAM *K. blossfeldiana* leaves also upregulate elements of the TCA cycle, along with a downregulation of ATP-citrate lyases (Table 3). Some have also suggested that citrate may play a role in nocturnal CO₂ assimilation at night in CAM (Lüttge, 1988). Together these data and recent studies point to the importance of mitochondrial metabolism as a potential source of ATP, yet there is a lack of clear experimental evidence to provide a complete understanding of changes in mitochondrial metabolism in CAM.

4.3.9 Down regulation of RUBISCO

There was a significant down regulation of transcript abundance of multiple genes relating to RUBISCO in the mature CAM *K. blossfeldiana* leaves, with multiple homologs of RBCS and RUBISCO ACTIVASE down-regulated. This was also observed in salt induced CAM induction in *M. crystallinum* (Cushman et al., 2008). However, it is not clear if this is a CAM specific response or due to ageing in mature CAM *K. blossfeldiana* leaves. Previous chapters showed a corresponding drop in both carbon uptake and soluble sugars in the mature leaves. Further work exploring changes in photosynthetic traits closer to the transition to CAM in ageing will be needed to determine changes to RUBISCO in CAM.

4.3.10 Vacuolar Transporters

Another key component of the CAM cycle is the storage of accumulated malate in the vacuole, with the vacuoles of CAM plants occupying up to 95% of volume within mesophyll cells (Steudle et al., 1980). The mature CAM *K. blossfeldiana* leaves showed increased expression of vacuolar ATPases, that create an energy gradient across the vacuolar membrane assisting in the import of malate into the vacuole. It is not clear which are the exact transporters for malate into or out of the vacuole, with some reports suggesting *ALMT1* or *ALMT9*. Here, in the mature CAM *K. blossfeldiana* leaves a homolog of *ALMT6* was upregulated, which is expressed at night in *K. fedtschenkoi* (Yang et al., 2017). Another potential vacuolar malate transporter, tonoplast dicarboxylate transporter (*tDT*), is also upregulated. Further molecular studies will be needed to reveal the exact components of vacuolar malate influx and efflux.

4.3.11 Overlap between ageing, drought and ABA CAM induction pathways.

The mechanisms by which CAM is induced as leaves age in *K. blossfeldiana* are not known. In the best studied inducible CAM species, CAM is often induced by abiotic stresses like drought or salt (Cushman & Borland, 2002). Throughout this thesis it has been postulated that age-induced CAM may be less stressful than abiotic stress induced CAM and thus provide insights into CAM induction that are not conflated with more general abiotic stress responses. At the transcriptome level this may be reflected by a lower number of genes differentially expressed due to ageing compared to CAM induction by abiotic stress; some 2260 differentially expressed genes in the mature leaves compared to the young leaves were found in *K. blossfeldiana*. This can be compared to 4737 differentially expressed genes in response to ABA in *T. triangulare* (Maleckova et al., 2019) and up to 3,245 differentially expressed genes in *S. album* in response to drought (Wai et al., 2019). It is possible that more genes will be involved in age-induced CAM in *K. blossfeldiana* that may only be active in the early stages of CAM induction. Work to determine the timings of age induced CAM and gene expression in the early stages may be needed to further elucidate the mechanisms of age induced CAM in *K. blossfeldiana*.

There was some overlap between ageing and ABA induced CAM, with genes reported to be upregulated in response to ABA induction of CAM in *T. triangulare* also upregulated in the mature *K. blossfeldiana* leaves. Five ABA responsive protein phosphatases were upregulated, homologous to *Highly ABA-Induced PP2C Gene 2* and *3*, as was also observed in ABA induced CAM induction in *T. triangulare* (Maleckova et al., 2019).-Downstream of this, several ABA responsive transcription factors were also upregulated in the mature *K. blossfeldiana* leaves that may be activated by *SnRK2s* and go onto regulate gene expression by binding to ABA-responsive elements. Genes involved in auxin and ethylene signalling were also upregulated in both ABA induced CAM in *T. triangulare*. Together this suggests that there is some overlap between the different CAM induction pathways. Future work could utilize the ability to induce CAM in *K. blossfeldiana* by ageing, drought, ABA, or short days to further explore the 'CORE' CAM induction pathways.

4.3.12 Identifying Guard Cell genes upregulated in mature CAM *K. blossfeldiana* leaves

In an effort to determine which of the genes upregulated in mature CAM *K. blossfeldiana* whole leaves may function in guard cell metabolism or stomatal regulation, two diel expression datasets, one proteomic (Abraham et al., 2020a) and one transcriptomic (James Hartwell, unpublished), from guard cell enriched epidermal peel tissues from constitutive CAM *K. fedtschenkoi* leaves were used. Of the 658 genes upregulated in age induced CAM in mature *K. blossfeldiana* leaves homologs of 94 and 186 were upregulated in *K. fedtschenkoi* epidermal peel proteome and transcriptome respectively.

Across these genes upregulated in the mature CAM *K. blossfeldiana* leaves and implicated in guard cell function there was an enrichment of genes involved in ABA signalling, salt and water stress signalling and carbohydrate metabolism (Figure 4.8, panel A and B). Of these genes a number have been implicated in stomatal regulation or guard cell metabolism in C₃ plants (Table 4).

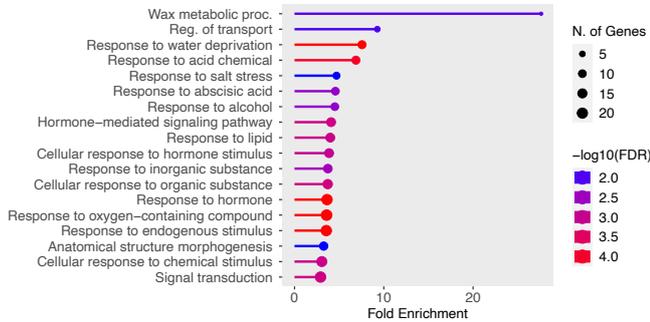
Table 4. Stomatal genes upregulated in mature *K. blossfeldiana* leaves at dusk and homologous to genes upregulated in both transcript (James Hartwell, unpublished) and protein (Abraham et al., 2020) abundance in *K. fedtschenkoi* guard cell enriched epidermal peels, apart from *CIPK5*, *MPK19*, *SUS3* that were detected only in the transcriptome.

Protein	<i>K. blossfeldiana</i> Gene ID	<i>K. fedtschenkoi</i> Gene ID	<i>A. thaliana</i> Gene ID
<i>H⁺-ATPase (AHA2)</i>	kblos_g18386	Kaladp0001s0196	AT4G30190
<i>H⁺-ATPase (AHA2)</i>	kblos_g19712	Kaladp0001s0196	AT4G30190
<i>OPEN STOMATA 1 (OST1)</i>	kblos_g26666	Kaladp0060s0144	AT4G33950
<i>OPEN STOMATA 1 (OST1)</i>	kblos_g26667	Kaladp0060s0144	AT4G33950
<i>SnRK2.3</i>	kblos_g39226	Kaladp0955s0013	AT5G66880
<i>MAP kinase 19 (MPK19)</i>	kblos_g3123	Kaladp0033s0169	AT3G14720
<i>CBL-interacting protein kinase 5 (CIPK5)</i>	kblos_g6309	Kaladp0095s0759	AT5G10930
<i>Beta-amylase 9 (BAM9)</i>	kblos_g24169	Kaladp0062s0212	AT5G18670
<i>Sucrose synthase 3 (SUS3)</i>	kblos_g11836	Kaladp0003s0158	AT4G02280
<i>Plasma membrane intrinsic protein (PIP1)</i>	kblos_g12096	Kaladp0037s0152	AT4G00430

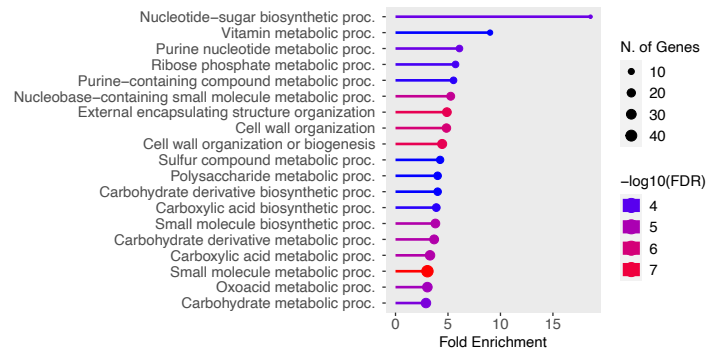
Enriched GO terms from genes upregulated in *K. blossfeldiana* CAM mature leaves

and *K. fedtschenkoi* epidermal peels:

A- Transcriptome (James Hartwell, unpublished):

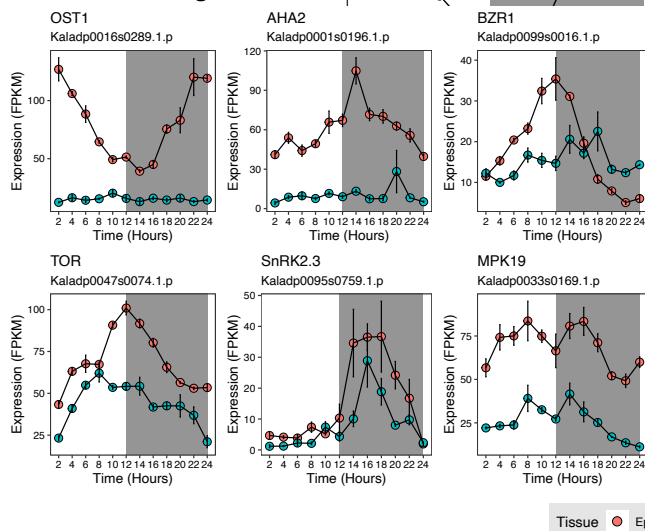


B- Proteome (Abraham et al., 2020):



Diel tissue specific transcript expression of key *K. fedtschenkoi* genes (James Hartwell, unpublished):

C- Stomatal Regulation:



D- Guard Cell Metabolism:

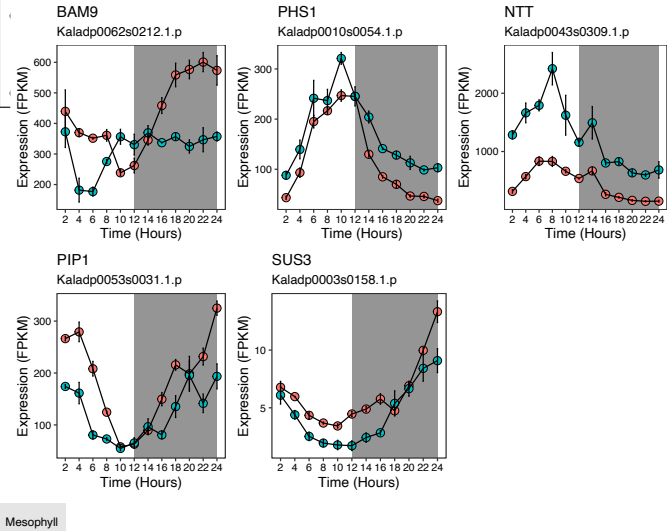


Figure 4.8 GO term enrichment of genes both upregulated in mature CAM *K. blossfeldiana* leaves at dusk and epidermal peels in both transcript (Panel A, James Hartwell, unpublished) and protein (Panel B, Abraham et al., 2020) abundance from constitutive CAM *K. fedtschenkoi* leaves. Upregulation of genes in the epidermal peels were calculated as means of expression over the diel periods. Lower section, diel tissue specific transcript expression of key genes implicated in CAM stomatal regulation (left) and guard cell metabolism (right) in epidermal (red circles) or mesophyll (blue circles) tissue in the constitutive CAM in *K. fedtschenkoi* (from James Hartwell, unpublished). Tissues sampled every 2hrs from respective leaf parts over a 12hr night/12hr day diel cycle.

4.3.13 Guard cell regulatory genes upregulated in mature CAM *K. blossfeldiana* leaves

A number of key stomatal regulatory genes were found to be up regulated in both CAM *K. blossfeldiana* leaves and in *K. fedtschenkoi* epidermal peels. *Plasma membrane H⁺-ATPase (AHA2)* and *OPEN STOMATA 1 (OST1)* are both upregulated in mature CAM *K. blossfeldiana* leaves and in *K. fedtschenkoi* epidermal peels and have opposing effects on stomatal opening show opposing diel transcript expression patterns in *K. fedtschenkoi* epidermal peels (Figure 4.8, panel C). *AHA2* shows greater expression during the end of day/night while *OST1* is expressed predominantly during the day, which was also observed in *A. americana* and *K. laxiflora* (Abraham et al., 2016; Boxall et al., 2020) and is retimed in comparison to the nocturnal expression pattern in *Arabidopsis*. *AHA2* induces guard cell plasma membrane hyperpolarisation in *Arabidopsis*, enabling K⁺ influx through voltage gated K⁺ channels ultimately resulting in stomatal opening (Ueno et al., 2005); with increased stomatal conductance observed in plants overexpressing *AHA2* specifically in *Arabidopsis* guard cells (Wang et al., 2014; Yang et al., 2008). Conversely *OST1*, a SnRK2 kinase, functions in high CO₂ induced closure in C₃ species with mutants displaying greater stomatal conductance and impaired ability to close in response to increased CO₂ (Xue et al., 2011). *OST1* has been shown to activate *SLAC1* driven Cl⁻ efflux from the guard cells resulting in plasma membrane depolarisation and ultimately stomatal closure (Geiger et al., 2009). *AHA2* and *OST1* were also primarily expressed in the *K. fedtschenkoi* epidermal proteomic dataset yet had slightly different expression patterns, with *AHA2* peaking towards the end of the day and *OST1* showing a flat expression profile (Abraham et al., 2020a). Transcripts of two other kinases, *MAP kinase 19 (MPK19)* and *CBL-interacting protein kinase 5 (CIPK5)*, were also upregulated in mature CAM *K. blossfeldiana* leaves and *K. fedtschenkoi* epidermal peels; *CIPK5* has been shown to be involved in wound induced stomatal closure in *Arabidopsis* by inducing potassium efflux (Förster et al., 2019), while *MPK19* as of yet has no recorded function in stomatal regulation.

4.3.14 Guard cell metabolic genes upregulated in mature CAM *K. blossfeldiana* leaves

Genes implicated in guard cell metabolism were also upregulated in mature CAM *K. blossfeldiana* leaves and showed greater diel expression in guard cell enriched epidermal peel tissue from CAM *K. fedtschenkoi* leaves. Transcripts of β -Amylase 9 (*BAM9*), which has been shown to positively regulate starch degradation in *Arabidopsis* (David et al., 2022), was significantly upregulated in mature CAM *K. blossfeldiana* leaves and showed a strong diel expression pattern peaking during the night in the epidermal peels of *K. fedtschenkoi* leaves (Figure 4.8, Panel D). *Sucrose synthase 3 (SUS3)*, which converts sucrose into hexoses for glycolysis and mitochondrial respiration during light induced stomatal opening (Antunes et al., 2012; Daloso et al., 2015), was upregulated in both the mature CAM *K. blossfeldiana* leaves and the epidermal peels of *K. fedtschenkoi* leaves. Transcript expression of *SUS3* showed a diel pattern increasing nocturnally in the epidermal peels of *K. fedtschenkoi* leaves (Figure 4.8, Panel D), corresponding to the period of increased stomatal opening in these CAM species; and stomatal aperture has been shown to increase when *SUS3* is specially overexpressed in *Nicotiana tabacum* guard cells (Daloso et al., 2016). Notably, *NUCLEOTIDE TRANSPORTER 1 (NTT1)* which has recently been shown to import ATP into the chloroplasts in *Arabidopsis* guard cells (Lim et al., 2022), was upregulated in CAM mature *K. blossfeldiana* leaves and highly expressed in both epidermal and mesophyll tissue in *K. fedtschenkoi* leaves (Figure 4.8, Panel D). In the guard cells ATP import into the chloroplasts via NTT is essential for enabling stomatal opening and guard cell starch synthesis (Lim et al., 2022). ATP import into the chloroplasts of mesophyll cells has not been reported in C₃ plants, implying this is a CAM specific function, which requires further study. Two regulatory genes, *Target of rapamycin (TOR)* and *BRASSINOALZOLE-RESISTANT1 (BZR1)*, that have been recently shown to positively regulate guard cell starch degradation via *BAM1* (Han et al., 2022) showed increased, but not statistically significant, transcript expression in the mature CAM *K. blossfeldiana* leaves and greater transcript expression in *K. fedtschenkoi* epidermal tissue with a similar diel pattern of expression (Figure 4.8, Panel D).

Together these data highlight identify a number genes that may play a role in the inverted stomatal opening in CAM *K. blossfeldiana* and suggest a retiming of key regulatory and metabolic elements occurs during the age induced transition from C₃ to CAM in *K. blossfeldiana* leaves. There are likely further genes that enable nocturnal stomatal opening that have not been detected in these analyses; detection may be improved by using guard cell enriched tissue and exploring the *K. blossfeldiana* transcriptome over the full diel period.

4.3.15 Endoreplication increases as *K. blossfeldiana* leaves age

Succulence and CAM often coexist, with greater leaf thickness and succulence observed in CAM species across many plant lineages (Nelson and Sage, 2008; Zambrano et al., 2014). *K. blossfeldiana* leaves also become more succulent and scanning electron microscopy has shown that cell size increases (Alexandra Sandéhn, Iwona Bernacka Wojcik and Till Dreier, unpublished) as leaves age and transition to CAM (Chapter 2). Increased succulence and cell size is thought to enable vacuolar storage of malic acid (Nelson & Sage, 2008).

Endoreplication has been previously reported to increase in the facultative CAM plant *Mesembryanthemum crystallinum* as leaf tissue ages and has been shown to occur in many succulent plants (De Rocher et al., 1990) and occurs in response to abiotic stress (Leitch & Dodsworth, 2017). It has been suggested that endoreplication and increased genome size may help support larger cells in succulent plants. Endoreplication occurs in many succulents including *K. blossfeldiana* and *K. fedtschenkoi* (de Rocher et al., 1990), but it is not clear if endoreplication occurs with ageing alongside the induction of CAM and the development of succulence in *K. blossfeldiana*. Early studies have shown that endoreplication can occur in *K. blossfeldiana* in response to changes in day length (Witsch & Flügel, 1951) which has separately been shown to induce CAM.

This chapter explored the hypothesis that endoreplication may occur as the leaves become more succulent and transition to CAM. Flow cytometry, performed at Kew, showed a significantly greater proportion of cells containing endoreplicated nuclei in the mature leaves compared to the young leaves (Appendix Table 2.6 , $P < 0.01$). Genes involved in the synthesis of nucleotides were also upregulated in the mature *K. blossfeldiana* leaves compared to the young (Figure 4.7.A). And precursors to nucleotide synthesis were observed in greater abundance in mature *K. blossfeldiana* leaves in metabolite data (Bethan Morris, unpublished). Together these data show that endoreplication occurs as the leaves age in *K. blossfeldiana*, and along with previous reports (Witsch & Flügel, 1951), suggests that endoreplication occurs alongside the induction of CAM and succulence. However, questions remain as to the relationship between CAM, succulence and endoreplication. For instance, does endoreplication assist in drought tolerance in CAM/succulent plants and how important is it for succulence or CAM? *K. blossfeldiana* may provide a good system for studying the mechanisms of endoreplication, its induction and role in CAM and succulence.

4.3.16 Conclusions

Overall, age induced CAM in the mature *K. blossfeldiana* leaves is similar to that of *K. fedtschenkoi*, homologs of many of the genes upregulated here also shown to be recruited for CAM in *K. fedtschenkoi* by CAM-like diel expression pattern or functional experiments. This is also true of less closely related starch storing CAM species like *S. album*, *T. triangulare* and *M. crystallinum*. The observed changes in transcription between the young C_3 and mature CAM *K. blossfeldiana* leaves suggest a substantial shift in photosynthetic and carbohydrate metabolism in the mature leaves, with the upregulation of key CAM genes and those involved in phosphorolytic starch degradation and PEP regeneration. Orthologs to many genes involved in CAM in *K. fedtschenkoi* were also upregulated in the mature *K. blossfeldiana* leaves. The data also suggests that CAM and PEP regeneration in the mature *K. blossfeldiana* leaves is similar to that of in *K. fedtschenkoi* and other starch storing CAM plants. This chapter has reinforced evidence of the importance of key changes in metabolism that occur to support the CAM cycle, such as the switch to phosphorolytic starch degradation. This work also highlights the importance of the provision of carbon skeletons and ATP for the CAM cycle,

with changes in metabolism occurring to provide both in the mature CAM leaves. The chapter has identified key genes implicated in stomatal regulation and guard cell metabolism that are upregulated in age induced CAM in *K. blossfeldiana* and are homologous to genes upregulated in the epidermis of *K. fedtschenkoi*. Many of these genes show CAM like patterns of diel expression in *K. fedtschenkoi* and may enable nocturnal opening in CAM stomatal. The assembled *K. blossfeldiana* genome will help in future efforts to functionally knock down genes that have shown conserved increases in transcript abundance across related CAM species to confirm the function and importance of these genes to CAM and to support to efforts to engineer CAM into C₃ plants.

This is the first reported work exploring transcriptional changes in CAM induction by ageing, with previous work focusing on NaCl (Cushman et al., 2008), ABA (Maleckova et al., 2019) or drought (Wai et al., 2019) induced CAM. The observed changes in transcription suggested significant overlap between the response to age induced CAM and that of NaCl, ABA and drought induced CAM, especially in the core CAM and metabolism genes upregulated, but also in potential regulatory pathways that coordinate CAM. The conserved regulatory changes may help outline the main CAM induction and regulation pathways. *K. blossfeldiana* could be of great future use in this respect, as CAM can be induced by NaCl, ABA, drought, short-days and ageing. Such a system for the comparative study of different modes of CAM induction could provide a path to understanding the 'core' mechanisms of CAM induction in inducible CAM plants.

Chapter 5. General Discussion

5.1 Key Findings

5.1.1 *Kalanchoe blossfeldiana* as a comparative system for studying C₃/CAM

A key goal of this thesis was to determine whether *K. blossfeldiana* would be a useful system for comparing C₃ and CAM physiology and guard cell metabolism by age induced CAM. In fact, the data showed a clear distinction between young (9th and 10th leaf pair from the bottom) C₃ and CAM performing mature (2nd and 3rd leaf pair from the bottom) leaves in terms of nocturnal CO₂ uptake, accumulation of titratable acidity, PEPC protein abundance and transcript abundance of key genes implicated in CAM (Chapters 2 and 4). Furthermore, there was a progressive increase in the amount of CAM activity observed by titratable acidity down the plant as the leaves increase in age. This, together with the genome and transcriptome of *K. blossfeldiana* will help to establish the plant as a model system for the comparative study of C₃ and CAM in multiple contexts within the same plant. The comparison of C₃ and CAM across a single plant reduces risk of conflation due to intraspecific differences between phylogenetically related species but also differences between individuals or batch effects, with many CAM studies comparing sometimes distantly related plants (Abraham et al., 2016; Moseley et al., 2019).

Age-induced CAM may be less stressful and 'cleaner', with fewer genes differentially expressed between young C₃ and mature CAM *K. blossfeldiana* leaves compared to other methods of induction, like drought (Wai et al., 2019), salt stress or ABA (Maleckova et al., 2019). However, an issue with using CAM induction by ageing is potential conflation between the impacts of leaf ageing and CAM induction on the leaves. This may be tackled in future work by either investigating CAM-related changes closer to the age induced transition from C₃ to CAM, or by larger experiments that separately induce CAM by different means to determine convergent elements important to CAM as well as to establish any unique elements associated with particular methods of CAM induction.

In keeping with previous studies and like other members of the *Kalanchoe* genus it is also possible to transform *K. blossfeldiana* with relative ease (Hartwell et al., 2016). In the present study, transformation was attempted using *Agrobacterium tumefaciens*, with a construct that produces betalain, which acts as an easy to see red marker for successful transformation, driven by a constitutive 35S promoter. However, this process still requires some optimisation since expression of betalain was only maintained for approximately a week (Appendix Figure A4). A working hypothesis is that betalain production may have been overly metabolically costly for the plant tissues and therefore led to the silencing of the transgene, however this remains to be investigated in detail and with alternative promoters.

Altogether, this work has highlighted *K. blossfeldiana* as an informative system for comparatively studying C₃/CAM in terms of gene expression, physiology and both mesophyll and guard cell metabolism.

5.1.2 Changes in guard cell metabolism and regulation in CAM are required for sustained nocturnal stomatal opening

A key question tackled by this thesis, with implications for CAM engineering, was: will stomata follow the pattern of mesophyll driven changes in C_i or will guard cells require separate changes to their regulation and metabolism to support nocturnal opening and diurnal closure? In *K. blossfeldiana* the data suggested that while young C_3 guard cells were responsive to reduced C_i at night, this signal alone was not enough to sustain the CAM-like pattern of nocturnal stomatal conductance observed in the mature CAM leaves for the entire night (Chapter 3). This contrasted with the response of the CAM-deficient *K. fedtschenkoi* *pepc1* mutant which showed CAM-like nocturnal stomatal conductance in response to reduced C_i over the entire night, despite the absence of PEPC-mediated carboxylation (Chapter 3). Together, this suggests a change occurs in the *K. blossfeldiana* guard cells on the transition from C_3 to CAM to enable nocturnal opening that is distinct from mesophyll PEPC-driven carboxylation.

This finding raises the question of what is changing between C_3 and CAM guard cells that enables sustained nocturnal opening in CAM in response to reduced C_i ? Chapter 2 and previous studies (Abraham et al., 2020) have shown a retiming of guard cell starch metabolism in CAM tissues compared to that in *Arabidopsis*, with starch degraded in the early night. The data collected in this thesis showed that the pattern of starch metabolism progressively changed as the leaves aged and CAM activity increased in *K. blossfeldiana* (Chapter 2, Figure 2). In C_3 plants, the rapid degradation of guard cell starch is associated with stomatal opening in response to light in the early morning, providing sugars for energy and osmoticum required for proper stomatal opening (Flütsch et al., 2020; Horrer et al., 2016). It is therefore possible that the retiming of starch metabolism in CAM guard cells is to support nocturnal opening both energetically and by supplying osmoticum. Previous work in *K. fedtschenkoi* has also suggested that guard cell starch synthesis during the day may work in the opposite direction by reducing sugar osmolytes by moving carbon into starch and assisting stomatal closure. This suggestion is supported by work on *pgm* mutants of *K. fedtschenkoi* impaired in starch synthesis which were unable to maintain proper stomatal closure during the day (Hurtado Castano, 2019).

It is also likely that guard cell regulatory pathways play a role in enabling sustained nocturnal opening in CAM in response to reduced C_i . Moseley et al., (2019) identified a number of genes implicated in stomatal regulation with CAM-like inverted transcript expression patterns in *K. fedtschenkoi*, including CAT2 which inhibits ABA induced stomatal closure in C_3 plants (Jannat et al., 2011). CAT2 was also found to be upregulated at dusk in the mature CAM *K. blossfeldiana* leaves (Chapter 4). Chapter four also identified a number of genes that have previously been implicated in stomatal regulation and guard cell metabolism in C_3 species, that were up regulated in both the mature CAM *K. blossfeldiana* leaves and in proteome/transcriptome datasets from guard cell enriched epidermal tissue from *K. fedtschenkoi*. Of these genes *Plasma membrane H⁺-ATPase (AHA2)* and *OPEN STOMATA 1 (OST1)* were of especial interest as they have opposing regulatory effects on stomatal opening (Ueno et al., 2005; Xue et al., 2011) and had opposing diel transcript expression patterns in *K. fedtschenkoi* epidermal peels. Transcripts encoding *β -Amylase 9 (BAM9)*, that has been shown to positively regulate starch degradation (David et al., 2022), and *Sucrose synthase 3 (SUS3)*, which converts sucrose into hexoses for glycolysis and mitochondrial respiration during light induced stomatal opening (Antunes et al., 2012; Daloso et al., 2015), were also upregulated in both the mature CAM *K. blossfeldiana* leaves and the epidermal peels of *K. fedtschenkoi* leaves. Together, the changes in gene expression observed here and in other studies suggest that changes to guard cell regulatory pathways play a role in nocturnal opening in CAM. There is a pressing need to determine how these regulatory pathways influence and interact with guard cell metabolism to coordinate both the regulatory and metabolic changes needed to control stomatal conductance in both C_3 and CAM.

The research conducted in this thesis also suggests that diurnal stomatal closure was largely driven by increases in C_i from the diurnal decarboxylation of malate, with CAM-deficient *pepc1* *K. fedtschenkoi* mutants displaying C_3 levels of diurnal stomatal conductance (Chapter 3). Curtailing nocturnal malate accumulation by growing *K. blossfeldiana* in reduced light also increased stomatal conductance during the day in mature CAM *K. blossfeldiana* leaves (Chapter 3). These findings are in contrast to experiments to curtail nocturnal malate accumulation by growing *Kalanchoe* species in reduced CO_2 both here and in previous work (von Caemmerer & Griffiths, 2009), which could suggest some additional regulatory control alongside increased C_i which together act to close stomata during the day in CAM. This thesis hypothesised that the sensitivity to C_i likely changes over the diel period and between C_3 and

CAM, with even small amounts of residual CO₂ decarboxylated able to cause diurnal stomatal closure. This could help in situations of extreme drought when little CO₂ has been taken up at night and day-time opening would be very costly.

This idea is supported by the upregulation of genes involved in ABA signalling and *OST1*, that promotes stomatal closure in response to ABA, in the mature CAM *K. blossfeldiana* leaves (Chapter 4). These genes also showed a rescheduled maximum daytime expression pattern in *K. laxiflora* and *A. americana* compared to maximal nocturnal expression in C₃ *Arabidopsis* (Abraham et al., 2016; Boxall et al., 2020). Both genes were , also shown to have epiderma-specific protein expression in *K. fedtschenkoi* (Abraham et al., 2020).

Though future works studying C₃ and CAM in *K. blossfeldiana* leaves with the aim of unravelling both nocturnal stomatal opening and diurnal closure in CAM will need to look at gene expression in isolated guard cell tissues and over the full diel period between C₃ and CAM tissues.

5.1.3 ATP/Carbon supply for CAM

This thesis has provided further evidence to support the increases in ATP that are required to enable mesophyll CAM which have previously been predicted by flux balance analysis (Shameer et al., 2018) and which is consistent with past transcriptomic and proteomic studies of multiple CAM species (Abraham et al., 2016; Brilhaus et al., 2016; Maleckova et al., 2019; Yang et al., 2017). As part of age-induced CAM induction in *K. blossfeldiana*, there was an upregulation of genes involved in multiple energy requiring and CAM supporting processes (Chapter 4). A major sink for ATP during CAM is the nocturnal transport of malate and H⁺ into the vacuole to maintain pH homeostasis in the cytosol during nocturnal carboxylation, with *ALMT* and *tDT* malate transporters and ATP consuming H⁺ pumping vacuolar ATPases shown to be upregulated in mature CAM *K. blossfeldiana* leaves (Chapter 4). ATP is also consumed through the cycling of carbon between transitory starch and PEP with many genes in this pathway upregulated in CAM mature *K. blossfeldiana* leaves.

In the transition from C_3 to CAM as *K. blossfeldiana* leaves age, a number of changes in gene expression occur to meet the energy demand of CAM, highlighting the importance for energy supply for CAM. In the mesophyll there is a conserved shift to the phosphorolytic starch degradation pathway upon CAM induction in mature *K. blossfeldiana* leaves which is energetically advantageous and also occurs in *K. fedtschenkoi* and *M. crystallinum*, with increased expression of *PHS1* and *GPT* and a decrease in *MEX1* expression observed in mature CAM *K. blossfeldiana* leaves (Chapter 4). A portion of this ATP will be provided by increased glycolytic processes, that were enriched in the genes upregulated in the mature CAM *K. blossfeldiana* leaves and from an upregulation of mitochondrial respiration. Increased mitochondrial respiration in CAM was suggested here by increased TCA cycle gene expression in the mature CAM *K. blossfeldiana* leaves (Chapter 4) and mitochondrial genes upregulated in constitutive CAM *Agave americana* (Abraham et al., 2016) and on CAM induction in the facultative CAM *Talinum triangulare* (Brilhaus et al., 2016; Maleckova et al., 2019). Increased nocturnal oxygen consumption was observed in CAM performing *Clusia* plants and determined to be a CAM-specific trait (Leverett et al., unpublished). The importance of ATP supply and the conservation of increases in mitochondrial respiration highlight the need for detailed metabolic analysis of ATP and carbon supply and demand in CAM.

This thesis also observed the upregulation of *NTT1*, which can import ATP into the chloroplasts, in CAM mature *K. blossfeldiana* leaves (Chapter 4) and its expression in both epidermal and mesophyll tissue in *K. fedtschenkoi* leaves suggests ATP import into the chloroplasts occurs in both the guard cells and mesophyll of CAM plants. In the guard cells, ATP import into the chloroplasts via NTT is essential for enabling stomatal opening and guard cell starch synthesis (Lim et al., 2022). ATP import into the chloroplasts of mesophyll cells has not been reported in C_3 plants, implying this may be a CAM-specific function, which requires further study. There is a need for future work to understand the movement of carbon into the guard cells and to combine guard cell metabolism and mesophyll CAM into an integrated metabolic model.

5.1.4 Core set of genes up-regulated in response to age, ABA, drought and NaCl-induced CAM

There are a core conserved set of metabolic genes required for CAM that are upregulated upon CAM induction across the different modes of CAM induction, i.e. age, ABA, drought and NaCl (Brilhaus, Bräutigam, et al., 2016; Cushman, Tillett, et al., 2008; Maleckova et al., 2019; Wai et al., 2019). These genes are also conserved across multiple, related CAM species and are discussed in detail in Chapter 4. Alongside this, there was overlap of regulatory genes that may be involved in the induction of CAM across age, drought, NaCl and ABA induced CAM (Brilhaus, Bräutigam, et al., 2016; Cushman, Tillett, et al., 2008; Maleckova et al., 2019; Wai et al., 2019), suggesting a core set of conserved genes involved in CAM induction. In keeping with the notion of ABA-induced CAM (Taybi & Cushman, 2002), Chapter 4 showed that many ABA signalling genes and responsive elements are also upregulated in response to age-induced CAM in *K. blossfeldiana* (Brilhaus et al., 2016; Cushman, Tillett, et al., 2008; Maleckova et al., 2019; Wai et al., 2019), suggesting that elements of ABA signalling play a core role in CAM induction across these different modes. It makes sense for the response to water deprivation and the induction of CAM to be somewhat interwoven, as both processes converge on the same goal which is to conserve water and improve the plants ability to tolerate drought. This thesis suggests that this goes so far as to share certain regulatory elements as shown, for example, by the upregulation of several ABA responsive transcription factors in age induced CAM in *K. blossfeldiana* and drought induced CAM in *S. album* and *T. triangulare* (Maleckova, 2020; Wai et al., 2019). There is precedent for similar overlap between regulatory pathways from other processes; for example in C_3 Arabidopsis there is overlap between age, photoperiod and temperature induced flowering (Kinoshita & Richter, 2021). This would suggest that CAM induction occurs in an analogous manner to flowering time regulation, which is influenced by multiple endogenous and external stimuli that converge on a common response regardless of the method of induction.

What is not yet understood is how age induces CAM and by extension how *K. blossfeldiana* leaves sense age? The above would suggest that age-induced CAM is mediated by the ABA signalling pathway, but it is likely that future studies will need to explore gene expression progressively as *K. blossfeldiana* leaves age in order to detect genes involved in the earlier stages of age-induced CAM. One hypothesis is the possibility of links between age-induced CAM and the flower timing or senescence pathways, which in *Arabidopsis* have been shown to be induced by the progressive reduction of miRNA-156 expression as the plants age (A. Kinoshita & Richter, 2021) and has thus been heralded as a potential 'age sensor' or at least close to one. However, there is not a clear link between CAM and flower induction in *K. blossfeldiana*, with CAM induction occurring at the individual leaf level much earlier than whole plant flower induction. Chapter four has shown few genes involved in flower timing to be differentially expressed in age-induced CAM in *K. blossfeldiana*, suggesting no link between age-induced CAM and the flower induction pathways. Interestingly, there was a difference in the expression of two *SQUAMOSA PROMOTER-BINDING PROTEIN-LIKE* (*SPL*) proteins in the mature CAM in *K. blossfeldiana* leaves. *SPL9*, which is implicated in the *SPL*-miRNA-156 age induced flower induction pathway in *Arabidopsis* (Kinoshita & Richter, 2021) was significantly downregulated while *SPL8*, the function of which is less well characterised, was significantly upregulated (Chapter 4). The dusk comparative transcriptome described in this thesis might provide the basis for future works exploring how age is detected and induces CAM in *K. blossfeldiana*.

5.2 Future Directions – where next on the road to CAM?

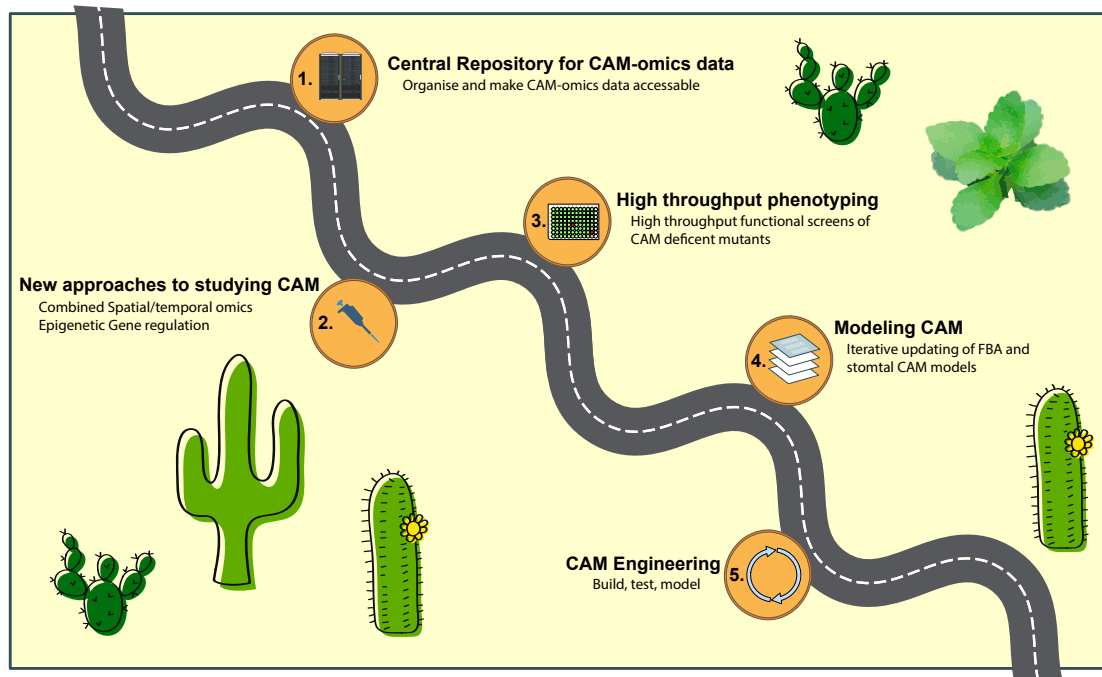


Figure 5.1 Roadmap for the future of CAM research and engineering CAM into C_3 species

5.2.1 Lots of omics data, but what to do with it?

As previously described, over the past decade there have been a spree of ‘CAM-omics’ studies including this one, using genomics, proteomics, transcriptomics and/or occasionally metabolomics to study gene expression and metabolic differences between C_3 and CAM. However, much of these data are hard to access and there has yet to be an effort to compile CAM omics data into an accessible and easy to use database. Examples of such include EFP browser for exploring gene expression data in *Arabidopsis* across various tissue and many different environmental conditions (Winter et al., 2007) and the broader TAIR database of the *Arabidopsis* genome and gene function (Berardini et al., 2015), which has become a core resource for gene information across plants. The CAM research community currently lacks such a resource that makes ‘omics’ data accessible. For example, most published transcriptomic data in CAM is stored on the NCBI Sequence Read Archive (SRA), which would require reassembly and quantification which in turn require significant computational resources, especially if applied to all available data. There are instances where some of these data are published, for instance there are many CAM genomes on Phytozome (Goodstein et

al., 2012) and there has been recent efforts to publish gene expression data from *K. fedtschenkoi* on the new Phytozome gene atlas repository (Sreedasyam et al., unpublished, Zhang et al., 2020). There is a need to organise the data from many CAM species into a central and accessible resource for studying CAM genomics, transcriptomics and metabolomics. Such a future project would allow for the easy and quick querying of many hypotheses across the complex CAM phenotype and speed up efforts to engineer CAM.

5.2.2 New Approaches – The role of methylation in age-induced CAM

One area of gene regulation that was also investigated by this thesis was the role of gene methylation in the regulation of gene expression in age-induced CAM in *K. blossfeldiana*.

This exploited the ability of the nanopore DNA sequencer to detect methylated base pairs by sequencing DNA samples from young and mature *K. blossfeldiana* leaves and a number of sites of differential methylation were detected (Appendix Figure A3.1). However, due to low coverage and a lack of replication the number of statistically significant sites were low. This work should be followed up with greater sequencing depth and replication, as from this preliminary data it appears that there are substantial differences in the methylation landscape of the *K. blossfeldiana* genome between young and mature leaves. Recent work has also shown that methylation detection by nanopore sequencers is influenced by species and has prompted work on plant specific models for basecalling DNA in plants (Ni et al., 2021). , Such methods may improve future attempts to detect differential methylation between young and mature *K. blossfeldiana* leaves.

5.2.3 Temporal and Spatial Approaches to studying CAM

Future studies on age-induced CAM in *K. blossfeldiana* could build upon the dusk transcriptome in this thesis by exploring differential gene expression patterns across the full diel period between C₃ and CAM tissues. As demonstrated in other studies, many genes involved in CAM show retimed gene expression rather than just increased or decreased gene expression (Abraham et al., 2020; Yang et al., 2017) meaning that some differentially expressed genes will likely have been missed in one-time point comparative transcriptome.

Another generalisation made in this thesis and across CAM research is a simplification of the CAM leaf into the photosynthetic CAM performing mesophyll and the guard cells at the epidermis; little is known about the potential roles of different leaf cells in CAM.

A recent study on C_4 -CAM in which CAM was induced by drought used laser capture and spatial transcriptomics to explore spatial changes in gene expression between mesophyll and bundle sheath cells in a C_4 -CAM plant before and after CAM induction by drought (Moreno-Villena et al., 2022). Such an approach in *K. blossfeldiana*, with comparisons made between guard cell and mesophyll cells before and after CAM induction would be useful in identifying further important CAM components with cell specific functions. High throughput spatial transcriptomics using single cell sequencing approaches may be useful in identifying potential functions across all cell types within the leaf. These approaches would be even more insightful if they also combined metabolomic and proteomic data and for completeness were carried out over the full diel period. These future approaches should also be taken in the context of recent rapid improvements in high throughput analytic methods and reducing sequencing costs. For instance advances in single molecule protein sequencing using nanopore like devices may allow the detailed study of both protein abundance (Restrepo-Pérez et al., 2018), which often differs from transcript abundance, and post translational modifications (Nova et al., 2022) that regulate many CAM functions (Abraham et al., 2020).

5.2.4 High Throughput Phenotyping

As a result of many CAM-omics studies over the last decade there are a large number of genes implicated in CAM that need to be functionally characterised. Methods to infer function from orthology to genes in C_3 are largely based on studies on *Arabidopsis* and may not hold true in CAM species. Furthermore, many of the genes that show expression patterns of interest from this thesis and across CAM-omics studies are poorly characterised. While there are methods of inferring function through homology, it is likely that many of these genes will need to be functionally characterised, especially in the context of their role in CAM.

High throughput studies of CAM-deficient mutants have been carried out in the past. Cushman et al. (2008) used a plate based colourimetric pH and starch assay to screen radioactively mutagenized *M. crystallinum* plants for CAM or starch metabolism deficiencies. Recently a library of CRISPR guide RNA targets were developed for *K. fedtschenkoi* which could allow for efficient linkage between phenotype and genotype (Liu et al., 2019). There is also need for the development of new methods to study and screen large number of CAM mutants, which may present subtle phenotypes. Most large-scale phenotyping facilities are setup for the study of C₃ or common crop species (Arend et al., 2016) and they also lack the ability to perform gas exchange experiments.

While TA's and other metabolic assays could be useful for large screening experiments, they might miss more subtle phenotypes. Impairment in CAM could be detected by screening for nocturnal conductance, with efforts made alongside this thesis with a group in Sweden to test the use of thermal imaging for detecting changes in conductance in response to metabolite injection. High throughput gas exchange would give a more detailed idea of phenotype and could enable both CO₂ uptake and stomatal conductance or even O₂ consumption to be measured across many plants. In this thesis gas exchange experiments were constrained by the LICOR-6400 ability to only test one leaf at a time. The ability to measure gas exchange characteristics over many plants and possibly assay them with varying conditions would provide a wealth of phenotypic information and may identify phenotypes that would go unnoticed using today's methods. Future detailed high throughput phenotyping may be needed to efficiently establish the function of many key genes in the context of their role in CAM and ultimately identify targets for CAM engineering. This approach could also work the other way as high throughput phenotyping could also be used to rapidly prototype plants for CAM engineering.

K. blossfeldiana is a good candidate species for high throughput experiments: it is easy to grow and CAM can be induced via multiple means, thus allowing comparisons between the different induction pathways. *K. blossfeldiana* has C₃ and CAM tissues within the same plant making it more efficient for C₃/CAM comparative studies.

5.2.5 CAM modelling and Engineering

Present and future CAM omics and functional phenotyping experiments will create vast amounts of complex data that will likely be only truly understood after applying these data to efforts to appropriately model the underlying metabolic and physiological characteristics of CAM. Such modelling efforts, reviewed by Chomthong & Griffiths (2020), will help condense these large omics data sets and have already helped to highlight key processes and targets for CAM engineering (Shameer et al., 2018).

Due to the complexity of implementing CAM into C_3 plants, engineering will have to make use of modelling to identify key metabolic control points that could potentially be manipulated to create CAM-like fluxes of carbon (Chomthong & Griffiths, 2020; Dodd et al., 2002). This approach may be simpler to implement, in terms of fewer transgenes, but will likely require a greater understanding of the regulation of metabolic fluxes in CAM. While complex transgenic constructs consisting of many transgenes can be introduced into C_3 plants (Engler et al., 2014), it may be wise to try to limit transgene introduction to avoid unintended consequences like transgene silencing or metabolic constraints by overexpression. A simple approach to engineering will also help in efforts to implement CAM-like stomatal regulation and guard cell metabolism, a key challenge that has been highlighted by the research presented in this thesis.

5.3 Overall Conclusions

This thesis has demonstrated the merits of *K. blossfeldiana* as a comparative system for studying C₃ and CAM physiologies and metabolism within a plant and has also identified substantial changes in the dusk transcriptome in between young C₃ and mature CAM *K. blossfeldiana* leaves in response to age-induced CAM. The research described here has shown the retiming of guard cell starch metabolism in CAM leaves and has provided evidence that changes in guard cell metabolism and stomatal regulation are likely necessary for CAM stomata to open in response to low C_i at night. It has identified genes implicated in stomatal regulation and guard cell metabolism that are differentially expressed between C₃ and CAM in *K. blossfeldiana* and may enable nocturnal stomatal opening in the mature CAM *K. blossfeldiana* leaves. The data described have also highlighted a need to further investigate the regulatory and metabolic processes that allow inverted stomatal conductance in CAM with nocturnal opening and diurnal closure. Substantial changes in whole leaf metabolism between the young C₃ and mature CAM *K. blossfeldiana* leaves have been identified and this has reinforced the need to further study the regulatory processes that orchestrate the diel cycle of carbon flux that enables nocturnal carboxylation and daytime decarboxylation.

Chapter 6. References

- Aasamaa, K., & Sober, A. (2011). Responses of stomatal conductance to simultaneous changes in two environmental factors. *TREE PHYSIOLOGY*, *31*(8), 855–864. <https://doi.org/10.1093/treephys/tpr078>
- Abraham, P. E., Hurtado Castano, N., Cowan-Turner, D., Barnes, J., Poudel, S., Hettich, R., Flütsch, S., Santelia, D., & Borland, A. M. (2020). Peeling back the layers of crassulacean acid metabolism: functional differentiation between *Kalanchoë fedtschenkoi* epidermis and mesophyll proteomes. *Plant Journal*, 1–20. <https://doi.org/10.1111/tpj.14757>
- Abraham, P. E., Yin, H., Borland, A. M., Weighill, D., Lim, S. D., de Paoli, H. C., Engle, N., Jones, P. C., Agh, R., Weston, D. J., Wullschleger, S. D., Tschaplinski, T., Jacobson, D., Cushman, J. C., Hettich, R. L., Tuskan, G. A., & Yang, X. (2016). Transcript, protein and metabolite temporal dynamics in the CAM plant *Agave*. *Nature Plants*, *2*. <https://doi.org/10.1038/nplants.2016.178>
- Allaway, W. G., & Setterfield, G. (1972). Ultrastructural observations on guard cells of *Vicia faba* and *Allium porrum*. *Canadian Journal of Botany*, *50*, 1405–1413.
- Alonge, M., Lebeigle, L., Kirsche, M., Aganezov, S., Wang, X., Lippman, Z. B., Schatz, M. C., & Soyk, S. (2021). Automated assembly scaffolding elevates a new tomato system for high-throughput genome editing. *BioRxiv*, 2021.11.18.469135. <https://doi.org/10.1101/2021.11.18.469135>
- Alonge, M., Soyk, S., Ramakrishnan, S., Wang, X., Goodwin, S., Sedlazeck, F. J., Lippman, Z. B., & Schatz, M. C. (2019). RaGOO: Fast and accurate reference-guided scaffolding of draft genomes. *Genome Biology*, *20*(1), 1–17. <https://doi.org/10.1186/s13059-019-1829-6>
- Andersson, M., Turesson, H., Arrivault, S., Zhang, Y., Fält, A.-S., Fernie, A. R., & Hofvander, P. (2018). Inhibition of plastid PPase and NTT leads to major changes in starch and tuber formation in potato. *Journal of Experimental Botany*, *69*(8), 1913–1924. <https://doi.org/10.1093/jxb/ery051>

- Ando, E., & Kinoshita, T. (2018). Red light-induced phosphorylation of plasma membrane H⁺-ATPase in stomatal guard cells. *Plant Physiology*, 178(October), DOI:10.1104/pp.18.00544. <https://doi.org/10.1104/pp.17.01829>
- Andrea Barrera Zambrano, V., Lawson, T., Olmos, E., Fernández-García, N., & Borland, A. M. (2014). Leaf anatomical traits which accommodate the facultative engagement of crassulacean acid metabolism in tropical trees of the genus *Clusia*. *Journal of Experimental Botany*, 65(13), 3513–3523. <https://doi.org/10.1093/jxb/eru022>
- Andrews, S. (2010). *FastQC: a quality control tool for high throughput sequence data*. Babraham Bioinformatics, Babraham Institute, Cambridge, United Kingdom.
- Antipov, D., Korobeynikov, A., McLean, J. S., & Pevzner, P. A. (2016). HybridSPAdes: An algorithm for hybrid assembly of short and long reads. *Bioinformatics*, 32(7), 1009–1015. <https://doi.org/10.1093/bioinformatics/btv688>
- Antunes, W. C., Provart, N. J., Williams, T. C. R., & Loureiro, M. E. (2012). Changes in stomatal function and water use efficiency in potato plants with altered sucrolytic activity. *Plant, Cell and Environment*, 35(4), 747–759. <https://doi.org/10.1111/j.1365-3040.2011.02448.x>
- Arend, D., Lange, M., Pape, J. M., Weigelt-Fischer, K., Arana-Ceballos, F., Mücke, I., Klukas, C., Altmann, T., Scholz, U., & Junker, A. (2016). Quantitative monitoring of *Arabidopsis thaliana* growth and development using high-throughput plant phenotyping. *Scientific Data*, 3. <https://doi.org/10.1038/sdata.2016.55>
- Assmann, S. M., Simoncini, L., & Schroeder, J. I. (1985). Blue light activates electrogenic ion pumping in guard cell protoplasts of *Vicia faba*. *Nature*, 318(6043), 285–287. <https://doi.org/10.1038/318285a0>
- Atkin, O. K., & Macherel, D. (2009). The crucial role of plant mitochondria in orchestrating drought tolerance. In *Annals of Botany* (Vol. 103, Issue 4, pp. 581–597). <https://doi.org/10.1093/aob/mcn094>
- Aubry, S., Kelly, S., Kümpers, B. M. C., Smith-Unna, R. D., & Hibberd, J. M. (2014). Deep Evolutionary Comparison of Gene Expression Identifies Parallel Recruitment of Trans-

- Factors in Two Independent Origins of C₄ Photosynthesis. *PLoS Genetics*, 10(6).
<https://doi.org/10.1371/journal.pgen.1004365>
- Azoulay-Shemer, T., Bagheri, A., Wang, C., Palomares, A., Stephan, A. B., Kunz, H. H., & Schroeder, J. I. (2016). Starch Biosynthesis in Guard Cells But Not in Mesophyll Cells Is Involved in CO₂-Induced Stomatal Closing. *PLANT PHYSIOLOGY*, 171(2), 788–798.
<https://doi.org/10.1104/pp.15.01662> WE - Science Citation Index Expanded (SCI-EXPANDED)
- Azoulay-Shemer, T., Palomares, A., Bagheri, A., Israelsson-Nordstrom, M., Engineer, C. B., Bargmann, B. O. R., Stephan, A. B., & Schroeder, J. I. (2015). Guard cell photosynthesis is critical for stomatal turgor production, yet does not directly mediate CO₂- and ABA-induced stomatal closing. *Plant Journal*, 83(4), 567–581.
<https://doi.org/10.1111/tpj.12916>
- Bates, G. W., Rosenthal, D. M., Sun, J., Chattopadhyay, M., Peffer, E., Yang, J., Ort, D. R., & Jones, A. M. (2012). A Comparative Study of the Arabidopsis thaliana Guard-Cell Transcriptome and Its Modulation by Sucrose. *PLoS ONE*, 7(11).
<https://doi.org/10.1371/journal.pone.0049641>
- Bauer, H., Ache, P., Lautner, S., Fromm, J., Hartung, W., Al-Rasheid, K. A. S., Sonnewald, S., Sonnewald, U., Kneitz, S., Lachmann, N., Mendel, R. R., Bittner, F., Hetherington, A. M., & Hedrich, R. (2013). The stomatal response to reduced relative humidity requires guard cell-autonomous ABA synthesis. *Current Biology*, 23(1), 53–57.
<https://doi.org/10.1016/j.cub.2012.11.022>
- Berardini, T. Z., Reiser, L., Li, D., Mezheritsky, Y., Muller, R., Strait, E., & Huala, E. (2015). The arabidopsis information resource: Making and mining the “gold standard” annotated reference plant genome. *Genesis*, 53(8), 474–485. <https://doi.org/10.1002/dvg.22877>
- Bode, O. (1942). Über Zusammenhänge zwischen CO₂-Assimilation und Photoperiodismus bei Kalanchoe Blossfeldiana. *Planta* 33, 278–289
- Borland, A. M., & Dodd, A. N. (2002). Carbohydrate partitioning in crassulacean acid metabolism plants: Reconciling potential conflicts of interest. *Functional Plant Biology*, 29(6), 707–716. <https://doi.org/10.1071/PP01221>

- Borland, A. M., Griffiths, H., Hartwell, J., & Smith, J. A. C. (2009). Exploiting the potential of plants with crassulacean acid metabolism for bioenergy production on marginal lands. *Journal of Experimental Botany*, *60*(10), 2879–2896. <https://doi.org/10.1093/jxb/erp118>
- Borland, A. M., Guo, H. B., Yang, X. H., & Cushman, J. C. (2016). Orchestration of carbohydrate processing for crassulacean acid metabolism. *CURRENT OPINION IN PLANT BIOLOGY*, *31*, 118–124. <https://doi.org/10.1016/j.pbi.2016.04.001>
- Borland, A. M., Hartwell, J., Jenkins, G. I., Wilkins, M. B., & Nimmo, H. G. (1999). Metabolite control overrides circadian regulation of phosphoenolpyruvate carboxylase kinase and CO₂ fixation in crassulacean acid metabolism. *Plant Physiology*, *121*(3), 889–896. <https://doi.org/10.1104/pp.121.3.889>
- Borland, A. M., Hartwell, J., Weston, D. J., Schlauch, K. A., Tschaplinski, T. J., Tuskan, G. A., Yang, X., & Cushman, J. C. (2014). Engineering crassulacean acid metabolism to improve water-use efficiency. *Trends in Plant Science*, *19*(5), 327–338. <https://doi.org/10.1016/j.tplants.2014.01.006>
- Borland, A. M., Wulschleger, S. D., Weston, D. J., Hartwell, J., Tuskan, G. A., Yang, X. H., & Cushman, J. C. (2015). Climate-resilient agroforestry: physiological responses to climate change and engineering of crassulacean acid metabolism (CAM) as a mitigation strategy. *PLANT CELL AND ENVIRONMENT*, *38*(9), 1833–1849. <https://doi.org/10.1111/pce.12479>
- Borland, A. M., Zambrano, V. A. B., Ceusters, J., & Shorrocks, K. (2011). The photosynthetic plasticity of crassulacean acid metabolism: an evolutionary innovation for sustainable productivity in a changing world. *NEW PHYTOLOGIST*, *191*(3), 619–633. <https://doi.org/10.1111/j.1469-8137.2011.03781.x>
- Boxall, S. F., Dever, L. v., Knerová, J., Gould, P. D., & Hartwell, J. (2017). Phosphorylation of phosphoenolpyruvate carboxylase is essential for maximal and sustained dark CO₂ fixation and core circadian clock operation in the obligate crassulacean acid metabolism species *Kalanchoë fedtschenkoi*. *Plant Cell*, *29*(10), 2519–2536. <https://doi.org/10.1105/tpc.17.00301>
- Boxall, S. F., Kadu, N., Dever, L. v., Knerová, J., Waller, J. L., Gould, P. J. D., & Hartwell, J. (2020). *Kalanchoë* PPC1 is essential for crassulacean acid metabolism and the regulation of core

- circadian clock and guard cell signaling genes[CC-BY]. *Plant Cell*, 32(4), 1136–1160. <https://doi.org/10.1105/TPC.19.00481>
- Brilhaus, D., Bräutigam, A., Mettler-Altmann, T., Winter, K., & Weber, A. P. M. (2016). Reversible burst of transcriptional changes during induction of crassulacean acid metabolism in *Talinum triangulare*. *Plant Physiology*, 170(1), 102–122. <https://doi.org/10.1104/pp.15.01076>
- Brulfert, J., Guerrier, D., & Queiroz, O. (1982). Photoperiodism and Crassulacean acid metabolism. *Planta*, 154(4), 332–338. <https://doi.org/10.1007/BF00393911>
- Brulfert, J., Ravelomanana, D., Güclü, S., & Kluge, M. (1996). Ecophysiological studies in *Kalanchoë porphyrocalyx* (Baker) and *K. miniata* (Hils et Bojer), two species performing highly flexible CAM. *Photosynthesis Research*, 49(1), 29–36. <https://doi.org/10.1007/BF00029425>
- Brúna, T., Hoff, K. J., Lomsadze, A., Stanke, M., & Borodovsky, M. (2021). BRAKER2: automatic eukaryotic genome annotation with GeneMark-EP+ and AUGUSTUS supported by a protein database. *NAR Genomics and Bioinformatics*, 3(1), lqaa108. <https://doi.org/10.1093/nargab/lqaa108>
- Buckley, T. N., & Mott, K. A. (2013). Modelling stomatal conductance in response to environmental factors. *PLANT CELL AND ENVIRONMENT*, 36(9), 1691–1699. <https://doi.org/10.1111/pce.12140> WE - Science Citation Index Expanded (SCI-EXPANDED)
- Carter, P. J., Nimmol, H. G., Fewson, C. A., & Wilkins, M. B. (1991). Circadian rhythms in the activity of a plant protein kinase. In *The EMBO Journal* (Vol. 10, Issue 8).
- Ceusters, J., Borland, A. M., Ceusters, N., Verdoodt, V., Godts, C., & de Proft, M. P. (2010). Seasonal influences on carbohydrate metabolism in the CAM bromeliad *Aechmea "Maya"*: consequences for carbohydrate partitioning and growth. *ANNALS OF BOTANY*, 105(2), 301–309. <https://doi.org/10.1093/aob/mcp275>

- Ceusters, N., Borland, A. M., & Ceusters, J. (2021). How to resolve the enigma of diurnal malate remobilisation from the vacuole in plants with crassulacean acid metabolism? *New Phytologist*, 229(6), 3116–3124. <https://doi.org/10.1111/nph.17070>
- Ceusters, N., Ceusters, J., Hurtado-Castano, N., Dever, L. v., Boxall, S. F., Kneřová, J., Waller, J. L., Rodick, R., van den Ende, W., Hartwell, J., & Borland, A. M. (2021). Phosphorolytic degradation of leaf starch via plastidic α -glucan phosphorylase leads to optimized plant growth and water use efficiency over the diel phases of Crassulacean acid metabolism. *Journal of Experimental Botany*, 72(12), 4419–4434. <https://doi.org/10.1093/jxb/erab132>
- Chomthong, M., & Griffiths, H. (2020). Model approaches to advance crassulacean acid metabolism system integration. In *Plant Journal* (Vol. 101, Issue 4, pp. 951–963). Blackwell Publishing Ltd. <https://doi.org/10.1111/tpj.14691>
- Christin, P. A., Salamin, N., Savolainen, V., Duvall, M. R., & Besnard, G. (2007). C4 Photosynthesis Evolved in Grasses via Parallel Adaptive Genetic Changes. *Current Biology*, 17(14), 1241–1247. <https://doi.org/10.1016/j.cub.2007.06.036>
- Cirelli, D., Equiza, M. A., Lieffers, V. J., & Tyree, M. T. (2016). Populus species from diverse habitats maintain high night-time conductance under drought. *TREE PHYSIOLOGY*, 36(2), 229–242. <https://doi.org/10.1093/treephys/tpv092>
- Cockburn, W., Ting, I. P., & Sternberg, L. O. (1979). Relationships between Stomatal Behavior and Internal Carbon Dioxide Concentration in Crassulacean Acid Metabolism Plants. *Plant Physiology*, 63(6), 1029–1032. <https://doi.org/10.1104/pp.63.6.1029>
- Cushman, J. C., Agarie, S., Albion, R. L., Elliot, S. M., Taybi, T., & Borland, A. M. (2008). Isolation and characterization of mutants of common ice plant deficient in Crassulacean acid metabolism. *PLANT PHYSIOLOGY*, 147(1), 228–238. <https://doi.org/10.1104/pp.108.116889>
- Cushman, J. C., & Borland, A. M. (2002). Induction of Crassulacean acid metabolism by water limitation. *Plant, Cell and Environment*, 25(2), 295–310. <https://doi.org/10.1046/j.0016-8025.2001.00760.x>

- Cushman, J. C., Tillett, R. L., Wood, J. A., Branco, J. M., & Schlauch, K. A. (2008). Large-scale mRNA expression profiling in the common ice plant, *Mesembryanthemum crystallinum*, performing C3 photosynthesis and Crassulacean acid metabolism (CAM). *Journal of Experimental Botany*, *59*(7), 1875–1894. <https://doi.org/10.1093/jxb/ern008>
- Daloso, D. M., Antunes, W. C., Pinheiro, D. P., Waquim, J. P., Araújo, W. L., Loureiro, M. E., Fernie, A. R., & Williams, T. C. R. (2015). Tobacco guard cells fix CO₂ by both Rubisco and PEPcase while sucrose acts as a substrate during light-induced stomatal opening. *Plant Cell and Environment*, *38*(11), 2353–2371. <https://doi.org/10.1111/pce.12555>
- Daloso, D. M., dos Anjos, L., & Fernie, A. R. (2016). Roles of sucrose in guard cell regulation. *New Phytologist*, *211*(3), 809–818. <https://doi.org/10.1111/nph.13950>
- Daloso, D. M., Medeiros, D. B., dos Anjos, L., Yoshida, T., Araújo, W. L., & Fernie, A. R. (2017). Metabolism within the specialized guard cells of plants. *New Phytologist*, *216*(4), 1018–1033. <https://doi.org/10.1111/nph.14823>
- Daloso, D. M., Williams, T. C. R., Antunes, W. C., Pinheiro, D. P., Müller, C., Loureiro, M. E., & Fernie, A. R. (2016). Guard cell-specific upregulation of sucrose synthase 3 reveals that the role of sucrose in stomatal function is primarily energetic. *New Phytologist*, *209*(4), 1470–1483. <https://doi.org/10.1111/nph.13704>
- David, L. C., Lee, S. K., Bruderer, E., Abt, M. R., Fischer-Stettler, M., Tschopp, M. A., Solhaug, E. M., Sanchez, K., & Zeeman, S. C. (2022). BETA-AMYLASE9 is a plastidial nonenzymatic regulator of leaf starch degradation. *Plant Physiology*, *188*(1), 191–207. <https://doi.org/10.1093/plphys/kiab468>
- Davison, C. W., Rahbek, C., & Morueta-Holme, N. (2021). Land-use change and biodiversity: Challenges for assembling evidence on the greatest threat to nature. In *Global Change Biology* (Vol. 27, Issue 21, pp. 5414–5429). John Wiley and Sons Inc. <https://doi.org/10.1111/gcb.15846>
- de Dios, V. R., Loik, M. E., Smith, R., Aspinwall, M. J., & Tissue, D. T. (2016). Genetic variation in circadian regulation of nocturnal stomatal conductance enhances carbon assimilation and growth. *PLANT CELL AND ENVIRONMENT*, *39*(1), 3–11. <https://doi.org/10.1111/pce.12598>

- de Rocher, E. J., Harkins, K. R., Galbraith, D. W., & Bohnert, H. J. (1990). Developmentally Regulated Systemic Endopolyploidy in Succulents with Small Genomes. *Science*, *250*(4977), 99–101.
- Dever, L., Boxall, S. F., Knerova, J., & Hartwell, J. (2015). Transgenic Perturbation of the Decarboxylation Phase of Crassulacean Acid Metabolism Alters Physiology and Metabolism But Has Only a Small Effect on Growth. *PLANT PHYSIOLOGY*, *167*(1), 44–59. <https://doi.org/10.1104/pp.114.251827>
- Dittrich, P., Campbell, W. H., & Black, C. C. (1973). Phosphoenolpyruvate Carboxykinase in Plants Exhibiting Crassulacean Acid Metabolism¹. In *Plant Physiol* 52.
- Dodd, A. N., Borland, A. M., Haslam, R. P., Griffiths, H., & Maxwell, K. (2002). Crassulacean acid metabolism: plastic, fantastic. *JOURNAL OF EXPERIMENTAL BOTANY*, *53*(369), 569–580. <https://doi.org/10.1093/jexbot/53.369.569>
- Dodd, A. N., Griffiths, H., Taybi, T., Cushman, J. C., & Borland, A. M. (2003). Integrating diel starch metabolism with the circadian and environmental regulation of Crassulacean acid metabolism in *Mesembryanthemum crystallinum*. *PLANTA*, *216*(5), 789–797. <https://doi.org/10.1007/s00425-002-0930-2>
- Dubois, M., Gilles, K. A., Hamilton, J. K., Rebers, P. A., & Smith, F. (1956). Colorimetric Method for Determination of Sugars and Related Substances. *Analytical Chemistry*, *28*(3), 350–356. <https://doi.org/10.1021/ac60111a017>
- Eckardt, N. A., Ainsworth, E. A., Bahuguna, R. N., Broadley, M. R., Busch, W., Carpita, N. C., Castrillo, G., Chory, J., Dehaan, L. R., Duarte, C. M., Henry, A., Jagadish, S. V. K., Langdale, J., Leakey, A. D. B., Liao, J. C., Lu, K.-J., Mccann, M. C., Mckay, J. K., Odeny, D. A., ... Zhang, X. (2022). Climate change challenges, plant science solutions. *The Plant Cell*. <https://doi.org/10.1093/plcell/koac303/6759373>
- Edwards, A., & Bowling, D. J. F. (1985). Evidence for a CO₂inhibited proton extrusion pump in the stomatal cells of *Tradescantia virginiana*. *Journal of Experimental Botany*, *36*(1), 91–98. <https://doi.org/10.1093/jxb/36.1.91>

- Eisenach, C., & de Angeli, A. (2017). Ion Transport at the Vacuole during Stomatal Movements. *PLANT PHYSIOLOGY*, *174*(2), 520–530. <https://doi.org/10.1104/pp.17.00130>
- Emmerlich, V., Linka, N., Reinhold, T., Hurth, M. A., Traub, M., Martinoia, E., & Neuhaus, H. E. (2003). The plant homolog to the human sodium/dicarboxylic cotransporter is the vacuolar malate carrier. *PROCEEDINGS OF THE NATIONAL ACADEMY OF SCIENCES OF THE UNITED STATES OF AMERICA*, *100*(19), 11122–11126. <https://doi.org/10.1073/pnas.1832002100>
- Emms, D. M., & Kelly, S. (2019). OrthoFinder: Phylogenetic orthology inference for comparative genomics. *Genome Biology*, *20*(1), 1–14. <https://doi.org/10.1186/s13059-019-1832-y>
- Engler, C., Youles, M., Gruetzner, R., Ehnert, T. M., Werner, S., Jones, J. D. G., Patron, N. J., & Marillonnet, S. (2014). A Golden Gate modular cloning toolbox for plants. *ACS Synthetic Biology*, *3*(11), 839–843. <https://doi.org/10.1021/sb4001504>
- Eurostat. (2020). *Eurostat Arable Land*. <https://ec.europa.eu/eurostat/web/agriculture/data>
- Ewels, P. A., Peltzer, A., Fillinger, S., Patel, H., Alneberg, J., Wilm, A., Garcia, M. U., Di Tommaso, P., & Nahnsen, S. (2020). The nf-core framework for community-curated bioinformatics pipelines. *Nature Biotechnology*, *38*(3), 276–278. <https://doi.org/10.1038/s41587-020-0439-x>
- Fan, Y., Asao, S., Furbank, R. T., von Caemmerer, S., Day, D. A., Tcherkez, G., Sage, T. L., Sage, R. F., & Atkin, O. K. (2022). The crucial roles of mitochondria in supporting C4 photosynthesis. In *New Phytologist* (Vol. 233, Issue 3, pp. 1083–1096). John Wiley and Sons Inc. <https://doi.org/10.1111/nph.17818>
- Farquhar, G. D., & Sharkey, T. D. (1982). STOMATAL CONDUCTANCE AND PHOTOSYNTHESIS. *ANNUAL REVIEW OF PLANT PHYSIOLOGY AND PLANT MOLECULAR BIOLOGY*, *33*, 317–345. <https://doi.org/10.1146/annurev.pp.33.060182.001533> WE - Science Citation Index Expanded (SCI-EXPANDED)

- Fichtner, F., & Lunn, J. E. (2021). The Role of Trehalose 6-Phosphate (Tre6P) in Plant Metabolism and Development. *Annu. Rev. Plant Biol.* 2021, 72, 737–760. <https://doi.org/10.1146/annurev-arplant-050718>
- Figuroa, C. M., Feil, R., Ishihara, H., Watanabe, M., Kölling, K., Krause, U., Höhne, M., Encke, B., Plaxton, W. C., Zeeman, S. C., Li, Z., Schulze, W. X., Hoefgen, R., Stitt, M., & Lunn, J. E. (2016). Trehalose 6-phosphate coordinates organic and amino acid metabolism with carbon availability. *Plant Journal*, 85(3), 410–423. <https://doi.org/10.1111/tpj.13114>
- Flis, A., Mengin, V., Ivakov, A. A., Mugford, S. T., Hubberten, H.-M., Encke, B., Krohn, N., Höhne, M., Feil, R., Hoefgen, R., Lunn, J. E., Millar, A. J., Smith, A. M., Sulpice, R., & Stitt, M. (2018). Multiple circadian clock outputs regulate diel turnover of carbon and nitrogen reserves. In *Plant, Cell & Environment*. <https://doi.org/10.1111/pce.13440>
- Flütsch, S. (2020). Glucose uptake to guard cells via STP transporters provides carbon sources for stomatal opening and plant growth. *Embo Rep.*, e49719, 1–13.
- Flütsch, S., Horrer, D., & Santelia, D. (2022). Starch biosynthesis in guard cells has features of both autotrophic and heterotrophic tissues. *Plant Physiology*, 189(2), 541–556. <https://doi.org/10.1093/plphys/kiac087>
- Flütsch, S., Nigro, A., Conci, F., Fajkus, J., Thalmann, M., Trtílek, M., Panzarová, K., & Santelia, D. (2020). Glucose uptake to guard cells via STP transporters provides carbon sources for stomatal opening and plant growth . *EMBO Reports*, 21(8), 1–13. <https://doi.org/10.15252/embr.201949719>
- Flütsch, S., & Santelia, D. (2021). Mesophyll-derived sugars are positive regulators of light-driven stomatal opening. *New Phytologist*, 230(5), 1754–1760. <https://doi.org/10.1111/nph.17322>
- Flütsch, S., Wang, Y., Takemiya, A., Violet-Chabrand, S. R. M., Klejchová, M., Nigro, A., Hills, A., Lawson, T., Blatt, M. R., & Santelia, D. (2020). Guard cell starch degradation yields glucose for rapid stomatal opening in Arabidopsis. *Plant Cell*, 32(7), 2325–2344. <https://doi.org/10.1105/tpc.18.00802>

- Flynn, J. M., Hubley, R., Goubert, C., Rosen, J., Clark, A. G., Feschotte, C., & Smit, A. F. (2020). RepeatModeler2 for automated genomic discovery of transposable element families. *Proceedings of the National Academy of Sciences of the United States of America*, *117*(17), 9451–9457. <https://doi.org/10.1073/pnas.1921046117>
- Förster, S., Schmidt, L. K., Kopic, E., Anschütz, U., Huang, S., Schlücking, K., Köster, P., Waadt, R., Larrieu, A., Batistič, O., Rodriguez, P. L., Grill, E., Kudla, J., & Becker, D. (2019). Wounding-Induced Stomatal Closure Requires Jasmonate-Mediated Activation of GORK K⁺ Channels by a Ca²⁺ Sensor-Kinase CBL1-CIPK5 Complex. *Developmental Cell*, *48*(1), 87–99.e6. <https://doi.org/10.1016/j.devcel.2018.11.014>
- Franco, A. C., Ball, E., & Liittge, U. (1990). Patterns of gas exchange and organic acid oscillations in tropical trees of the genus *Clusia*. In *Oecologia* (Vol. 85).
- Fujita, T., Noguchi, K., & Terashima, I. (2013). Apoplastic mesophyll signals induce rapid stomatal responses to CO₂ in *Commelina communis*. *New Phytologist*, *199*(2), 395–406. <https://doi.org/10.1111/nph.12261>
- Gabriel, L., Hoff, K. J., Brůna, T., Borodovsky, M., & Stanke, M. (2021). TSEBRA: transcript selector for BRAKER. *BMC Bioinformatics*, *22*(1), 1–12. <https://doi.org/10.1186/s12859-021-04482-0>
- Gao, X. Q., Li, C. G., Wei, P. C., Zhang, X. Y., Chen, J., & Wang, X. C. (2005). The dynamic changes of tonoplasts in guard cells are important for stomatal movement in *Vicia faba*. *PLANT PHYSIOLOGY*, *139*(3), 1207–1216. <https://doi.org/10.1104/pp.105.067520>
- Garcês, H. M. P., Champagne, C. E. M., Townsley, B. T., Park, S., Malhó, R., Pedroso, M. C., Harada, J. J., & Sinha, N. R. (2007). Evolution of asexual reproduction in leaves of the genus *Kalanchoë*. *Proceedings of the National Academy of Sciences of the United States of America*, *104*(39), 15578–15583. <https://doi.org/10.1073/pnas.0704105104>
- Gehrig, H., Gaußmann, O., Marx, H., Schwarzott, D., & Kluge, M. (2001). Molecular phylogeny of the genus *Kalanchoe* (Crassulaceae) inferred from nucleotide sequences of the ITS-1 and ITS-2 regions. *Plant Science*, *160*(5), 827–835. [https://doi.org/10.1016/S0168-9452\(00\)00447-7](https://doi.org/10.1016/S0168-9452(00)00447-7)

- Gehrig, H., Taybi, T., Kluge, M., & Brulfert, J. (1995). Identification of multiple PEPC isogenes in leaves of the facultative crassulacean acid metabolism (CAM) plant *Kalanchoe blossfeldiana* Poelln. cv. Tom Thumb. *FEBS Letters*, *377*(3), 399–402. [https://doi.org/10.1016/0014-5793\(95\)01397-0](https://doi.org/10.1016/0014-5793(95)01397-0)
- Geiger, D., Scherzer, S., Mumm, P., Stange, A., Marten, I., Bauer, H., Ache, P., Matschi, S., Liese, A., Al-Rasheid, K. A. S., Romeis, T., & Hedrich, R. (2009). Activity of guard cell anion channel SLAC1 is controlled by drought-stress signaling kinase-phosphatase pair. *Proceedings of the National Academy of Sciences*, *106*(50), 21425–21430. <https://doi.org/10.1073/pnas.0912021106>
- Gilman, I. S., Moreno-Villena, J. J., Lewis, Z. R., Goolsby, E. W., & Edwards, E. J. (2022). Gene co-expression reveals the modularity and integration of C4 and CAM in *Portulaca*. *Plant Physiology*, *189*(2), 735–753. <https://doi.org/10.1093/plphys/kiac116>
- Goh, C.-H., Oku, T., & Shimazaki, K.-I. (1997). Photosynthetic properties of adaxial guard cells from *Vicia* leaves. *Plant Science*, *127*(2), 149–159. [https://doi.org/10.1016/S0168-9452\(97\)00122-2](https://doi.org/10.1016/S0168-9452(97)00122-2)
- Goodstein, D. M., Shu, S., Howson, R., Neupane, R., Hayes, R. D., Fazo, J., Mitros, T., Dirks, W., Hellsten, U., Putnam, N., & Rokhsar, D. S. (2012). Phytozome: A comparative platform for green plant genomics. *Nucleic Acids Research*, *40*(D1), 1178–1186. <https://doi.org/10.1093/nar/gkr944>
- Gotoh, E., Oiawamoto, K., Inoue, S., Shimazaki, K., & Doi, M. (2018). Stomatal response to blue light in crassulacean acid metabolism plants *Kalanchoe pinnata* and *Kalanchoe daigremontiana*. *Journal of Experimental Botany*, 1–8. <https://doi.org/10.1093/jxb/ery450>
- Gotow, K., Taylor, S., & Zeiger, E. (1988). Photosynthetic carbon fixation in guard cell protoplasts of *Vicia faba* L.: Evidence from radiolabel experiments. *Plant Physiology*, *86*, 700–705.
- Gregory, F. G., Spear, I., & Thimann, K. v. (1954). The Interrelation between CO₂ Metabolism and Photoperiodism in *Kalanchoë*. *Plant Physiology*, *29*(3), 220–229. <https://doi.org/10.1104/pp.29.3.220>

- Griffiths, H., Cousins, A. B., Badger, M. R., & Von Caemmerer, S. (2007). Discrimination in the dark. Resolving the interplay between metabolic and physical constraints to phosphoenolpyruvate carboxylase activity during the crassulacean acid metabolism cycle. *Plant Physiology*, *143*(2), 1055–1067. <https://doi.org/10.1104/pp.106.088302>
- Griffiths, H., Robe, W. E., Girnus, J., & Maxwell, K. (2008). Leaf succulence determines the interplay between carboxylase systems and light use during Crassulacean acid metabolism in *Kalanchoë* species. *Journal of Experimental Botany*, *59*(7), 1851–1861. <https://doi.org/10.1093/jxb/ern085>
- Gross, S. M., Martin, J. A., Simpson, J., Abraham-Juarez, M. J., Wang, Z., & Visel, A. (2013). De novo transcriptome assembly of drought tolerant CAM plants, *Agave deserti* and *Agave tequilana*. *BMC Genomics*, *14*(1), 563. <https://doi.org/10.1186/1471-2164-14-563>
- Guan, D., Guan, D., McCarthy, S. A., Wood, J., Howe, K., Wang, Y., Durbin, R., & Durbin, R. (2020). Identifying and removing haplotypic duplication in primary genome assemblies. *Bioinformatics*, *36*(9), 2896–2898. <https://doi.org/10.1093/bioinformatics/btaa025>
- Haider, M. S., Barnes, J. D., Cushman, J. C., & Borland, A. M. (2012). A CAM- and starch-deficient mutant of the facultative CAM species *Mesembryanthemum crystallinum* reconciles sink demands by repartitioning carbon during acclimation to salinity. *JOURNAL OF EXPERIMENTAL BOTANY*, *63*(5), 1985–1996. <https://doi.org/10.1093/jxb/err412>
- Han, C., Hua, W., Li, J., Qiao, Y., Yao, L., Hao, W., Li, R., Fan, M., de Jaeger, G., Yang, W., & Bai, M. Y. (2022). TOR promotes guard cell starch degradation by regulating the activity of β -AMYLASE1 in *Arabidopsis*. *The Plant Cell*, *34*(3), 1038–1053. <https://doi.org/10.1093/plcell/koab307>
- Han, S., Bi, D., Yi, R., Ding, H., Wu, L., & Kan, X. (2022). Plastome evolution of *Aeonium* and *Monanthes* (Crassulaceae): insights into the variation of plastomic tRNAs, and the patterns of codon usage and aversion. *Planta*, *256*(2). <https://doi.org/10.1007/s00425-022-03950-y>
- Hartwell, J., Dever, L. V., & Boxall, S. F. (2016). Emerging model systems for functional genomics analysis of Crassulacean acid metabolism. *Current Opinion in Plant Biology*, *31*, 100–108. <https://doi.org/10.1016/j.pbi.2016.03.019>

- Hartwell, J., Gill, A., Nimmo, G. A., Wilkins, M. B., Jenkins, G. I., & Nimmo, H. G. (1999). Phosphoenolpyruvate carboxylase kinase is a novel protein kinase regulated at the level of expression. *The Plant Journal*, *20*(3), 333–342. <https://doi.org/10.1046/j.1365-313x.1999.00609.x>
- Haruta, M., Burch, H. L., Nelson, R. B., Barrett-Wilt, G., Kline, K. G., Mohsin, S. B., Young, J. C., Otegui, M. S., & Sussman, M. R. (2010). Molecular characterization of mutant Arabidopsis plants with reduced plasma membrane proton pump activity. *Journal of Biological Chemistry*, *285*(23), 17918–17929. <https://doi.org/10.1074/jbc.M110.101733>
- Hashimoto, M., Negi, J., Young, J., Israelsson, M., Schroeder, J. I., & Iba, K. (2006). Arabidopsis HT1 kinase controls stomatal movements in response to CO₂. *Nature Cell Biology*, *8*(4), 391–397. <https://doi.org/10.1038/ncb1387>
- Hausler, R. E., Baur, B., Scharte, J., Teichmann, T., Eicks, M., Fischer, K. L., Flugge, U. I., Schubert, S., Weber, A., & Fischer, K. (2000). Plastidic metabolite transporters and their physiological functions in the inducible crassulacean acid metabolism plant *Mesembryanthemum crystallinum*. *PLANT JOURNAL*, *24*(3), 285–296. <https://doi.org/10.1046/j.1365-313x.2000.00876.x>
- Hayashi, M., Inoue, S. I., Takahashi, K., & Kinoshita, T. (2011). Immunohistochemical detection of blue light-induced phosphorylation of the plasma membrane H⁺-ATPase in stomatal guard cells. *Plant and Cell Physiology*, *52*(7), 1238–1248. <https://doi.org/10.1093/pcp/pcr072>
- Hedrich, R. (2012). Ion Channels in Plants. *Physiological Reviews*, *92*(4), 1777–1811. <https://doi.org/10.1152/physrev.00038.2011>
- Hedrich, R., Kurkdjian, A., Guern, J., & Flugge, U. I. (1989). Comparative studies on the electrical properties of the H⁺ translocating ATPase and pyrophosphatase of the vacuolar-lysosomal compartment. *EMBO Journal*, *8*(10), 2835–2841. <https://doi.org/10.1002/j.1460-2075.1989.tb08430.x>
- Hedrich, R., Marten, I., Lohse, G., Dietrich, P., Winter, H., Lohaus, G., & Heldt, H. -W. (1994). Malate-sensitive anion channels enable guard cells to sense changes in the ambient CO₂

- concentration. *The Plant Journal*, 6(5), 741–748. <https://doi.org/10.1046/j.1365-313X.1994.6050741.x>
- Hedrich, R., Raschke, K., & Stitt, M. (1985). A role for fructose 2,6-bisphosphate in regulating carbohydrate metabolism in guard cells. *Plant Physiol.*, 79, 977–982.
- Heyduk, K., McAssey, E., & Leebens-Mack, J. (2022). Differential timing of gene expression and recruitment in independent origins of CAM in the Agavoideae (Asparagaceae). *New Phytologist*, 235(5), 2111–2126. <https://doi.org/10.1111/nph.18267>
- Heyduk, K., Ray, J. N., Ayyampalayam, S., Moledina, N., Borland, A., Harding, S. A., Tsai, C. J., & Leebens-Mack, J. (2019). Shared expression of crassulacean acid metabolism (CAM) genes pre-dates the origin of CAM in the genus *Yucca*. *Journal of Experimental Botany*, 70(22), 6597–6609. <https://doi.org/10.1093/jxb/erz105>
- Hiyama, A., Takemiya, A., Munemasa, S., Okuma, E., Sugiyama, N., Tada, Y., Murata, Y., & Shimazaki, K. I. (2017). Blue light and CO₂ signals converge to regulate light-induced stomatal opening. *Nature Communications*, 8(1). <https://doi.org/10.1038/s41467-017-01237-5>
- Holtum, J. A. M., Smith, J. A. C., & Neuhaus, H. E. (2005). Intracellular transport and pathways of carbon flow in plants with crassulacean acid metabolism. *Functional Plant Biology*, 32(5), 429–449. <https://doi.org/10.1071/FP04189>
- Hong-Hermesdorf, A., Brück, A., Grüber, A., Grüber, G., & Schumacher, K. (2006). A WNK kinase binds and phosphorylates V-ATPase subunit C. *FEBS Letters*, 580(3), 932–939. <https://doi.org/10.1016/j.febslet.2006.01.018>
- Horrer, D., Flütsch, S., Pazmino, D., Matthews, J. S. A., Thalmann, M., Nigro, A., Leonhardt, N., Lawson, T., & Santelia, D. (2016). Blue light induces a distinct starch degradation pathway in guard cells for stomatal opening. *Current Biology*, 26(3), 362–370. <https://doi.org/10.1016/j.cub.2015.12.036>
- Hu, R., Zhang, J., Jawdy, S., Sreedasyam, A., Lipzen, A., Wang, M., Ng, V., Daum, C., Keymanesh, K., Liu, D., Lu, H., Ranjan, P., Chen, J.-G., Muchero, W., Tschaplinski, T. J., Tuskan, G. A., Schmutz, J., & Yang, X. (2022). Comparative genomics analysis of drought response

- between obligate CAM and C3 photosynthesis plants. *Journal of Plant Physiology*, 153791. <https://doi.org/https://doi.org/10.1016/j.jplph.2022.153791>
- Hudspeth, R. L., Grula, J. W., Dai, Z., Edwards, G. E., & Ku, M. S. B. (1992). Expression of Maize Phosphoenolpyruvate Carboxylase in Transgenic Tobacco Effects on Biochemistry and Physiology. In *Plant Physiol* (Vol. 98).
- Inoue, S., & Kinoshita, T. (2017). Blue Light Regulation of Stomatal Opening and the Plasma Membrane H⁺ -ATPase. *Plant Physiology*, 174(2), 531–538. <https://doi.org/10.1104/pp.17.00166>
- Jackman, S. D., Vandervalk, B. P., Mohamadi, H., Chu, J., Yeo, S., Hammond, S. A., Jahesh, G., Khan, H., Coombe, L., Warren, R. L., & Birol, I. (2017). ABySS 2 . 0 : Resource-Efficient Assembly of Large Genomes using a Bloom Filter Effect of Bloom Filter False Positive Rate. *Genome Research*, 27, 768–777. <https://doi.org/10.1101/gr.214346.116>. Freely
- Jannat, R., Uraji, M., Morofuji, M., Hossain, M. A., Islam, M. M., Nakamura, Y., Mori, I. C., & Murata, Y. (2011). The roles of catalase2 in abscisic acid signaling in arabidopsis guard cells. *Bioscience, Biotechnology and Biochemistry*, 75(10), 2034–2036. <https://doi.org/10.1271/bbb.110344>
- Jezek, M., & Blatt, M. R. (2017). The membrane transport system of the guard cell and its integration for stomatal dynamics. *Plant Physiology*, 174(2), 487–519. <https://doi.org/10.1104/pp.16.01949>
- Jin, J. J., Yu, W. bin, Yang, J. B., Song, Y., Depamphilis, C. W., Yi, T. S., & Li, D. Z. (2020). GetOrganelle: A fast and versatile toolkit for accurate de novo assembly of organelle genomes. *Genome Biology*, 21(1). <https://doi.org/10.1186/s13059-020-02154-5>
- Jin, X., Wang, R.-S., Zhu, M., Jeon, B. W., Albert, R., Chen, S., & Assmann, S. M. (2013). Abscisic acid-responsive guard cell metabolomes of Arabidopsis wild-type and gpa1 G-protein mutants. *Plant Cell*, 25(12), 4789–4811. <https://doi.org/10.1105/tpc.113.119800>
- Jung, M., Reichstein, M., Margolis, H. A., Cescatti, A., Richardson, A. D., Arain, M. A., Arneeth, A., Bernhofer, C., Bonal, D., Chen, J., Gianelle, D., Gobron, N., Kiely, G., Kutsch, W., Lasslop, G., Law, B. E., Lindroth, A., Merbold, L., Montagnani, L., ... Williams, C. (2011).

- Global patterns of land-atmosphere fluxes of carbon dioxide, latent heat, and sensible heat derived from eddy covariance, satellite, and meteorological observations. *Journal of Geophysical Research: Biogeosciences*, 116(3). <https://doi.org/10.1029/2010JG001566>
- Kalyaanamoorthy, S., Minh, B. Q., Wong, T. K. F., von Haeseler, A., & Jermin, L. S. (2017). ModelFinder: Fast model selection for accurate phylogenetic estimates. *Nature Methods*, 14(6), 587–589. <https://doi.org/10.1038/nmeth.4285>
- Katoh, K., & Standley, D. M. (2013). MAFFT multiple sequence alignment software version 7: Improvements in performance and usability. *Molecular Biology and Evolution*, 30(4), 772–780. <https://doi.org/10.1093/molbev/mst010>
- Kebeish, R., Niessen, M., Oksaksin, M., Blume, C., & Peterhaensel, C. (2012). Constitutive and dark-induced expression of *Solanum tuberosum* phosphoenolpyruvate carboxylase enhances stomatal opening and photosynthetic performance of *Arabidopsis thaliana*. *Biotechnology and Bioengineering*, 109(2), 536–544. <https://doi.org/10.1002/bit.23344>
- Keb-Llanes, M., González, G., Chi-Manzanero, B., & Infante, D. (2002). A rapid and simple method for small-scale DNA extraction in Agavaceae and other tropical plants. *Plant Molecular Biology Reporter*, 20(3). <https://doi.org/10.1007/BF02782465>
- Keenan, T. F., Hollinger, D. Y., Bohrer, G., Dragoni, D., Munger, J. W., Schmid, H. P., & Richardson, A. D. (2013). Increase in forest water-use efficiency as atmospheric carbon dioxide concentrations rise. *Nature*, 499(7458), 324–327. <https://doi.org/10.1038/nature12291>
- Kelley, C. P., Mohtadi, S., Cane, M. A., Seager, R., & Kushnir, Y. (2015). Climate change in the Fertile Crescent and implications of the recent Syrian drought. *Proceedings of the National Academy of Sciences of the United States of America*, 112(11), 3241–3246. <https://doi.org/10.1073/pnas.1421533112>
- Kelly, G., Moshelion, M., David-Schwartz, R., Halperin, O., Wallach, R., Attia, Z., Belausov, E., & Granot, D. (2013). Hexokinase mediates stomatal closure. *Plant Journal*, 75(6), 977–988. <https://doi.org/10.1111/tpj.12258>

- Kinoshita, A., & Richter, R. (2021). Genetic and molecular basis of floral induction in *Arabidopsis thaliana*. In *Journal of Experimental Botany* (Vol. 71, Issue 9, pp. 2490–2504). Oxford University Press. <https://doi.org/10.1093/JXB/ERAA057>
- Kinoshita, T., Doi, M., Suetsugu, N., Kagawa, T., Wada, M., & Shimazaki, K. (2001). phot1 and phot2 mediate blue light regulation of stomatal opening. *NATURE*, *414*(6864), 656–660. <https://doi.org/10.1038/414656a>
- Kinoshita, T., & Shimazaki, K. (1999). Blue light activates the plasma membrane H⁺-ATPase by phosphorylation of the C-terminus in stomatal guard cells. *EMBO Journal*, *18*(20), 5548–5558.
- Kinoshita, T., & Shimazaki, K. ichiro. (2002). Biochemical evidence for the requirement of 14-3-3 protein binding in activation of the guard-cell plasma membrane H⁺-ATPase by blue light. *Plant and Cell Physiology*, *43*(11), 1359–1365. <https://doi.org/10.1093/pcp/pcf167>
- Klein, D.P., Shtein, R., Nusbaumer, L., & Callmander, M. W. (2021). *Kalanchoe darainensis* (Crassulaceae), a new species from northeastern Madagascar. *Candollea*, *76*(1). <https://doi.org/10.15553/c2021v761a12>
- Kluge, M., Brulfert, J., Ravelomanana, D., Lipp, J., & Ziegler, H. (1991). Crassulacean acid metabolism in *Kalanchoë* species collected in various climatic zones of Madagascar: a survey by $\delta^{13}\text{C}$ analysis. *Oecologia*, *88*(3), 407–414. <https://doi.org/10.1007/BF00317586>
- Kogami, H., Shono, M., Koike, T., Yanagisawa, S., Izui, K., Sentoku, N., Tanifuji, S., Uchimiya, H., & Toki, S. (1994). Molecular and physiological evaluation of transgenic tobacco plants expressing a maize phosphoenolpyruvate carboxylase gene under the control of the cauliflower mosaic virus 35S promoter. *Transgenic Research*, *3*(5), 287–296. <https://doi.org/10.1007/BF01973588>
- Kolmogorov, M., Yuan, J., Lin, Y., & Pevzner, P. A. (2019). Assembly of long, error-prone reads using repeat graphs. *Nature Biotechnology*, *37*(5), 540–546. <https://doi.org/10.1038/s41587-019-0072-8>

- Kondo, A., Shibata, K., Sakurai, T., Tawata, M., & Funaguma, T. (2006). Intracellular positioning of nucleus and mitochondria with clumping of chloroplasts in the succulent CAM plant *Kalanchoe blossfeldiana*: an investigation using fluorescence microscopy. *PLANT MORPHOLOGY*, *18*(1), 69–73. <https://doi.org/10.5685/plmorphol.18.69>
- Kong, W., Yoo, M. J., Zhu, D., Noble, J. D., Kelley, T. M., Li, J., Kirst, M., Assmann, S. M., & Chen, S. (2020). Molecular changes in *Mesembryanthemum crystallinum* guard cells underlying the C3 to CAM transition. *Plant Molecular Biology*, *103*(6), 653–667. <https://doi.org/10.1007/s11103-020-01016-9>
- Koreeda, S., & Kanai, R. (1997). Induction of glucose 6-phosphate transport activity in chloroplasts of *Mesembryanthemum crystallinum* by the C-3-CAM transition. *PLANT AND CELL PHYSIOLOGY*, *38*(8), 895–901. <https://doi.org/10.1093/oxfordjournals.pcp.a029249>
- Koreeda, S., Nozawa, A., Okada, Y., Takashi, K., Azad, M. A. K., Ohnishi, J., Nishiyama, Y., & Tozawa, Y. (2013). Characterization of the Plastidic Phosphate Translocators in the Inducible Crassulacean Acid Metabolism Plant *Mesembryanthemum crystallinum*. *BIOSCIENCE BIOTECHNOLOGY AND BIOCHEMISTRY*, *77*(7), 1511–1516. <https://doi.org/10.1271/bbb.130174>
- Kovermann, P., Meyer, S., Hortensteiner, S., Picco, C., Scholz-Starke, J., Ravera, S., Lee, Y., & Martinoia, E. (2007). The *Arabidopsis* vacuolar malate channel is a member of the ALMT family. *PLANT JOURNAL*, *52*(6), 1169–1180. <https://doi.org/10.1111/j.1365-313X.2007.03367.x>
- Kriventseva, E. V., Kuznetsov, D., Tegenfeldt, F., Manni, M., Dias, R., Simão, F. A., & Zdobnov, E. M. (2019). OrthoDB v10: Sampling the diversity of animal, plant, fungal, protist, bacterial and viral genomes for evolutionary and functional annotations of orthologs. *Nucleic Acids Research*, *47*(D1), D807–D811. <https://doi.org/10.1093/nar/gky1053>
- Ku, M. S. B., Agarie, S., Nomura, M., Fukayama, H., Tsuchida, H., Ono, K., Hirose, S., Toki, S., Miyao, M., & Matsuoka, M. (1999). High-level expression of maize phosphoenolpyruvate carboxylase in transgenic rice plants. In *NATURE BIOTECHNOLOGY* (Vol. 17). <http://biotech.nature.com>

- Lasceve, G., Leymarie, J., & Vavasseur, A. (1997). Alterations in light-induced stomatal opening in a starch-deficient mutant of *Arabidopsis thaliana* L deficient in chloroplast phosphoglucomutase activity. *PLANT CELL AND ENVIRONMENT*, *20*(3), 350–358. <https://doi.org/10.1046/j.1365-3040.1997.d01-71.x> WE - Science Citation Index Expanded (SCI-EXPANDED)
- Lawson, T., & Blatt, M. R. (2014). Stomatal Size, Speed, and Responsiveness Impact on Photosynthesis and Water Use Efficiency. *PLANT PHYSIOLOGY*, *164*(4), 1556–1570. <https://doi.org/10.1104/pp.114.237107>
- Lawson, T., Lefebvre, S., Baker, N. R., Morison, J. I. L., & Raines, C. A. (2008). Reductions in mesophyll and guard cell photosynthesis impact on the control of stomatal responses to light and CO₂. *Journal of Experimental Botany*, *59*(13), 3609–3619. <https://doi.org/10.1093/jxb/ern211>
- Lawson, T., & Matthews, J. (2020). Guard Cell Metabolism and Stomatal Function. *Annual Review of Plant Biology*, *71*, 273–302. <https://doi.org/10.1146/annurev-arplant-050718-100251>
- Lawson, T., Oxborough, K., Morison, J. I. L., & Baker, N. R. (2003). The responses of guard and mesophyll cell photosynthesis to CO₂, O₂, light, and water stress in a range of species are similar. *Journal of Experimental Botany*, *54*(388), 1743–1752. <https://doi.org/10.1093/jxb/erg186>
- Lawson, T., Simkin, A. J., Kelly, G., & Granot, D. (2014). Mesophyll photosynthesis and guard cell metabolism impacts on stomatal behaviour. *New Phytologist*, *203*(4), 1064–1081. <https://doi.org/10.1111/nph.12945>
- Lawson, T., von Caemmerer, S., & Baroli, I. (2011). *Photosynthesis and Stomatal Behaviour BT - Progress in Botany 72* (U. E. Lüttge, W. Beyschlag, B. Büdel, & D. Francis, Eds.; pp. 265–304). Springer Berlin Heidelberg. https://doi.org/10.1007/978-3-642-13145-5_11
- Lee, M., Choi, Y., Burla, B., Kim, Y. Y., Jeon, B., Maeshima, M., Yoo, J. Y., Martinoia, E., & Lee, Y. (2008). The ABC transporter AtABCB14 is a malate importer and modulates stomatal response to CO₂. *NATURE CELL BIOLOGY*, *10*(10), 1217–1223. <https://doi.org/10.1038/ncb1782> WE - Science Citation Index Expanded (SCI-EXPANDED)

- Leitch, I. J., & Dodsworth, S. (2017). Endopolyploidy in Plants. In *eLS* (pp. 1–10). <https://doi.org/https://doi.org/10.1002/9780470015902.a0020097.pub2>
- Leonhardt, N., Kwak, J. M., Robert, N., Waner, D., Leonhardt, G., & Schroeder, J. I. (2004). Microarray expression analyses of Arabidopsis guard cells and isolation of a recessive abscisic acid hypersensitive protein phosphatase 2C mutant. *PLANT CELL*, *16*(3), 596–615. <https://doi.org/10.1105/tpc.019000>
- Lerman, J. C., & Queiroz, O. (1974). Carbon Fixation and Isotope Discrimination by a Crassulacean Plant: Dependence on the Photoperiod. *Science*, *183*(4130), 1207 LP – 1209. <https://doi.org/10.1126/science.183.4130.1207>
- Leverett, A., Hartzell, S., Winter, K., Garcia, M., Aranda, J., Virgo, A., Smith, J. A., Focht, P., Rasmussen-Arda, A., Willats, W. G. T., Cowan-Turner, D., & Borland, A. M. (2022). Dissecting Succulence : Crassulacean Acid Metabolism and Hydraulic Capacitance are Independent Adaptations in Clusia Leaves. *BioRxiv*.
- Lim, S. D., Lee, S., Choi, W.-G., Yim, W. C., & Cushman, J. C. (2019). Laying the Foundation for Crassulacean Acid Metabolism (CAM) Biodesign: Expression of the C4 Metabolism Cycle Genes of CAM in Arabidopsis. *Frontiers in Plant Science*, *10*. <https://www.frontiersin.org/articles/10.3389/fpls.2019.00101>
- Lim, S. L., Flütsch, S., Liu, J., Distefano, L., Santelia, D., & Lim, B. L. (2022). Arabidopsis guard cell chloroplasts import cytosolic ATP for starch turnover and stomatal opening. *Nature Communications*, *13*(1). <https://doi.org/10.1038/s41467-022-28263-2>
- Lima, V. F., Erban, A., Daubermann, A. G., Freire, F. B. S., Porto, N. P., Cândido-Sobrinho, S. A., Medeiros, D. B., Schwarzländer, M., Fernie, A. R., dos Anjos, L., Kopka, J., & Daloso, D. M. (2021). Establishment of a GC-MS-based ¹³C-positional isotopomer approach suitable for investigating metabolic fluxes in plant primary metabolism. *Plant Journal*, *108*(4), 1213–1233. <https://doi.org/10.1111/tpj.15484>
- Liu, D., Chen, M., Mendoza, B., Cheng, H., Hu, R., Li, L., Trinh, C. T., Tuskan, G. A., & Yang, X. (2019). CRISPR/Cas9-mediated targeted mutagenesis for functional genomics research of crassulacean acid metabolism plants. *Journal of Experimental Botany*, *70*(22), 6621–6629. <https://doi.org/10.1093/jxb/erz415>

- Lloyd, F. E. (1908). *The physiology of Stomata*. Carnegie Institute.
- Loureiro, J., Rodriguez, E., Dolezel, J., & Santos, C. (2007). Two new nuclear isolation buffers for plant DNA flow cytometry: a test with 37 species. *Annals of Botany*, *100*(4), 875–888. <https://doi.org/10.1093/aob/mcm152>
- Love, M. I., Huber, W., & Anders, S. (2014). Moderated estimation of fold change and dispersion for RNA-seq data with DESeq2. *Genome Biology*, *15*(12), 1–21. <https://doi.org/10.1186/s13059-014-0550-8>
- Lüttge, U. (1988). Day-night changes of citric-acid levels in crassulacean acid metabolism: phenomenon and ecophysiological significance. *Plant, Cell & Environment*, *11*(6), 445–451. <https://doi.org/https://doi.org/10.1111/j.1365-3040.1988.tb01782.x>
- Lüttge, U. (2010). *Clusia: A Woody Neotropical Genus of Remarkable Plasticity and Diversity*. Springer Berlin Heidelberg. <https://books.google.co.uk/books?id=WMdQcgAACAAJ>
- Luttge, U., Smith, J., Marigo, G., & Osmond, C. B. (1981). Energetics Of Malate Accumulation In The Vacuoles Of Kalanchoe Tubiflora. *FEBS* *126*(1).
- MacRobbie, E. A. C., & Kurup, S. (2007). Signalling mechanisms in the regulation of vacuolar ion release in guard cells. *New Phytologist*, *175*(4), 630–640. <https://doi.org/10.1111/j.1469-8137.2007.02131.x>
- Madhavan, S., & Smith, B. N. (1982). Localization of ribulose biphosphate carboxylase in the guard cells by an indirect, immunofluorescence technique. *Plant Physiol*, *69*, 273–277.
- Maleckova, E. (2020). *Regulation of crassulacean acid metabolism (CAM) in the facultative CAM species Talinum triangulare*. Dissertation, Düsseldorf, Heinrich-Heine-Universität, 2020.
- Maleckova, E., Brilhaus, D., Wrobel, T. J., & Weber, A. P. M. (2019). Transcript and metabolite changes during the early phase of abscisic acid-mediated induction of crassulacean acid metabolism in *Talinum triangulare*. *Journal of Experimental Botany*, *70*(22), 6581–6596. <https://doi.org/10.1093/jxb/erz189>

- Males, J., & Griffiths, H. (2017). Stomatal Biology of CAM Plants. *Plant Physiology*, *174*(2), 550–560. <https://doi.org/10.1104/pp.17.00114>
- Manni, M., Berkeley, M. R., Seppey, M., Simão, F. A., & Zdobnov, E. M. (2021). BUSCO Update: Novel and Streamlined Workflows along with Broader and Deeper Phylogenetic Coverage for Scoring of Eukaryotic, Prokaryotic, and Viral Genomes. *Molecular Biology and Evolution*, *38*(10), 4647–4654. <https://doi.org/10.1093/molbev/msab199>
- Marçais, G., & Kingsford, C. (2011). A fast, lock-free approach for efficient parallel counting of occurrences of k-mers. *Bioinformatics*, *27*(6), 764–770. <https://doi.org/10.1093/bioinformatics/btr011>
- Marigo, G., Ball, E., Lüttge, U., & Smith, J. A. C. (1982). Use of the DMO Technique for the Study of Relative Changes of Cytoplasmic pH in Leaf Cells in Relation to CAM. *Zeitschrift Für Pflanzenphysiologie*, *108*(3), 223–233. [https://doi.org/10.1016/s0044-328x\(82\)80122-0](https://doi.org/10.1016/s0044-328x(82)80122-0)
- Martinoia, E., Maeshima, M., & Neuhaus, H. E. (2007). Vacuolar transporters and their essential role in plant metabolism. *Journal of Experimental Botany*, *58*(1), 83–102. <https://doi.org/10.1093/jxb/erl183>
- Matthews, J. S. A., Vialet-Chabrand, S. R. M., & Lawson, T. (2017). Diurnal Variation in Gas Exchange: The Balance between Carbon Fixation and Water Loss. *PLANT PHYSIOLOGY*, *174*(2), 614–623. <https://doi.org/10.1104/pp.17.00152> WE - Science Citation Index Expanded (SCI-EXPANDED)
- Mawson, B. T. (1993). Modulation of photosynthesis and respiration in guard and mesophyll cell protoplasts by oxygen concentration. *Plant, Cell & Environment*, *16*(2), 207–214. <https://doi.org/10.1111/j.1365-3040.1993.tb00862.x>
- McAdam, S. A. M., & Brodribb, T. J. (2012). Stomatal innovation and the rise of seed plants. *Ecology Letters*, *15*(1), 1–8. <https://doi.org/10.1111/j.1461-0248.2011.01700.x>
- McAusland, L., Vialet-Chabrand, S., Davey, P., Baker, N. R., Brendel, O., & Lawson, T. (2016). Effects of kinetics of light-induced stomatal responses on photosynthesis and water-use efficiency. *NEW PHYTOLOGIST*, *211*(4), 1209–1220. <https://doi.org/10.1111/nph.14000>

- McLachlan, D. H., Lan, J., Geilfus, C. M., Dodd, A. N., Larson, T., Baker, A., Hörak, H., Kollist, H., He, Z., Graham, I., Mickelbart, M. v., & Hetherington, A. M. (2016). The Breakdown of Stored Triacylglycerols is Required during Light-Induced Stomatal Opening. *Current Biology*, *26*(5), 707–712. <https://doi.org/10.1016/j.cub.2016.01.019>
- Medeiros, D. B., Perez Souza, L., Antunes, W. C., Araújo, W. L., Daloso, D. M., & Fernie, A. R. (2018). Sucrose breakdown within guard cells provides substrates for glycolysis and glutamine biosynthesis during light-induced stomatal opening. *Plant Journal*, *94*(4), 583–594. <https://doi.org/10.1111/tpj.13889>
- Meinhard, M., & Schnabl, H. (2001). *Fusicoccin- and light-induced activation and in vivo phosphorylation of phosphoenolpyruvate carboxylase in vicia guard cell protoplasts*. *160*, 635–646.
- Merlot, S., Leonhardt, N., Fenzi, F., Valon, C., Costa, M., Piette, L., Vavasseur, A., Genty, B., Boivin, K., Müller, A., Giraudat, J., & Leung, J. (2007). Constitutive activation of a plasma membrane H⁺-ATPase prevents abscisic acid-mediated stomatal closure. *EMBO Journal*, *26*(13), 3216–3226. <https://doi.org/10.1038/sj.emboj.7601750>
- Messerschmid, T. F. E., Klein, J. T., Kadereit, G., & Kadereit, J. W. (2020). Linnaeus's folly – phylogeny, evolution and classification of *Sedum* (Crassulaceae) and Crassulaceae subfamily Sempervivoideae. *Taxon*, *69*(5), 892–926. <https://doi.org/10.1002/tax.12316>
- Messinger, S. M. (2006). Evidence for Involvement of Photosynthetic Processes in the Stomatal Response to CO₂. *Plant Physiology*, *140*(2), 771–778. <https://doi.org/10.1104/pp.105.073676>
- Ming, R., VanBuren, R., Wai, C. M., Tang, H., Schatz, M. C., Bowers, J. E., Lyons, E., Wang, M. L., Chen, J., Biggers, E., Zhang, J., Huang, L., Zhang, L., Miao, W., Zhang, J., Ye, Z., Miao, C., Lin, Z., Wang, H., ... Yu, Q. (2015). The pineapple genome and the evolution of CAM photosynthesis. *Nature Genetics*, *47*(12), 1435–1442. <https://doi.org/10.1038/ng.3435>
- Minh, B. Q., Schmidt, H. A., Chernomor, O., Schrempf, D., Woodhams, M. D., von Haeseler, A., Lanfear, R., & Teeling, E. (2020). IQ-TREE 2: New Models and Efficient Methods for Phylogenetic Inference in the Genomic Era. *Molecular Biology and Evolution*, *37*(5), 1530–1534. <https://doi.org/10.1093/molbev/msaa015>

- Misra, B. B., de Armas, E., Tong, Z. H., & Chen, S. X. (2015). Metabolomic Responses of Guard Cells and Mesophyll Cells to Bicarbonate. *PLOS ONE*, *10*(12). <https://doi.org/10.1371/journal.pone.0144206>
- Molina-Hidalgo, F. J., Vazquez-Vilar, M., D'Andrea, L., Demurtas, O. C., Fraser, P., Giuliano, G., Bock, R., Orzáez, D., & Goossens, A. (2021). Engineering Metabolism in Nicotiana Species: A Promising Future. *Trends in Biotechnology*, *39*(9), 901–913. <https://doi.org/https://doi.org/10.1016/j.tibtech.2020.11.012>
- Moraes, T. A., Mengin, V., Peixoto, B., Encke, B., Krohn, N., Höhne, M., Krause, U., & Stitt, M. (2022). The circadian clock mutant *lhy cca1 elf3* paces starch mobilization to dawn despite severely disrupted circadian clock function. *Plant Physiology*, *189*(4), 2332–2356. <https://doi.org/10.1093/plphys/kiac226>
- Moreno-Villena, J. J., Zhou, H., Gilman, I. S., Tausta, S. L., Cheung, C. Y. M., & Edwards, E. J. (2022). Spatial resolution of an integrated C₄ +CAM photosynthetic metabolism. In *Sci. Adv* (Vol. 8).
- Mort, M. E., O'Leary, T. R., Carrillo-Reyes, P., Nowell, T., Archibald, J. K., & Randle, C. P. (2010). Phylogeny and evolution of Crassulaceae: past, present, and future. *Schumannia*, *6*, 69–86.
- Moseley, R. C., Tuskan, G. A., & Yang, X. (2019). Comparative genomics analysis provides new insight into molecular basis of stomatal movement in *Kalanchoë fedtschenkoi*. *Frontiers in Plant Science*, *10*. <https://doi.org/10.3389/fpls.2019.00292>
- Mott, K. A., Sibbersen, E. D., & Shope, J. C. (2008). The role of the mesophyll in stomatal responses to light and CO₂. *PLANT CELL AND ENVIRONMENT*, *31*(9), 1299–1306. <https://doi.org/10.1111/j.1365-3040.2008.01845.x>
- Nelson, E. A., & Sage, R. F. (2008). Functional constraints of CAM leaf anatomy: Tight cell packing is associated with increased CAM function across a gradient of CAM expression. *Journal of Experimental Botany*, *59*(7), 1841–1850. <https://doi.org/10.1093/jxb/erm346>

- Neuhaus, H. E., & Schulte, N. (1996). Starch degradation in chloroplasts isolated from C-3 or CAM (crassulacean acid metabolism)-induced *Mesembryanthemum crystallinum* L. *BIOCHEMICAL JOURNAL*, *318*, 945–953. <https://doi.org/10.1042/bj3180945>
- Ni, P., Huang, N., Nie, F., Zhang, J., Zhang, Z., Wu, B., Bai, L., Liu, W., Xiao, C. le, Luo, F., & Wang, J. (2021). Genome-wide detection of cytosine methylations in plant from Nanopore data using deep learning. *Nature Communications*, *12*(1). <https://doi.org/10.1038/s41467-021-26278-9>
- Nova, I. C., Ritmejeris, J., Brinkerhoff, H., Koenig, T. J. R., Gundlach, J. H., & Dekker, C. (2022). Mapping phosphorylation post-translational modifications along single peptides with nanopores. *BioRxiv*, 2022.11.11.516163. <https://doi.org/10.1101/2022.11.11.516163>
- Obermayer, R., Leitch, I. J., Hanson, L., & Bennett, M. D. (2002). Nuclear DNA C-values in 30 species double the familial representation in pteridophytes. *Annals of Botany*, *90*(2), 209–217. <https://doi.org/10.1093/aob/mcf167>
- O’Leary, B., & Plaxton, W. C. (2020). Multifaceted functions of post-translational enzyme modifications in the control of plant glycolysis. In *Current Opinion in Plant Biology* (Vol. 55, pp. 28–37). Elsevier Ltd. <https://doi.org/10.1016/j.pbi.2020.01.009>
- Osakabe, Y., Watanabe, T., Sugano, S. S., Ueta, R., Ishihara, R., Shinozaki, K., & Osakabe, K. (2016). Optimization of CRISPR/Cas9 genome editing to modify abiotic stress responses in plants. *Scientific Reports*, *6*(February), 1–10. <https://doi.org/10.1038/srep26685>
- Osmond, C. B. (1978). Crassulacean Acid Metabolism: A Curiosity in Context. *Annual Review of Plant Physiology*, *29*(1), 379–414. <https://doi.org/10.1146/annurev.pp.29.060178.002115>
- Ossa, P. G., Moreno, A. A., Orellana, D., Toro, M., Carrasco-Valenzuela, T., Riveros, A., Meneses, C. C., Nilo-Poyanco, R., & Orellana, A. (2022). Transcriptomic analysis of the C3-CAM transition in *Cistanthe longiscapa*, a drought tolerant plant in the Atacama Desert. *BioRxiv*, 2022.03.16.484649. <https://doi.org/10.1101/2022.03.16.484649>

- Ota, K. (1988). Stimulation of CAM Photosynthesis in *Kalanchoë blossfeldiana* by Transferring to Nitrogen-Deficient Conditions. *Plant Physiology*, 87(2), 454–457. <https://doi.org/10.1104/pp.87.2.454>
- Ou, S., Chen, J., & Jiang, N. (2018). Assessing genome assembly quality using the LTR Assembly Index (LAI). *Nucleic Acids Research*, 46(21), e126. <https://doi.org/10.1093/nar/gky730>
- Outlaw, W. H., & Manchester, J. (1979). Guard Cell Starch Concentration Quantitatively Related to Stomatal Aperture. *Plant Physiology*, 64, 79–82.
- Outlaw, W. H., Manchester, J., Dicamelli, C. A., Randall, D. D., Rapp, B., & Veith, G. M. (1979). Photosynthetic carbon reduction pathway is absent in chloroplasts of *Vicia faba* guard cells. *Proc Natl Acad Sci USA*, 76, 6371–6375.
- Patro, R., Duggal, G., Love, M. I., Irizarry, R. A., & Kingsford, C. (2017). Salmon provides fast and bias-aware quantification of transcript expression. *Nature Methods*, 14(4), 417–419. <https://doi.org/10.1038/nmeth.4197>
- Pellicer, J., Powell, R. F., & Leitch, I. J. (2021). The Application of Flow Cytometry for Estimating Genome Size, Ploidy Level Endopolyploidy, and Reproductive Modes in Plants. *Methods in Molecular Biology (Clifton, N.J.)*, 2222, 325–361. https://doi.org/10.1007/978-1-0716-0997-2_17
- Pertuit, A. J. (1992). 17 - *Kalanchoe* (R. A. B. T.-I. to F. (Second E. Larson, Ed.; pp. 429–450). Academic Press. <https://doi.org/https://doi.org/10.1016/B978-0-12-437651-9.50022-1>
- Qu, X., Peterson, K. M., & Torii, K. U. (2017). Stomatal development in time: the past and the future. *CURRENT OPINION IN GENETICS & DEVELOPMENT*, 45, 1–9. <https://doi.org/10.1016/j.gde.2017.02.001>
- Quinlan, A. R., & Hall, I. M. (2010). BEDTools: A flexible suite of utilities for comparing genomic features. *Bioinformatics*, 26(6), 841–842. <https://doi.org/10.1093/bioinformatics/btq033>
- Raghavendra, A. S. (1981). Energy supply for stomatal opening in epidermal strips of *Commelina benghalensis*. *PLANT PHYSIOLOGY*, 67, 385–387.

- Ranallo-Benavidez, T. R., Jaron, K. S., & Schatz, M. C. (2020). GenomeScope 2.0 and Smudgeplot for reference-free profiling of polyploid genomes. *Nature Communications*, *11*(1). <https://doi.org/10.1038/s41467-020-14998-3>
- Reckmann, U., Scheibe, R., & Raschke, K. (1990). Rubisco activity in guard cells compared with the solute requirement for stomatal opening. *Plant Physiology*, *92*(1), 246–253. <https://doi.org/10.1104/pp.92.1.246>
- Resco de Dios, V., Chowdhury, F. I., Granda, E., Yao, Y., & Tissue, D. T. (2019). Assessing the potential functions of nocturnal stomatal conductance in C3 and C4 plants. *New Phytologist*, *223*(4), 1696–1706. <https://doi.org/10.1111/nph.15881>
- Restrepo-Pérez, L., Joo, C., & Dekker, C. (2018). Paving the way to single-molecule protein sequencing. In *Nature Nanotechnology* (Vol. 13, Issue 9, pp. 786–796). Nature Publishing Group. <https://doi.org/10.1038/s41565-018-0236-6>
- Roach, M. J., Schmidt, S., & Borneman, A. R. (2018). Purge Haplotigs: allelic contig reassignment for third-gen diploid genome assemblies. *BMC Bioinformatics*, 1–10.
- Robaina-Estévez, S., Daloso, D. M., Zhang, Y., Fernie, A. R., & Nikoloski, Z. (2017). Resolving the central metabolism of Arabidopsis guard cells. *Scientific Reports*, *7*(1). <https://doi.org/10.1038/s41598-017-07132-9>
- Roelfsema, M. R. G., Steinmeyer, R., Staal, M., & Hedrich, R. (2001). Single guard cell recordings in intact plants: light-induced hyperpolarization of the plasma membrane. *Plant Journal*, *26*(1), 1–13.
- Rustin, P., & Queiroz-Claret, C. (1985). Changes in oxidative properties of Kalanchoe blossfeldiana leaf mitochondria during development of Crassulacean acid metabolism. *Planta*, *164*(3), 415–422. <https://doi.org/10.1007/BF00402955>
- Santelia, D., & Lawson, T. (2016). Rethinking Guard Cell Metabolism. *PLANT PHYSIOLOGY*, *172*(3), 1371–1392. <https://doi.org/10.1104/pp.16.00767>

- Santelia, D., & Lunn, J. E. (2017). Transitory Starch Metabolism in Guard Cells: Unique Features for a Unique Function. *Plant Physiology*, *174*(2), 539–549. <https://doi.org/10.1104/pp.17.00211>
- Schiller, K., & Bräutigam, A. (2021). Engineering of Crassulacean Acid Metabolism. *Annual Review of Plant Biology*, *72*(1), 77–103. <https://doi.org/10.1146/annurev-arplant-071720-104814>
- Schneider, C. A., Rasband, W. S., & Eliceiri, K. W. (2012). NIH Image to ImageJ: 25 years of image analysis. *Nature Methods*, *9*(7), 671–675. <https://doi.org/10.1038/nmeth.2089>
- Schwartz, A., & Zeiger, E. (1984). Metabolic energy for stomatal opening. Roles of photophosphorylation and oxidative phosphorylation. *Planta*, *161*(2), 129–136. <https://doi.org/10.1007/BF00395472>
- Scott, A. D., Zimin, A. V., Puiu, D., Workman, R., Britton, M., Zaman, S., Caballero, M., Read, A. C., Bogdanove, A. J., Burns, E., Wegrzyn, J., Timp, W., Salzberg, S. L., & Neale, D. B. (2020). A reference genome sequence for giant sequoia. *G3: Genes, Genomes, Genetics*, *10*(11), 3907–3919. <https://doi.org/10.1534/g3.120.401612>
- Serrano, E. E., Zeiger, E., & Hagiwara, S. (1988). Red light stimulates an electrogenic proton pump in *Vicia* guard cell protoplasts. *Proceedings of the National Academy of Sciences*, *85*(2), 436–440. <https://doi.org/10.1073/pnas.85.2.436>
- Shameer, S., Baghalian, K., Cheung, C. Y. M., Ratcliffe, R. G., & Sweetlove, L. J. (2018). Computational analysis of the productivity potential of CAM. *Nature Plants*, *4*(3), 165–171. <https://doi.org/10.1038/s41477-018-0112-2>
- Shi, J., Yi, K., Liu, Y., Xie, L., Zhou, Z., Chen, Y., Hu, Z., Zheng, T., Liu, R., Chen, Y., & Chen, J. (2015). Phosphoenolpyruvate carboxylase in arabidopsis leaves plays a crucial role in carbon and nitrogen metabolism. *Plant Physiology*, *167*(3), 671–681. <https://doi.org/10.1104/pp.114.254474>
- Shimada, T., Nakano, R., Shulaev, V., Sadka, A., & Blumwald, E. (2006). Vacuolar citrate/H⁺ symporter of citrus juice cells. *Planta*, *224*(2), 472–480. <https://doi.org/10.1007/s00425-006-0223-2>

- Shimazaki, K., Doi, M., Assmann, S. M., & Kinoshita, T. (2007). Light regulation of stomatal movement. *ANNUAL REVIEW OF PLANT BIOLOGY*, *58*, 219–247. <https://doi.org/10.1146/annurev.arplant.57.032905.105434>
- Shimazaki, K., Iino, M., & Zeiger, E. (1986). Blue light-dependent proton extrusion by guard-cell protoplasts of *vicia faba*. *Nature*, *319*(6051), 324–326. <https://doi.org/10.1038/319324a0>
- Shimazaki, K.-I., Terada, J., Tanaka, K., & Kondo, N. (1989). Calvin-Benson cycle enzymes in guard-cell protoplasts from *vicia faba* L: Implications for the greater utilization of phosphoglycerate/dihydroxyacetone phosphate shuttle between chloroplasts and the cytosol. *Plant Physiology*, *90*(3), 1057–1064. <https://doi.org/10.1104/pp.90.3.1057>
- Shukla, J. S., Slade, R., Khourdajie, A. A., Diemen, R., McCollum, D., Pathak, M., Some, S., Vyas, P., Fradera, R., Belkacemi, M., Hasija, A., Lisboa, G., Luz, S., & Malley, J. (2022). *IPCC, 2022: Climate Change 2022: Mitigation of Climate Change. Contribution of Working Group III to the Sixth Assessment Report of the Intergovernmental Panel on Climate Change*. Cambridge University Press. <https://doi.org/10.1017/9781009157926>
- Smith, A. M., & Stitt, M. (2007). Coordination of carbon supply and plant growth. In *Plant, Cell and Environment* (Vol. 30, Issue 9, pp. 1126–1149). <https://doi.org/10.1111/j.1365-3040.2007.01708.x>
- Steudle, E., Andrew, J., Smith, C., & Luttge, U. (1980). Water-relation Parameters of Individual Mesophyll Cells of the Crassulacean Acid Metabolism Plant *Kalanchoe daigremontiana*. In *Plant Physiol* (Vol. 66). <https://academic.oup.com/plphys/article/66/6/1155/6077712>
- Suetsugu, N., Takami, T., Ebisu, Y., Watanabe, H., Iiboshi, C., Doi, M., & Shimazaki, K. (2014a). Guard Cell Chloroplasts Are Essential for Blue Light-Dependent Stomatal Opening in *Arabidopsis*. *PLOS ONE*, *9*(9). <https://doi.org/10.1371/journal.pone.0108374>
- Talbott, L. D., & Zeiger, E. (1993). Sugar and Organic Acid Accumulation in Guard Cells of *Vicia faba* in Response to Red and Blue Light. *Plant Physiology*, *102*(4), 1163 LP – 1169. <https://doi.org/10.1104/pp.102.4.1163>

- Talbott, L. D., & Zeiger, E. (1996). Central roles for potassium and sucrose in guard-cell osmoregulation. *PLANT PHYSIOLOGY*, *111*(4), 1051–1057. <https://doi.org/10.1104/pp.111.4.1051>
- Talbott, L. D., & Zeiger, E. (1998). The role of sucrose in guard cell osmoregulation. *JOURNAL OF EXPERIMENTAL BOTANY*, *49*(Annual Meeting of the Society-for-Experimental-Biology on Stomatal Biology), 329–337. https://doi.org/10.1093/jexbot/49.suppl_1.329 WE - Science Citation Index Expanded (SCI-EXPANDED) WE - Conference Proceedings Citation Index - Science (CPCI-S)
- Talbott, L. D., & Zeiger, E. (1993). SUGAR AND ORGANIC-ACID ACCUMULATION IN GUARD-CELLS OF VICIA-FABA IN RESPONSE TO RED AND BLUE-LIGHT. *PLANT PHYSIOLOGY*, *102*(4), 1163–1169. <https://doi.org/10.1104/pp.102.4.1163> WE - Science Citation Index Expanded (SCI-EXPANDED)
- Tallman, G., & Zeiger, E. (1988). Light quality and osmoregulation in Vicia guard cells. Evidence for involvement of three metabolic pathways. *Plant Physiol.*, *88*, 887–895.
- Tan, X. L. J., & Cheung, C. Y. M. (2020). A multiphase flux balance model reveals flexibility of central carbon metabolism in guard cells of C3 plants. *Plant Journal*, *104*(6), 1648–1656. <https://doi.org/10.1111/tpj.15027>
- Tarailo-Graovac, M., & Chen, N. (2009). Using RepeatMasker to Identify Repetitive Elements in Genomic Sequences. *Current Protocols in Bioinformatics*, *25*(1), 4.10.1-4.10.14. <https://doi.org/https://doi.org/10.1002/0471250953.bi0410s25>
- Tavakoli, N., Kluge, C., Gollack, D., Mimura, T., & Dietz, K. J. (2001). Reversible redox control of plant vacuolar H⁺-ATPase activity is related to disulfide bridge formation in subunit E as well as subunit A. *Plant Journal*, *28*(1), 51–59. <https://doi.org/10.1046/j.1365-313X.2001.01130.x>
- Taybi, T., & Cushman, J. C. (2002). Abscisic acid signaling and protein synthesis requirements for phosphoenolpyruvate carboxylase transcript induction in the common ice plant. In *J. Plant Physiol* (Vol. 159). <http://www.urbanfischer.de/journals/jpp>

- Taybi, T., Cushman, J. C., & Borland, A. M. (2017). Leaf carbohydrates influence transcriptional and post-transcriptional regulation of nocturnal carboxylation and starch degradation in the facultative CAM plant, *Mesembryanthemum crystallinum*. *Journal of Plant Physiology*, *218*(July), 144–154. <https://doi.org/10.1016/j.jplph.2017.07.021>
- Taybi, T., Sotta, B., Gehrig, H., Güçlü, S., Kluge, M., & Brulfert, J. (1995). Differential Effects of Abscisic Acid on Phosphoenolpyruvate Carboxylase and CAM Operation in *Kalanchoë blossfeldiana*. *Botanica Acta*, *108*(3), 240–246. <https://doi.org/10.1111/j.1438-8677.1995.tb00856.x>
- Taylor, A. R., & Assmann, S. M. (2001). Apparent absence of a redox requirement for blue light activation of pump current in broad bean guard cells. *Plant Physiology*, *125*(1), 329–338.
- Thi Hoang, D., Chernomor, O., von Haeseler, A., Quang Minh, B., Sy Vinh, L., & Rosenberg, M. S. (2017). UFBoot2: Improving the Ultrafast Bootstrap Approximation. *Mol. Biol. Evol.*, *35*(2), 518–522. <https://doi.org/10.5281/zenodo.854445>
- Tian, X., Guo, J., Zhou, X., Ma, K., Ma, Y., Shi, T., & Shi, Y. (2021). Comparative and Evolutionary Analyses on the Complete Plastomes of Five *Kalanchoe* Horticultural Plants. *Frontiers in Plant Science*, *12*. <https://doi.org/10.3389/fpls.2021.705874>
- Tillich, M., Lehwark, P., Pellizzer, T., Ulbricht-Jones, E. S., Fischer, A., Bock, R., & Greiner, S. (2017). GeSeq - Versatile and accurate annotation of organelle genomes. *Nucleic Acids Research*, *45*(W1), W6–W11. <https://doi.org/10.1093/nar/gkx391>
- Tominaga, M., Kinoshita, T., & Shimazaki, K. (2001). Guard-cell chloroplasts provide ATP required for H⁺ pumping in the plasma membrane and stomatal opening. *PLANT AND CELL PHYSIOLOGY*, *42*(8), 795–802. <https://doi.org/10.1093/pcp/pce101>
- Tominaga, M., Kinoshita, T., & Shimazaki, K.-I. (2001c). Guard-cell chloroplasts provide ATP required for H⁺ pumping in the plasma membrane and stomatal opening. *Plant and Cell Physiology*, *42*(8), 795–802. <https://doi.org/10.1093/pcp/pce101>

- Toreti, A., Bavera, D., Acosta Navarro, J., Cammalleri, C., Jager, A., Ciollo, C., Hrast Essenfelder, A., Maetens, W., Magni, D., Masante, D., Mazzeschi, M., Niemeyer, S., & Spinoni, J. (2022). *Drought in Europe August 2022*. Publications Office of the European Union. <https://doi.org/10.2760/264241>
- Ueno, K., Kinoshita, T., Inoue, S. I., Emi, T., & Shimazaki, K. I. (2005). Biochemical characterization of plasma membrane H⁺-ATPase activation in guard cell protoplasts of *Arabidopsis thaliana* in response to blue light. *Plant and Cell Physiology*, *46*(6), 955–963. <https://doi.org/10.1093/pcp/pci104>
- UNEP. (2012). *United Nations Environment Programme 2012 Annual Report UNEP United Nations Environment Programme*.
- Witsch, H., & Flügel, A. (1951). Über photoperiodisch induzierte Endomitose bei *Kalanchoë Blossfeldiana*. *Naturwissenschaften*, *38*(6), 138–139. <https://doi.org/10.1007/BF00589268>
- Vahisalu, T., Kollist, H., Wang, Y. F., Nishimura, N., Chan, W. Y., Valerio, G., Lamminmäki, A., Brosché, M., Moldau, H., Desikan, R., Schroeder, J. I., & Kangasjärvi, J. (2008). SLAC1 is required for plant guard cell S-type anion channel function in stomatal signalling. *Nature*, *452*(7186), 487–491. <https://doi.org/10.1038/nature06608>
- van Dingenen, J., Vermeersch, M., de Milde, L., Hulsmans, S., de Winne, N., van Leene, J., Gonzalez, N., Dhondt, S., de Jaeger, G., Rolland, F., & Inzé, D. (2019). The role of HEXOKINASE1 in *Arabidopsis* leaf growth. *Plant Molecular Biology*, *99*(1–2), 79–93. <https://doi.org/10.1007/s11103-018-0803-0>
- van Voorst, A., & Arends, J. C. (1982). The origin and chromosome numbers of cultivars of *Kalanchoe blossfeldiana* V on P oelln.: Their history and evolution. *Euphytica*, *31*(3), 573–584. <https://doi.org/10.1007/BF00039195>
- Vani, T., & Raghavendra, A. S. (1994). High mitochondrial activity but incomplete engagement of the cyanide-resistant alternative pathway in guard cell protoplasts of pea. *Plant Physiology*, *105*(4), 1263–1268.

- Violet-Chabrand, S. R. M., Matthews, J. S. A., McAusland, L., Blatt, M. R., Griffiths, H., & Lawson, T. (2017). Temporal Dynamics of Stomatal Behaviour: Modelling and Implications for Photosynthesis and Water Use. *PLANT PHYSIOLOGY*, *174*(2), 603–613. <https://doi.org/10.1104/pp.17.00125>
- von Caemmerer, S., & Griffiths, H. (2009). Stomatal responses to CO₂ during a diel Crassulacean acid metabolism cycle in *Kalanchoe daigremontiana* and *Kalanchoe pinnata*. *Plant, Cell and Environment*, *32*(5), 567–576. <https://doi.org/10.1111/j.1365-3040.2009.01951.x>
- Vurture, G. W., Sedlazeck, F. J., Nattestad, M., Underwood, C. J., Fang, H., Gurtowski, J., & Schatz, M. C. (2017). GenomeScope: Fast reference-free genome profiling from short reads. *Bioinformatics*, *33*(14), 2202–2204. <https://doi.org/10.1093/bioinformatics/btx153>
- Wai, C. M., Weise, S. E., Ozersky, P., Mockler, T. C., Michael, T. P., & Vanburen, R. (2019). Time of day and network reprogramming during drought induced CAM photosynthesis in *Sedum album*. *PLoS Genetics*, *15*(6). <https://doi.org/10.1371/journal.pgen.1008209>
- Walker, B. J., Abeel, T., Shea, T., Priest, M., Abouelliel, A., Sakthikumar, S., Cuomo, C. A., Zeng, Q., Wortman, J., Young, S. K., & Earl, A. M. (2014). Pilon: An integrated tool for comprehensive microbial variant detection and genome assembly improvement. *PLoS ONE*, *9*(11). <https://doi.org/10.1371/journal.pone.0112963>
- Wang, C., Zhang, J., Wu, J., Brodsky, D. E., & Schroeder, J. I. (2018). Cytosolic malate and oxaloacetate activate S-type anion channels in *Arabidopsis* guard cells. *New Phytologist*, *220*(1), 178–186. <https://doi.org/10.1111/nph.15292>
- Wang, P., Khoshravesht, R., Karki, S., Tapia, R., Balahadia, C. P., Bandyopadhyay, A., Quick, W. P., Furbank, R., Sage, T. L., & Langdale, J. A. (2017). Re-creation of a Key Step in the Evolutionary Switch from C₃ to C₄ Leaf Anatomy. *Current Biology*, *27*(21), 3278–3287.e6. <https://doi.org/10.1016/j.cub.2017.09.040>
- Wang, S. W., Li, Y., Zhang, X. L., Yang, H. Q., Han, X. F., Liu, Z. H., Shang, Z. L., Asano, T., Yoshioka, Y., Zhang, C. G., & Chen, Y. L. (2014). Lacking chloroplasts in guard cells of crumpled leaf attenuates stomatal opening: Both guard cell chloroplasts and mesophyll

- contribute to guard cell ATP levels. *Plant, Cell and Environment*, 37(9), 2201–2210. <https://doi.org/10.1111/pce.12297>
- Wang, W., Das, A., Kainer, D., Schalamun, M., Morales-Suarez, A., Schwessinger, B., & Lanfear, R. (2020). The draft nuclear genome assembly of *Eucalyptus pauciflora*: A pipeline for comparing de novo assemblies. *GigaScience*, 9(1), 1–12. <https://doi.org/10.1093/gigascience/giz160>
- Warzecha, H., & Mason, H. S. (2003). Benefits and risks of antibody and vaccine production in transgenic plants. *Journal of Plant Physiology*, 160(7), 755–764. <https://doi.org/https://doi.org/10.1078/0176-1617-01125>
- Wickell, D., Kuo, L. Y., Yang, H. P., Dhabalia Ashok, A., Irisarri, I., Dadras, A., de Vries, S., de Vries, J., Huang, Y. M., Li, Z., Barker, M. S., Hartwick, N. T., Michael, T. P., & Li, F. W. (2021). Underwater CAM photosynthesis elucidated by *Isoetes* genome. *Nature Communications*, 12(1). <https://doi.org/10.1038/s41467-021-26644-7>
- Wille, A. C., & Lucas, W. J. (1984). Ultrastructural and histochemical studies on guard cells. *Planta*, 160(2), 129–142. <https://doi.org/10.1007/BF00392861>
- Willmer, C. M., & Dittrich, P. (1974). Carbon dioxide fixation by epidermal and mesophyll tissues of *Tulipa* and *Commelina*. *Planta*, 117(2), 123–132. <https://doi.org/10.1007/BF00390794>
- Winter, D., Vinegar, B., Nahal, H., Ammar, R., Wilson, G. v., & Provart, N. J. (2007). An “electronic fluorescent pictograph” Browser for exploring and analyzing large-scale biological data sets. *PLoS ONE*, 2(8). <https://doi.org/10.1371/journal.pone.0000718>
- Winter, H., Robinson, D. G., & Heldp, H. W. (1993). Subcellular volumes and metabolite concentrations in barley leaves. In *Planta* (Vol. 191). Springer-Verlag.
- Winter, K. (2019). Ecophysiology of constitutive and facultative CAM photosynthesis. *Journal of Experimental Botany*, 70(22), 6495–6508. <https://doi.org/10.1093/jxb/erz002>
- Winter, K., Garcia, M., & Holtum, J. A. M. (2008). On the nature of facultative and constitutive CAM: Environmental and developmental control of CAM expression during early growth

- of *Clusia*, *Kalanchoë*, and *Opuntia*. *Journal of Experimental Botany*, 59(7), 1829–1840.
<https://doi.org/10.1093/jxb/ern080>
- Winter, K., & Holtum, J. A. M. (2014). Facultative crassulacean acid metabolism (CAM) plants: powerful tools for unravelling the functional elements of CAM photosynthesis. *JOURNAL OF EXPERIMENTAL BOTANY*, 65(13), 3425–3441. <https://doi.org/10.1093/jxb/eru063>
- Wong, S. C., Cowan, I. R., & Farquhar, G. D. (1979). Stomatal conductance correlates with photosynthetic capacity. *Nature*, 282(5737), 424–426.
<https://doi.org/10.1038/282424a0>
- Wyka, T. P., Duarte, H. M., & Lüttge, U. E. (2005). Redundancy of stomatal control for the circadian photosynthetic rhythm in *Kalanchoë daigremontiana* Hamet et Perrier. *Plant Biology*, 7(2), 176–181. <https://doi.org/10.1055/s-2005-837541>
- Xue, S., Hu, H., Ries, A., Merilo, E., Kollist, H., & Schroeder, J. I. (2011). Central functions of bicarbonate in S-type anion channel activation and OST1 protein kinase in CO₂ signal transduction in guard cell. *EMBO Journal*, 30(8), 1645–1658.
<https://doi.org/10.1038/emboj.2011.68>
- Yamauchi, S., Takemiya, A., Sakamoto, T., Kurata, T., Tsutsumi, T., Kinoshita, T., & Shimazaki, K. (2016). Plasma membrane H⁺-ATPase1 (AHA1) plays a major role in *Arabidopsis thaliana* for stomatal opening in response to blue light. *Plant Physiology*, 171(August), pp.01581.2016. <https://doi.org/10.1104/pp.16.01581>
- Yang, X., Hu, R., Yin, H., Jenkins, J., Shu, S., Tang, H., Liu, D., Weighill, D. A., Cheol Yim, W., Ha, J., Heyduk, K., Goodstein, D. M., Guo, H. B., Moseley, R. C., Fitzek, E., Jawdy, S., Zhang, Z., Xie, M., Hartwell, J., ... Tuskan, G. A. (2017). The *Kalanchoë* genome provides insights into convergent evolution and building blocks of crassulacean acid metabolism. *Nature Communications*, 8(1). <https://doi.org/10.1038/s41467-017-01491-7>
- Yang, Y., Costa, A., Leonhardt, N., Siegel, R. S., & Schroeder, J. I. (2008). Isolation of a strong *Arabidopsis* guard cell promoter and its potential as a research tool. *Plant Methods*, 4(1), 1–15. <https://doi.org/10.1186/1746-4811-4-6>

- Zeiger, E., & Zhu, J. X. (1998). Role of zeaxanthin in blue light photoreception and the modulation of light-CO₂ interactions in guard cells. *JOURNAL OF EXPERIMENTAL BOTANY*, 49(Annual Meeting of the Society-for-Experimental-Biology on Stomatal Biology), 433–442. https://doi.org/10.1093/jexbot/49.suppl_1.433 WE - Science Citation Index Expanded (SCI-EXPANDED) WE - Conference Proceedings Citation Index - Science (CPCI-S)
- Zeppel, M. J. B., Lewis, J. D., Chaszar, B., Smith, R. A., Medlyn, B. E., Huxman, T. E., & Tissue, D. T. (2012). Nocturnal stomatal conductance responses to rising [CO₂], temperature and drought. *NEW PHYTOLOGIST*, 193(4), 929–938. <https://doi.org/10.1111/j.1469-8137.2011.03993.x>
- Zeppel, M. J. B., Lewis, J. D., Phillips, N. G., & Tissue, D. T. (2014). Consequences of nocturnal water loss: a synthesis of regulating factors and implications for capacitance, embolism and use in models. *TREE PHYSIOLOGY*, 34(10), 1047–1055. <https://doi.org/10.1093/treephys/tpu089>
- Zhang, J., De-oliveira-ceciliato, P., Takahashi, Y., Schulze, S., Dubeaux, G., Hauser, F., Kollist, H., Rappel, W., & Schroeder, J. I. (2018). Minireview Insights into the Molecular Mechanisms of CO₂-Mediated Regulation of Stomatal Movements Minireview. *Current Biology*, 28, 1356–1363. <https://doi.org/10.1016/j.cub.2018.10.015>
- Zhang, J., Hu, R., Sreedasyam, A., Garcia, T. M., Lipzen, A., Wang, M., Yerramsetty, P., Liu, D., Ng, V., Schmutz, J., Cushman, J. C., Borland, A. M., Pasha, A., Provar, N. J., Chen, J. G., Muchero, W., Tuskan, G. A., & Yang, X. (2020a). Light-responsive expression atlas reveals the effects of light quality and intensity in *Kalanchoë fedtschenkoi*, a plant with crassulacean acid metabolism. *GigaScience*, 9(3), 1–17. <https://doi.org/10.1093/gigascience/giaa018>
- Zhang, J., Wang, N., Miao, Y., Hauser, F., McCammon, J. A., Rappel, W.-J., & Schroeder, J. I. (2018). Identification of SLAC1 anion channel residues required for CO₂/bicarbonate sensing and regulation of stomatal movements. *Proceedings of the National Academy of Sciences*, 115(44), 11129–11137. <https://doi.org/10.1073/pnas.1807624115>

- Zhao, Z., & Assmann, S. M. (2011). The glycolytic enzyme, phosphoglycerate mutase, has critical roles in stomatal movement, vegetative growth, and pollen production in *Arabidopsis thaliana*. *Journal of Experimental Botany*, *62*(14), 5179–5189. <https://doi.org/10.1093/jxb/err223>
- Zhao, Z. X., Zhang, W., Stanley, B. A., & Assmann, S. M. (2008). Functional Proteomics of *Arabidopsis thaliana* Guard Cells Uncovers New Stomatal Signaling Pathways. *PLANT CELL*, *20*(12), 3210–3226. <https://doi.org/10.1105/tpc.108.063263>
- Zhu, M. M., Dai, S. J., McClung, S., Yan, X. F., & Chen, S. X. (2009). Functional Differentiation of *Brassica napus* Guard Cells and Mesophyll Cells Revealed by Comparative Proteomics. *MOLECULAR & CELLULAR PROTEOMICS*, *8*(4), 752–766. <https://doi.org/10.1074/mcp.M800343-MCP200>
- Zimin, A. V., Puiu, D., Luo, M. C., Zhu, T., Koren, S., Marçais, G., Yorke, J. A., Dvořák, J., & Salzberg, S. L. (2017). Hybrid assembly of the large and highly repetitive genome of *Aegilops tauschii*, a progenitor of bread wheat, with the MaSuRCA mega-reads algorithm. *Genome Research*, *27*(5), 787–792. <https://doi.org/10.1101/gr.213405.116>

Chapter 7. Appendix

7.1 Appendix 1. Supplementary Data for Chapter 3.

Modelling Stomatal Kinetics

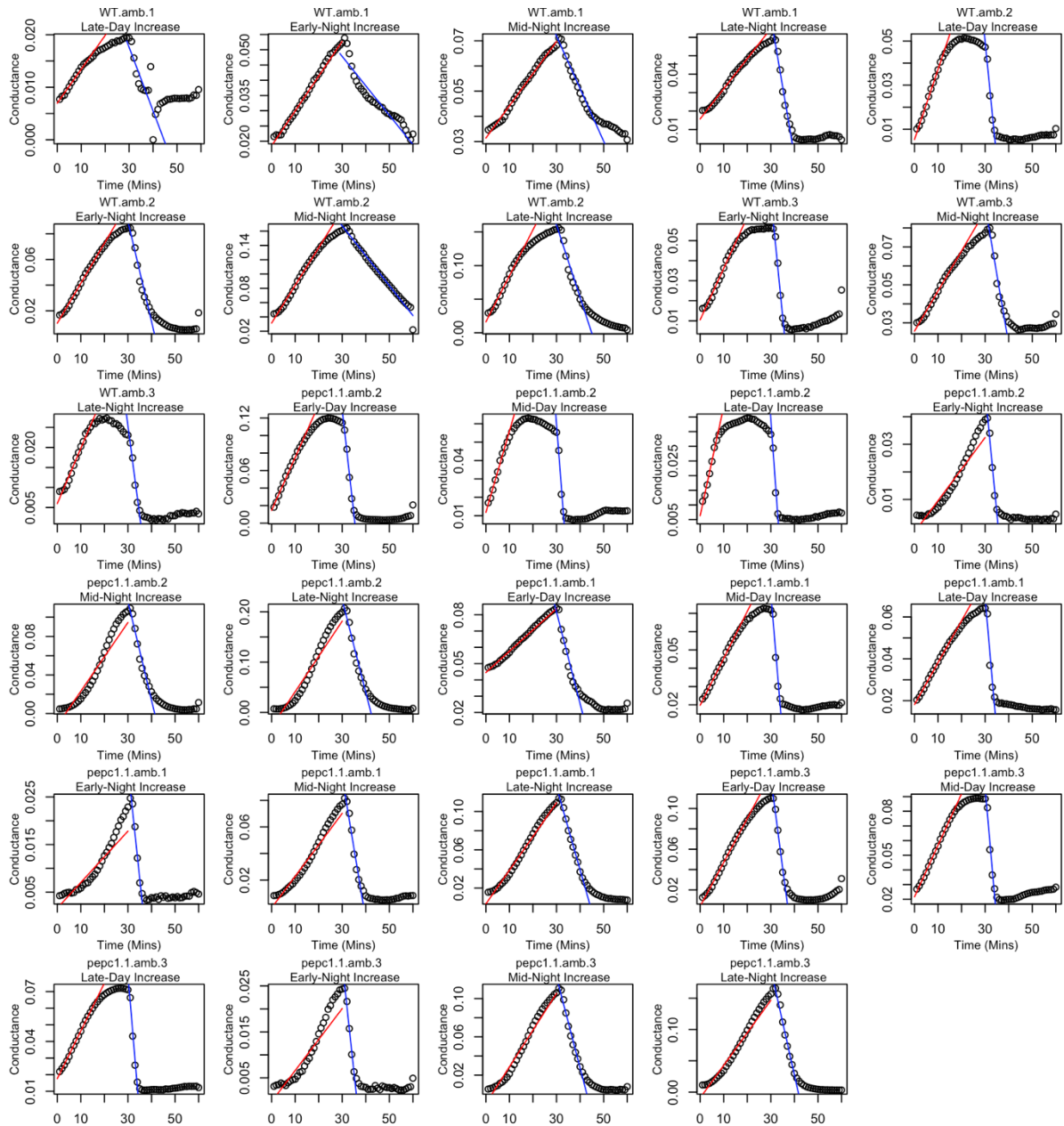


Figure A1.1 Low CO₂ Response Stomatal Kinetics. Exponential equations fail to capture response. Conditions and method as described in Chapter 3. *K. fedtschenkoii* wild type and *pepc1* mutant graphs used for example.

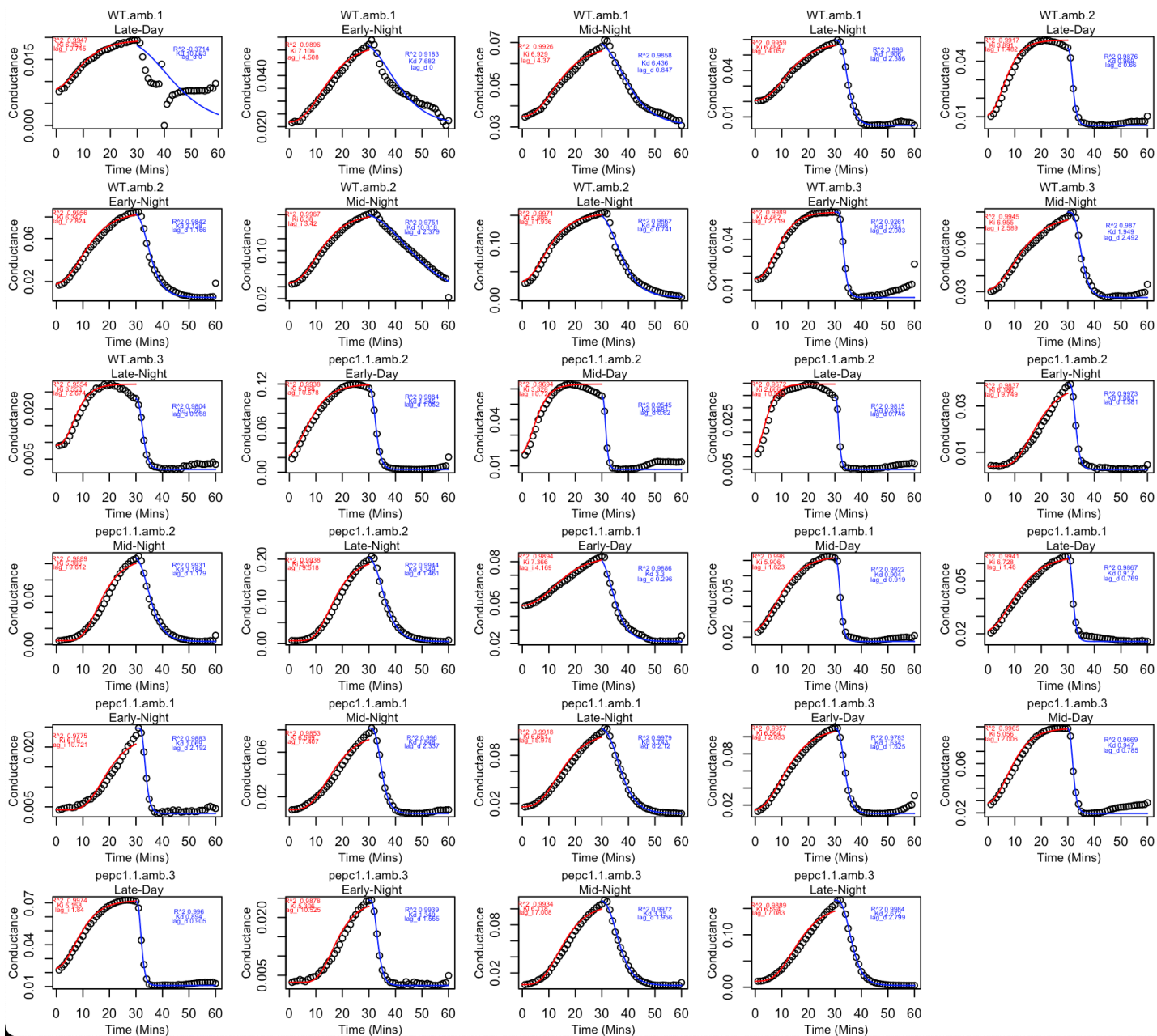


Figure A1.2 Low CO₂ Response Stomatal Kinetics. Sigmoidal equations fit the data better than the exponential equations and was therefore used for response kinetics modelling in Chapter 3. Conditions and method as described in Chapter 3. *K. fedtschenkoi* wild type and *pepc1* mutant graphs used for example.

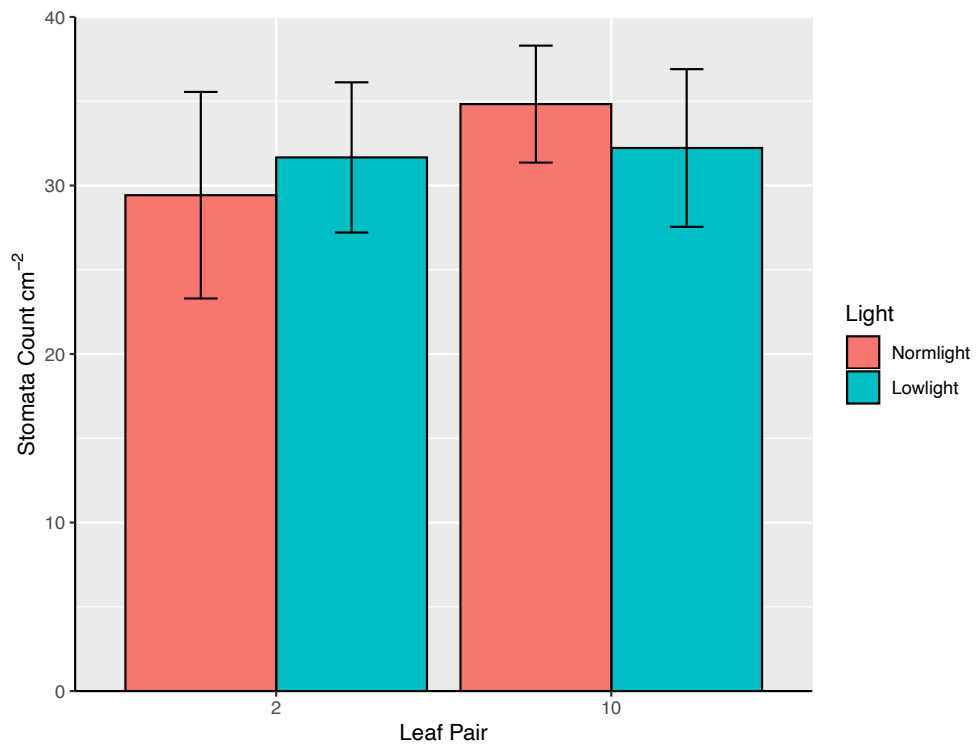


Figure A1.3. *Kalanchoe blossfeldiana* stomatal density, number of stomata per cm² on the abaxial epidermis of young (10th leaf pair from the bottom) and mature (2nd leaf pair from the bottom) *Kalanchoe blossfeldiana* leaves counted at 90 days after propagation. Error bars = +/- standard deviation.

7.2 Appendix 2. Supplementary Data for Chapter 4.

Sequencing Read Statistics

Table A2.1 Raw DNA Short Sequencing Read Counts and QC

Sample	Raw reads	Raw data (Gb)	Effective(%)	Error(%)	Q20(%)	Q30(%)	GC(%)
M3	124931528	18.74	99.82	0.02	98.29	94.62	37.76
M3	311285030	46.69	99.76	0.03	97.45	92.83	37.76
M3	174885886	26.20	99.8	0.03	97.91	93.81	37.78

Table A2.2 Raw DNA Long Reads Nanopore Read Counts (After QC filtering)

Raw reads	Raw data (Gb)	N50 (Kb)
3490000	10	~10

Table A2.3 Raw RNA Sequencing Read Counts and QC

Sample	Leaf Pair	Raw reads	Raw data					
			(Gb)	Effective(%)	Error(%)	Q20(%)	Q30(%)	GC(%)
A5T1	9	42958464	6.4	98.99	0.03	96.44	90.8	48.66
A6T1	9	31891616	4.8	98.83	0.03	96.32	90.71	48.58
A7T1	9	37386098	5.6	98.94	0.03	96.51	90.89	48.9
B7T5	3	44191658	6.6	99.08	0.03	97.22	92.15	47.94
B5T2	3	41715744	6.3	98.74	0.03	97.3	92.3	47.74
B8T1	3	40890964	6.1	99	0.03	96.3	90.45	47.94

Table A2.4. *Kalanchoe blossfeldiana* Genome Assembly Size through scaffold and duplicate purging. Order is progressive down, with top being MaSuRCA output and bottom being the final assembly.

Scaffold No.	N75 (Mb)	N50 (Mb)	N25 (Mb)	Max (Mb)	Sum (Mb)	Notes
2528	0.3	1.0	2.3	8.5	772	MaSuRCA
13145	1.6	9.4	21.6	30.2	772	Scaffolded with <i>K. laxiflora</i>
173	5.6	19.3	23.5	30.2	593	PurgeHaplotigs
172	5.0	18.7	23.4	29.6	556	PurgeHaplotigs +PurgeDups
18	18.7	21.3	24.1	29.6	377	Chromosome only assembly
143	18.2	20.6	23.4	29.6	461	Chromosomes + Busco Optimised Scaffolds

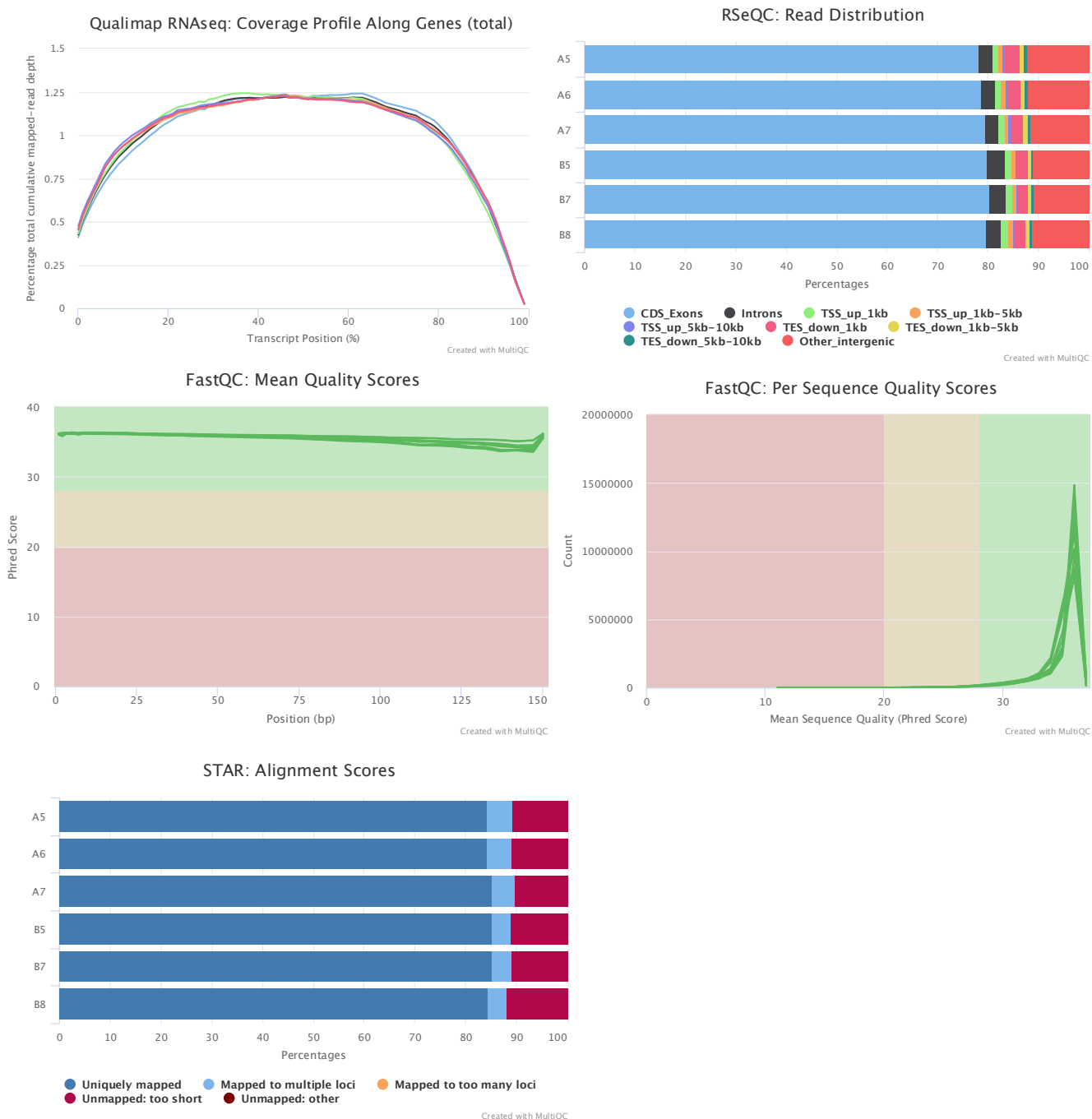


Figure A2.1 Raw RNA Sequencing Quality Statistics. Compiled with multiQC, methods as described in Chapter 4.

Table A2.5. *Kalanchoe blossfeldiana* Genome Size Flow Cytometry from Robyn Powel (Kew Gardens)

Sample	Genus	Species	Standard	2C (pg)	1C (pg)	CV sample	CV Standard
young leaf 1	Kalanchoe	blossfeldiana	<Petroselinum	2.07	1.03	3.44	2.97
young leaf 2	Kalanchoe	blossfeldiana	<Petroselinum	1.94	0.97	3.55	3.08
young leaf 3	Kalanchoe	blossfeldiana	<Petroselinum	1.98	0.99	3.56	3.49
young leaf 4	Kalanchoe	blossfeldiana	<Petroselinum	2.01	1.01	4.11	2.78
mature leaf 1	Kalanchoe	blossfeldiana	<Petroselinum	2.04	1.02	5.34	3.05
mature leaf 2	Kalanchoe	blossfeldiana	<Petroselinum	1.95	0.98	5.3	2.67
mature leaf 3	Kalanchoe	blossfeldiana	<Petroselinum	1.95	0.97	2.17	2.33
mature leaf 4	Kalanchoe	blossfeldiana	<Petroselinum	1.95	0.97	3.21	2.56

Table A2.5. *Kalanchoe blossfeldiana* Endoreplication Flow Cytometry from Robyn Powel (Kew Gardens)

Sample	Genus	Species	1(2C)	2(4C)	3(8C)	4(16C)	EI	no. of peaks
young leaf 1	Kalanchoe	blossfeldiana	1651	3517	5280	430	1.413	4
young leaf 2	Kalanchoe	blossfeldiana	2331	5637	7564	146	1.352	4
young leaf 3	Kalanchoe	blossfeldiana	1804	4977	8442	163	1.453	4
young leaf 4	Kalanchoe	blossfeldiana	1219	3035	6131	716	1.571	4
mature leaf 1	Kalanchoe	blossfeldiana	390	960	3467	1770	2.005	4
mature leaf 2	Kalanchoe	blossfeldiana	406	844	1610	1079	1.854	4
mature leaf 3	Kalanchoe	blossfeldiana	1091	2215	4484	1232	1.649	4
mature leaf 4	Kalanchoe	blossfeldiana	725	1825	4662	1709	1.824	4

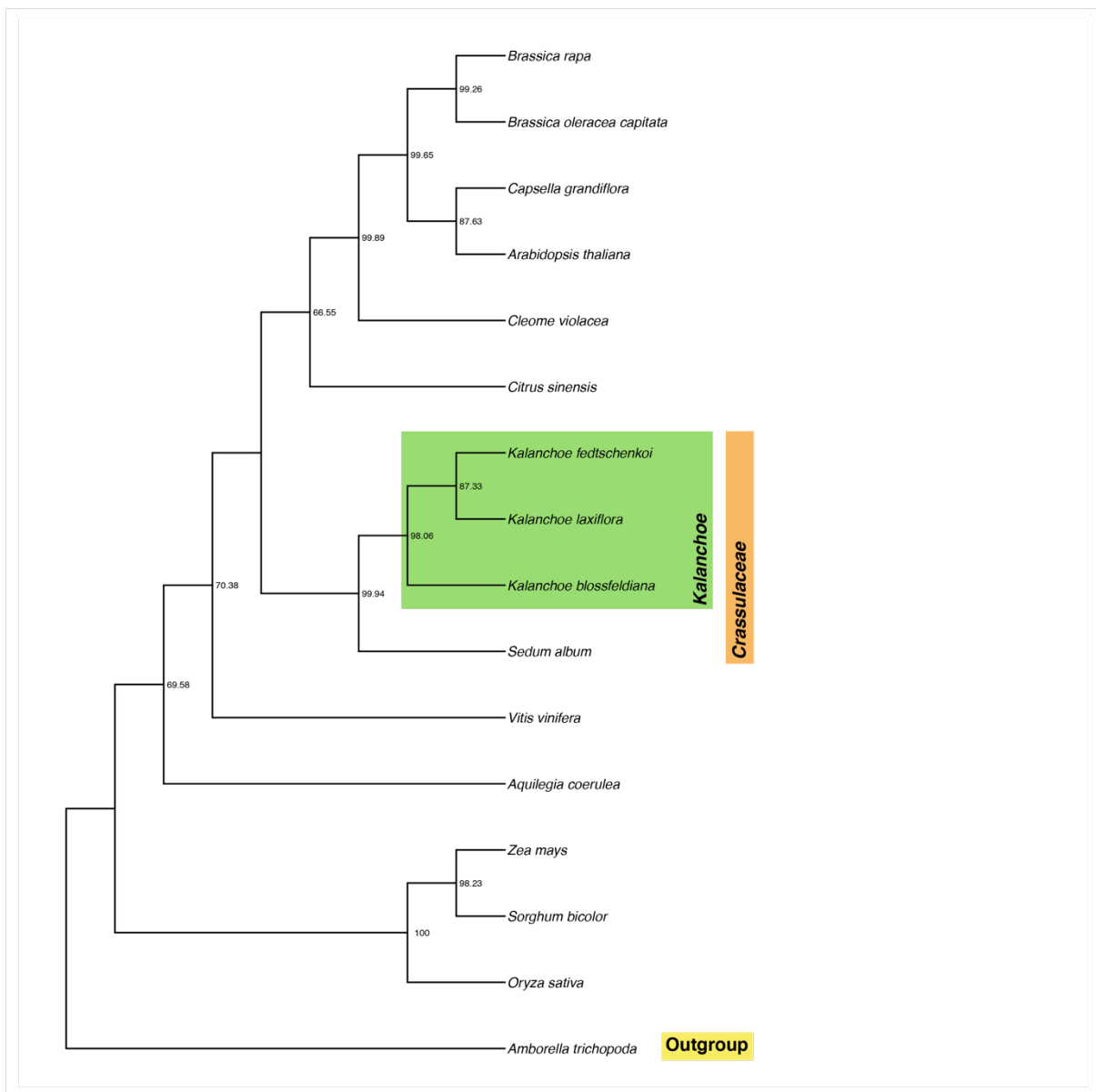
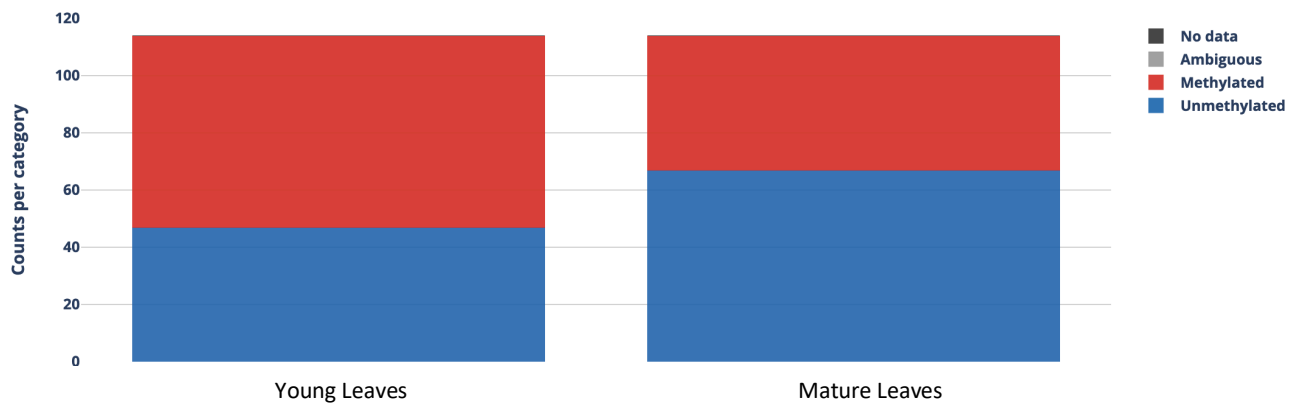


Figure A2.1 Species gene tree constructed from 285 single copy gene trees identified by OrthoFinder (Emms & Kelly, 2019), grouped sequences were aligned with Mafft 7.505 (Kato & Standley, 2013) individual trees were constructed using maximum likelihood with IQ-TREE 2.2.0.3 (Minh et al., 2020) and combined into a single summarised tree with ASTRAL-II (Mirarab & Warnow, 2015). Node values represent % individual tree support.

7.3 Appendix 3 Investigating differential methylation in age induced CAM in *K. blossfeldiana*

A.

Methylation category counts by sample for significant CpG intervals



B.

Methylation log-likelihood ratio by significant CpG interval

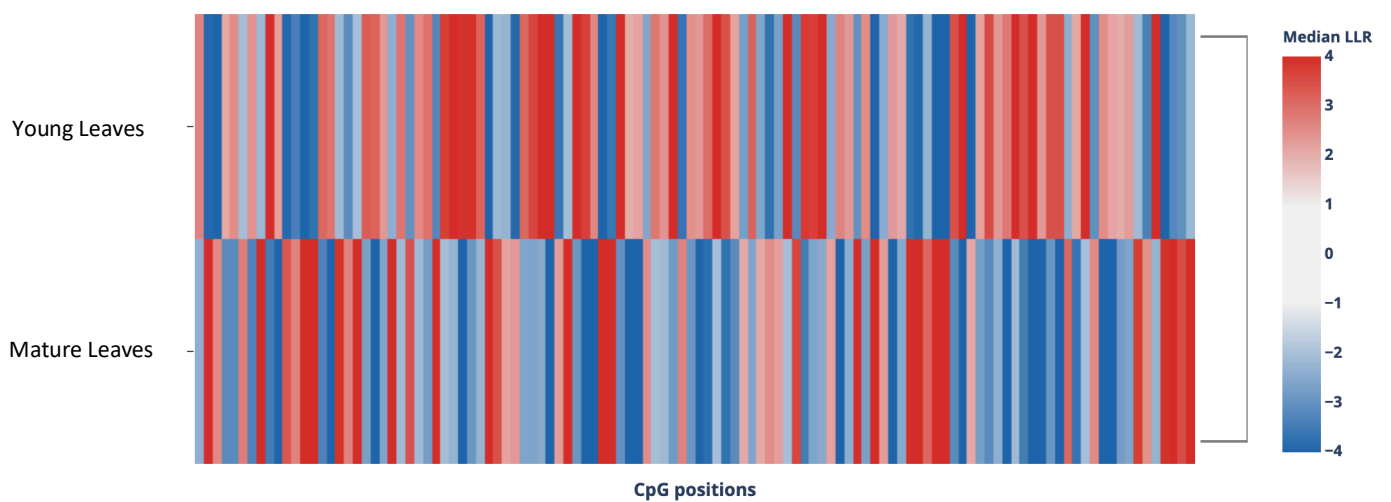


Figure A3.1. Differentially methylated sites detected by PycoMeth between young (10th leaf pair from the bottom) C₃ and mature (2nd leaf pair from the bottom) CAM *K. blossfeldiana* leaves, methylation category counts (Panel A), methylation log-likelihood ratio by CpG interval (Panel B).

The nanopore DNA sequencer was used to detect methylated base pairs by sequencing DNA samples from young and mature *K. blossfeldiana* leaves and a number of sites of differential methylation were detected (Appendix 4, Figure A4.1). However, due to low coverage and a lack of replication the number of statistically significant sites were low. This work should be followed up with greater sequencing depth and replication, as from this preliminary data it appears that there are substantial differences in the methylation landscape of the *K. blossfeldiana* genome between young and mature leaves with 467 differentially methylated sites detected by PycoMeth (2.2.1, Snajder et al., 2022). Recent work has also shown that methylation detection by nanopore sequencers is influenced by species and has prompted work on plant specific models for basecalling DNA in plants (Ni et al., 2021). Such methods may improve future attempts to detect differential methylation between young and mature *K. blossfeldiana* leaves.

7.4 Appendix 4. Testing transformations of *K. blossfeldiana*

A- WT *K. blossfeldiana*



B- 35S:RUBYRED *K. blossfeldiana*



Figure A4.1. Test transformation of *K. blossfeldiana*, an un-transformed wild type *K. blossfeldiana* plantlet (Panel A), a *K. blossfeldiana* plantlet 10 days after *Agrobacterium* mediated transformation with a 35S:RUBYRED plasmid.

Transformation of *K. blossfeldiana* was attempted using *Agrobacterium tumefaciens*, with a construct that produces betalain, which acts as an easy to see red marker for successful transformation, driven by a constitutive 35S promoter. This construct was kindly gifted by Sebastian S. Cocioba and featured a betalain biosynthesis cassette from He et al., (2020) that expressed three enzymes driven by a constitutive 35S promoter, along with kanamycin resistance genes and a bacterial eforCP expression cassette that enabled easy handling in *E.coli* and *A. tumefaciens* (Figure A4.2). However, this process still requires some optimisation since expression of betalain was only maintained for approximately a week (Figure A4.1). A working hypothesis is that betalain production may have been overly metabolically costly for the plant tissues and therefore led to the silencing of the transgene, however this remains to be investigated in detail and with alternative promoters and genes.

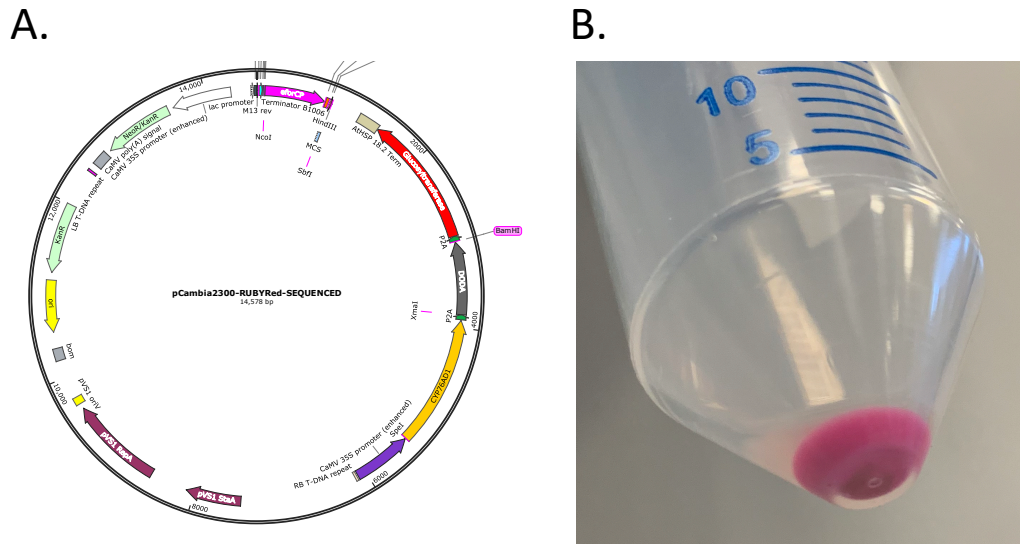


Figure A4.2. 35S:RUBYRED plasmid constructed by Sebastian S. Cocioba for *Agrobacterium* mediated plant transformation (Panel A) and expression of eforCP within an *Agrobacterium* cell pellet as an alternative plasmid marker.

7.5 Appendix 5. Reduced Light Intensity Reduces CAM

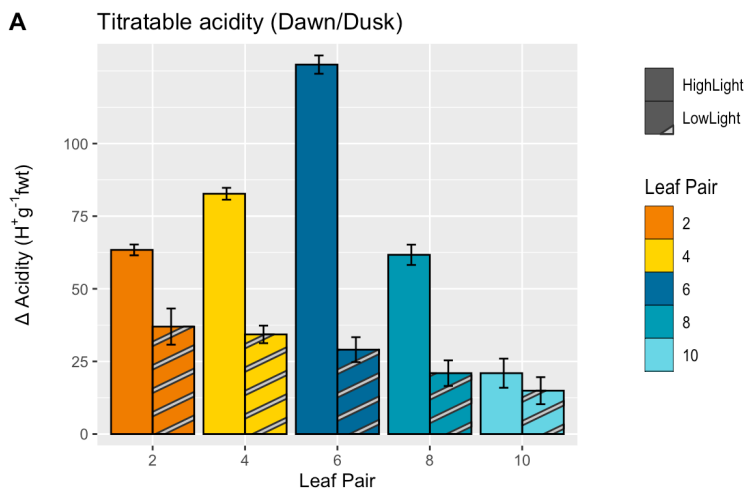


Figure A5.1. Dawn/Dusk whole leaf overnight accumulation of titratable acidity across different leaf pairs in *K. blossfeldiana* plants sampled 90 days after propagation, grown in normal light (normal bars, 190 μmol Photons) or low light (dashed bars, 50 μmol Photons). Leaf pairs are numbered up the plant, with 10 being the youngest sampled. Values are means \pm SEM.

